



SMAC 83

Proceedings of the Stockholm Music Acoustics
Conference
July 28—August 1, 1983

Anders Askenfelt Si Felicetti Erik Jansson Johan Sundberg
Editors



Volume II

Publications issued by the Royal Swedish Academy of Music No. 46:2
1985

SMAC 83

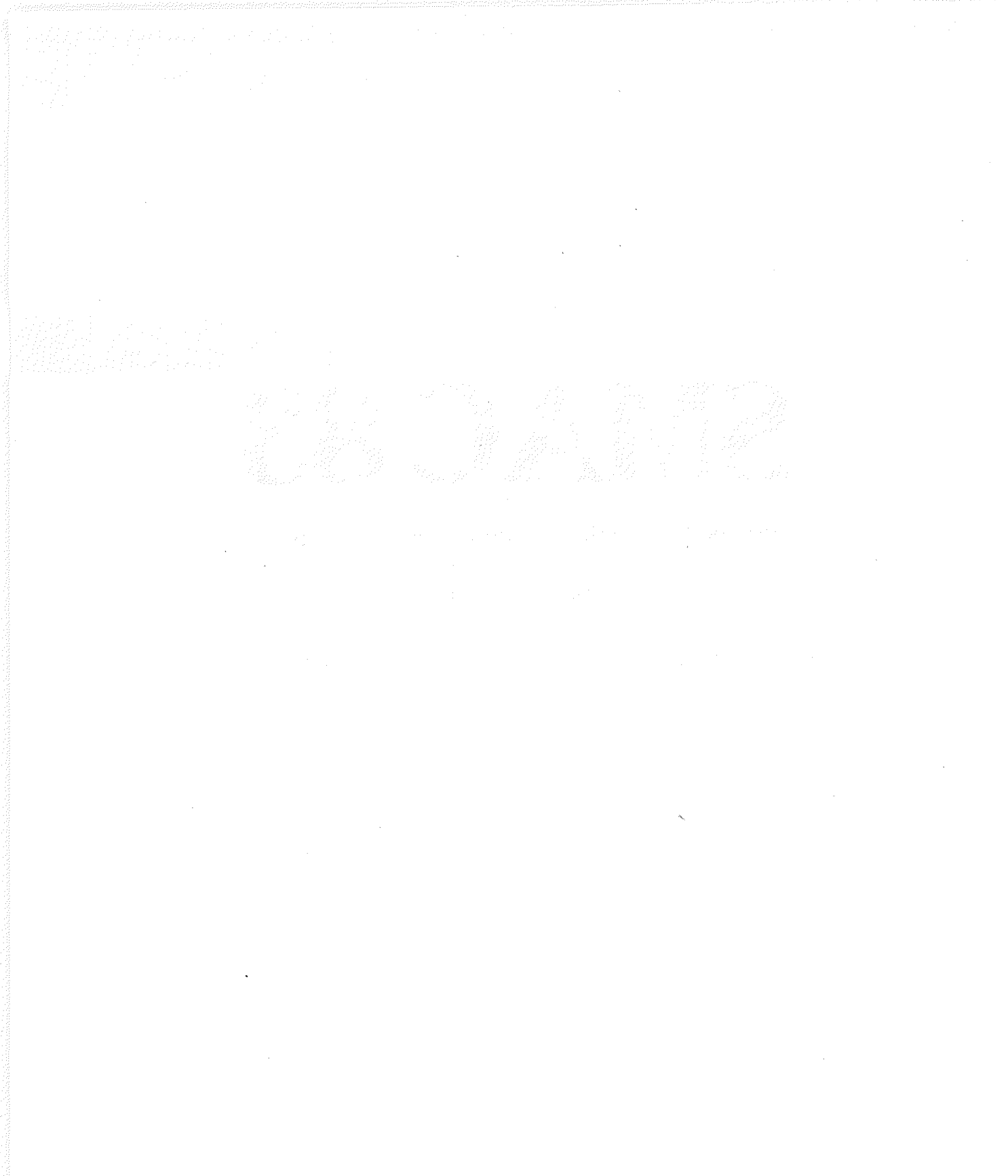
Proceedings of the Stockholm Music Acoustics
Conference
July 28—August 1, 1983

Anders Askenfelt Si Felicetti Erik Jansson Johan Sundberg
Editors

Volume II

Publications issued by the Royal Swedish Academy of Music No. 46:2

1985



VOLUME I

TABLE OF CONTENTS

PREFACE

SINGING - INVITED PAPERS

G. FANT: Acoustic Parameters of The Voice Source	11
H. HOLLIEN: Report on Vocal Registers	27
Z. PAWLOWSKI, R. PAWLUCZYK & Z. KRASKA: Epiphysis Vibrations of Singers Studied by Holographic Interferometry	37
I. TITZE: The Importance of Vocal Tract Loading in Maintaining Vocal Fold Oscillation	61

SINGING - CONTRIBUTED PAPERS

M.C. AMETRANO JACKSON: The Quality of Children's Singing Voice	73
L. BOVES & B. CRANEN: Spectral and Temporal Differences between Glottal Flow Pulses as a Function of Speaker and Supra-Glottal Load	87
G. BROCK-NANNESTAD: The Masking of Characteristic Spectra by The Acoustico-Mechanical Recording Process	105
M. CASTELLENGO, B. ROUBEAU & C. VALETTE: Study of The Acoustical Phenomena Characteristic of The Transition between Chest Voice and Falsetto	113
D.G. CHILDERS, J.J. YEA & E.L. BOCCHIERI: Source/Vocal Tract Interaction in Speech and Singing Synthesis	125
T. CLEVELAND & J. SUNDBERG: Acoustic Analysis of Three Male Voices of Different Quality	143

J. ESTILL, T. BAER, K. HONDA & K.S. HARRIS: Supralaryngeal Activity in a Study of Six Voice Qualities	157
B. FRITZELL, J. GAUFFIN, B. HAMMARBERG, I. KARLSSON & J. SUNDBERG: Measuring Insufficient Vocal Fold Closure during Phonation	175
A. JOHNSON, J. SUNDBERG & H. WILBRAND: "Kölning". Study of Phonation and Articulation in a Type of Swedish Herding Song	187
C. JOHANSSON, J. SUNDBERG & H. WILBRAND: X-ray Study of Articulation and Formant Frequencies in Two Female Singers	203
F. McCURTAIN & G. WELCH: Vocal Tract Gestures in Soprano and Bass: A Xeroradiographic- Electro-Laryngographic Study	219
C. OCKER, W. PASCHER & M. RÖHRS: Investigations of The Vibration Modes of The Vocal Cords during Different Registers	239
C. SCULLY & E. ALLWOOD: Simulation of Singing with a Composite Model of Speech Production	247
W. SEIDNER, H.K. SCHUTTE, J. WENDLER & A. RAUHAUT: Dependence of The High Singing Formant on Pitch and Vowel in Different Voice Types	261
T. SHIPP, P. MORRISSEY & S. HAGLUND: Laryngeal Muscle Adjustments for Sustained Phonation at Lung Volume Extremes	269
J. SUNDBERG, R. LEANDERSON, C. von EULER & H. LAGERCRANTZ: Activation of The Diaphragm during Singing	279
S. TERNSTRÖM, J. SUNDBERG & A. COLLDEN: Articulatory Perturbation of Pitch in Singers Deprived of Auditory Feedback	291
G.J. TROUP & H. LUKE: Some Radiological Observations of Vocal Source - Vocal Tract Interactions	305
S. WANG: Singing Voice: Bright Timbre, Singer's Formants and Larynx Positions	313

G.F. WELCH: A Schema Theory of How Children Learn to Sing In-Tune: An Empirical Investigation	323
J. WENDLER, S. FISCHER, W. SEIDNER, A. RAUHUT & U. WENDLER: Stroboglottometric and Acoustic Measures of Natural Vocal Registers	333
<hr/>	
SOUND EXAMPLES	341

VOLUME II

TABLE OF CONTENTS

PANEL ON VOICE QUALITY IN BOWED INSTRUMENTS	
A. RAKOWSKI (Moderator): Bowed Instruments - Close Relatives of The Singing Voice	9

STRINGS - INVITED PAPERS

C. GOUGH: Acoustical Studies of String Instruments Using String Resonances	19
C. HUTCHINS: What The Violin Maker Wants to Know	47
J. MEYER: Tonal Quality of Violins	69
G. WEINREICH: Violin Radiativity: Concepts and Measurements	99

STRINGS - CONTRIBUTED PAPERS

J. ALONSO MORAL: Input Admittances and The Sound Radiation of Four Violins	111
A. ASKENFELT: Study Your Bowing Technique!	123

A. ASKENFELT & E. JANSSON: Piano Touch, Hammer Action and String Motion	137
G. BISSINGER & C. HUTCHINS: Tracking "Enclosed Air-Plate" Coupling with Interior Gas Exchange	145
O. CHRISTENSEN: An Oscillator Model for Analysis of Guitar Sound Pressure Response	151
I.M. FIRTH & A.J. Bell: On The Acoustics of The Concert Harp's Soundboard and Soundbox	167
S. FREDIN, G. HAMMEL, J.A. STRAIN, P.D. TOWNSEND & L. WILZEN: Some Analyses of Viola Tone	185
C. GOUGH: Acoustic Resonant Scattering - A Possible New Method for Studying Musical Instruments	197
H. HARAJDA: Characteristics of Dynamic Possibilities of Sound in Contemporary Master Bowed Instruments	207
E. JANSSON: The Function of The Violin Body - What The Physicist Does Not Know!	223
C. KARP: Evidence of Bridge and Soundboard Contributions to Keyboard Inharmonicity	239
M. KONDO & H. KUBOTA: A New Identification Expression of Helmholtzian Waves and Their Formation Mechanism	245
J. PHILIPP: Automatic Transcription of Polyphonic Music by Linear Predictive Analysis	263
M. RAFFERTY & A. LEE: Fast Decay of Longitudinal Vibrations in Violin Strings	269
R. RASCH: Jitter in Violin Tones	275

B. RICHARDSON & G. ROBERTS: The Adjustment of Mode Frequencies in Guitars: A Study by Means of Holographic Interferometry and Finite Element Analysis	285
R. ROSS & T. ROSSING: Plate Vibrations and Response of Classical and Folk Guitars	303
T. ROSSING, J. POPP & D. POLSTEIN: Acoustical Response of Guitars	311
R. SENGUPTA, B. BANERJEE, S. SENGUPTA & D. NAG: Tonal Qualities of The Indian Tanpura	333

BOWED INSTRUMENTS - CLOSE RELATIVES OF THE SINGING VOICE

Andrzej Rakowski

Academy of Music, Warsaw, Poland

Introduction

The similarity between stringed bowed instruments and the human voice in singing may not seem very obvious either to an amateur listener or to a researcher in one of the domains in question. However, as we start looking at the problem from certain perspectives this similarity becomes more and more evident and finally appears as striking.

In looking for the common feature in these two kinds of musical instruments we should concentrate separately on such problems as the spectral characteristic of the source, the filtering action of a transmitting system, the specific features of the timbre and the specific character of the melodic intonation. Let us briefly review these problems.

Input vibrations

I am certain that someone trying to find an analogy between a violin and a singing voice as two musical instruments may raise a serious objection: "These instruments belong to different groups of classification. The violin is a chordophone and the singing voice is an aerophone. Not only are their "vibrators" different (a string and a vibrating column of air), but they are also driven by entirely different mechanical systems: the moving bow in the one case and the vibrating vocal cords in the other."

I have deliberately put forward this simplified picture, which most of you recognize as improper, but this is exactly how the great majority of

music students would describe differences between the emission of bowed and sung tones. As a matter of fact, this is a consequence of some controversies inherent in the commonly adopted classification of musical instruments. It is beyond the scope of the present lecture to talk about these controversies at large, so let us adopt a slightly different point.

Let us concentrate our attention on that particular place inside the complex musical instrument where the vibrations, induced externally, enter into the multi-resonance chain of transmission and transformation. Such transmission-transformation chains for the two instruments in question are the violin body and the human vocal tract. Our place of interest will be located respectively in the violin bridge and in the larynx, just above the vocal folds. We shall call the vibrations that arise in these particular places "input vibrations". The medium in which input vibrations occur (the air or solid matter) is essential in classifying a given instrument as an aerophone or not an aerophone. (E.g., a chordophone as in the case of instruments where input vibrations are imposed by vibrating chords.) However, as we shall see, this appears not to be essential at all if we consider the situation on a somewhat higher level of abstraction.

One of the important features that makes many bowed instruments sound so similar to the human voice is the general similarity of spectrum envelopes. This fact arises mostly from the basic correspondence in the form of the input vibrations in both kinds of instruments. That, in turn, is partly due to somewhat similar driving mechanisms (relaxation oscillations). Violin bridge vibrations are at the first approximation saw-tooth shaped. They have a harmonic spectrum with the envelope falling down at the rate of 6 dB per octave. The shape of these input vibrations and corresponding spectrum envelope may be to some degree mediated by the violinist through changing the place upon the string (e.g., *sul tasto* or *sul ponticello*), or the force of playing.

When the violinist places his bow on the string relatively far from the bridge, then the vibrations become triangular rather than saw-tooth

shaped and the sound is less rich in harmonics. The opposite effect, i.e., sound particularly bright and rich in harmonics, may be obtained when the bow is placed near to the bridge (sul ponticello). The level of high harmonics may also be raised by applying greater force to the bow.

The form of the input vibrations in singing generally implies a spectrum less rich in harmonics than that of the violin; its average envelope falls down with the rate of abt. 12 dB per octave. Here, however, the correction is applied to the final product. The radiation of sound from the mouth enhances higher parts of the spectrum with the rate of 6 dB per octave, so the cumulative effect for the spectral envelope of the radiated sound is similar to that of a violin: falling down at the rate of 6 dB per octave.

The possibility of changing the shape of input vibrations and consequently that of their spectrum envelope is much more at the disposal of a singer than it is at the disposal of a violinist. This comes naturally from the fact that all the driving mechanism in singing belongs to a living human body while in violin playing only part of this mechanism, namely the right hand of a violinist, constitutes a living structure.

Transmission transformation chain

There are several groups of instruments in which the transmission-transformation chain does not exist at all or plays only a totally marginal role. These are most idiophones, like a triangle, the tymbals or wooden blocks, some aerophones like a mechanical siren or an accordion, and some chordophones like a primitive hunters' bow. The input vibrations in these instruments should be considered as identical with the "output vibrations" or vibrations in the air around the instrument when the correction for directional radiation is taken into account.

In the instruments which concern us during this conference, the transmission-transformation chain constitutes their most essential part. (In a somewhat trivial manner, let us think of the dollar price of a

Stradivarius violin body and compare it with the price of its strings and bow.) The transmission-transformation chain of a violin is a complicated multiresonance mechano-acoustic system that imposes a rich formant structure on the spectral envelope of the input vibrations. Both the frequency location and the Q-value of the formants are constant for a given instrument and cannot be corrected by the player.

This situation, though similar, differs in some essential details in the singer's instrument. At first the transmission-transformation chain is based here on acoustical rather than mainly mechanical resonances. Then, the damping in soft organic tissues of the vocal tract is generally larger than it is in a wooden violin box, so the formant Q-values in the singing voice are lower. Finally, and perhaps what is most important, the formant frequencies in the singing voice apparatus may to some degree be mediated by a singer.

This possibility plays a very essential role in shaping the timbre of the voice (vowel quality) and in acquiring a desired intensity level in singing (particularly high soprano notes).

The above differences should not mask the basic similarity of a bowed instrument and a singing voice as far as the relation of their input vibrations to the characteristic of the resonance system is concerned. As a matter of fact, both instruments belong to the same family of "formant-spectrum" or "fixed formant" sound sources, in opposition to some other groups of instruments which may be characterized as "non-formant", or, (though not very correctly) "moving formant" instruments.

The typical non-formant sound source is a single organ register taken as a separate instrument. The shapes of successive pipes along the tone scale exactly mirror each other while the dimensions change in a fixed proportion. As a consequence, the spectral patterns of corresponding sound vibrations remain the same. There are more or less fixed proportions among the amplitudes of various harmonics and the enhancement of a harmonic of a given number remains constant. This particular enhancement, occurring at various frequencies as tones of various pitch are

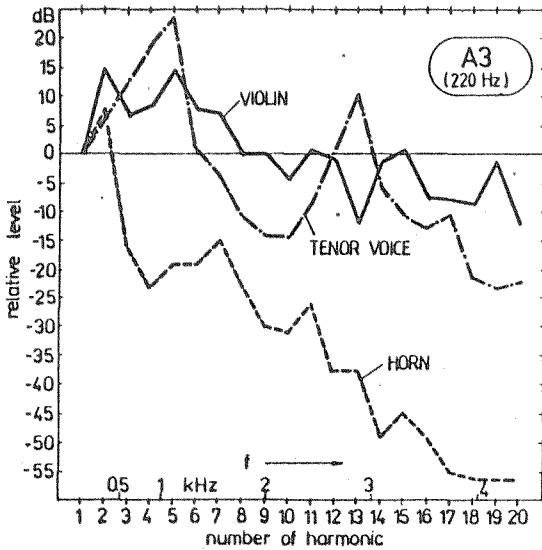


Fig. 1. Spectrum envelopes of a violin, a tenor voice and a French horn.

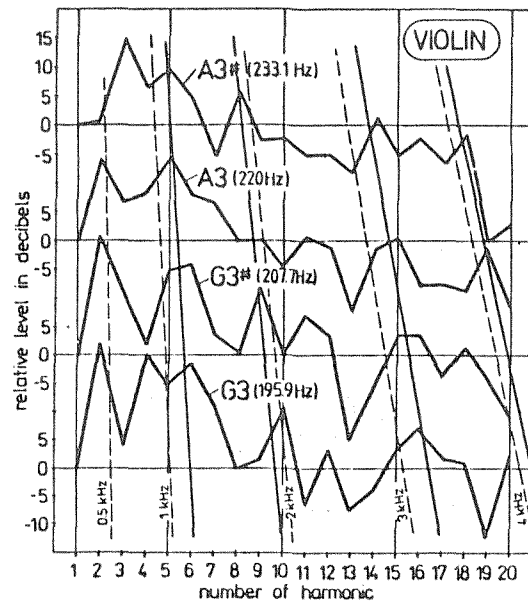


Fig. 2. Spectrum envelopes of four tones of a violin. Continuous straight lines across the diagrams show supposed formant frequencies.

played, is sometimes called a "moving formant". It occurs in most wind instruments in which input vibrations and the vibrations of a transmitting system are frequency-locked.

This situation may be seen in an example. In Fig. 1 the spectrum envelopes of three instruments were compared. The instruments were: an old Italian violin, a tenor voice, and a French horn. The fundamental tone was G_3 (about 196 Hz) and levels of 20 harmonics relative to the level of a first harmonic were shown in dB. The first impression from looking at this figure is that of the basic similarity of the violin and voice spectra while compared to that of a French horn. Their spectral envelopes are falling down at nearly the same rate.

Let us now follow the changes in spectral relations that occur while

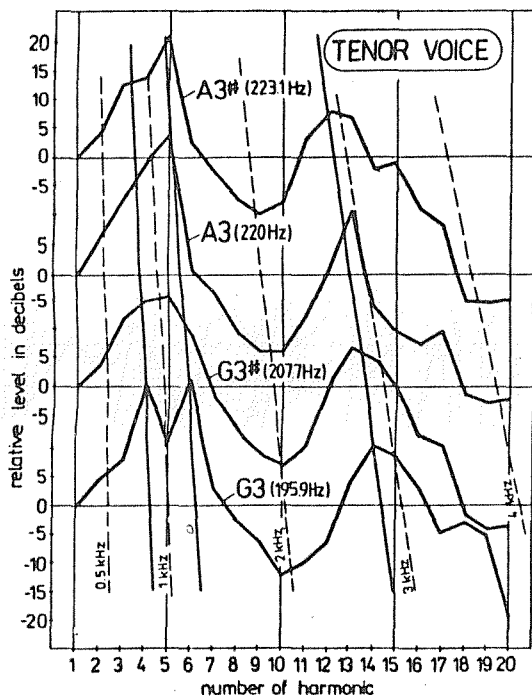


Fig. 3. Spectrum envelopes of four tones sung by a tenor voice. Continuous straight lines across the diagrams show supposed formant frequencies.

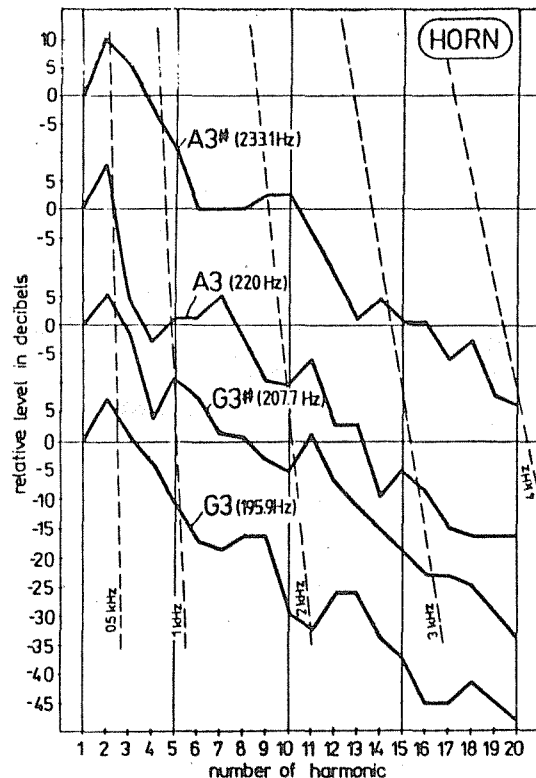


Fig. 4. Spectrum envelopes of four tones of a French horn.

the fundamental frequency changes within a minor third (about 20%). This situation is presented separately for the violin, the singing voice, and the horn in Figs. 2, 3, and 4. In these figures numbers of harmonics have been taken as a common abscissa scale independently of the fundamental frequency of a tone, so the frequency scale can be represented according to thin broken lines across the figures. Following the amplitude maxima of the harmonics in violin and voice tones one can easily come to a conclusion about the virtual position of formant frequencies.

Some of them have been marked on the drawings by thick straight lines. It is, however, not possible to find any fixed-frequency formant looking at the subsequent tones of a horn. The only definite conclusion which can be drawn from Fig. 4 is that in this particular part of a horn's scale

the second harmonic was always most pronounced in the spectrum. As has been mentioned, such a phenomenon is sometimes described as a "moving formant".

There is one additional fact which seems to be significant from a perceptual point of view and sheds some light at our sense of timbre perception. Due to the fixed values of formant frequencies the amplitudes of tone harmonics change as the fundamental frequency increases according to the semitone musical scale. To evaluate these changes the variance of separate harmonics levels was computed and averaged for ten

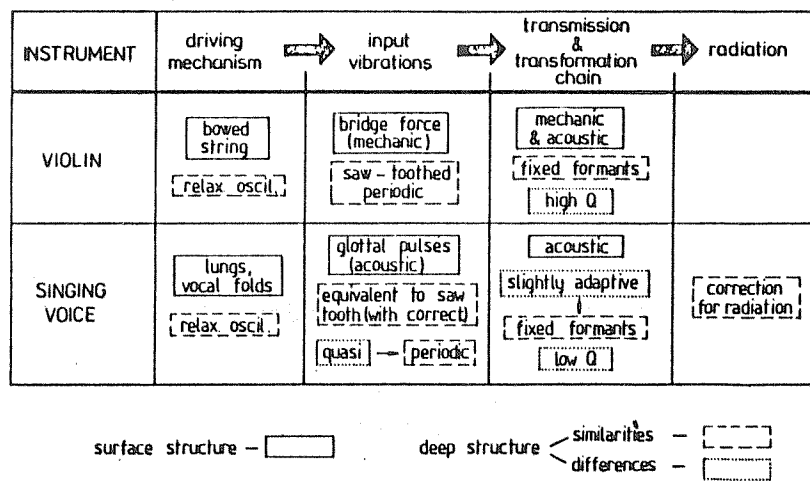


Fig. 5. Functional similarities and differences between a violin and a singing voice.

lower harmonics in the range of four subsequent notes separated by semitones from G_3 to A_3 . The results are: 32 dB^2 for a violin, 29 dB^2 for a singing voice, and 16 dB^2 for a French horn. As was to be expected, the formant-spectrum instruments reveal much larger step-to-step spectral variability than the non-formant-spectrum instruments do. It should be noted that tones taken a semitone apart - from the same register of a given instrument - are supposed to be practically identical as far as

their timbre is concerned. Nevertheless, as may be seen in Fig. 2, their harmonics may vary as much as 18 dB. Consequently, these tones must be perceptually quite different. This fact seems to be a new illustration of the general feature of a human perception mechanism: a categorical perception. The perceptually different signals belonging to the same category (in this case a common timbre category) are accepted as practically identical, and the differences between them are neglected. This is exactly the same perceptual phenomenon as the one that we shall observe in the following section in the pitch domain. However, before we pass to that last section, let us summarize some of the problems looking at the functional scheme on Fig. 5.

The instruments compared differ in many ways. However, they appear to be similar in many functional aspects. The apparent differences constitute a "surface structure", often in contrast to less evident though more important "deep structure" of functional similarities.

Fundamental frequency regulation

Despite the great similarities in spectrum forms, it is not so much the timbre, but rather the ways of processing pitch that make the bowed instrument and the singing voice so very similar to each other in producing music. Both belong to the same group of free-intonation instruments. This is to a large extent due to the fact, previously described, that in both cases the input vibrations are not frequency-locked to the resonance vibrations in the transmitting system.

The unlimited freedom of intonation within the instrument's range secured to the bows and to the singing voice gives them a unique position among other musical instruments. It was claimed that they are the only instruments that practically perform music in natural "pure" scales not distorted by the artificially introduced musical temperament (by "pure" scales were meant Pythagorean or just intonations). This view has for many years been put forward as a very strong point in official music theory. The most effective blow to this theory came with the results of

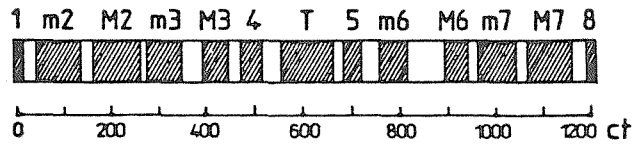


Fig. 6. "Zones of tolerance" of musical interval widths in violin playing measured by Garbuzon (after Golachowski and Drobner, 1953).

a very simple and modestly instrumented experiment by Nickolai Garbuzow of the Moscow Conservatory (after Golachowski and Drobner, 1953). Garbuzow had two eminent violinists play and record on the taperecorder the Air on G string by Johan Sebastian Bach.

The fundamental frequencies of all tones were then measured and exact frequency distances in cents calculated for all tone successions in the melody. This large set of data, taken jointly for both music performances, was next analyzed in terms of maximum deviations occurring in each of the twelve within-octave musical intervals. The result of this analysis is shown in Fig. 6.

It appeared that top professional violinists in a recorded performance fully accepted by them as correct from the musical point of view, performed musical intervals that were mostly neither "natural", nor "Pythagorean" nor even tempered, but rather taken "at random" (as it might have seemed at the first sight) from a very large range of possible intonations. The resulting "zones of tolerance" were really very wide. For some intervals they stretched for nearly 100 cents around the tempered values. (It is good to remember that the differences between just, Pythagorean, and tempered intonation do not exceed 20 cents.) However, the intonation here was far from being "random". Later investigations (Rags, 1960) have shown that there are quite definite rules that govern melodic intonation. These rules derive mostly from the harmonic background of the melody. They aim at strengthening harmonic tensions. According to them the pitch of a leading note is shifted towards its solution, dis-

sonances lean towards dissolving into consonances, and the major character of a mode is strengthened through enlarging a major third.

The above-described situation is typical of a solo melodic performance. It is different when chords are played. In such a case a new important factor takes the lead. This factor is the tendency to minimize beats between partials of the tones. In such cases "natural" intervals, expressed by small integer ratios are often performed.

Nearly everything that has been said so far about the bowed-string intonation may be repeated in reference to singing. A few years ago Hagerman and Sundberg (1980) in their work on barbershop-quartet singing showed the great precision attained by experienced singers in controlling the pitch. This precision, reaching the order of a few cents, does not prevent singers from making wide deviations from the average interval values. These deviations are, however, scarcely accidental. In most cases they reflect a subconscious striving to obtain a given musical effect.

And here we come to an important conclusion. Both bowed instruments and the singing voice are given a unique and powerful means of musical expression that nearly all other instruments are deprived of. This means of musical expression is attained by the absolute freedom of within-interval pitch intonation. It can be used in the way that makes the performance of bowed instruments and of singing most impressive and makes us believe that these instruments keep the highest position in the kingdom of music.

References

Golachowski, S. and Drobner, M. (1953): Akustyka muzyczna, PWSM, Warsaw.

Rags, J. (1960): "Intonirovaniye melodii v sviazi s niekotorimi jejo elementami", Trudy Kafiedry Teorii Muzyki Moskovskoj Konservatorii, Muzgiz, Moscow.

Hagerman, B. and Sundberg, J. (1980): "Fundamental frequency adjustment in barbershop singing", J.Res. in Singing 4, 4-17.

ACOUSTICAL STUDIES OF STRINGED INSTRUMENTS USING STRING RESONANCES

Colin E. Gough

Department of Physics, University of Birmingham, Great Britain

Abstract

In this paper we briefly outline the way that coupling at the bridge between the vibrating string and acoustical resonances of a stringed instrument strongly influences the vibrational characteristics of the string itself. We show that measurement of low amplitude string resonances can provide quantitative information about the acoustical properties that determine the tone of an instrument - the position and Q-factor of body resonances, the strength of their coupling to the vibrating string and even their radiation efficiencies. It will be argued that it is important to take such interaction into account in interpreting the characteristic vibrational response of any stringed instrument, however this is measured. Examples of string resonances that illustrate the importance of the string-body interaction will be shown for the violin, cello and piano. The possible musical significance of large amplitude, non-linear, string resonances will also be illustrated.

Introduction

In view of the importance of string vibrations in the history and science of acoustics, it is perhaps surprising that until very recently no reliable measurements existed for the response of a string at resonance. Indeed, Benade (1976) in his relatively recent book on musical acoustics listed a number of anticipated difficulties in making such measurements, largely associated with the expected narrowness of string resonance and the demands that this would make on the stability and resolution of measurements. In practice, however, these difficulties appear to have been overestimated and in this paper we demonstrate that it is possible to measure the resonant response of a string with sufficient accuracy and resolution to reveal a number of unexpected, but predictable, features that had not previously been reported.

We shall now show that the resonant response of a string can provide quantitative information about the acoustically important structural vibrations of the instrument on which the string is mounted. In particular, measurements of string resonances can give the position of structural resonances, their Q -values, their effective masses, their coupling directions to the string and even their acoustic efficiencies. In addition to providing such information, measurements of string resonances have also helped to illuminate a number of interesting aspects of the dynamics of the vibrating string and the acoustically radiating vibrations of the body of the instrument to which the strings are coupled via the bridge.

The idea of using string resonances to study the acoustics of the violin was suggested by Schelleng's analysis of the interaction of string vibrations and the vibrational modes of the body of an instrument in his important paper on the theory of the violin treated as an electric circuit (1963). Schelleng used the electrical analogue of a transmission line terminated by a series resonant circuit to represent the string and coupled mechanical resonator. He showed that, if coupling was sufficiently strong, the imaginary component of the mechanical admittance (velocity/force) at the bowing point measured as a function of frequency would pass through zero three times when the frequencies of the uncoupled string and structural resonance were coincident. He proposed that excitation of stable vibrations at the outer two zero-crossing frequencies was responsible for the characteristic beating associated with the wolf-note on the bowed string.

Although the excitation of wolf notes is probably rather more complicated than suggested by Schelleng's original analysis (see, for example the discussion given by McIntyre and Woodhouse, 1978) the predicted value for the critical coupling constant for excitation of the wolf-note was shown to be close to the value described from experiments (see also Firth and Buchanan, 1973; Gough, 1980). The coupling constant can be expressed in terms of the mass m of the vibrating string and the effective mass and Q -value, M and Q , of the coupled resonance.

Irrespective of the validity of his analysis of the wolf-note problem, Schelleng's analysis showed that measurement of the resonant response of a string, when tuned to frequencies in the neighbourhood of a coupled structural resonance, could in principle provide useful quantitative information about the acoustically important modes of the instrument on which the string was mounted.

In this paper we will use a simple mechanical model (described more fully in Gough, 1981a) to describe the interactions between a string and any structural resonance to which the string is coupled via the supporting bridge. The experimental techniques that we have developed to study string resonances will be briefly described and illustrated by measurements on both the violin and cello as well as for the piano. We show that it is not only the string vibrations that are modified by their interaction with the resonances of the body of an instrument but that the structural resonances themselves can be appreciably perturbed by their interaction with the string. Finally, we show that it is even possible to study the radiation loading of structural resonances by measurement of string resonances.

Theory

Before attempting to analyse the dynamics of a real string on an actual musical instrument, it is instructive to consider the simpler text-book example of a string terminated at one end by a mass M , see Fig. 1. We assume that the induced displacement of the terminating mass is small, so that to a good approximation the string displacement y along its length is given by $y = a \sin kx \exp j\omega t$, where $k \approx n\pi/l$ for the n th partial mode. The sinusoidally varying transverse component of the tension T causes the mass M to vibrate according to the equation

$$M \ddot{z} = T \sin \theta. \tag{1}$$

The motion of the end-point changes the effective nodal position and therefore the wavelength at resonance by an amount

$$dl/l = d\lambda/\lambda = z/(1 \tan \theta) \tag{2}$$

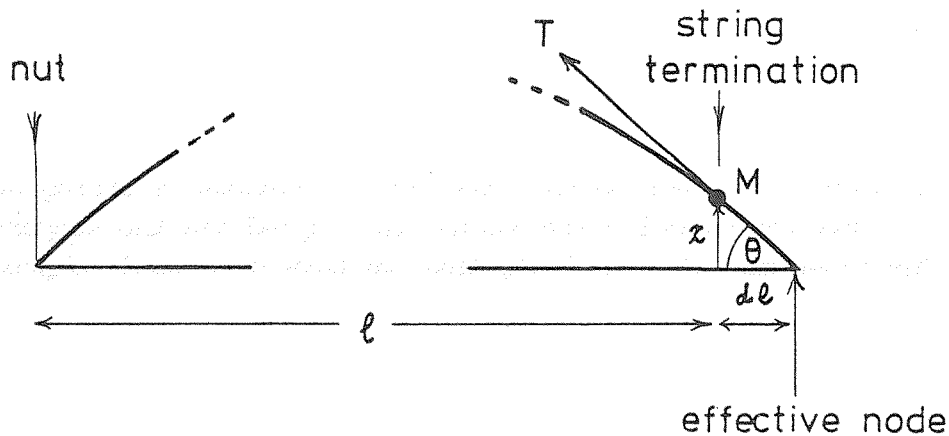


Fig. 1. Motion of end-support.

so that on substituting from Eq. (1) and assuming θ is small, we obtain

$$\begin{aligned}
 d\lambda/\lambda &= -T/(M\omega^2 l) \\
 &= -\frac{1}{(n\pi)^2} \left(\frac{m}{M}\right) \\
 &= -df/f
 \end{aligned}
 \tag{3}$$

where m is the mass of the vibrating string, $c = \omega k = (Tl/m)^{\frac{1}{2}}$ and df/f is the fractional change in resonant frequency of the string.

For a terminating mass the end support moves in anti-phase with the transverse force exerted by the string, effectively shortening the effective wavelength and therefore increasing the resonant frequency of the string. For a spring-like termination the wavelength is increased and the resonant frequency decreased. The two cases are illustrated schematically in Fig. 2.

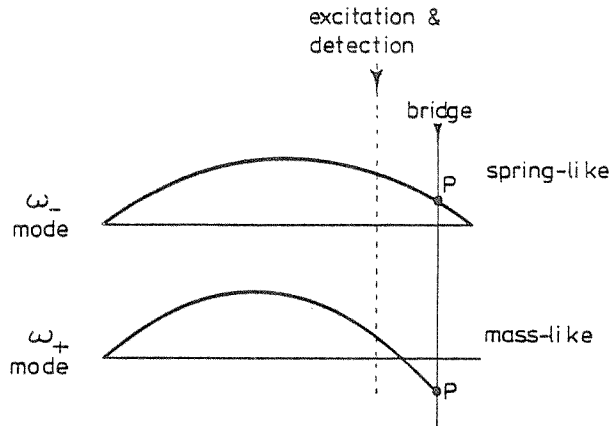


Fig. 2. Motion of end-supports and normal modes of system.

The most interesting situations arise when a resonating string is coupled to one of the structural modes of an instrument. The motion of the end support can then be described by an equation of the form

$$M_B(\ddot{z} + \frac{w}{Q_B} \dot{z} + w_B^2 z) = T \sin \theta \quad (4)$$

where Q_B is the quality-factor of the coupled resonance, M_B is its effective mass at the point of string support and w_B its resonant frequency. We then obtain

$$\frac{df}{f} = \frac{1}{(n\pi)^2} \cdot \left(\frac{m}{M}\right) \cdot \frac{8}{(1 - (w_B/w)^2 - j/Q_B)} \quad (5)$$

For string resonances at frequencies well above the resonant frequency of the coupled structural resonance the end support appears mass-like, whereas for frequencies below the structural resonance the support is spring-like. When the frequencies of string and structural resonance coincide, the predicted frequency shift is purely imaginary. This corresponds to a damping of the string resonance giving rise to a string

resonance with a half-width $|df/f|$ and quality-factor Q_S given by

$$2|df/f| = 1/Q_S = \frac{1}{(n\pi)^2} Q_B \left(\frac{2m}{M}\right). \quad (6)$$

We would like to take this opportunity to draw attention to an algebraic mistake, see Gough (1981b), where in every expression that m appears it should be replaced by $2m$.

In all the above expressions for the shifts and broadening of string resonances resulting from coupling to structural modes of an instrument, it is only the mass of the string that is important. A strong case could be made for manufacturers to indicate the mass of a string rather than its diameter, as it is largely the mass that will determine the tonal quality of a string on a particular instrument.

On a musical instrument the string can couple to more than one structural resonance and in general one can express the terminating admittance (velocity/force) at the point of string support on the bridge as

$$A = A' + jA'' = \sum \frac{1}{M_B} \cdot \frac{jw}{(w_B^2 - w^2)(1 - j/Q_B)} \quad (7)$$

where A' and A'' are the resistive and reactive components of the admittance. The shift in resonant frequency of the string can then be expressed as

$$df/f = \frac{jz_0}{n\pi} (A' + jA'') \quad (8)$$

where $z_0 = mc/l$ is the characteristic mechanical impedance of the string.

The measured shift and broadening of a string resonance can therefore be used to determine the real and imaginary components of the terminating impedance. Although the broadening can be observed directly, any shift in resonant frequency of the string has to be measured relative to the unshifted value. Fortunately, the directional nature of the coupling at the bridge makes the determination of any such shift relatively straightforward, as we will now show.

Consider a violin string supported at a position P on the bridge, as shown in Fig. 3. At low frequencies, the right hand foot of the bridge close to the soundpost is approximately a nodal point for the vibrations of the instrument associated with the main body resonance and the air resonance. Since at these frequencies the bridge moves as a rigid body (Reinicke, 1973), the vibrations of the top-plate will cause the bridge to rock in its own plane taking the string with it along what we will call the "coupling" or rocking direction. It is only the component of string vibrations polarised in this direction that can interact with the structural resonances excited. String vibrations polarised in a direction orthogonal to the "coupling" direction will not be perturbed and so will remain unshifted and unbroadened by any interaction with the air and main body resonance. If a string is excited in an arbitrary direction, two distinct modes of string vibration can therefore be excited, which we will refer to as the "coupled" and "uncoupled" modes of string vibration. Any shift in resonant frequency of the coupled string resonance can be measured relative to the unshifted resonant frequency of the uncoupled mode, as we have illustrated schematically in Fig. 4.

There are of course complications to our simple model which become increasingly important at higher frequencies. In particular, a string will generally be coupled to more than one structural resonance and, if these involve different coupling directions, the modes of string vibration will no longer be linearly polarised but will be elliptically polarised, though in practice the degree of ellipticity is rather small. Furthermore, even at low frequencies the "uncoupled" string vibrations will be slightly broadened and shifted in frequency by coupling to all the structural modes at higher frequencies that involve motion of the point of bridge support in the "noncoupling" direction. We shall see an illustration of this in a later section.

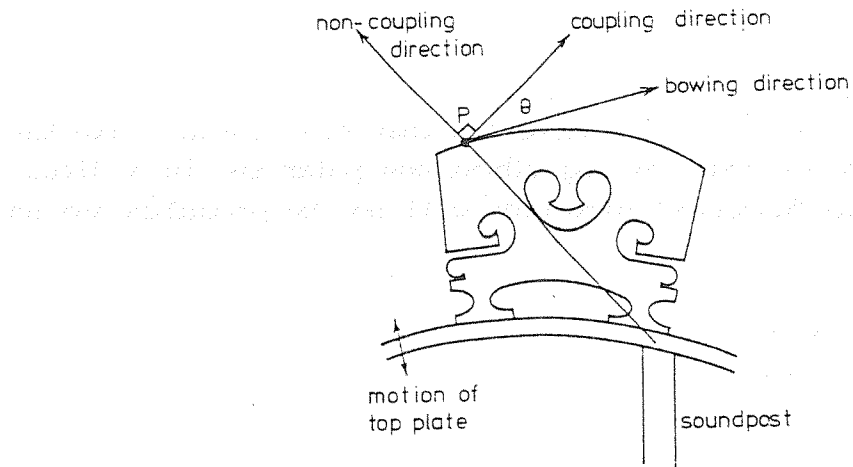


Fig. 3. Rocking motion of bridge.

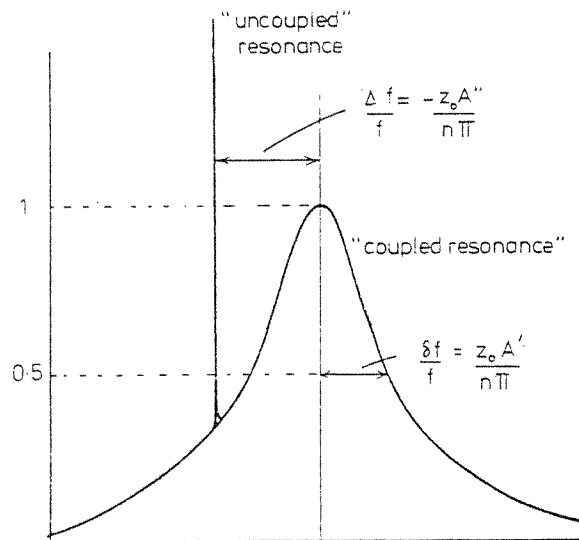


Fig. 4. Shift and broadening of coupled resonance.

Experiment

Hancock (1975; 1977) was the first to publish measurements for the resonant response of a sinusoidally excited string on a stringed instrument. His initial experiments (1975) were carried out with the electromagnetically excited violin string in one arm of a sensitive ac-bridge, the out of balance signal being induced by the motion of the metal-covered string in a magnetic field. Subsequently Hancock developed a rather more sophisticated technique (1977) based on the Doppler shift of laser light reflected from the moving string. In both cases some very interesting results were reported but no very clear picture of the essential physics of the vibrating string emerged.

With the help of two undergraduate students, Chris Baker and Carolyn Thair, we developed a rather simple technique for monitoring string vibrations (Baker et al, 1980), which is illustrated schematically in Fig. 5. Like Hancock, we excite the string electromagnetically by passing an ac-current through the wire or metal-covered string and use a permanent magnet to produce a localised driving force at a position fairly close to the end of the fingerboard. The amplifier delivering current to the string is driven by a voltage controlled oscillator (VCO), which enables us to scan the exciting current slowly through the string resonance.

The induced displacement of the string is monitored by a photo-detector, the shadow of the moving string modulating the current through the device. Initially we used a filament lamp for illumination and a Darlington photo-detector but we now prefer to use a matched infra-red LED and photo-diode because of its faster response (the Radio Spares slotted opto-electronic switch is a very convenient commercial device). A phase sensitive detector with the frequency from the VCO as reference monitors the resulting modulation in current through the detector in phase and in phase-quadrature with the current passing through the string. For measurements on thin strings, we half-mask the small (≈ 3 mm diameter) active area so that one side of the strings shadow lies permanently in the masked region. Using such a detector we can measure string displacements

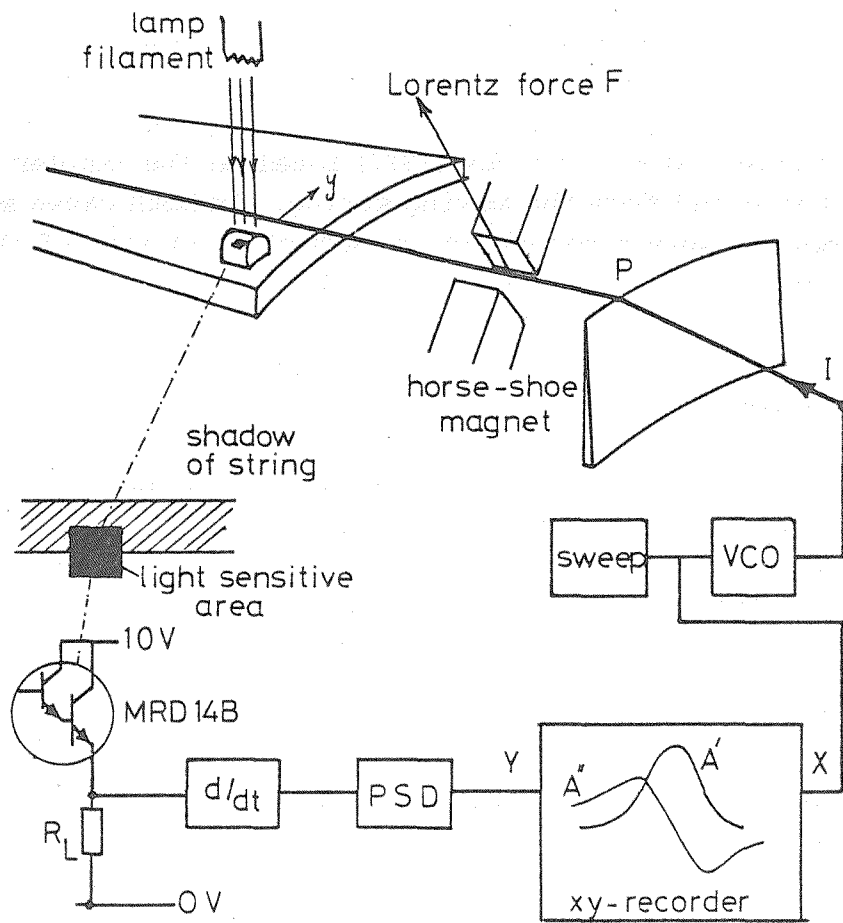


Fig. 5. Original experimental arrangement (see Gough, 1981b).

from as little as 10^{-6} mm to about 0.5 mm over an almost linear dynamic range. At such small amplitudes we can safely ignore any complications from the nonlinearity associated with the increase in tension with amplitude of string vibration, which we will discuss elsewhere (Gough, 1983).

By varying the direction of the magnetic field providing the Lorentz driving force and noting the relative intensities of the "uncoupled" and "coupled" string vibrations, it is relatively straightforward, if a little tedious, to derive the coupling directions for relatively strongly coupled structural vibrations of the body.

Measurements

A typical measurement of a string resonance is shown in Fig. 6, which can be interpreted as the superposition of a "coupled" and "uncoupled" string vibration. The broadened coupled string vibration is shifted to a lower frequency than the uncoupled mode. This is to be expected because at this frequency the dominant coupling is to the main body resonance, which for this instrument lies at the slightly higher frequency of about 465 Hz.

Fig. 7 shows a sequence of string resonances tuned by increasing the tension in the string so that the resonances scanned across a relatively weakly coupled structural resonance at around 630 Hz. In this case the field direction was carefully adjusted so that only the coupled mode of string vibration was strongly excited. The frequency at which the string resonances are most strongly damped identifies the position of the coupled structural resonance, while the width of the string resonance and its variation in the neighbourhood of the minimum can be used to determine the effective mass and quality factor of the coupled resonance using Eq. (5). A correction has to be made for the slowly varying background damping from vibrational modes of the body of the instrument with resonant frequencies some way away from the string resonance.

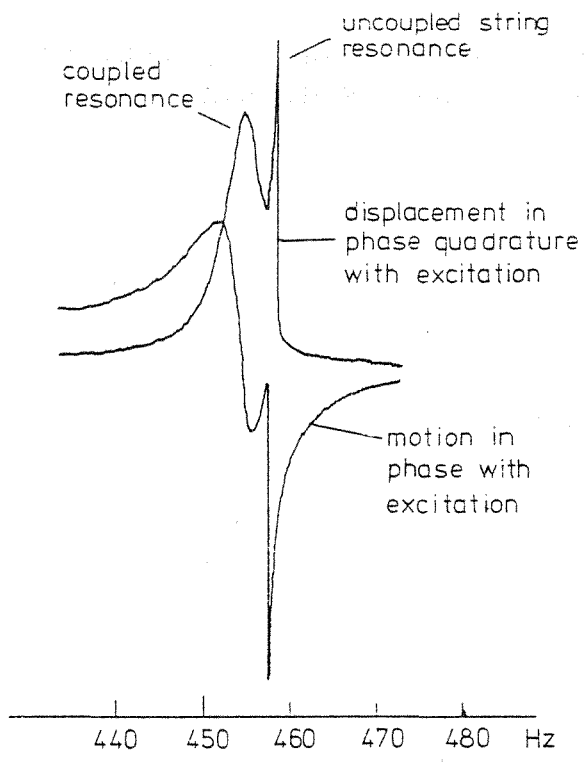


Fig. 6. A typical string resonance.

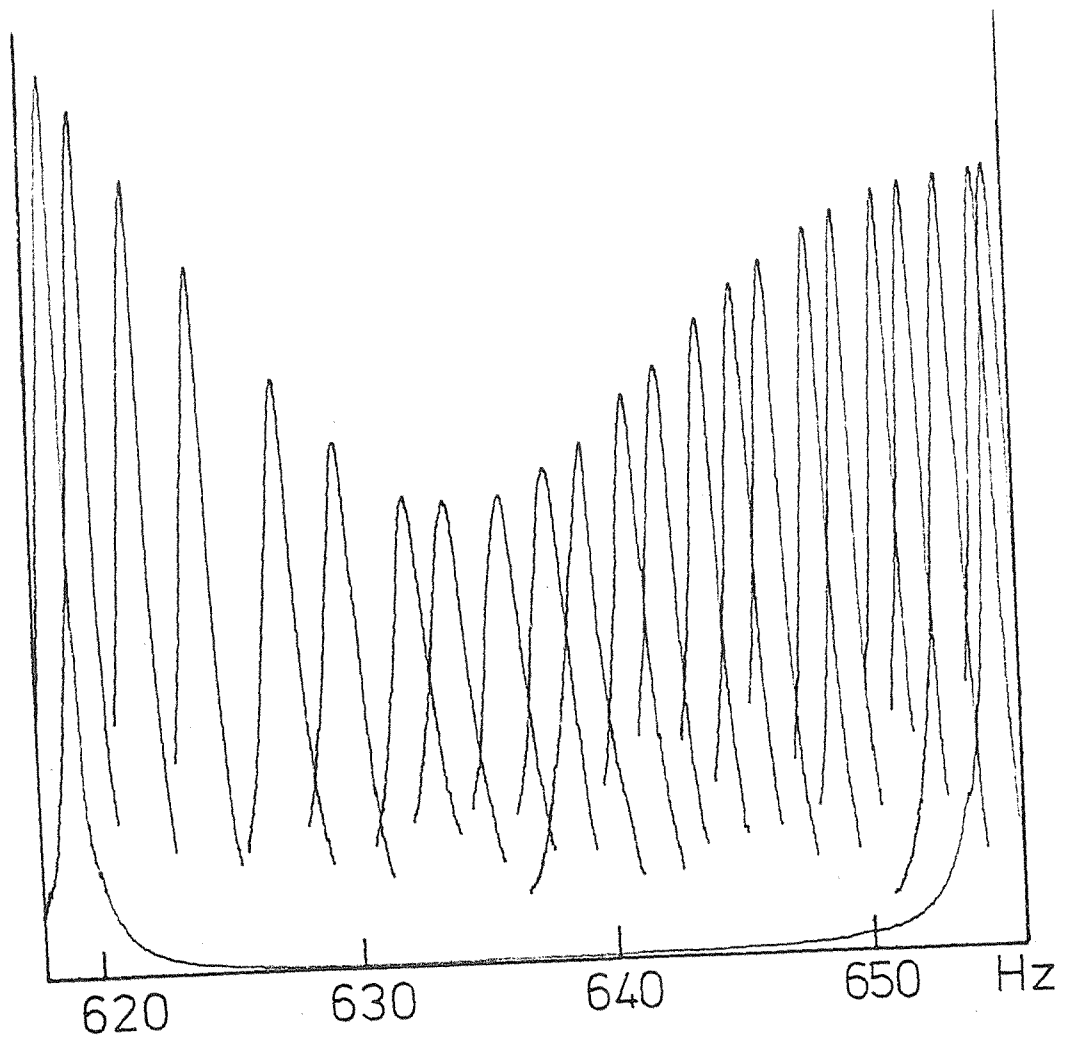


Fig. 7. A sequence of string resonances ($n=2$, E string).

It is often assumed that the finite flexibility of a string will be the major cause of deviations from harmonicity in the frequencies of the partials of a vibrating string. However, measurements on a violin G-string show that for the lowest 10 or so partials coupling to the vibrational modes of the body of an instrument is the major cause of anharmonicity. Fig. 8 shows a series of resonances for the lowest few partials of a Pirastro Gold-label G-string. The wide variation in scanning ranges and widths of the string resonances should be noted. In Fig. 9 we plot the normalised frequencies, f_n/n , of the partials in a form that allows comparison with the n^2 variation predicted from the finite flexibility. The dashed line gives the predicted dependence extrapolated from measurements of the higher partials - we could measure the first 21. Where both coupled and uncoupled string resonances were observed, they are both plotted.

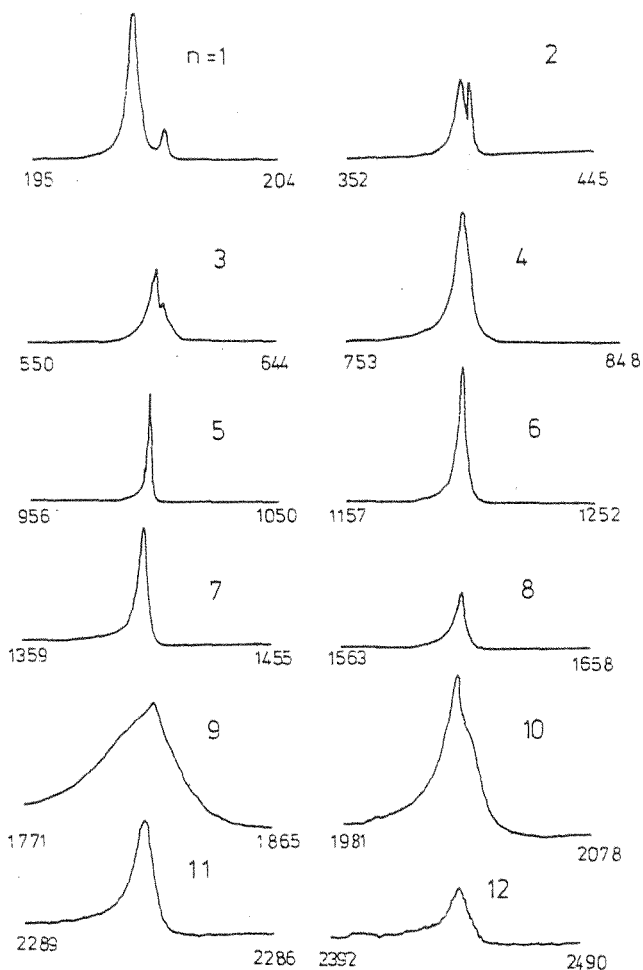


Fig. 8. Resonances of partials of a Pirastro G-string.

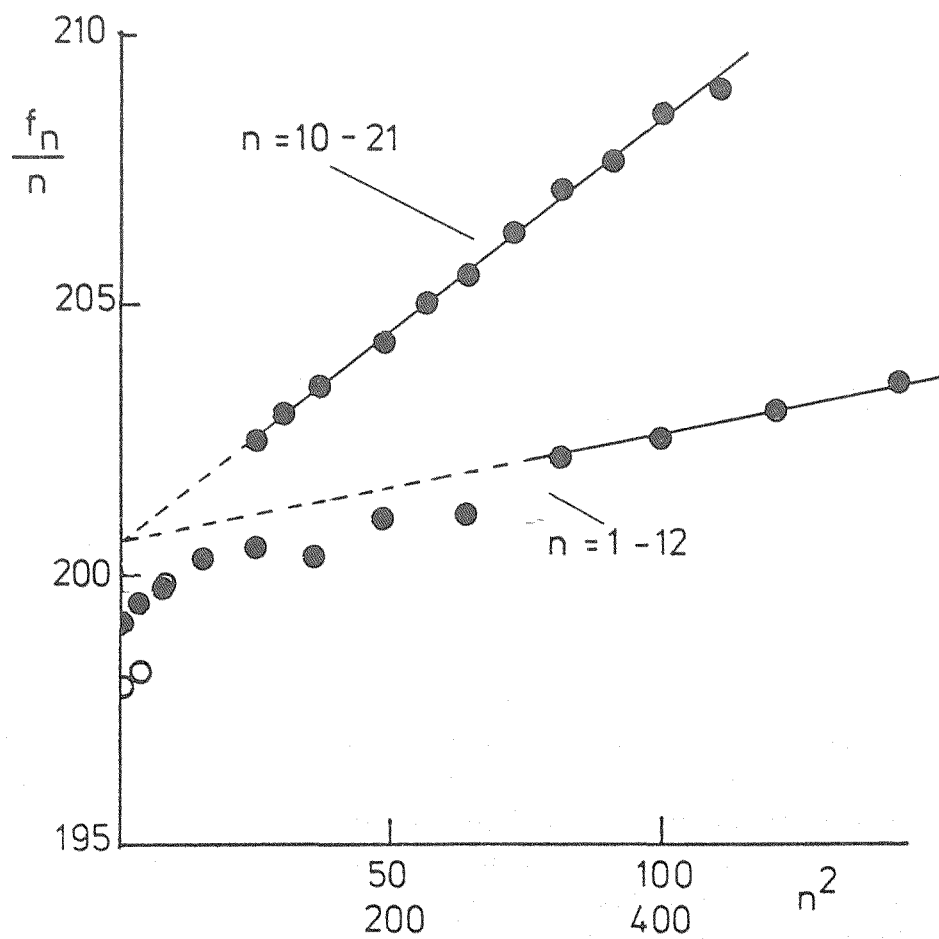


Fig. 9. Anharmonicity of G-string partials.

The n^2 dependence for the higher partials is confirmed but the extrapolated frequencies of the lower partials are considerably higher than those measured. The "coupled" string resonances deviate most strongly by an amount that depends critically on their position relative to the coupled structural resonances. The lowest partials are depressed in frequency by the compliance of the point of string support on the bridge, which will be different for a force in the "uncoupled" and "coupled" directions of the lowest string resonances. This compliance can be considered as the low frequency limit of the admittance arising from all the structural resonances of the instrument as expressed by Eq. (7). The relatively large amount of unharmonicity introduced by coupling to the body modes will clearly affect the establishment of stable Helmholtz vibrations of the bowed string. It would be interesting to compare the frequency of vibration of the bowed string with the frequencies of the unharmonic lower partials to see whether the observations could be understood in terms of Fletcher's analysis of the non-linear excitation of an unharmonic multimode system (1978).

The bridge and soundboard of the piano present a rather more rigid termination for the string than on the violin. Consequently string resonances are less strongly perturbed. Nevertheless, Weinreich (1977) has shown that the coupling of strings to the soundboard can play an important role in the tuning and production of tone of pairs and triplets of strings on the piano. Since, in addition, relatively few measurements have been made on the acoustical properties of the piano, we decided to investigate the resonances of single strings, with all other strings damped, on a 6'10" Steinway Grand piano (Baxandall et al, 1981). For the upper octaves we made measurements on individual strings using much the same techniques as those described for the violin. However, in the lower octaves the damping of the string resonances was so small that our normal scanning techniques could not be used. In this range we derived frequency shifts and damping coefficients from the free decay of string vibrations using a Fourier Transform method.

In Fig. 10 we have plotted the damping of the two string modes observed, which we again identify with the "coupled" and "uncoupled" modes

of string vibration. The scales are logarithmic and on the left gives the width deduced from the string resonances, $\Gamma = f_s/Q_s$ and on the right gives the corresponding 60 dB decay times, $\tau_{60} = 6 \ln 10 Q_s/w_s$.

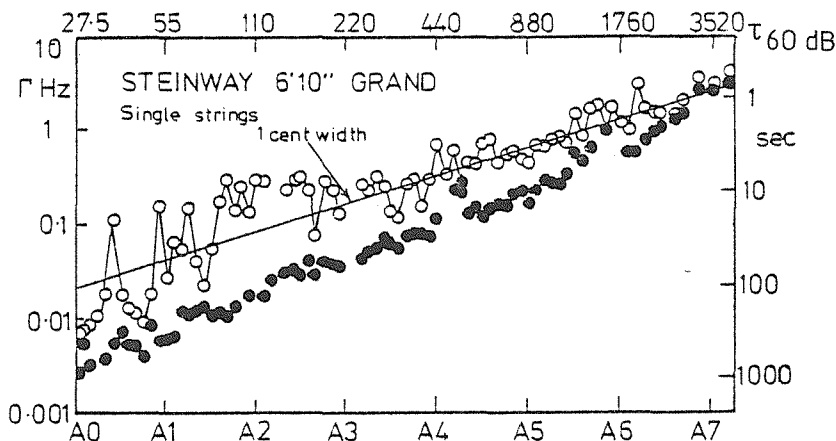


Fig. 10. Damping of coupled and uncoupled modes of a single piano strings.

The uncoupled modes of the lowest string have extremely long decay times but radiate very little sound. The stronger damping of the coupled mode of string vibrations reflects coupling to the structural resonances of the soundboard. There is clear evidence for a strong soundboard resonance in the first octave but unambiguous identification of higher frequency resonances is not possible because of the semi-tone spacing of the string resonances which rapidly becomes larger than the spacing of soundboard resonances.

Fig. 11 shows the corresponding measurements of the difference in frequency between the coupled and uncoupled string resonances. Note the reversals in sign, which are indicated by the dotted lines through zero connecting solid and open circles. The changes in frequency shifts are of the same order as the damping widths as anticipated from the general form of the terminating admittance, Eq. (7).

As an example of the way that coupling via the bridge can affect the motion of adjacent strings, we show some measurements of the induced motion of the centre string of a string triplet when only the outer

string is excited. Coupling between the strings via their common support on the bridge leads to the excitation of the "normal modes" of the coupled system. For the example shown, two of the normal modes involve the motion of the centre string in phase with the exciting force, whereas for the third it moves in antiphase. String resonance spectroscopy could be a powerful tool in the study of the acoustics of the piano and of the influence on tuning and tone production of the mutual interaction of pairs and triplets of strings in particular.

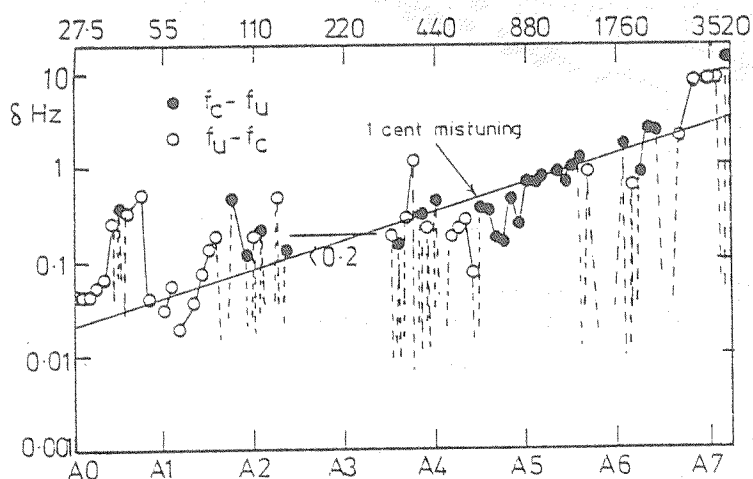


Fig. 11. Difference in frequency of coupled and uncoupled modes on piano.

Normal modes

Until now we have only considered the influence of the body resonances on the strings and have neglected any change in the structural resonances arising from the coupling. For piano strings such an approximation is justified but for instruments of the violin family the coupling between the strings and body resonances can be so large that it is not even possible to consider the string and body resonances as distinguishable vibrational modes of the system. Instead we have to consider the coupled, normal modes of the system as a whole. The problem is closely analogous to the well known textbook example of the oscillations of a pair of identical pendula swinging in the vertical plane and suspended

from a common horizontal thread. The two normal modes then comprise, in the first case, of the two bobs swinging together in the same phase at a lower frequency than the frequency of the pendula when rigidly supported and, in the second case, of the two pendula vibrating in antiphase at a higher frequency.

To consider the motion of a string coupled via the bridge to a structural resonance of the main body of an instrument, we consider the following pair of coupled equations (Gough, 1981a), which describes the influence of body resonances on the motion of the string as well as the reverse process considered in the earlier sections;

$$M(\ddot{z} + \frac{w}{Q_B} \dot{z} + w_B^2 z) = Tka \quad (9)$$

$$\frac{m}{2}(\ddot{a} + w_S^2 a) = Tka \quad (10)$$

where a is the amplitude of string vibration, and we neglect any intrinsic damping of the motion of the string. For simplicity, we only consider solutions of the above equations when the uncoupled string and structural resonance have the same resonant frequencies, $w_S = w_B$. We look for a solution for a and z varying as $\exp j\omega t$. By substitution we obtain a quadratic equation in w^2 , which has the following solutions

$$w_{\pm}^2 = w_B^2 \left[1 + \frac{1}{2Q_B} (j \pm \sqrt{K^2 - 1}) \right] \quad (11)$$

where $K = \frac{2}{n\pi} Q_B \sqrt{\frac{2m}{M}}$. Essentially the same result was derived by Meamari (1978) in an interesting theoretical and experimental investigation of string modes and the excitation of wolf notes on a specially prepared monochord.

Eq. (11) shows that the character of the normal modes of the coupled system depends critically on the magnitude of the coupling constant K relative to unity. For small K (weak coupling) we recover the results of the previous section with the w_+ mode corresponding to the scarcely perturbed structural resonance with Q -value $\sim Q_B$ and the w_- mode to the

string mode damped via its coupling to the structural resonance with a large Q -value = $K^2/4 Q_B$. In the small coupling limit the two modes remain unshifted in frequency.

In contrast, when $K > 1$ the term inside the square root is positive so that the two modes have different frequencies but the same damping. The normal modes have frequencies on either side of the uncoupled resonant frequencies with a splitting such that the difference in their frequencies is given by

$$\frac{f_+ - f_-}{\bar{f}} = \frac{1}{n\pi} \sqrt{\frac{2m}{M}} \quad (12)$$

These are equivalent to the modes of the two pendula referred to above with the string and body vibrating in phase (the w_- mode) and in anti-phase (the w_+ mode) as represented schematically in Figs. 2a and b.

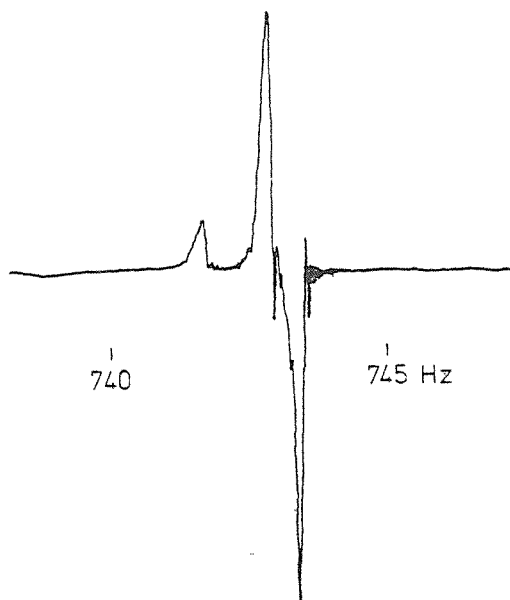


Fig. 12. Response of centre string of an F triplet with only the outer string excited.

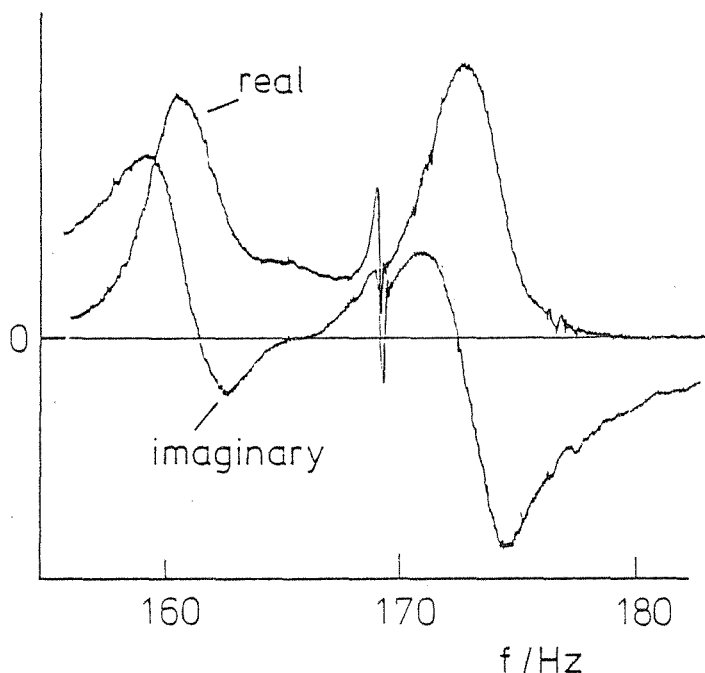


Fig. 13. Splitting of coupled, $n=2$, C-string resonance on a cello with a bad wolf-note.

Fig. 13 illustrates the magnitude of the splitting of string resonances that can occur in practice when the coupling is large. These measurements were obtained on a cello with the C-string purposely tuned sharp so that its first harmonic coincided with the main body resonance known to be responsible for a bad wolf note on this instrument. The two broad peaks are the split normal modes of the coupled system with half-widths just half that of the coupled structural resonance (Eq. 12). Although care was taken to excite the string in such a way that only resonances in the "coupling" direction were strongly excited, it was not possible to eliminate the "uncoupled resonance" lying between them entirely because of the slight degree of ellipticity referred to earlier.

The very large shifts in frequency of the string resonances resulting from the coupling should be noted. From the known mass of the vibrating string and the observed splitting and widths of resonances, it is easy to derive values for the frequency of the strongly coupled resonance = 166 Hz, its Q-value = 23 and its effective mass = 94 g. The direction of magnetic field to minimise excitation of the "uncoupled" string resonance gives the coupling direction relative to the bowing direction, which in this case was almost parallel.

In practice we have found that any instrument with a wolf note gives a double resonance similar to Fig. 13 with the imaginary component of the measured admittance passing through zero 3 or 5 times within the region of interest (the presence of the "uncoupled" string resonance is responsible for 2 of the zero crossings) thereby confirming Schelleng's prediction that such a feature could be expected on any instrument that suffered from a wolf-note. The condition for 3 zero crossings is that $k > 2$ - the coupling has to be sufficiently large to produce a splitting of the string resonances larger than their width.

The split "string resonances" are of course normal modes of the system as a whole and could equally well be studied by a direct measurement of, say, the vibrations of the top plate of the instrument or of the admittance at the point of string support on the bridge. It seems very probable that several of the split main body resonances reported from

time to time in the literature on structural resonances of the violin may be attributed to a strong interaction via the bridge to a nearly coincidentally tuned string resonance - on the violin the main body resonance is generally close to the fundamental of the A-string, for example.

The two normal modes can always be observed in any measurement of structural or string resonances even when there is a considerable degree of mistuning between the uncoupled modes (Gough, 1981b). Figs. 14 and 15 illustrate how the frequencies of the normal modes vary with the degree of mistuning for both weak and strong coupling. The shaded areas indicate the widths of the resonances. These dispersion curves again emphasise the very different characteristics for weak and strong coupling. Indeed, it is just as well that structural resonances are quite strongly damped, otherwise every time a string was played at the frequency of a structural resonance a wolf-note would occur.

Air loading

Finally, we consider the influence of air-loading on the body resonances as an interesting example of the way that string resonance spectroscopy can be used as a sensitive probe of relatively small changes in the properties of structural resonances.

Fig. 16 shows three sets of measurements taken on the same violin within a few minutes of each other. In the first the violin was freely suspended in a small room; in the second the violin was placed inside a totally enclosing heavy metal cylinder of diameter 9" and length 24"; and in the third the cylinder was evacuated. The G-string was initially adjusted so that its second partial was approximately tuned to the main body resonance to give a split string resonance with almost equal amplitudes on either side of the uncoupled resonance.

When placed inside the enclosing volume, there is a very slight increase in the frequency of the main body resonance - the string would

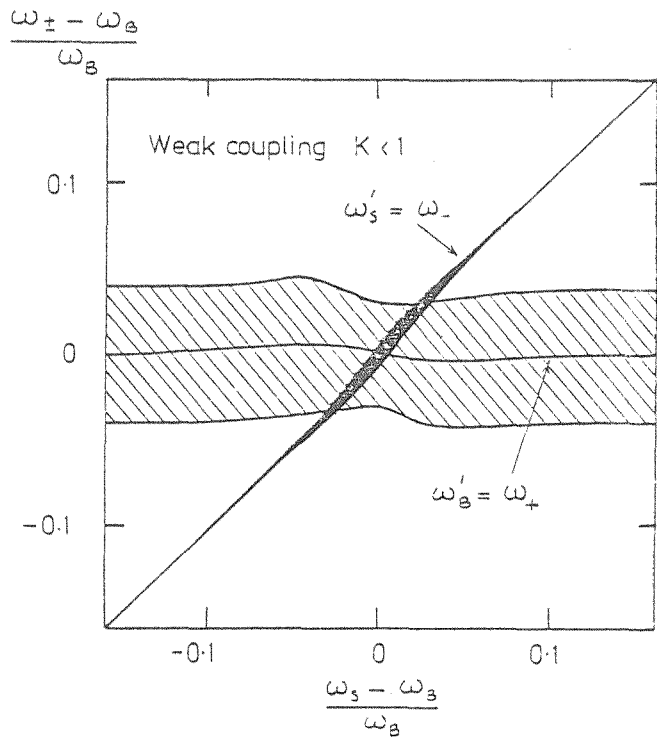


Fig. 14. The frequency and damping of normal modes for $k < 1$ - weak coupling.

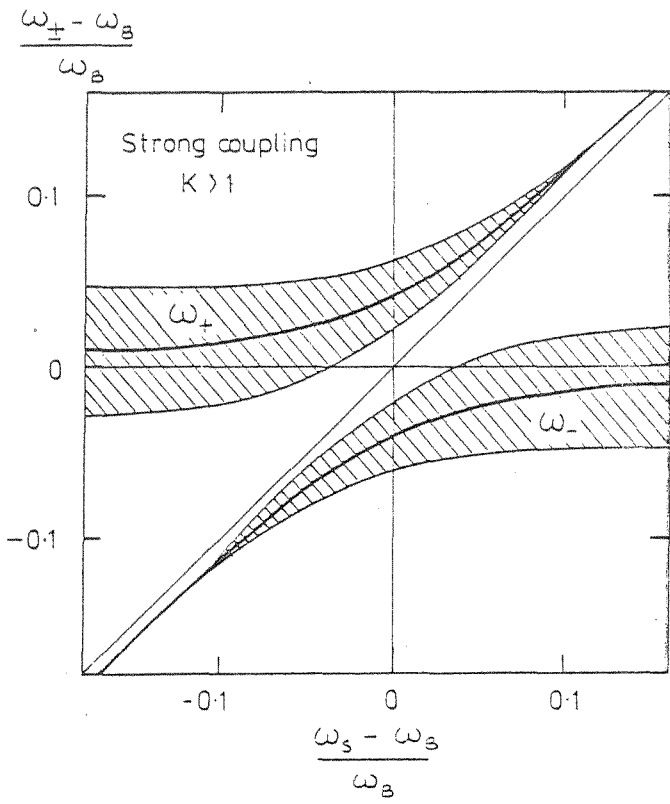


Fig. 15. The frequency and damping of normal modes for $k > 1$ - strong coupling.

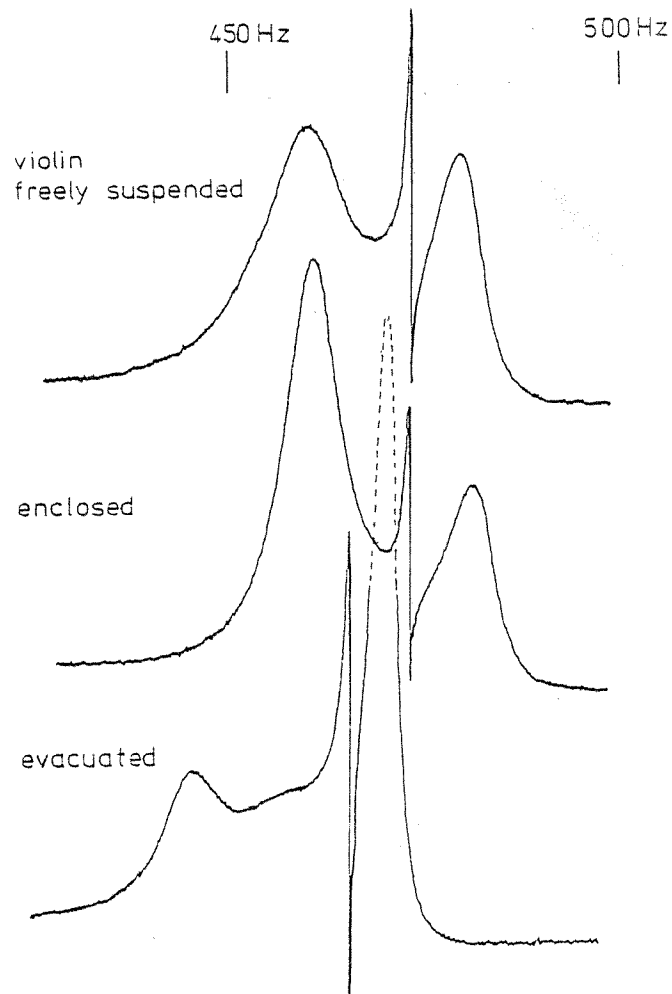


Fig. 16. The influence of air loading on string and structural resonances.

have to be tuned to a slightly higher frequency to make the split resonances of equal height again. However, much more interestingly, the combined widths of the split resonances are decreased, which implies from Eq. 11 that the width of the structural resonance has been decreased by the same amount. The Q-value of the main body resonance has been increased from about 17 to almost 30. This increase occurs because the violin inside the enclosing volume loses none of its energy by acoustic radiation, it is only coupled reactively to the non-radiating standing waves of the air inside the enclosing volume. This large rise in Q-value implies that almost half of the damping of the main body resonance arises from direct acoustic radiation, which is a very high value but is in line with the much earlier observations of Rohloff (1940) who observed the decrease in damping for several violins when placed inside an evacuated chamber.

The effect of evacuating the chamber can be seen in the third measurement of Fig. 16. The current passing through the string now leads to some heating of the string, which lowers its resonant frequency. However, the main body resonance is lowered by a much larger value and can now be seen as the small resonance well to the left of the now much stronger "coupled" string resonance. Comparison between the first and third set of measurements shows that the reactive component of the normal air loading on the body of the instrument increases the frequency of the main body resonance by about a quarter of a tone.

Conclusion

In this paper we have outlined the theory and practice of string resonance spectroscopy as a technique for investigating the acoustically important vibrations of stringed instruments. It will be clear that most of our work to date has been of an exploratory nature. We now need to undertake a rather more systematic application of these techniques to study instruments having a range of tonal qualities. Thereby we might hope to obtain a clearer indication of the relative importance of the various measured properties in relation to the subjective quality of an

instrument assessed by player and listener.

It may turn out that there are simpler and somewhat more direct methods for obtaining the information that we have shown can be derived from our measurements. Nevertheless, we hope that our measurements will have served to highlight a number of interesting aspects of the physics of the violin and other stringed instruments that need to be recognised to explain fully the acoustics of sound production by any stringed instrument.

Acknowledgements

Much of the work reported here was supported by a grant from the Royal Society and could not have been undertaken without the enthusiastic help of undergraduates working on student projects in this area. I would also like to express my appreciation for the encouragement and advice received from many members of the Catgut Society and would like to mention Carleen Hutchins, Gaby Weinreich, Art Benade, Robert Schumacher, Maurice Hancock and Bernard Richardson in particular.

References

- Baker, C., Thair, C., and Gough, C.E. (1980): "A photo-detector for measuring resonances of violin strings", *Acustica*, 44, 70.
- Baxandall, A., Brown, I.S., and Gough, C.E. (1981): "Vibrations of piano strings and coupling to the keyboard", *Proc. Inst. Acoust. Acoustics 81*, 339-342.
- Benade, A.H. (1976): Fundamentals of Musical Acoustics, Oxford University Press, London.
- Firth, I.M. and Buchanan, J.M. (1973): "The wolf on the cello", *J. Acoust. Soc. Am.*, 53, 457-463.
- Fletcher, N.H. (1978): "Mode locking in nonlinearly excited inharmonic musical oscillators", *J. Acoust. Soc. Am.*, 64, 1566-1569.
- Gough, C.E. (1980): "The resonant response of a violin G-string and the excitation of the wolf note", *Acustica*, 44, pp. 113-123.

- Gough, C.E. (1981a): "The theory of string resonances on musical instruments", *Acustica*, 49, 124-141.
- Gough, C.E. (1981b): "The acoustics of string instruments studied by string resonances", *Catgut Acoust.Soc. NL*, 35, 22-28.
- Gough, C.E. (1983): "The free decay of a nonlinear string", published in this volume.
- Hancock, M. (1975): "The mechanical impedance of violin strings", *Catgut Acoust.Soc. NL*, 23, 17-25.
- Hancock, M. (1977): "The mechanical impedance of violin strings. II", *Catgut Acoust.Soc.NL*, 28, 14-16.
- McIntyre, M.E. and Woodhouse, J. (1978): "The acoustics of stringed instruments", *Interdiscip.Sci.Rev.*, 3, 157-173.
- Meamari, E. (1978): "Experimentelle Untersuchungen zur Entstehung des Wolfons beim Cello", *Acustica*, 41, 94-101.
- Reinicke, W. (1973): "Übertragungseigenschaften des Streichinstrumentensteges", *Catgut Acoust.Soc. NL*, 19, 26-34.
- Rohloff, E. (1940): "Über die innere Reibung und die Strahlungsdämpfung von Geigen", *Ann.Phys.*, 38, 177-198.
- Schelleng, J.C. (1963): "The violin as a circuit", *J.Acoust.Soc.Am.*, 35, 326-336.
- Weinreich, G. (1977): "Coupled piano strings", *J.Acoust.Soc.Am.*, 62, 1474-1484.

WHAT THE VIOLIN MARKER WANTS TO KNOW
Carleen M. Hutchins
Catgut Acoustical Society, Inc.
Montclair, N.J., USA

Abstract

There are two main areas of importance to the violin maker - the construction and the adjustments of the violin for the production of fine sound and playing qualities.

The first includes selection and seasoning of wood for top and back plates, as well as for blocks, liners and ribs; the carving of the plates, their archings, contours, thicknesses, placement of F-holes, purfling groove, rib thicknesses and rib height in relation to the inside air modes; how to tune top and back plates with varying wood qualities; effect of varnish and how to compensate ahead of time for these effects.

The second on how to adjust an instrument for optimum tone includes the soundpost - its wood quality, shape and placement; the bridge - its wood quality and tuning; the strings - their gross action under the bow, tension and balancing.

Scientific investigations have thrown light on some of these areas, others are still being researched; while others are not yet understood. Each area will be discussed briefly in light of present knowledge related to violin making and its practices and problems.

The term "scientific investigation" can be broadly construed to mean a way of looking at a given phenomenon either natural (such as the cat sitting on my paper as I write) or man-made (such as the violin on the table before me). Both can be petted and cherished and are capable of giving much pleasure when properly handled. Both are extremely complicated from a structural as well as a functional point of view, and their physical parameters are as yet incompletely understood.

So much for the cat, for I don't intend here to go into the medical sciences and DNA chemistry.

For the trained master violin maker who has worked most of his life to absorb all the fine points of the age-old tradition of violin making, there is little need for scientific investigation. His senses are sharpened to assess properly the stiffness characteristics of the wood he selects and carves with such care and precision and to see variations of 1/10 millimeter in arching contours.

The tradition of apprentice training over a period of many years conveys the knowledge and skills of "how to do it" as well as the historical tradition involved in the work of the early makers and the development of fine violins.

Unfortunately, the values inherent in our technological society do not encourage many brilliant capable young men and women to spend 8 or 10 years in apprentice training learning a profession which will bring them 5 to 6 dollars per hour for their labors. Present scientific investigations are beginning to help the violin maker to learn his art and skills more readily, but as yet there are not answers to all his questions.

Five areas of potentially useful scientific information are considered here:

- I. Wood technology
 - A. Wood testing
 - B. Growth, selection, cutting, seasoning
- II. Constructional parameters
 - A. Ribs
 - B. Arching contours
 - C. Plate graduation
 - D. Purfling
 - E. F-holes

- III. Plate tuning
- IV. Effects of coatings
- V. Effects of moisture

I.

A. Wood testing

What physical properties of violin top and back wood, so carefully selected by the violin maker, are most important to the sound of a fine instrument? Researchers in this area generally agree on five criteria: (1) Elasticity both along and across the grain, (2) Shear, (3) Internal friction (damping) resulting in dissipation of energy, (4) Density, (5) Velocity of sound.

The most important aspects of elasticity are the values of Young's modulus along and across the grain. Young's modulus is a measure of the resistance to bending and resistance to stretching of the material, and is based on the force applied per unit area as related to the fractional change in length produced.

The shear modulus is a measure of the resistance to distortion such as occurs when the top of a very thick book, lying on a flat surface, is pushed sideways thus shifting the upper surface with respect to the lower.

Internal friction or damping is a measure of the ratio of energy stored to energy dissipated and can be expressed in two ways: (1) by the decay time, or the time during which vibration persists after excitation is cut off. (The violin maker listens for a long decay time in the tap-tone as he tunes a violin plate). (2) by the width of the frequency interval within which there is a specific response to continuous excitation as frequency is varied about a resonance. Internal friction, damping, is often expressed as the "quality factor" or "Q". Damping is frequency dependent, rising slowly as frequency increases, but the members given here generally hold good up to about 700 Hz.

Density is weight per unit volume and is found by multiplying length, width, and thickness of a strip and dividing the product into its weight.

Velocity of sound in the wood is found by dividing Young's modulus by density and taking the square root. One of the desirable characteristics of spruce for musical instrument soundboards is its high ratio of stiffness to density which is given the term velocity.

Fig. 1. Log and strips. The diagram shows a section of a spruce tree and four types of test strips cut from it. The strips are labeled: longitudinal-vertical, cross-vertical, horizontal, and end-vertical-vertical.

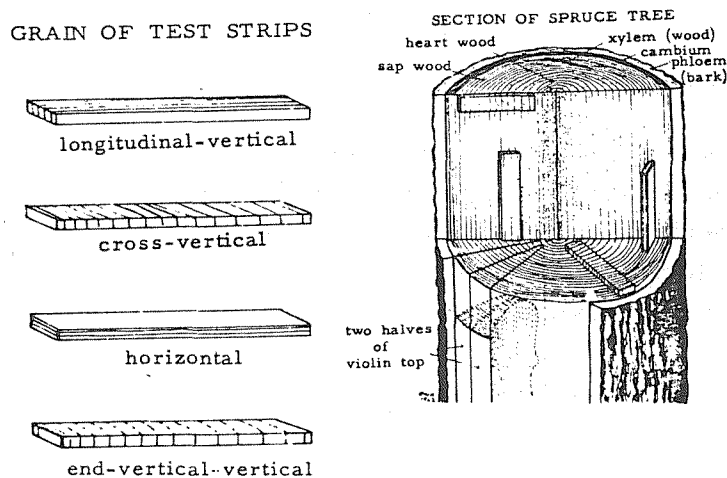


Fig. 1. Log and strips.

These characteristics are most often measured on small bars or strips (Fig. 1) of rectangular cross-section from which something about the larger pieces can be inferred. A simple and useful test of various woods of interest can be set up by cutting bars of exactly similar dimensions and mounting them as a xylophone, a method first suggested by Felix Savart in 1830. When the bars are struck, the pitch of the sound and the decay time can be heard clearly, enabling frequency and Q comparisons with specimens of known suitability. By combining this with the weight of the bars, a rough judgement can be formed of the new samples, at least for properties along the grain. It is difficult to identify the sounds in crossgrain strips by ear.

Acoustical testing of wood strips, using electronic methods, has been done by a number of researchers, notably Rohloff and Kruger in Germany (1938, 1940), Barducci and Pasqualini in Italy (1948), Daniel Haines (1979, 1980) at the University of South Carolina and Morton Hutchins (1981). Their findings indicate an average ratio of Young's modulus along to across the grain of about 15 to 1 in spruce selected for the tops of violins, guitars and piano soundboards, while the maple selected for violin backs has a ratio of about 5 to 1 along to across the grain. Measurements of internal friction indicate an average Q for spruce along the grain of about 140 and across the grain of 50; for maple along the grain of about 80 and across the grain of 50.

The effect of shear is to cause a slight lowering of all the resonance frequencies above the fundamental with the result that they are more closely packed, an effect felt about 4 kHz to 5 kHz in softwoods such as spruce and cedar much more than in hardwoods such as maple. In crossgrain strips shear stiffness as well as Young's modulus is markedly dependent on the angle of the grain or reeds. In wood with the reeds at a 45° angle to the flat surface, shear modulus is at a maximum, while Young's modulus is at a minimum. Through an experiment involving several hundred pieces of selected spruce, Haines found a Young's modulus of 15 to 1 with reeds at 90°, but as much as 100 to 1 with reeds at 45° to the flat surface. Since the ratio of Young's modulus along to across the grain in the wood selected for top and back violin plates is critical to the tuning of the eigenmodes in each plate, this can explain why violin makers always avoid wood with reeds at a 45° angle. In slab-cut wood sometimes used for backs where the reeds are parallel to the flat surface, the crossgrain stiffness is again high.

B. Wood growth, selection, and cutting

The vibrational properties of each finished shell-like top and back plate are the result of the whole "life story" of that particular piece of wood. It begins with the life of a great tree, from the sprouting of the seed through its many years of growth in winds and weather until its

crown is high above the ground and its trunk at least two feet in diameter. Then the tree is ready for the saw and axe of the violin maker, the long seasoning process, and the final crafting of the wood into a beautiful instrument -- a story that can span as much as 200 years.

When a violin maker climbs up into the high forest areas where the big spruce tree with wood suitable for violin tops can still be found, he is looking for a tall straight trunk with a clear span of 20 to 30 feet with no visible branches. He does this usually in winter, for not only is the water content in the wood lower than in the growing season - a desirable characteristic - but it is possible to slide the logs down the icy slopes from the more inaccessible ridges where the biggest trees have often been skipped on previous cuttings. Certain trees are ruled out because of abnormal growth characteristics such as a twisted trunk, or a marked lean from the vertical which causes undesirable cell growth known as "reaction wood", (Fig. 2.) In a given area where all the spruces have grown from

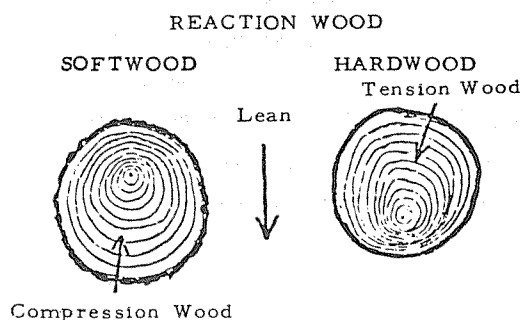


Fig. 2. Reaction wood.

seedlings at about the same time, it is often possible to assess some of their vibrational characteristics by whacking the trunks with an axe as high up as one can reach and listening to the sounds ringing through the forest. A clear full ring usually indicates that a tree has a straight grain without too many big knots from hidden branch butts, as well as lack of the twist where the grain spirals somewhat like the stripes of a barber pole. A hollow, non-resonant sound can indicate rot in the center of the trunk. The pitch of the sound from one tree to another, as well as

the diameter of the trunk of similar species in a given growth area, can indicate the pattern of the annual growth rings - the higher sound usually the narrower the spacing and vice versa.

It is possible to make test borings straight into the heart of the tree with a special device known as an increment borer that brings out a 1/4 inch diameter core showing the actual pattern and spacing of the alternating soft hard areas of so called early and late wood. As a tree grows, the single layer of activity dividing cells, known as the cambium, between the wood and the bark, produces new wood cells on one side and new bark cells on the other. Each year these new wood cells form a soft, light colored layer of thin-walled wood and a harder, darker layer of thick-walled cells over the whole tree - trunk, branches and twigs. In the cross-cut section of a tree the ring-like appearance of these successive pairs of hard and soft layers has given them the name annual rings.

The growth pattern of the cambium is affected by seasonal changes such as temperature, hours of sunlight, water supply, and wind as well as the mineral content of the soil, not to mention insect infestations and forest fires. In the mountains, particularly where the winters are cold and the snow accumulates, the trees tend to get a great deal of water in the warm sun of the spring thaws that may last into early summer. During this time the cambium grows quickly, forming thin-walled cells of both wood and bark in layers whose thickness depends on the supply of water, sunlight and temperature. This is called earlywood or springwood. Then in the drier, cooler conditions of late summer, fall and winter cambium produces tightly packed, thick-walled darker looking cells called latewood or summerwood. In spruce, these dark and light layers which form the grain of the wood are very prominent.

Violin makers call the latewood or darker segments of the annual rings the reeds, and look for spruce that has thin dark reeds with wider, light, earlywood areas between. This criterion is a good indication of low density as well as of a high ratio between the stiffness along the grain to that across the grain. It is quite possible for the density to be too low and the crossgrain flexibility too great. But here again the

experienced violin maker has learned to judge these characteristics by the appearance and feel of the wood. He also looks for spruce that has close, narrow growth rings near the outside of the log, where the tree has grown more slowly as it ages, with gradually wider ring spacing toward the center. Ideally the spruce for a top plate comes from a tree that has not only well-spaced, thin reeds, but straight grain in all directions. When such a trunk is cut into proper lengths and split on the quarter, as shown in the figure, the grain of the two halves of the joined top runs parallel, not only to the center join, but also to the flat bottom surface of the plate, (Fig. 3.) Also when two of the adja-

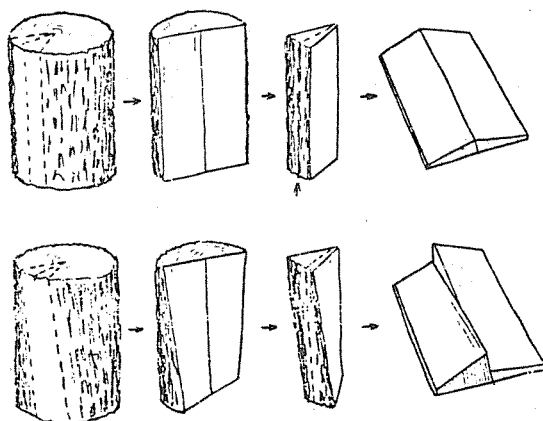


Fig. 3. Run out.

cent split-quarter flitches are cut and joined, the closer grain from the outside of the tree lies at the center of the plate with the gradually widening growth rings of the early more vigorous years opening out toward the flanks. The importance of this is shown later.

Traditionally violin makers discard the bottom six or eight feet of a spruce trunk because the wood is not uniform in this area. Root damage causes changes in cell structure several feet up the trunk. The static load of the hugh trunk, as well as the enormous stresses produced as a tall tree with a full crown of branches bends and twists in the wind alter the character of the wood.

Splitting a log on the quarter not only helps to assure the proper grain orientation, but also to detect twists in the growth fibers. The tendency of trees to grow with slightly spiral grain creates what is known as RUN OUT in the two halves of a violin plate, making it impossible for the fibers of the halves to be oriented parallel in two directions. Run-out tends to change the stiffness characteristics in different areas of the finished plate, for on one side the uncut fibers of the arch will be longer than those on the opposite side, skewing somewhat the bilateral symmetry of the two joined halves. Bilateral symmetry has been found to be important in the proper tuning, especially of the top plate of a violin.

Seasoning

Tradition also indicates that both spruce for violin tops and the maple for the backs should be stack-seasoned in a covered outdoor shed for some years, the spruce for at least five to ten years and the maple somewhat longer. In the past when a violin maker had a supply of selected flitches laid down for him by his father and then cut a supply of wood for his son, the long natural seasoning process did not constitute a real problem. Today such traditions are rarely followed. With the increasing worldwide demand for seasoned tone wood, the supplies are dwindling rapidly. The big trees in Europe are almost gone. Kiln drying of wood for violins has long been considered undesirable, particularly if the water is drawn out of the cells so rapidly that the cell walls are broken down. A violin maker can usually distinguish, by the sound and the feeling in his fingers, between the crackly shavings of well-seasoned spruce and maple and the shavings of kiln dried wood with their dull sound and slippery feel. Some makers indicate that it is best to season both the spruce and maple for at least fifty years, a judgement which may be reinforced by the findings of several wood technologists, who report that the ratio of crystalline-to-amorphous areas in the cell structure of wood seems to increase as the wood seasons. This concept fits rather nicely into violin making traditions, since amorphous material absorbs and loses water readily, and crystalline material does not. This could be one explanation of why many older instruments are less susceptible to mois-

ture changes than new ones - and why wood seasoned for many years is preferred over relatively new wood by most violin makers. Tests to check this amorphous-to-crystalline ratio in wood seasoned from 2 to 200 years are under way, but definitive results are not yet available.

II.

Certain CONSTRUCTIONAL PARAMETERS, well known in good violin making have been found to be important and can be explained by analogies to scientific principles. The effect of some of these parameters can be evaluated by present scientific test methods; while others are still too subtle for current technologies to unravel and measure.

A. Hologram interferometry has shown that the RIBS, (sides) of a violin actual bend considerably at certain frequencies. Thin ribs will bend more readily under vibration and do not split as easily as thicker ones. Also they are easier to shape when building the rib structure. Italian tradition based on the work of Stradivari as interpreted by Simone F. Sacconi (1962) indicates that violin and viola ribs should be an even 1.0 mm thick all around; cello ribs 1.5 mm and bass ribs 2.0 mm. Stradivari sometimes even went as thin as 1.3 mm for his cello ribs, reinforcing with thin cloth strips glued inside vertically at intervals.

B. Although there has as yet been no definitive analysis of the considerable effects that different ARCHING CONTOURS have on tone qualities, test made on several hundred pairs of free plates of all sizes of violin family instruments show that smooth, even contours are extremely important. Uneven, lumpy arches have been found to inhibit the vibrations of the normal plate bending modes, even suppressing them entirely at times.

C. The same is true of PLATE GRADUATIONS. This can be observed when working with Chladni patterns of free plates where even the smooth arching contours do not result in actively vibrating modes (particularly of mode #5) if the graduations are uneven and lumpy. (Plate tuning is discussed later.)

The Chladni pattern method of plate tuning (a technique originated by Ernst F.F. Chladni (1809) is intended for use by the skilled violin maker. It involves the vibration of free violin (also viola, cello and bass) top and back plates by means of sine wave sound of variable frequency emitted from a loudspeaker. By observing frequency, shape and activity (amplitude) of vibrations of the plates, made visible by motion of powder sprinkled on them, the experienced luthier can often decide where to remove the last half millimeter of wood that will complete his instrument.

The three most prominent, and most useful bending vibrations, or modes, in a violin plate are the first, the second and the fifth, which lie in that order of ascending frequency in every violin shaped top and back plate. These three mode shapes for a top and back plate are shown in Fig. 4 indicating not only the proper placement of the loudspeaker, but also of the four soft foam mounting pads.

Mode #1 entails a twisting of the plate, with one corner up and the other down. Thus, when a violin maker holds a plate at each end, twisting it between his hands to feel its resistance, he is sensing the stiffness of mode #1.

When a maker holds one end of a plate in both hands with thumbs on top and fingers spread out underneath across the wood, squeezing and bending it slightly to assess the cross-grain stiffness of first one end and then the other, he is comparing the relative stiffness of mode #2 across the two ends.

When he holds a plate around the two ends in his fingertips and pushes down in the middle with his thumbs, he is sensing the stiffness of mode #5. The same test can be made holding the plate around the edges and gently pressing the top of the arch against a flat surface to feel the bending.

Holding the plate at the midpoint of one end or in the edge of a C-bout and tapping with the soft part of a finger around the upper and

D. The effect of the PURFLING GROOVE open and closed.

We know from engineering principles that a thin edge to a bending plate enhances its vibrating potential. In the early 1930s, F.A. Saunders observed a fine hair-line crack around the purfling, particularly in the upper and lower bouts of instruments that had been played for many years, which would indicate considerable bending around the plate edges. Saunders suggested that this loosening of the purfling around the edge may well be an important factor in the "playing in" of an instrument, an idea confirmed in one of my experimental violas in the 1950s. This explains the importance of instructions given by Sacconi to set the purfling in its groove evenly and easily (not hammered in tightly) with constant wood thickness of 1.5 mm left under the groove, particularly around the upper and lower bouts (Sacconi, 1962).

E. The EDGES OF THE F-HOLES traditionally are left sharp and clean by the expert knife work of the trained luthier. On older violins these edges have often been marred by soundpost adjusting and other inside operations with the result that the sharp edges are smoothed off and touched up. These rounded edges reduce considerably the impedance or drag to the airflow in and out of the f-holes created by the sharp edges. Arthur H. Benade has indicated that the wear from years of playing actually rounds off the edges of the finger holes on some wind instruments, such as the recorder, giving a more "friendly" speaking quality (Benade, 1968). Many tests on old violins show larger amplitudes for the Helmholtz, or "main air" resonance than we find on new violins with sharp edges to their f-holes. Rounding off the edges of the f-holes somewhat seem to help this, though we do not have definitive tests as yet.

III.

PLATE TUNING is the most helpful finding so far in aiding the violin maker to construct consistently fine sounding instruments with smooth, easy playing qualities. This method has been explained in detail in SCIENTIFIC AMERICAN and the Catgut Acoustical Society NEWSLETTER (Hutchins, 1981, 1983). Some excerpts from the latter are included here.

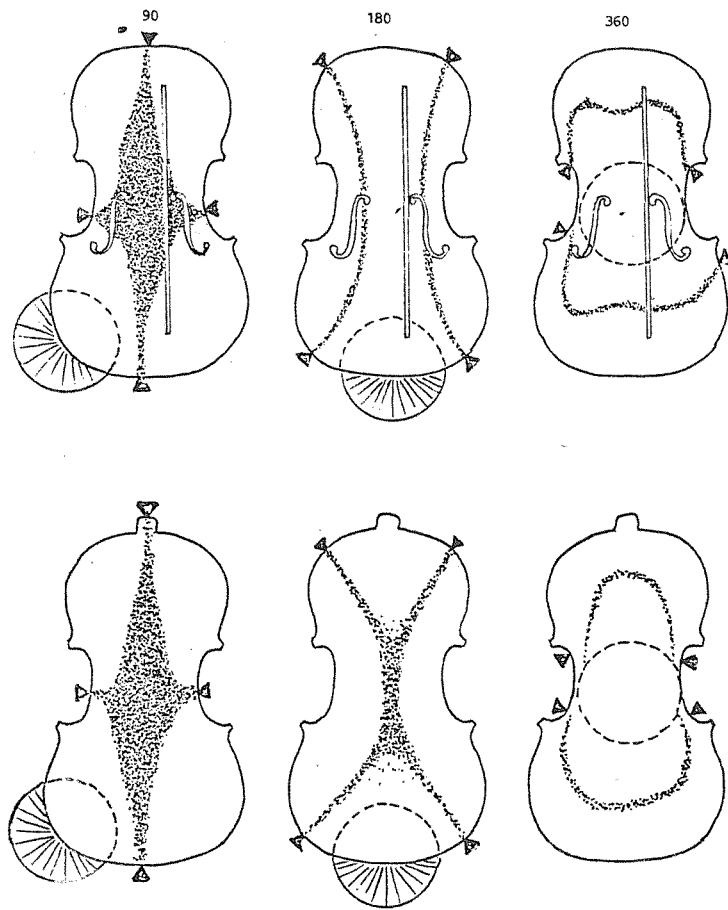


Fig. 4. Chladni patterns in a pair of tree top and back violin shaped plates showing the proper placement of soft foam pads (black triangles) for mounting modes #1, #2 and #5 as near as possible to the dark nodal lines where the black particles are piled up. The active areas are white. The large circles show the position of the plate over the speaker cone centered at an antinode for each mode.

lower bout edges will activate the sound of mode #1 quite clearly, because the holding point is a node and the curves of the upper and lower edges are antinodes for that mode. Holding at one of the four points where the nodal lines of mode #2 intersect the edges and tapping on the antinodal area near the midline at either end of the plate activates

primarily mode #2. Holding at a point along the nearly oval nodal line of mode #5 and tapping in the center of the plate causes the sound of mode #5 to predominate. The best holding place for modes #2 and #5 is, of course, where their nodal lines cross, near one end and just off the midline. In this situation, tapping in the center will produce primarily mode #5 and tapping at the mid-line of the opposite end activates primarily mode #2.

All the modes, however, contribute in greater or lesser degree to the sound heard when the plate is tapped. In a well-tuned plate, particularly if the modes are an octave apart, the sounds will be relatively clear and easy to distinguish. But if the plate is not well-tuned, it is often difficult to differentiate and analyze by ear the pitches of the sounds produced by tapping. This indeterminateness explains in part why violin makers are often very subjective in interpreting tap tones, and highlights the importance of this "Chladni pattern method." By its use many of the luthier's problems with thickness and stiffness can be visualized objectively, and are thus on the way to being solved.

From 20 years of experimentation in tuning the free pairs of plates of over 200 violin family instruments of all sizes, four findings stand out:

1. Fine sounding instruments, which project in a large hall and have smooth easy playing qualities, have resulted when mode #5 in both top and back lie at the same frequency in the range of 360 to 370 Hz with mode #2 an octave below in both; also mode #1 in the top plate an octave below #2 giving a harmonic sequence of modes #1, #2 and #5 in the top plate. Because of structure, the back plate's mode #1 cannot be adjusted to lie an octave below #2 without altering the #2 - #5 relationship.
2. Instruments of good quality have resulted when mode #5 has a relatively large amplitude and its frequency in the top plate lies within a tone of the frequency in the back.
3. Smooth easy playing characteristics have resulted when the frequency of mode #2 in the top plate lies within 1.4% of that in the back. (1.4% is about 5 Hz in violin and viola plates.)

4. If mode#5 lies at the same frequency in top and back, then mode#2 should be adjusted to lie at matching frequencies between top and back else a harsh gritty playing quality may result.

Different schools of violin making teach different methods of graduating violin plates which can be adapted to the Chladni pattern method. The graduation patterns shown here were developed from those indicated by Simone A. Sacconi in his book "The Secrets of Stradivari" as we have adapted them for plate tuning.

Thinning the wood in practically any plate area affects all the modes to some extent. Also, no two pieces of wood are exactly alike, and have different stiffness characteristics. This means that any set of instructions on how to reduce the frequency of mode#2 or mode#5 selectively must take into account the relative stiffnesses in a given top or back plate. The feel of the bending stiffnesses of the plate in one's fingers is the best indication of this.

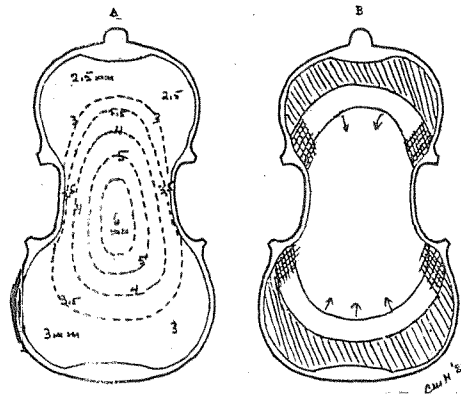


Fig. 5. Suggested starting thicknesses and tuning process of modes#2 and#5 for a violin back plate.

The diagram at the left, Fig. 5A, shows approximate thickness for a violin back before tuning, using well selected curly maple with fairly

high pitched sound. If wood quality is uncertain, it is well to start with thicknesses 1/2 to 1 mm greater than these. The long oval pattern through the center helps to keep the frequency of mode #2 up.

The diagram on the right, Fig. 5B, suggests where to thin the plate to reduce the frequency of mode #5  more than mode #2 around the edge area of the upper and lower bouts. Thinning the cross hatched  area particularly JUST INSIDE THE CORNERS usually reduces the frequency of both modes #2 and #5. To lower the frequency of mode #2 more than #5 in the back plate we usually start by pulling in the thickness contours - thinning the 3 mm line to 2.5 mm; the 3.5 line to 3.0, etc. - gradually working in toward the center. Also, the elongated shape of the central area can be gradually made more circular (arrows), which also helps reduce the frequency of mode #2 more than #5.

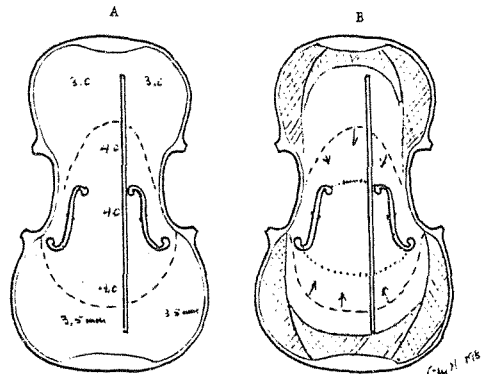


Fig. 6. Suggested starting thicknesses and tuning process of modes #2 and #5 for a violin top plate.

The diagram at the left, Fig. 6A, shows approximate thicknesses for a violin top plate before tuning which is finished on the outside with purfling installed, f-holes cut and bassbar in. Shaving down the height of the bassbar will lower the frequency of mode #5 without appreciably lowering that of mode #2. This happens because the bassbar is in the center of the actively bending antinode of mode #5, but lies approximately along a nodal line of mode #2 where there is almost no bending.

Thinning the wood in the cross hatched areas,  first in the crescent shapes at the sides of the upper and lower bouts, then across the upper and lower ends will reduce the frequencies of both modes#2 and#5.

The elongated center area at 4.0 mm is to help keep the frequency of mode#2 up. This gives the violin maker a chance to lower mode#2 frequency gradually, first by thinning the area inside the dashed lines to 3.5 or 3 mm and then shortening it if desired to the dotted lines between the f-holes in Fig. 6B.

I should like to emphasize that the Chladni pattern method takes years to learn properly and should be adopted by each violin maker to suit his own practices. It is an extremely useful tool that has been used successfully in hundreds of instruments. A maker can not only sense and hear the vibrations in his nearly finished plates, but, with this method, he can actually see and record their mode shapes and the frequencies at which they occur. Through using this method and keeping careful records of his construction parameters (wood qualities, arching, contours, thickness distributions, sealer and varnish), a maker can build up his own body of information to be related to the tone and playing qualities of his finished instruments.

IV.

The effects of coatings

Application of SEALER AND VARNISH will change the physical characteristics of each violin plate, adding mass, stiffening the outermost fibers of the wood, and increasing damping. Since these changes depend on the physical properties of the coatings related to those in the wood, there can be no general rules for compensation ahead of time.

There is, however, one important effect that sealer and varnish usually have on a top plate, namely to increase the crossgrain stiffness of the spruce. Since spruce is about 15 times stiffer along the grain than across it, the effect of the coating is to stiffen the crossgrain direction more than along the grain. Such stiffening tends to raise the fre-

quency of mode #2 as well as to change the contours of mode #5. The modes of the back are affected much less because the wood itself is somewhat stiffer. Therefore, if you are using a sealer-varnish combination that adds stiffness, we suggest for violin plates tuning mode #2 to be 5-8 Hz lower in the top than in the back. Then the stiffening of the coatings will tend to raise the mode #2 frequency in the top so that it nearly matches that of the back in the finished instrument.

In the top plate the stiffening effect of the coatings on mode #5 tends to detune the bassbar. To offset this, we usually leave the bar slightly higher than optimum with the nodal line at the lower right not quite up to the right corner. Then when the sealer and varnish are completely dry (usually about 2 years) the nodal line moves to the corner. See Fig. 7.

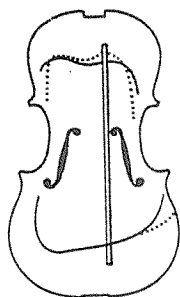


Fig. 7. Effect of varnish seasoning on mode #5. Dry one week (dotted line) - two years (solid line).

To help offset changes caused by coatings, we have established the practice of putting sealer and several coats of varnish on the free plates at least a year before final tuning. When the instrument is assembled and ready for final varnishing, the so-called "tuning varnish" is rubbed back almost to the wood.

V.

Effects-of-moisture

All luthiers are well aware of the drastic effects of humidity changes not only on finished violins, but also on the wood as it is being fash-

ioned into instruments. Robert E. Fryxell reported that both varnished and unvarnished violin plates absorbed water slowly over a period of months when maintained in an environment of 100% relative humidity. Yet after being returned to a dry environment the water loss took place in a matter of few hours (Fryxell, 1965).

This finding has important implications for the violin maker particularly when tuning plates. A sudden change to a lower humidity can set up stresses in the wood as the outside layers lose moisture quickly. These stresses will alter the mode patterns and their frequencies in the free plates making proper tuning practically impossible until the entire thickness of the wood has adapted to the new ambient.

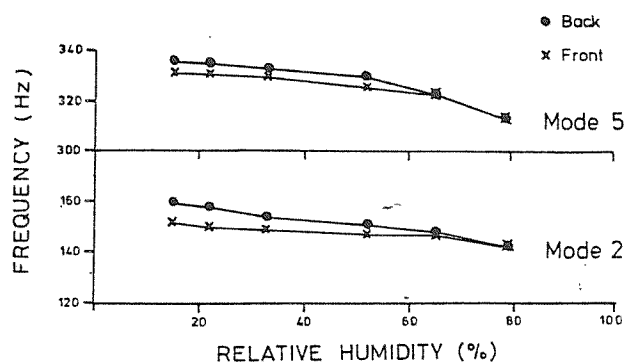


Fig. 8. Effect of humidity on the frequency of response of mezzo violin plates SUS 108.

Rex Thompson also reported this in his study of the effect of variations in relative humidity on the frequency response of free violin plates, indicating that if plates are tested when moisture is not evenly distributed throughout the wood, erroneous reading will be obtained due to distortion, Fig. 8. He found that the difference between the top and back plates (varnished) did not exceed 5 Hz at the same relative humidity in the range between 15% and 79%. However, he found mode #2 quite sensitive to humidity changes and suggested that a safe procedure would be to match mode #2 as closely as possible at a relative humidity of 50% (Thompson, 1979).

Currently a variety of sophisticated testing systems are being applied to the violin such as modal analysis, finite element analysis, acoustical holography, acoustical spectroscopy and electro-optical studies of the violin via string resonances. It will be some time, however, before practical applications to violin making can be gleaned from this research.

References

- Barducci, I. and Pasqualini, G. (1948): "Misure dell'attrito interno e delle costanti elastiche del legno", *Il Nuovo Cimento* 5(5), 416-466. (English translation: Measurement of the internal friction and elastic constants of wood.)
- Benade, A.H. (1968): Personal communication.
- Chladni, E.F.F. (1809): Traite d'Acoustique, Courcier, Paris.
- Fryxell, R.E. (1965): "The hazards of weather on the violin", *Am.String Teacher*, Fall, 26-27.
- Haines, D.W. (1979): "On musical instrument wood", *Catgut Acoust.Soc. Newsletter* 31, 23-32.
- Haines, D.W. (1980): "On musical instrument wood, part II: Surface finishes, plywood, light and water exposure", *Catgut Acoust.Soc. Newsletter* 33, 19-23.
- Hutchins, C.M. (1981): "The acoustics of violin plates", *Scientific American* (Oct.), 170-186.
- Hutchins, C.M. (1983): "Plate tuning for the violin maker", *Catgut Acoust.Soc. Newsletter* 39, 25-32.
- Hutchins, M.A., (1981): "Acoustical parameters for violin and viola back wood", *J.Acoust.Soc.Am. Suppl.* 1 69, S89; *Catgut Acoust.Soc. Newsletter* 36, 29-31.
- Krüger, E. and Rohloff, E. (1938): "Über die innere Reibung von Holz", *Z. Phys.* 110 (1-10), 58-68.
- Rohloff, E. (1940): "Über die innere Reibung und die Strahlungsdämpfung von Geigen", *Ann.Phys.* 38 (3), 177-198.

Sacconi, S.F. (1962): Personal communication.

Sacconi, S.F. (1979): The "Secrets of Stradivari", Libreria Del Convegno, Cremona, Italy.

Saunders, F.A. (1937): "The mechanical action of violins," J.Acoust.Soc. Am. 9, 81-98.

Thompson, R. (1979): "The effect of variations in relative humidity on the frequency response of free violin plates", Catgut Acoust Soc. Newsletter 32, 25-27.

THE TONAL QUALITY OF VIOLINS
Jürgen Meyer
Physikalisch-Technische Bundesanstalt
Braunschweig, BRD

Abstract

The tonal quality of violin sounds depends as well on the quality of the instruments as on the player's quality. For a critical examination of the violin, it is necessary to separate the influences of the instrument and the player as far as it is possible because of the feedback between instrument and player. The most important properties of the instrument are the resonance characteristics of body and bridge. Several measuring methods for getting response curves are compared and methods of evaluating these curves are discussed in order to get typical criteria of high qualified violins.

The total radiation for all violins lies in a very narrow range of variations, whereas the frequency range of strongest resonances differs from violin to violin, especially at lower and medium frequencies. In the higher frequency range, the response curves show a structure like a comb-filter, which is important for time-overtone-structure of violin sounds.

The sound quality of a musical instrument depends upon a great number of factors. Some of these are acoustic factors to do with the instruments' vibration properties and sound radiation. Some, however, are non-acoustical factors which can exert a psychological influence on the player. If an instrument does not look beautiful, the player subconsciously believes that it must also have a poor sound. If, however, an instrument looks as if it had been made by a master, the player believes he is playing an instrument of high sound quality: here we probably encounter the not very logical idea that every instrument-maker who is

able to make something beautiful to the eye is also able to make something beautiful to the ear.

The consequence of this idea is that the player allows his judgement of the instrument's sound quality to be influenced by its appearance and that a handsome instrument will inspire him to play better than one which is not so well made. This results in the situation that the better-looking instrument actually sounds better to the listener; he does not realize that this is due only to the player. Indeed, a concert audience seldom judges a player and his instrument objectively: When, for example, in a violin concerto with orchestra, a violin could be heard well against the orchestra, the listener is often induced to say that the violinist's instrument had a strong tone. If, however, the violin could not be heard well enough, the typical judgement will be that the violinist's tone is weak.

When we are dealing with the sound quality of violins, it is evidently important to try to distinguish between the player's influence on his instrument, and the influence of the instrument itself. As regards the purely physical aspects, this is quite possible, for the various parameters of playing technique by which the player can influence the vibrations of the strings are widely known today, and a large number of the resonance properties of the instrument which are responsible for the radiated sound are also known. It is much more difficult to make a distinction between instrument and player in a subjective judgement formed by listening to violin music, for even the room can influence this judgement.

But it is just this listening to first-class artists performing in concerts that forms our conception of what is judged to be a good or beautiful sound. This sound conception has developed over a long period; it has been handed down in continuity from teachers to students, even if in the process it has been subjected to stylistic changes or changes in fashion. However, since great artists have played old Italian violins almost exclusively for generations, the memory of particularly beautiful

concerts is almost always combined with the memory of the sound of old Italian violins. The question of the sound quality of violins therefore leads to the question whether these instruments are really superior to other violins or whether it is only a matter of the psychological effect upon the player, resulting in his playing better. This raises two concrete questions:

(1) Does the vibration behavior of old Italian violins differ from that of other violins?

(2) Is it possible to imagine sound qualities of a violin making it appear superior to an old Italian violin, without its losing the typical sound of a violin?

To find an answer to these questions, let us first try to distinguish between the influences of the player on his instrument, and those of the instrument itself. Let us take the case where the strings are excited to vibration by the bow, and let us disregard pizzicato and similar techniques.

As regards the playing technique of the right hand, there are three parameters which the player can vary within certain limits. These parameters are the velocity of the bow, the force with which the bow is applied to the string, and the bow position, i.e. the distance of the bow from the bridge (Cremer, 1971; 1981; Meyer, 1978; Schelleng, 1973). Naturally, the left hand is first and foremost primarily responsible for correct intonation, but its influence upon the tone quality should not be underestimated. Thus the pressure of the finger against the string is important, and the time structure of a tone is influenced by the vibrato. Finally, in some cases, the player also has the choice of string on which to play a certain note.

As is generally known, the string - when excited by the bow to vibrate - always takes the form of a triangle whose vertex runs along the string, the amplitude being directly proportional to the speed of the bow. It therefore forms an important basis of the dynamics of play. On the

assumption that the bow speed can be varied between 12 and 120 cm/s, a dynamic range of some 20 dB results. It is not, however, always possible to reach these limits of speed. Another choice open to the player is the bow position: the nearer it is to the bridge, the greater the amplitude of the string becomes, the bow speed remaining the same. The ratio between the minimum and maximum distance from the bridge is 1:9, which yields an additional dynamic range of 18 dB (Bradley, 1976).

On the whole, it should thus be possible to reach a dynamic range of 38 dB on the violin. In practice, however, this value can be reached only with individual notes; in particular in the case of rapid sequences of notes, the dynamic range shrinks to some 20 dB, the quality of the instrument playing a relatively small part. Fig. 1 shows the dynamic

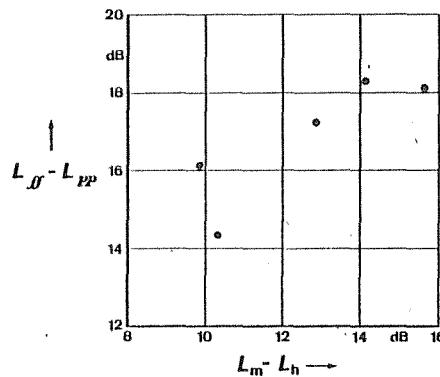


Fig. 1. Dynamic range of 5 violins playing scales $A_3 \dots C_6^\#$.

L_{ff} : maximum sound power level

L_{pp} : minimum sound power level

L_m : averaged level of the response curve between 180 Hz and 1400 Hz

L_h : averaged level of the response curve between 1400 Hz and 4500 Hz

range of five violins playing rapid scales (Meyer and Angster, 1982). On the horizontal axis the difference between the average sound pressure level in the frequency range of 200 Hz to 1400 Hz and the corresponding level between 1400 Hz and 4500 Hz is plotted. These levels have been determined on the basis of response curves measured with the strings excited artificially. As can be seen, the dynamic range becomes somewhat larger when the radiation of the high frequency components is weaker.

The bow force is particularly important for the playing technique of the violinist. In order to produce a continuous variation a minimum bow force value is necessary, as otherwise the damping losses cannot be compensated. The greater the losses, i.e.,

the higher the bow speed,
the nearer the bow position to the bridge,
the thicker the string,
the smaller the pressure of the finger on the string,
and the more energy the instrument takes from the string,
the higher this minimum value must be.

On the other hand, the bow force must not exceed a definite maximum value, because otherwise the frictional force would be too great at the moment when the string detaches from the bow. If this maximum value is exceeded, the sound will show statistical variations and audible noise components. The bow force with which it is possible to produce sound is thus restricted to a field as is shown in Fig. 2 (Meyer, 1978). On the horizontal axis the distance between the bow position and the bridge is plotted, whereas the vertical axis represents the bow force. The diagram is valid for constant bow speed. As can be seen, the playing range narrows towards the bridge and the needed bow force clearly increases.

The influence of the bow force on the sound consists in the fact that with increasing force the peaks of the triangular vibration of the string and, thus, also the peaks of the mode of vibration with respect to time become sharper, whereas they are clearly rounded when the force is reduced. This means that the overtone level of vibration increases with

increasing bow force. In Fig. 2 this tendency is indicated by the shading of the area of play being the lighter, the higher the bow force. In

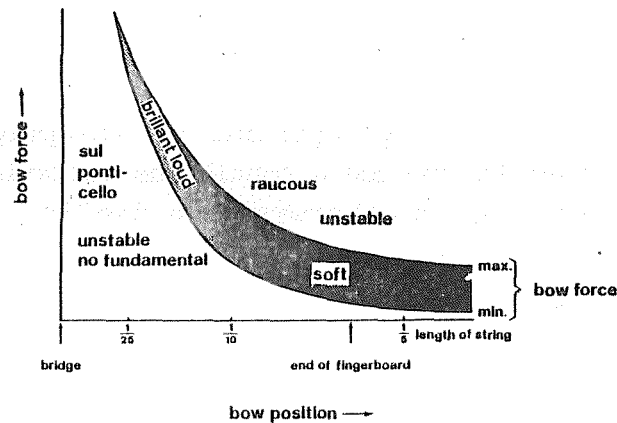


Fig. 2. Connection of bow position, bow force and timbre in case of constant bow velocity.

particular, in connection with the choice of the bow position, the bow force gives the player some opportunity to influence the timbre. This influence is, however, restricted by the fact that the basic mode of the string's vibration must always remain a more or less rounded sawtooth vibration.

Two examples will illustrate this: Fig. 3 shows three sound spectra of a violin for A_3 ; all of them are played with the same bow position. In the upper diagram bow force and bow speed are high; a strong sound with overtones of up to some 6000 Hz is produced. In the middle diagram the bow force is the same, but the speed is lower than in the upper diagram. The envelope of the upper diagram has been taken for comparison. It can be seen that on the whole the amplitudes of the individual partials have become smaller. For the upper partials, however, this weakening is not greater than in the range of the lower partials. In the lower diagram the force is reduced but the bow speed remains the same. The result is a weakening of the upper partials, the amplitude of the lower partials remains unaltered.

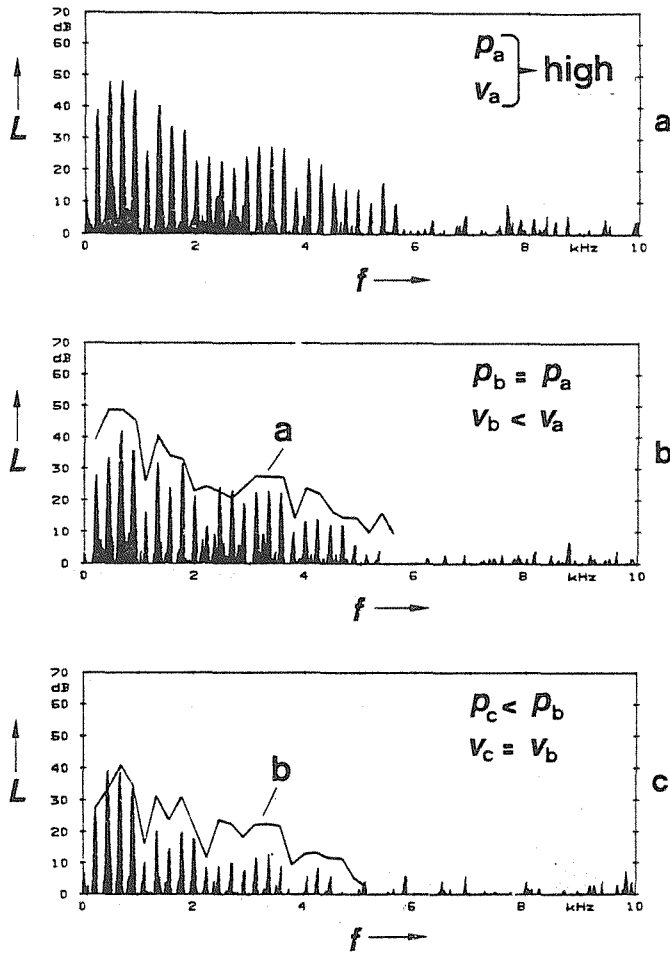


Fig. 3. Spectra of violin sounds, note A_3 , constant bow position, but different bow forces (p) and velocities (v).

Fig. 4 shows three sound spectra of a violin for the note A_4 . In the lower diagram the bow position is as near to the bridge as possible in order to achieve a strong sound rich in overtones. In the diagram in the middle, the bow position is near to the finger board; the speed is more or less maintained and the bow force is adapted to the speed. The consequence is a lowering of the spectrum which is largely independent of the frequency; according to the bow position, at about 1/5 of the string

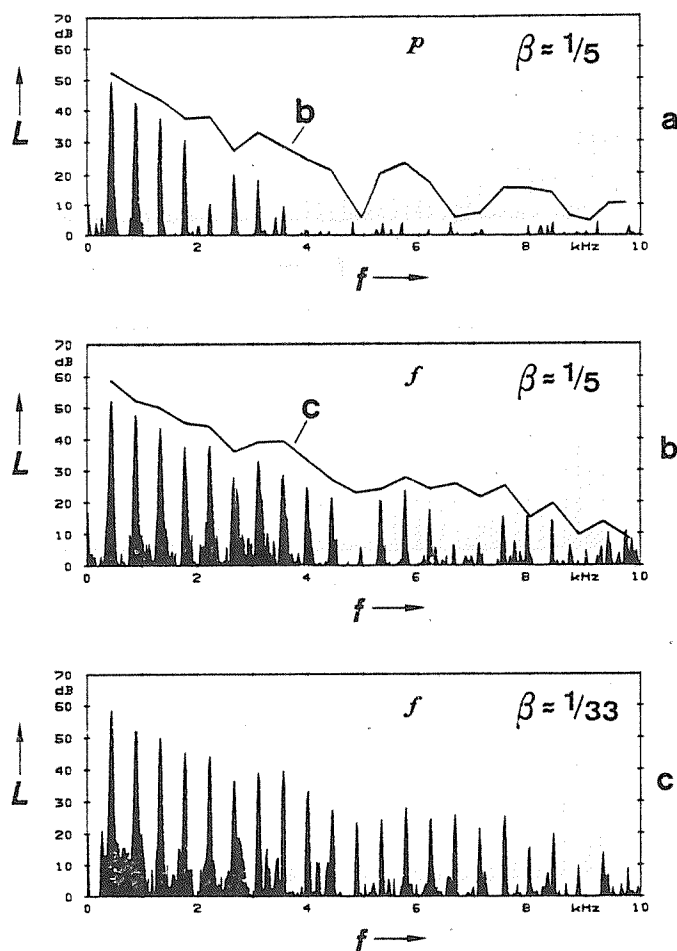


Fig. 4. Spectra of violin sounds, note A_4 , different bow positions (β) and dynamics (p and f).

length, there are, however, gaps at the 6th, 11th, and 16th partial. When a piano is played at low speed with the same point of contact and with corresponding force (upper diagram), a weak sound poor in overtones is produced.

The influence of the string on the timbre is illustrated by Fig. 5 (Meyer and Angster, 1982). It represents the sound power spectra of A_5

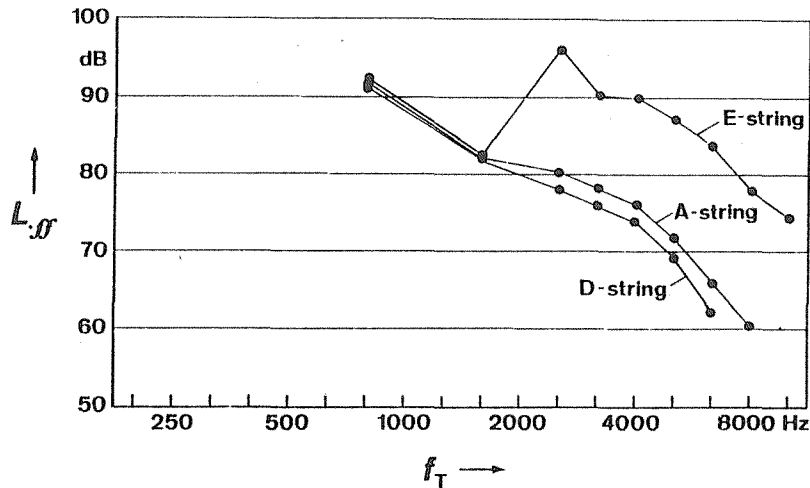


Fig. 5. Sound power spectra of the violin sound A_5 played in ff on different strings.

played once each on the E-string, on the A-string, and on the D-string. The measurements were carried out in a reverberation room so that the sound radiation of the instrument could be recorded in all directions. Because of the third-octave band filters used, the upper overtones are combined in third-octave bands. It is a remarkable feature of the measurement result that the fundamental and the octave partial change by only approx. 1 dB at the transition to the neighbouring string. In the case of the upper partials the D-string and the A-string differ by 3 to 5 dB whereas the E-string is stronger by approx. 15 dB, which gives the tone a completely different sound character. This must not, however, obscure the fact that the choice of string does not usually lie within the player's discretion but results from the musical context and from the requirements of the playing technique.

To what extent the sound power spectra can vary between different

violins is shown in Fig. 6 which represents the spectra for A_3 and A_6 which were each played on 5 violins, the dynamic level being the strong-

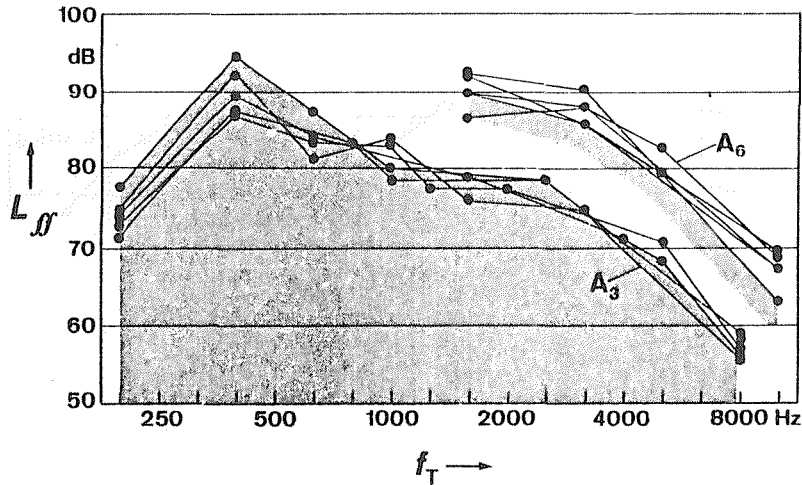


Fig. 6. Sound power spectra of 5 violins played in ff. The shadow area marks the spectrum of an old Italian violin.

est fortissimo possible which could be played. When considering the results for A_3 , it is conspicuous that the differences between the violins are greater for the lower partials up to 1000 Hz than for the upper partials. Here the different resonance properties of the individual instruments become apparent. Furthermore, the ratio between the fundamental tone and the octave partial is almost equal for all violins, whereas the spectra run together in confusion at higher frequencies.

Among the five violins was an old Italian violin; the area below the pertaining spectra has been shaded. As can be seen, the spectrum of A_3 is situated at a very high level; only in the 1000 Hz third as well as above 4000 Hz is it surpassed by other instruments. With the exception of the fundamental, the spectrum for A_6 is situated at the lower edge of the variation range. For the rest, the individual violins differ for A_6 more or less to the same extent as for the lower A_3 . It is conspicuous

that the fundamental which is always the strongest partial in A_6 shows more or less the same intensity as the octave partial in the spectra for A_3 , which here is always the strongest partial.

A rather good general idea of the sound power radiated by a violin is obtained when measuring the spectra for scales which are played rapidly over a greater range. To allow the results of several instruments to be compiled in one figure, an exact representation of the frequency dependence must, however, be dispensed with. In order to be able to make a

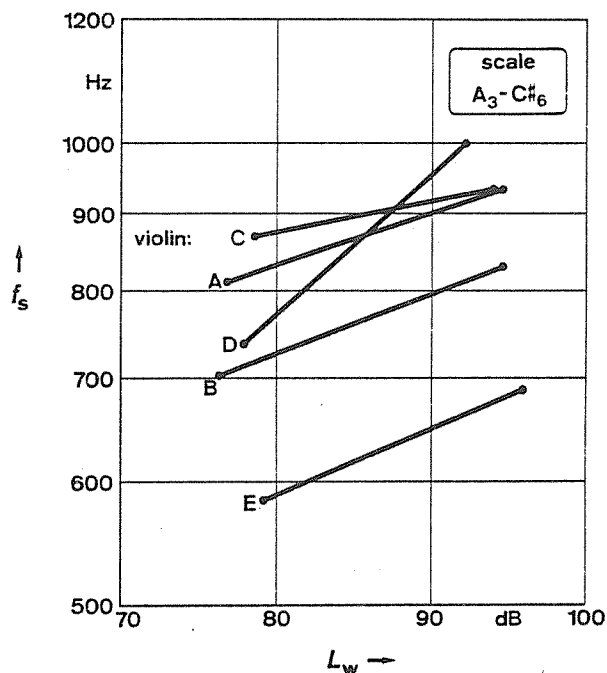


Fig. 7. Dynamic range of 5 violins.

f_s : first order momentum frequency of the third-octave band spectra

L_w : linear sound power level

distinction with respect to the timbre, it is advisable to determine the first order momentum of the energy distribution from the sound power spectra; for each spectrum a first order momentum frequency is then obtained (Angster and Meyer, 1983). Together with the linear sound power level, this frequency is represented in Fig. 7 for five violins. The

ends of the straight line represent the measurement values for pp and ff.

The higher the measuring points for a violin in this diagram, the clearer the timbre of the instrument. The (old Italian) instrument "E" is conspicuous by its particularly deep timbre. For all violins the rise of the first order momentum frequency from pp to ff is apparent. For most of the violins this rise is somewhat more than a whole-tone step. For instrument "C" which shows the highest first order momentum frequency in the pp, the rise is particularly flat. For instrument "D" it comprises more than a fourth; the timbre dependence of the dynamics is thus particularly strong for this instrument.

When evaluating the results of these examples, it can clearly be seen that the player's influence upon the sound spectrum is relatively small; it is restricted in the main to the steepness of the slope of the envelope towards high frequencies. Both the frequency-related energy distribution on the whole and the fine structure of the partial spectrum depend to a large extent upon the resonance properties of the instrument; added to this is the fact that the playable dynamic range, too, is influenced by the resonance properties. If several violinists each play on several instruments, the spectra produced by the various violinists on the same instrument are much more similar than the spectra produced by one violinist on the various instruments.

Nevertheless, there are professional violinists who only require of a violin that it should be loud, as they themselves can "produce" the beauty of the tone. And it is well known that a violin played by a good violinist has a better sound than when played by a bad violinist, even if both of them play "correctly". It obviously follows that the sound spectra and, thus, the frequency-related energy distribution do not alone constitute the quality of a violin's tone. Correct intonation assumed, qualitative differences between various players have a strong effect on the time-dependent fine structure of the sound. This applies both to the intonation and to the subsequent development of the tone. A rapid movement of the finger into the final position immediately creates a defined end for the vibrating string and avoids an additional damping during the

starting transient. In addition, the bow force must be varied in time in the attack, as the string must store energy at the beginning. But the final bow force should be reached as quickly as possible and then maintained as uniform as possible in order to produce a stable tone. The vibrato first produces frequency variations of the string vibrations. The resonance system of the body then adds amplitude variations of the individual partials which - according to the position of the individual partials with respect to the individual resonances - must by no means be equally phased. When a good player varies the frequency and the width of the vibrato, he interferes with the partial spectrum's time-dependent fine structure. This time-dependent fine structure is probably a most essential criterion for the production of a beautifully sounding violin tone. To what extent the time-dependent mode of vibration during a vibrato period - which can be different depending on whether the movement is performed only by the finger, by the hand, or by the arm - also plays a role, has not yet been investigated.

In developing an apparatus for the objective measurement of the quality of a violin, it is scarcely possible to reproduce the great number of components with which the player can influence the sound of the violin. One of the main difficulties is the fact that all these components are controlled - through the player's hearing - in a feedback controlled system. Thus devices for the artificial bowing of violins always sound as if it were a beginner playing. Although such devices allow spectral differences between various violins to be measured, the assignment to a subjective judgement of the sound is almost impossible. It is therefore interesting to see that in the great number of historical works in the field of violin research, such bowing devices have been used mainly for solving problems of string vibration but scarcely for judging the resonance behavior.

In contrast to this, early attempts were made at exciting the instrument at the bridge, the string vibrations being dispensed with. I do not wish to go into a historical survey of this development, as C.M. Hutchins published a detailed paper on the history of violin research only a short time ago (Hutchins, 1983). I prefer to single out two methods with which

investigations on the sound quality of violins are at present being carried out in Germany. One method dates back to the work of W. Lottermoser in the Physikalisch-Technische Bundesanstalt in Braunschweig which was taken up some 25 years ago (Lottermoser and Meyer, 1968; Meyer, 1982). The other method was developed in the last few years by H. Dünwald at the Institute for Technical Acoustics of the Rheinisch-Westfälische Technische Hochschule in Aachen (Dünwald, 1982; 1983). In both cases the basic principle consists in the recording of the resonance behavior of body and bridge with unchanging excitation, and in the interpretation of the differences between the curves obtained - in particular in comparison with the results obtained with old Italian violins.

In Braunschweig the excitation of violins is still produced with an electro-dynamic system made by Messrs. Ling Dynamic Systems Ltd. This system has a small vibrating needle which is laterally pressed into the bridge near the upper left corner. Thus the direction of vibration of the needle corresponds to the direction with which the force of the vibrating string acts upon the bridge. The electro-dynamic system is driven by a sliding sinusoidal current at constant voltage.

This measuring set-up is installed in an anechoic chamber. In contrast to earlier investigations, six microphones are arranged around the instrument to compensate the influence of the directivity on sound radiation. They are always placed at a distance of 1 m from the belly of the violin. Each microphone is connected to its own amplifier; the rectified voltage output of these amplifiers is coupled in a mean-value forming network so that the phase relationship of the sound waves at the individual microphones has no influence on the resonance curve.

As an example, Fig. 8 shows the resonance curves of three violins recorded with the method described. At first sight, there is a very strong resemblance between the three curves. This is not surprising, for in principle, the listener will recognize each of these instruments as a typical violin even if he perceives differences in the tonal quality. Upon closer consideration, however, it is noticeable that the curves differ clearly both with respect to the frequency position and strength

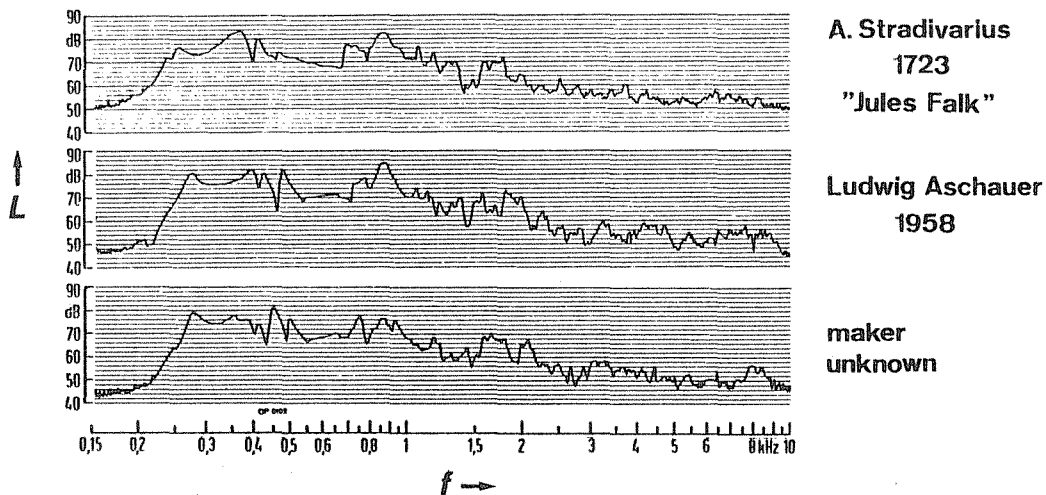


Fig. 8. Response curves of 3 violins.

of the individual resonances in the lower frequency range and with respect to the distribution of the resonance groups at higher frequencies. In this connection the relatively even course of the curves, due to the use of the six microphones, should be noted. Curves which are plotted with only one microphone show a great number of deep crevasses above about 1000 Hz.

Particular importance is attached to the frequency position of the two lowest resonances, the first being due to the cavity and the second to plate vibrations. In Fig. 2 it can be seen that in the case of the Stradivari violin, the cavity is tuned particularly deep and that the following resonance forms the highest point of the whole curve, this resonance, too, being tuned very low. To show that these are properties typical of old Italian violins, Fig. 9 shows the tuning of the lowest resonances of some 100 violins. As can be seen, the measuring points for the old Italian violins are situated almost without exception in the lower quarter of the range of scattering where they are, however, distributed over the whole width. The violins made by Stradivari and Guarneri del Gesu are concentrated at the lower corner on the left-hand

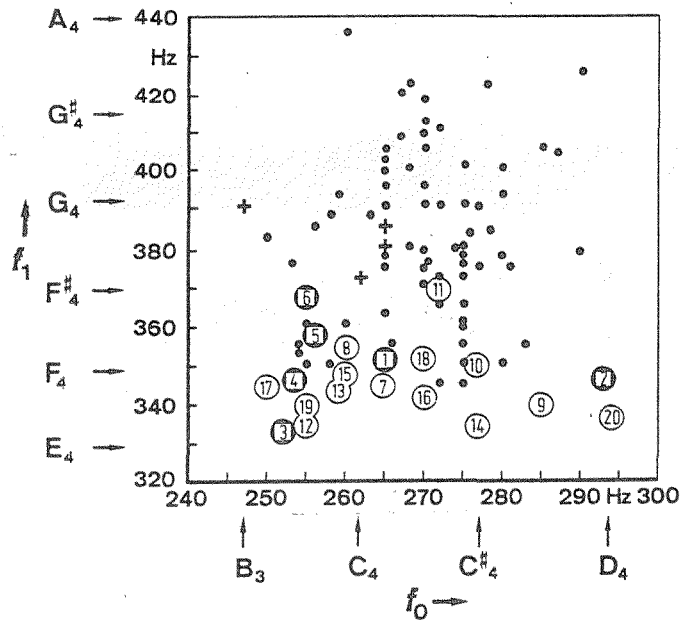


Fig. 9. Tuning of the two lowest resonances of different violins.
 numbers: old Italian violins
 no. 1...6: Stradivarius violins

side. It can thus be concluded that a particularly low tuning of the plate resonance is characteristic of old Italian instruments. In the case of both of the particularly famous violin makers mentioned, there is also an especially low tuning of the cavity resonance.

The frequency-related energy distribution within the resonance curve can be clearly represented by subdividing the analyzed frequency range into third-octave bands and by determining a mean level value for each of these bands. Fig. 10 contains the results for the two third-octave bands with the central frequencies 315 Hz and 400 Hz. Each violin is again represented by a measuring point. If the measuring point is situated below the diagonal, this means that the mean level in the 315 Hz third-octave band is higher than the level in the 400 Hz third-octave band.

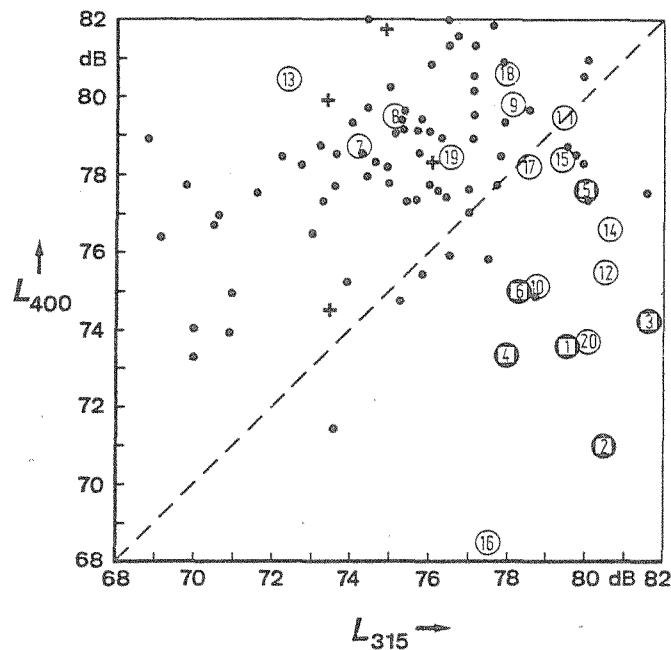


Fig. 10. Averaged level of the response curves of different violins.

L_{315} : level of the 315 Hz third-octave band

L_{400} : level of the 400 Hz third-octave band

This is the case with most of the old Italian violins, whereas it is relatively rare with other violins; in particular, at a greater distance from the diagonal, only old Italian violins are found. However, it should be pointed out that the measuring points for the Guarneri del Gesu violins and for the 19th century French violins are situated above the diagonal; for these instruments the intensity in the 400 Hz third-octave band is obviously higher than that in the 315 Hz third-octave band.

As is generally known, there are far fewer genuine Stradivari violins in existence today than there are fakes, that is, violins which bear a label with the name Stradivari but which were made in his time or later by other violin-makers. The exteriors of some of these instruments al-

ready show such a poor workmanship that it can easily be seen that the instrument cannot be an original Stradivari violin. In other cases it is much more difficult to distinguish a fake from the original. Fig. 11 shows the mean level values for the 315 Hz third-octave band and the 400 Hz third-octave band for six genuine Stradivari violins and for 14 fakes. This diagram clearly shows the difference with respect to the vibration behavior in the frequency range mentioned.

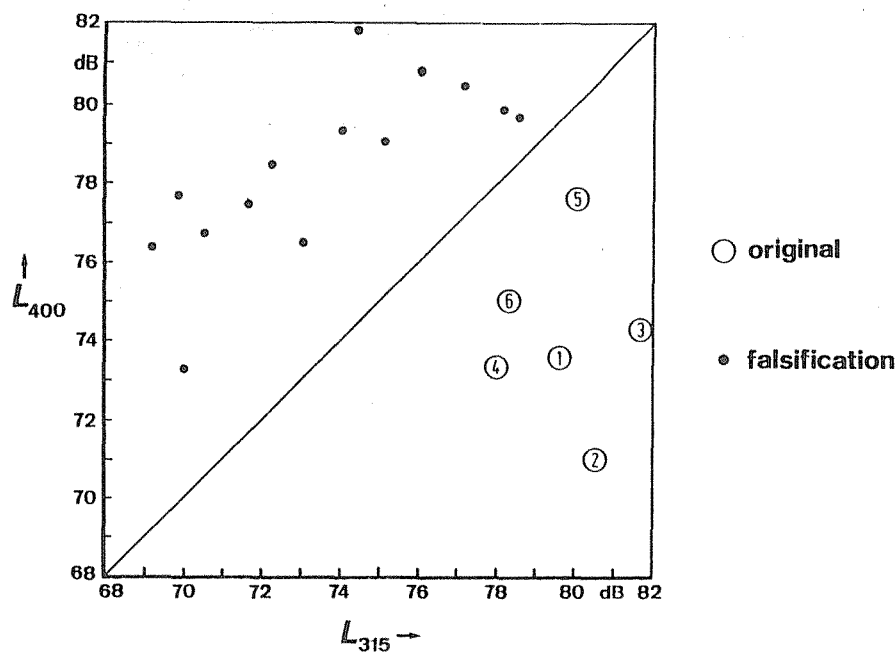


Fig. 11. Averaged level of the response curves of original Stradivarius violins and of falsifications.

As can be seen in Fig. 8, the first group of plate resonances is followed by a gap which in its turn is followed by another group of strong resonances. By the latter a second maximum is produced in the series of the mean level values for the third-octave band but in the case of some violins it already appears in the 630 Hz third-octave band. This

frequency distribution is shown in Fig. 12 together with the position of the first maximum: In the left-hand half there are the instruments with the first maximum in the 315 Hz third-octave band and in the right-hand half, those with the maximum in the 400 Hz third-octave band. The lower half of the diagram contains the instruments with the second maximum in the 630 Hz third-octave band and the upper half those with the maximum in the 800 Hz third-octave band.

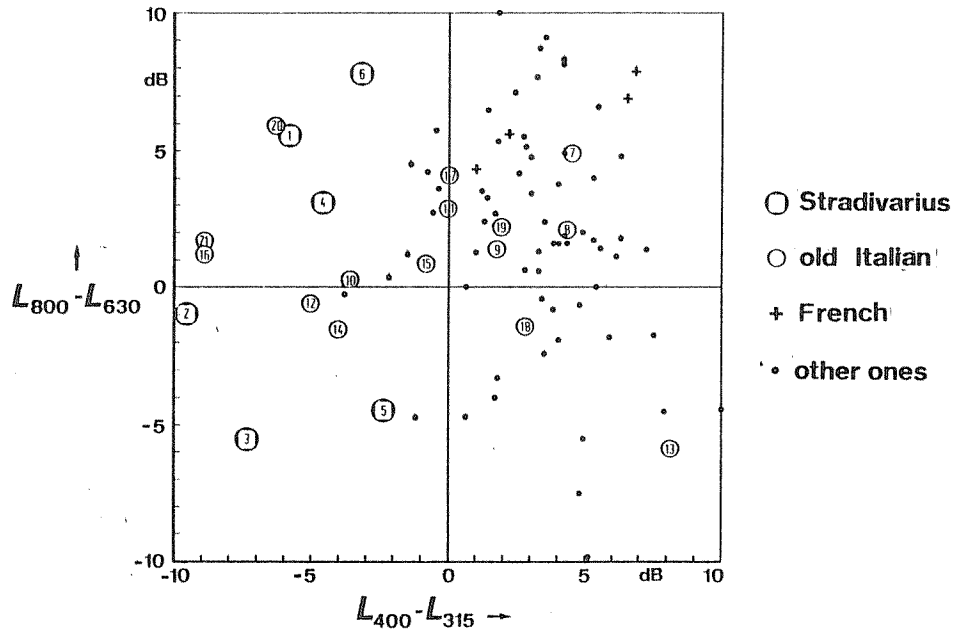


Fig. 12. Frequency distribution of the third-octave bands containing maximum levels.

It can be seen that the old Italian violins have a second maximum both in the 630 Hz and in the 800 Hz third-octave band. If it appears in the 630 Hz third-octave band, it will almost always be connected with a first maximum at 315 Hz. The 400 Hz/630 Hz combination is mainly shown by violins whose sound is not so good. Like most of the other violins, the older French violins show the 400 Hz/800 Hz combination.

The level of this second maximum is also important. It is of particular interest when relating it to the level in the 315 Hz third-octave band, which has already proved to be essential for the characterization

of the old Italian violins. In Fig. 13 these two numerical values are plotted for all violins under test. While almost all of the old Italian violins are to be found below the diagonal, one half of the other instruments is above and the other half below the diagonal. The difference between the Stradivari violins and most of the other old Italian violins

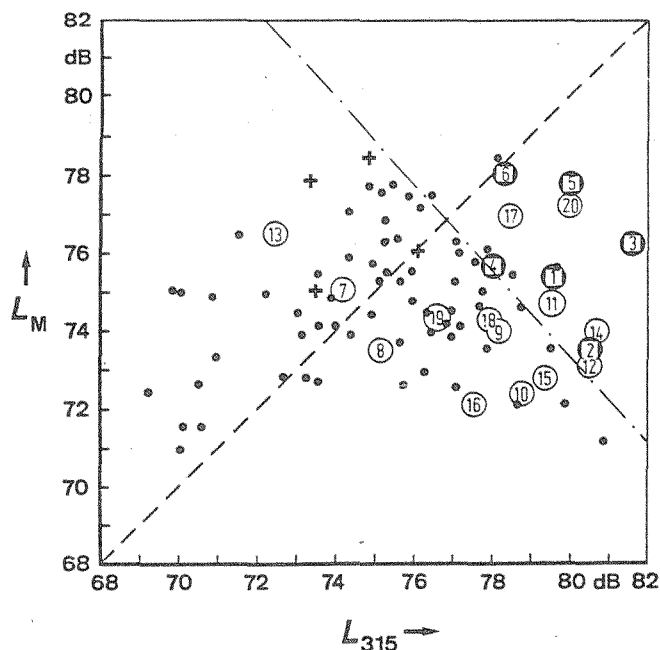


Fig. 13. Averaged level of the response curves of different violins.
 L_M : level of the second maximum third-octave band

lies not only in the fact that the Stradivari violins are situated relatively far on the right-hand side but also in the rather high level of their measuring points. This means that the old Italian violins not only have a strong resonance effect in the low frequency range but also show a particularly strong second maximum.

Towards the high frequencies, the Italian violins no longer differ clearly from the other instruments. It is true that many Italian instruments have a higher level in the 1600 Hz than in the 1250 Hz third-octave band, but a similar energy distribution is also shown by many other instruments. It is remarkable, however, that the level of the Guarneri

del Gesu violins as well as of the instruments Stradivari made in his later years is higher both in the 1000 Hz range and in the 4000 Hz range than almost all other old Italian violins, which constitutes the particular brilliance of these instruments.

Dünnwald's excitation system is based on the objective that the force transmitted by the system to the bridge should be independent of the frequency and that it should not represent an additional mass load for the instrument. This is achieved by the use of a copper wire only 0.3 mm thick as the vibrating element. This wire runs through two air gaps of a strong permanent magnet which are arranged at a distance of some millimeters from each other, the magnet's field of force being perpendicular to the wire. Through this wire passes a sinusoidal current producing a force which acts perpendicular to the wire and perpendicular to the magnetic field. With the free-lying part between the air gaps of the magnet, the wire is in contact with the string edge of the bridge near the upper corner. To avoid intrinsic resonances, the wire passes not only through the excitation system proper but also through two small tubes filled with a highly viscous grease.

The measurement is carried out in an anechoic chamber with a reflecting floor. Both the violin with the excitation system and the microphone are arranged close to the floor. The microphone is installed at an angle of 45° to the belly (bass-bar side) at a distance of 3 m. The frequency curves of the violins are recorded with a dynamic range of 25 dB.

Fig. 14 shows some typical measurement results obtained with this method. In each section, the curves of ten instruments with similar acoustic properties are plotted one above the other. As can clearly be seen in particular in the upper section, the curves consist of three individual resonances at low frequencies and a close sequence of resonances at high frequencies. The lowest of the individual resonances is the Helmholtz resonance; the two following peaks which are particularly pronounced are due to vibrations of the violin body. While the frequency of the Helmholtz resonance of the individual instruments varies only slightly, the body resonances show somewhat more pronounced differences.

The essential differences between the three groups of violins represented are, however, to be found in the frequency range above 700 Hz. The older Italian violins show an increase in level up to a maximum of some 2500 Hz, followed by a more or less symmetrical drop of the curve.

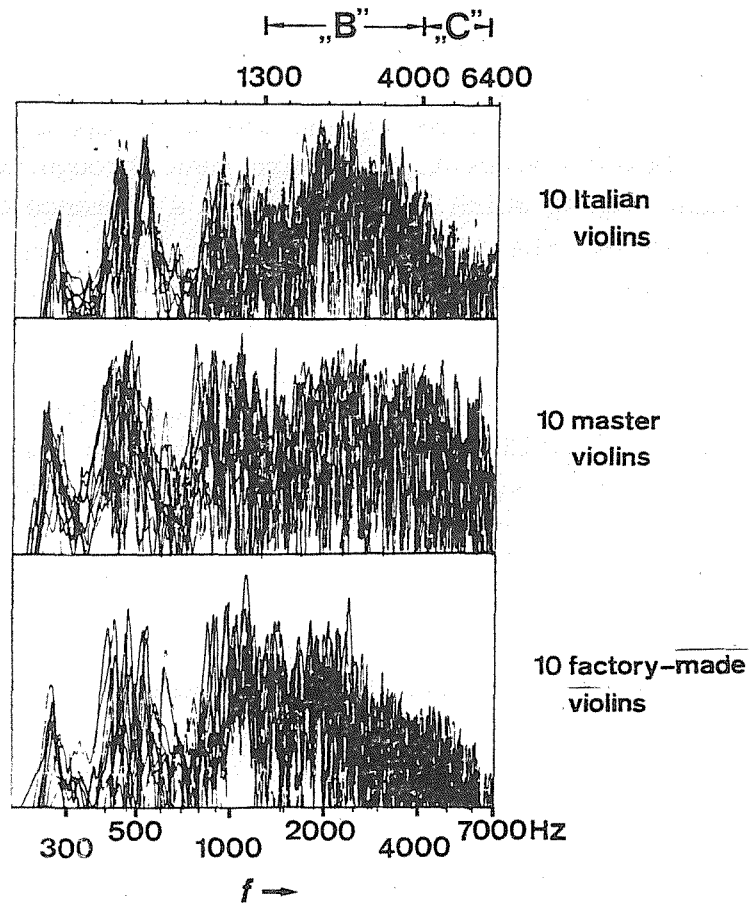


Fig. 14. Response curves of different violins (Dünnwald).

In contrast to this, in the case of the new master violins, the frequency range from 700 Hz to more than 5000 Hz is filled rather uniformly with resonances, whereas the factory-made violins already show a maximum at 1200 Hz and decrease strongly towards the high frequencies.

In the meantime about 350 violins have been tested according to the method described. A representation of the results in a diagram presup-

poses that some numerical value criteria are derived from the curve to describe the quality. Two such criteria are shown in Fig. 15 for all violins: On the horizontal axis the scattering of the level differences is shown, which appear in the sound spectra (calculated tone by tone) between components in the range between 650 Hz and 1300 Hz and components

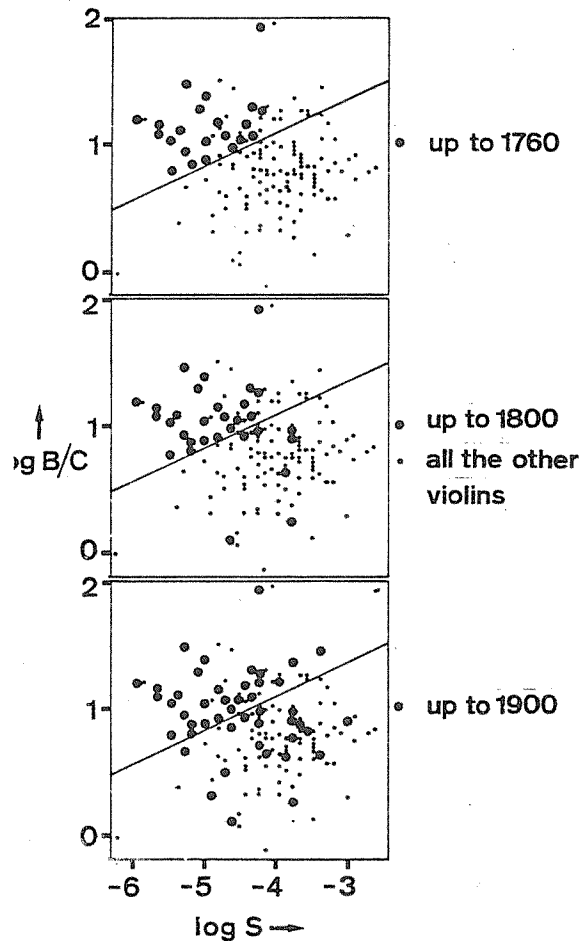


Fig. 15. Intensity ratio of the frequency ranges B and C (see Fig. 14) and the scattering of the levels in lower frequency ranges (see text) (Dünwald).

in the range between 1300 Hz and 2600 Hz. A slight scattering means that the individual resonances in the frequency ranges stated lie harmonically to one another. To the ear, the effect of the relatively strong partials

in the range from 650 Hz to 1300 Hz is reduced by correspondingly strong components between 1300 and 2600 Hz, for - as can be seen in the upper section of Fig. 14 - too strong sound components between 650 Hz and 1300 Hz seem to be disadvantageous for the sound impression.

On the vertical axis in Fig. 15 the intensity ratio between the components from 1300 Hz to 4000 Hz and the components from 4000 Hz to 6400 Hz is plotted. This intensity ratio seems to be closely connected with the clarity of sound. To show the distribution of the measurement results for various groups of violins, Fig. 15 is subdivided into three sections. Each of them contains the results of all violins, but the results of the violins up to a definite year of manufacture have been emphasized. Thus the upper picture shows an accumulation of the old violins until 1760 in the upper left-hand zone of the range of scattering; this range which is obviously typical of old violins is separated from the rest by a straight line. When considering the violins up to 1800, we see that this line is already clearly exceeded and the instruments made before 1900 cover the whole range of scattering.

An interesting result is obtained when considering the frequency distribution perpendicular to this dividing line (Fig. 16). Three char-

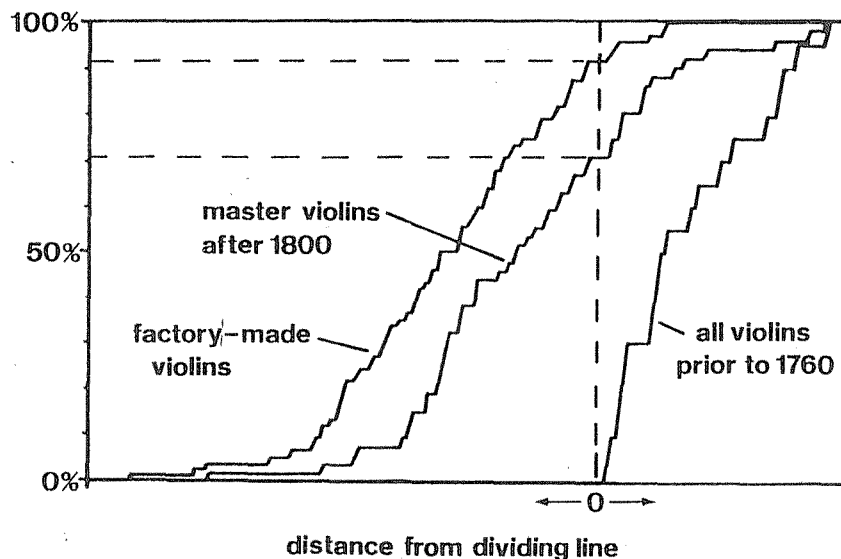


Fig. 16. Cumulative frequency perpendicular to the dividing line in Fig. 15 (Dünnwald).

acteristic curves are obtained for the cumulative frequency of the violins from various periods. The curves for the instruments made after 1800 and for the factory-made violins show a more or less Gaussian distribution, i.e., starting from a medium quality, there is a scattering which decreases towards a higher and a lower quality, corresponding more or less to a random distribution. In the case of the group of violins made before 1760, values for the worst instruments are not available, and the curve therefore no longer represents a Gaussian distribution. The reason for this is not easily ascertainable, though Dinnwald puts forward three possible explanations:

- (1) In the course of the last 200 years, only the good instruments have been preserved and handed down to posterity.
- (2) The old violin-makers sold only the good instruments and destroyed the bad ones.
- (3) The violin-makers were able to improve inferior instruments by subsequently working on them until the desired quality was obtained.

In a comparison of the resonance curves obtained with the two different methods, at first the differences are not visible at a glance. This is due to (Lottermoser and Meyer, 1968; and Meyer, 1982; Dinnwald, 1982; 1983) several reasons: above all, of course, the difference in the kind of excitation but also the differences in the distance and the number of microphones and the scale on which the level is represented are responsible. Fig. 17 shows the two curves for one violin. In both cases, first the cavity resonance is distinguished which is somewhat more pronounced in the lower curve. Two other resonances follow, which in the lower curve are to be found at somewhat higher frequencies than in the upper diagram. Towards the high frequencies a great number of individual resonances follow which in their fine structure are difficult to assign in the two curves; the envelope in the upper picture shows a shift of the maxima towards the lower frequencies.

The influence of the excitation system's mass on the resonance curves

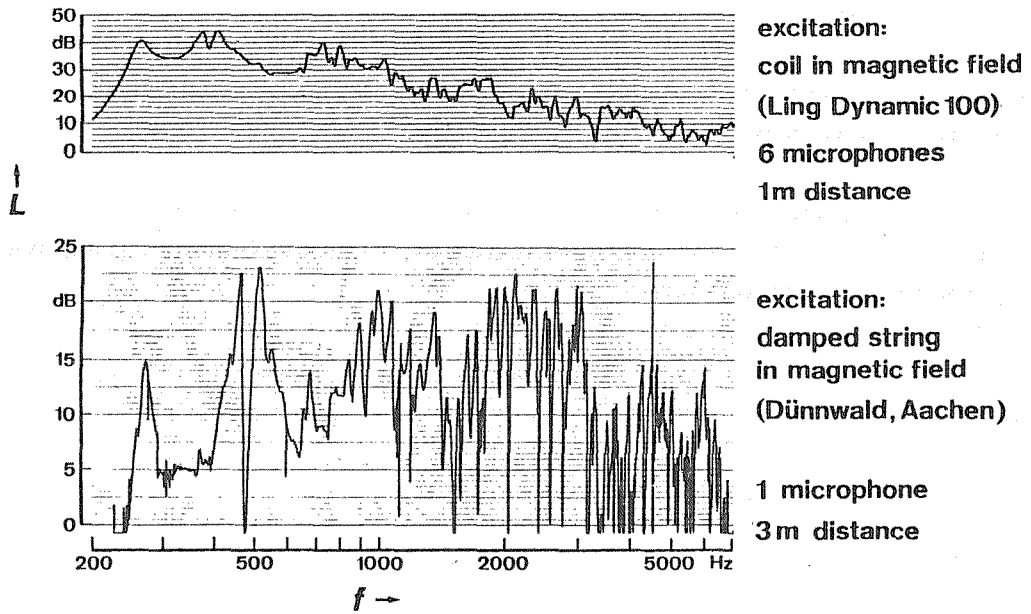
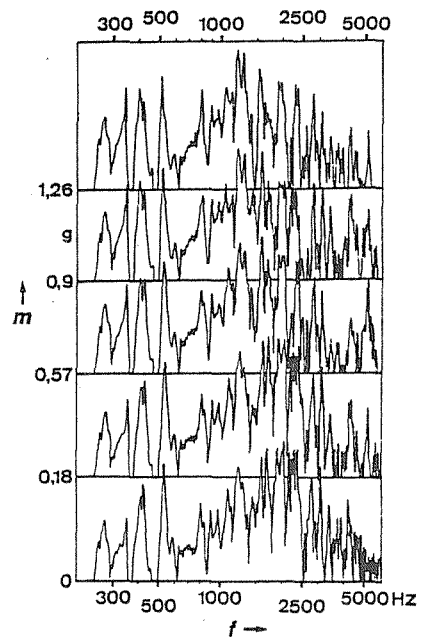


Fig. 17. Response curves of a violin got by different methods.

Fig. 18. Influence of additional masses (acting upon the bridge) on the response curve of a violin (Dünwald).



has been investigated by Dünnwald. Fig. 18 shows the curves of an instrument when different additional masses act upon the bridge. It can easily be seen that the envelope in the lowest curve which represents the normal condition has its maximum at about 2000 Hz. With increasing mass this maximum is shifted towards the lower frequencies, the frequency position of the individual resonances remaining almost unchanged.

As has been mentioned at the beginning, the basic principle of both methods is based on the fact that all instruments are always examined according to the same method and that the results are compared with one another. The differences of the curves obtained with the different methods should not therefore be overrated, though a certain degree of caution is necessary when interpreting the optimum energy distribution in the low frequency range.

The far more balanced course of the upper curve at high frequencies is due to the fact that the resonances lying increasingly closer together overlap one another. These resonances result in different directional characteristics at neighboring frequencies; this has the effect of changing above all the direction of the minima in the directivity diagrams. The deep valley in the lower curve should therefore be interpreted to mean that only little energy is radiated in the direction of the microphone at the respective frequency, whereas there is a strong sound radiation in other directions.

The distinct subdivision of the curve plotted with only one microphone has a certain resemblance to a comb filter curve, although there are different widths between the valleys in the individual frequency ranges, which is in contrast to the usual comb filter. In dependence upon the slope steepness, frequency movements of the partials result in amplitude modulations as known from the comb filter, and thus give the sound a particular characteristic. As is generally known, in the case of natural sounds, comb filters result in a certain hardness of timbre which is felt to be unpleasant. In the case of the violin a moderate change of the spectrum produced by the string is quite desirable, as the sound then gains in incisiveness.

When we consider that the energy distribution at lower frequencies can mould the spectra of individual tones but not the overall character of an instrument, it is obvious that essential quality criteria are to be found in the range of very high frequencies and are therefore associated with the comb filter effect mentioned. In this connection the change of the internal damping of the wood with time can play an important part. As is shown in Fig. 19, the internal damping of the belly wood decreases during

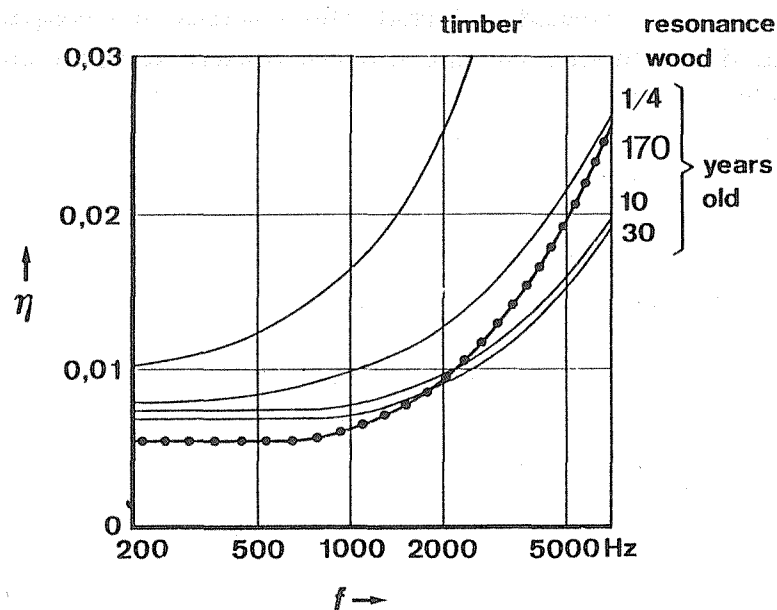


Fig. 19. Internal damping of wood of different age (Ptacnik).

the first few decades in the whole frequency range and increases again above about 2000 Hz after more than a century (Ptacnik, 1953). This increase in damping would effect a flattening of the comb filter flanks, which would result in a reduction of the sharpness of the sound. With this theory it is quite possible to explain the "mellowness" of sound for which old violins are praised.

It is also conceivable that a good player can adapt his playing technique to the comb filter effect in different instruments. If the very high frequencies are modulated too strongly by the vibrato, he can reduce

the breadth of the vibrato a little but he can also reduce the level of the highest sound components by adapting the bow position and the bow force. If the comb filter effect is not too strong in the case of a good instrument, the player need not make allowances for it when selecting the bow position and the bow force; the possibilities open to him of varying the sound are therefore greater, which is felt both by the player and the listeners to be a higher sound quality. In addition, he can play a stronger vibrato and thus obtain a richer sound.

It appears that the resonance behavior of the violins at very high frequencies allows not only important criteria of the instrument quality to be derived, but also explains the differing beauty of sound of the same instrument when played by different players. For this purpose, however, unequivocal measurement results are still lacking. In spite of the progress made in the last few years in various institutes all over the world, interesting work is still to be done to answer the question: "What constitutes the tonal quality of a violin?"

References

Angster, J. and Meyer, J. (1983): "Zur Schalleistungsmessung bei Musikinstrumenten", Tag.-Ber. "Akustik der Musikinstrumente und ihre Konstruktionsaspekte", Kraslice.

Bradley, J.S. (1976): "Effects of bow force and speed on violin response", J.Acoust.Soc.Am. 60, p. 24.

Cremer, L. (1971): "Die Geige aus der Sicht des Physikers", Nachr.Akad. Wiss.Göttingen, II. Math.-Phys. Klasse, Nr. 12.

Cremer, L. (1981): Die Physik der Geige, S. Hirzel Verlag, Stuttgart.

Dünnwald, H. (1982): "Zur Messung von Geigenfrequenzgängen", Acustica 51, p. 281.

Dünnwald, H. (1983): "Auswertung von Geigenfrequenzgängen", p. 373 in Proc. 11 ICA Paris, Vol. 4.

Hutchins, C.M. (1983): "A history of violin research", J.Acoust.Soc.Am. 73, p. 1421.

Lottermoser, W. and Meyer, J. (1968): "Über den Klang der Stradivari-Geige 'Prince Khevenhuller'", Instr.-Bau Z. 22, p. 140.

Meyer, J. (1978): Physikalische Aspekte des Geigenspiels, Verlag der Instrumentenbau-Zeitschrift, Siegburg.

Meyer, J. (1982): "Zum Klangphänomen der altitalienischen Geigen", Acustica 51, p. 1.

Meyer, J. and Angster, J. (1982): "Zur Schalleistungsmessung bei Violinen", Acustica 49, p. 192.

Ptacnik, E. (1953): "Experimentelle Prüfung der inneren Reibung von Holz", Acta Phys.Austr. 8, p. 28.

Schelleng, J.C. (1973): "The bowed string and the player", J.Acoust.Soc. Am. 53, p. 26.

VIOLIN RADIATIVITY: CONCEPTS AND MEASUREMENTS

Gabriel Weinreich

University of Michigan, Ann Arbor, MI, USA

and

IRCAM, 31, rue Saint Merri, Paris, France

Abstract

If we define the "violin corpus" as that physical system which interposes between the vibrating string and the ultimately produced acoustic radiation field, and if we assume that its action is to a great degree linear, then the performance of the system should be completely specified by two quantities: the admittance presented to the string at its termination, and the "radiativity", that is, the sound field produced per unit force exerted by the string on the bridge. Each quantity is, of course, a complex function of frequency, and involves two degrees of freedom corresponding to the possible polarizations of the string. In addition, the radiativity must, in principle, couple to an infinite number of degrees of freedom corresponding to some convenient parametrization of the radiation field.

By concentration our attention on the radiativity we do not imply that the bridge admittance is unimportant. Since it determines the response of the string to the bow it must have a major effect on the "feel" of the instrument as perceived by the player. Nonetheless, even here the radiativity must play a role since the feedback to the player is, to some degree at least, acoustic.

At low frequencies, where the wavelength of the sound is comparable to, or greater than, the size of the violin, the radiativity is conveniently defined in terms of the radiative multipole moments. For the monopole radiativity, for example, we imagine a small pulsating sphere as the source of the sound, and specify the equivalent radial air flux corresponding to unit force applied to the bridge. At higher frequencies, where the different parts of the corpus become radiatively independent of each other, an absolute definition that does not depend on incidental idiosyncracies of the experiment setup involves some serious problems.

This paper will discuss some aspects of radiativity from a theoretical point of view, as well as present data on measured absolute radiativities of a number of violins of varied quality.

Introduction

Although there has been a great deal of investigation of the amount of sound produced by violins under various controlled circumstances, the procedures have not generally been specified in terms that allow an absolute evaluation of the measured quantity independently of the experimental setup. Useful as such an approach may sometimes be, it remains an engineer's "test" rather than a scientist's "measurement". For this reason we prefer to introduce a new word -- "radiativity" -- to characterize a precisely defined ratio of the outgoing acoustic field produced by a violin at a given frequency to the force applied to the bridge by the vibrating string. It must be stated immediately that this simple-sounding definition in fact hides some concepts of great complexity. First, the sound produced depends on the direction of the force exerted on the bridge, so that at each frequency two components of the radiativity must be specified -- for example, with the force applied parallel to the violin top and perpendicular to it. Secondly, an acoustic field, even when limited to outgoing waves, needs an infinite number of parameters for its quantitative specification, so that an understanding of radiativity depends on an appropriate parametrization of the field.

This paper describes the acoustic field in terms of a multipole expansion of the radiated wave. Although this expansion can be shown to converge under all circumstances, its terms do not begin to decrease strongly until a multipole order which is approximately equal to the number of wavelengths that fit into the circumference of the source. Thus, if this number is large, the expansion may not be particularly useful even though its convergence is, in principle, assured. If, on the other hand, the source is not large compared to a wavelength -- and in the case of a violin this claim might be made up to, perhaps, 1 kHz -- an expansion in multipole fields is decidedly fruitful, because not many terms are required. We thus arrive at a classification of the radiativity components in terms of multipoles: the "monopole radiativity", for example, measures the radiative monopole moment developed per unit force applied to the bridge at the frequency in question (the two components of force must, of course, still be specified separately).

Principle of reciprocity

To measure the radiativity in practice, it is convenient to have recourse to a very general principle, called "the principle of reciprocity", which applies to all linear mechanical systems. In its simplest form, it states that if one particle of a system, say particle A, is displaced from equilibrium by a certain amount, with no other particle being allowed to move, and the force on particle B is measured, the result will be the same as if the measurement were repeated with the roles of A and B interchanged. In this form, we have nothing other than Newton's Third Law. It may, however, be shown that, if linearity of the system is assumed, the principle maintains its form under very general transformations to other types of coordinates and forces. In the present case, the reciprocity principle leads to the following conclusion: if one wishes to know the radiativity component for a certain force direction and a certain multipole order, one can equivalently measure the displacement of the bridge in that same direction when the violin is immersed in an incoming field of unit amplitude having that same multipole character. The derivation of this theorem, which must take into account the effect of reaction forces exerted on the violin by the radiation field, will be given in a later publication.

Intuitively speaking, an acoustic monopole moment is most easily conceived by imaging a small body whose volume is fluctuating, and taking the amplitude of volume fluctuation as the magnitude of the moment. Higher moments then correspond to the fluctuation amplitude of the higher moments of the volume: for example, the dipole moment is equal to the volume of the source times the amplitude of displacement of its geometrical center of gravity. We shall use this picture in our qualitative discussion. Quantitatively, however, the monopole moment is conventionally defined not as a volume but as a rate of change of volume, that is, a volume flow, obtained from the volume amplitude by multiplying it by 2π times the frequency. This is the quantity that will be plotted in our data graphs.

Method of measurement

In our experimental arrangement, the violin rests horizontally on three small foam rubber supports in a semi-anechoic chamber. A stereo phonograph cartridge is mounted so that the tip of its stylus touches the bridge between the A and D strings. The incoming field is generated by a number of loudspeakers whose individual radiation fields have been previously ascertained, so that we know with what amplitudes and phases they have to be superposed at each frequency to produce the desired angular characteristics. This superposition is not in fact performed acoustically; rather, the response of the violin is measured with each speaker separately, and the superposition is done by the computer.

Because of the linearity of the system -- which, for our circumstances, has been verified with considerable precision -- we can measure the radiativity simultaneously at a large number of frequencies by using a stimulus in which the corresponding frequencies are contained. For example, a pulse train at a 1 Hz repetition rate contains all frequencies which are multiples of 1 Hz, limited at the upper end by the width of the pulses. This is, however, the worst possible signal to use in practice because its instantaneous power is concentrated in a very small part of the cycle. To avoid overloading the apparatus during the pulse, its amplitude would have to be kept very low, resulting in an abominable overall signal-to-noise ratio. A random "white-noise" signal is much better in this respect, but still not optimum; as always, one does better by careful signal design than by a throw of dice.

We use a specially constructed signal which contains equal amplitudes of all integer frequencies from 190 Hz to 3000 Hz, with phases selected so as to minimize power fluctuations in the course of its one-second cycle. It is generated by an LSI-11/23 computer which repetitively reads a table of 8192 values, at a sampling interval of 122 microseconds, into a D/A converter and synchronously samples and digitizes the returning signal from the phonograph cartridge. After the one-second cycle has been traversed for each permutation of loudspeaker and cartridge channel, the results are Fourier-analyzed and normalized to previously measured sound amplitudes at each of the 2811 frequencies.

Low-frequency model

Before looking at experimental data, we give a short discussion of the expected behavior of a violin, especially at relatively low frequencies. For this purpose we imagine first that the violin is a closed shell without any f-holes, and that its volume can be made to change by a force applied to the bridge. We may think of this volume change, when divided by the applied force amplitude, as the monopole radiativity. Now at low frequencies the volume change will be static, that is, determined entirely by the elastic properties of the shell, so that the radiativity will be independent of frequency. As the frequency is raised, the shell's inertial properties enter, so that the amplitude of motion increases, leading ultimately to a resonance which we can roughly identify with the "main body resonance" of violin lore. Above this frequency, the volume change will have the opposite phase relative to the applied force, so that the radiativity will change its sign. This behavior is shown schematically in Fig. 1. (We neglect dissipation in this discussion, since it has no effect on the general argument.)

If we now add f-holes to our model, it is easily seen that at very low frequencies, where the air behaves as an incompressible fluid, the change in volume of the shell will be exactly compensated by the volume of air which emerges from the f-holes, just as the overall volume of a tube of toothpaste is not affected when the tube is squeezed. Thus the monopole radiativity must vanish at frequencies small compared to the Helmholtz frequency. As the Helmholtz frequency is approached, the inertia of the air begins to exert its influence, so that the volume motion of the air becomes larger than that of the shell (assuming that the Helmholtz frequency is lower than the main body resonance, which is the case in actual violins). In this regime the monopole radiativity thus has the opposite sign from the "static" one characteristic of the shell alone. It vanishes at low frequencies in proportion to the square of the frequency, becomes large at the Helmholtz frequency, then again changes sign and joins to the "static" response of the shell. This behavior is shown in Fig. 2.

It is important to note that, unlike the monopole radiativity, the dipole radiativity remains finite as the frequency goes to zero, since the "toothpaste behavior" does not preclude an overall displacement of

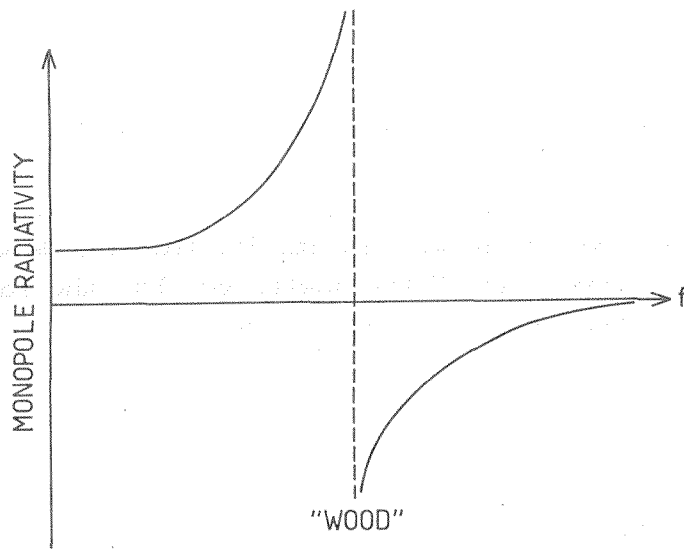


Fig. 1

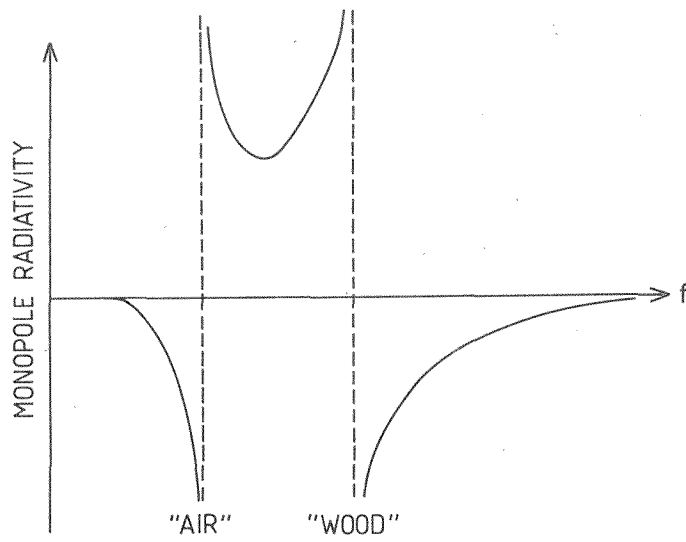


Fig. 2

the center of gravity of the system volume. Consequently the radiation of a violin (as well as of other string instruments that have sound holes) must, at low enough frequencies, have a pure dipole character. At the lowest playing frequency of the violin -- about 196 Hz -- this effect, though not overriding, is sufficient to give the violin's directional radiation pattern a decidedly anisotropic character.

Experimental results

Fig. 3 shows the monopole radiativity of a violin of medium quality (a "good amateur violin") from 200 to 1000 Hz. The solid curves give the amplitude and phase of the radiativity when the force is applied parallel to the violin top, that is, in the nominal bowing direction. The dotted curve gives the amplitude of the radiativity when the force is applied perpendicularly to the top. It is impressive to note that the ratio of the two is, for much of the range, close to a factor of ten, indicating

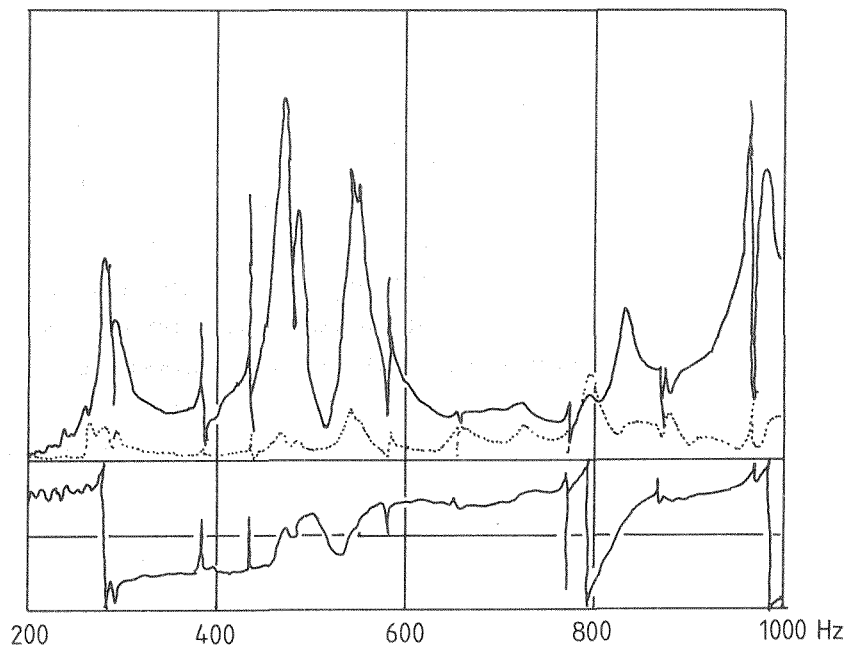


Fig. 3

that the instrument is less sensitive by almost 20 dB to forces in the "wrong" direction than it is to forces in the "right" direction.

In these measurements, we always leave the open strings undamped. The common practice of damping the strings so as to "eliminate their influence" is questionable in that one can never eliminate a normal mode, only displace it: hence, a damped string may masquerade as a broad body mode at an unexpected position. In Fig. 3, by contrast, one clearly distinguishes the string resonances by their sharpness: the D-string fundamental at 293 Hz, the G-string second harmonic at 392 Hz, the A-string fundamental at 440 Hz, and so on. On the other hand, since the measurements are made via the principle of reciprocity, the radiativity must then be interpreted as the multipole moment produced per unit force applied to the bridge by an agent external to the strings, which is not, of course, correct. In fact, however, the impedance presented by a string to the bridge is very low except very near to a string resonance. Thus, if we are interested, for example, in sounds produced on the A-string, we can take Fig. 3 at face value except at frequencies very close to 440 Hz and its harmonics, where the curve is to be corrected by smoothing it out so as to eliminate the sharp resonance.

The phase scale ranges from $+180^\circ$ at the top of the phase graph to -180° at the bottom. As we mentioned, these graphs are based on a definition of the monopole moment as a volume velocity rather than the volume amplitude itself. Hence, the "static" behavior we discussed earlier, in which the shell response to an applied force is governed only by its elasticity, is here characterized by a phase of -90° rather than 0° . We see this "static" behavior in the range from about 320 Hz to about 450 Hz. The region around 280 Hz is the Helmholtz resonance, associated with a phase reversal; at lower frequencies the radiativity phase is "antistatic", as the motion of the toothpaste exceeds that of the tube. Above 450 Hz we enter a cluster of resonances which together comprise the "main body resonance". In traversing this region, the phase again changes by 180° , as the behavior of the shell begins to be governed by inertia rather than elasticity.

Figs. 4-6 show monopole radiativities, in the range from 200 to 4000 Hz, of the following instruments:

- Fig. 4: Vuillaume #2390 (1862);
- Fig. 5: Hutchins #SUS296;
- Fig. 6: "LARK", a cheap Chinese violin.

One may note that, superficially at least, all instruments of more or less "normal" construction show a great deal of similarity in their radiativities. It must be emphasized that the vertical scale of the graphs, although not explicitly labeled, is the same in all of them. That there were not greater differences in the overall level of radiativity for instruments of varying quality was something of a surprise.

If, on the other hand, one deviates from the "normal" construction, radical differences immediately appear. Thus Fig. 7 is a violin with a brass "practice mute" on the bridge, and Fig. 8 is a "sixteenth-size" instrument. Finally, Fig. 9 is the radiativity of one of Carleen Hutchins' "mezzo" violins. This instrument, a member of the "New Violin Octet", has the normal string length and tuning, but is built with a larger plate area and narrower ribs. The consequent emphasis of the low-frequency resonances in the radiativity is clear.

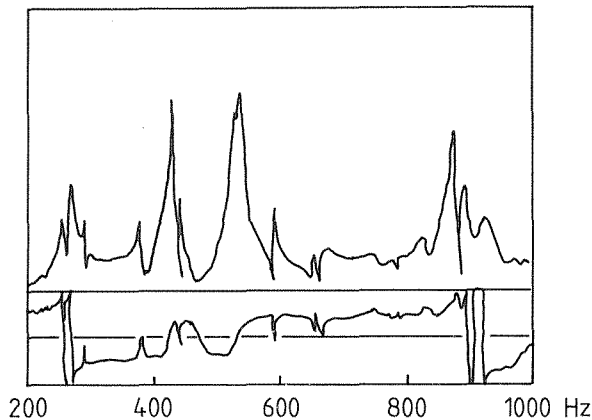


Fig. 4

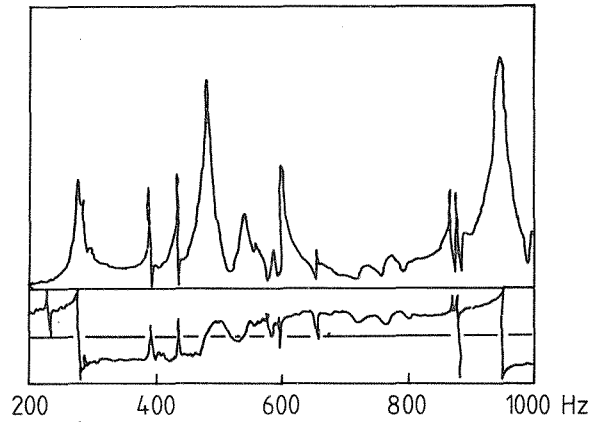
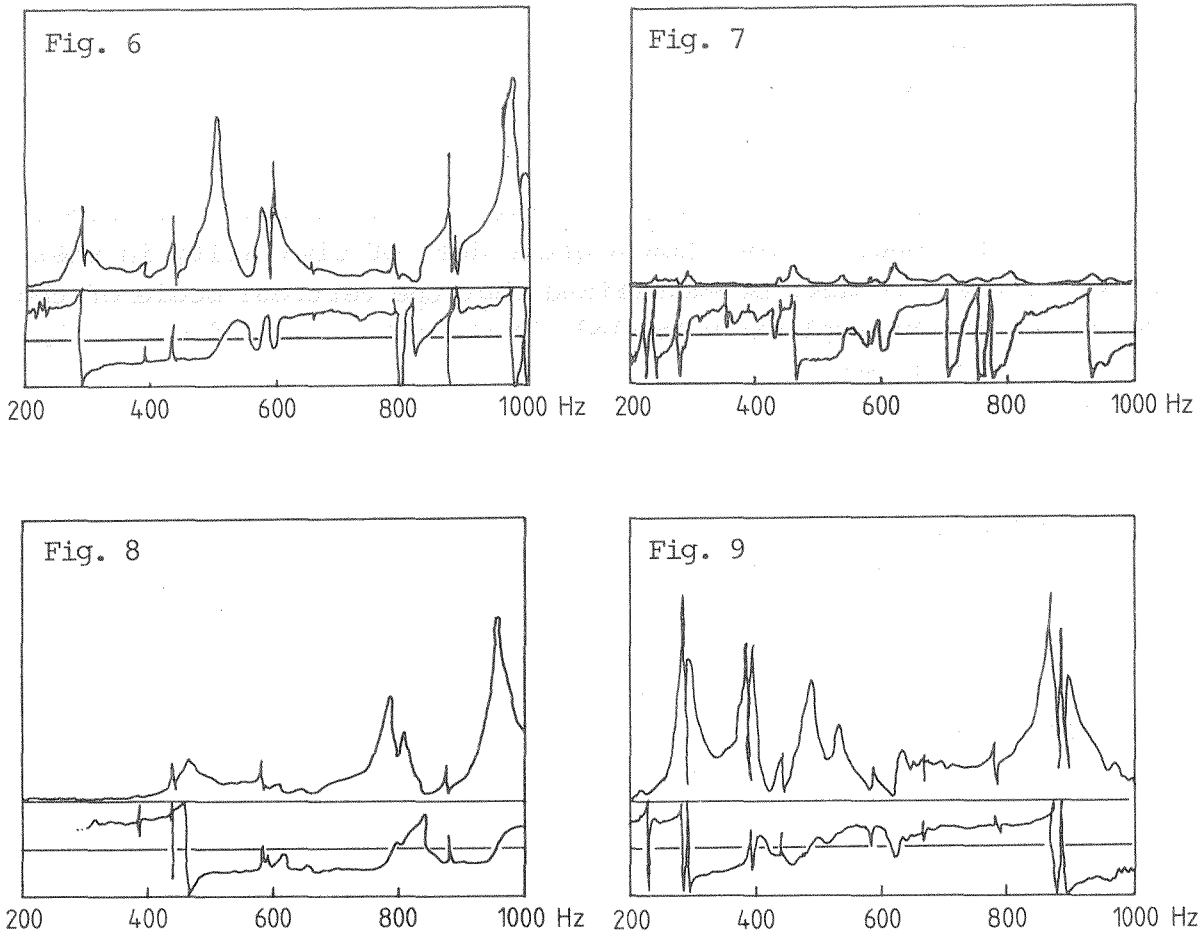


Fig. 5



Concluding remarks

It is known, of course, that violin qualities are importantly affected by behavior at frequencies above 1 kHz. Although our raw data extends to 3 kHz, its analysis in terms of absolute radiativities is complicated by the fact that to tailor the incoming fields up to a certain multipole order requires a number of independent parameters (that is, loudspeakers) equal to the square of the number of multipole orders to be treated. Thus the four speakers that we have used suffice only if monopole and dipole radiation is all that we have. But, in addition to the technical

difficulty of making such measurements, it may be questioned whether this type of expansion remains fruitful at higher frequencies, since the number of simultaneously active violin modes also becomes large. The extension of absolute measurements into higher frequency ranges will, accordingly, have to go hand in hand with further elaboration of the theoretical framework.

INPUT ADMITTANCES AND SOUND RADIATION OF FOUR VIOLINS

J. Alonso Moral

Dept. of Speech Communication and Music Acoustics, KTH, Stockholm

Abstract

Four violins were selected to study input admittance and sound radiation. The study was conducted to obtain answers to two questions:

- 1) How many positions and directions of the input admittance measures are needed to achieve the most essential information of the vibration properties? and
- 2) Is it possible to predict the radiation level with the input admittance known?

The results show that the input admittance outside the G-string and perpendicularly to the top plate is the most informative. Furthermore, they show that the ratio of radiation to input admittance is considerably higher at the Helmholtz resonance than at the following single resonances but considerably lower in the range of the main bridge resonance and above.

The radiation of the violins is for low frequencies insensitive to the direction but for high frequencies strongly dependent of the direction. The radiation is stronger perpendicular to the top plate than perpendicular to the back plate and, furthermore, it is stronger "along" the violin than "across" it.

The radiation effectivity varies from a violin to another; thus the radiation level cannot be predicted better than 3 dB from the input admittance curve. The results indicate that violins with higher input admittance level have a higher radiation level but a lower ratio of radiation to input admittance.

1. Introduction

The input admittance curve is easy to measure and summarizes the vibration properties in an illustrative way. Furthermore, by means of a reciprocal method the radiation properties can be studied.

Four violins were analyzed and answers were sought to the following questions:

1. How many and which positions of the input admittances should be used to achieve the essential information on the vibrational properties?
2. Can the sound radiation be predicted from the input admittance?

The investigation method is described in short. The major results of the measurements will be analyzed and conclusions will be drawn.

2. Experimental Violins

Four violins of different origins were analyzed: (1) a cheap Chinese violin, (2) a Czech violin, made in a non-traditional way, (3) a violin made by Sundin for the Jansson, Molin and Sundin investigations (Jansson et al., 1970; Jansson, 1976), an old violin of unknown origin.

3. Input Admittance Measurements

In my study the so-called input admittance was recorded, that is, the resulting velocity at the driving point for constant driving force. The input admittance gives a measure of how the violin accept the applied driving force from the strings.

3.1. Position of the Measurements

The most important forces caused by the strings on the bridge can be separated into two directions of the plane of the bridge: The first in perpendicular to the top plate and the second in parallel with the top plate. The string forces act in different points on the bridge. Therefore, the input admittance was recorded at five positions: three perpen-

dicular to and two in parallel with the top plate, see Fig. 1.

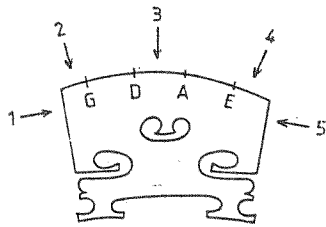


Fig. 1. Definition of the five tested positions and directions of the input admittance.

3.2. Results

An example of input admittance curve outside the G-string perpendicularly to the top plate is shown in Fig. 2. We can see five prominent

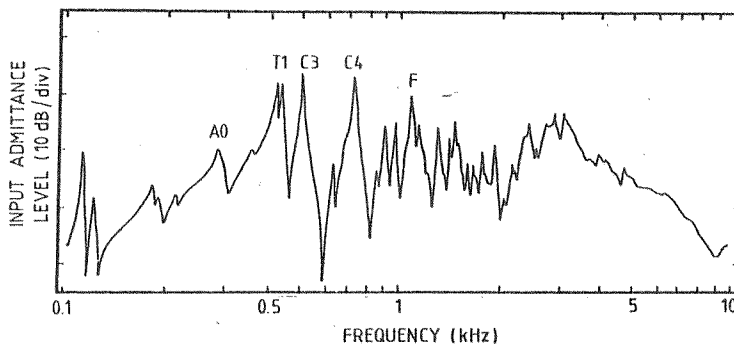


Fig. 2. Input admittance level as function of the frequency at position 2 for the old violin.

resonances marked with A0, C2, T1, C3, and C4. They correspond to the Helmholtz-, Corpus 2-, Top plate-, Corpus 3- and Corpus 4-resonances (Alonso Moral and Jansson, 1982a). A broad hill around 3 kHz is in large the results of a bridge resonance.

3.3. Input Admittance at Different Positions

The input admittance level as a function of the position for the resonances A0, C2, T1, C3, C4, and the average of those resonances are shown in Fig. 3.

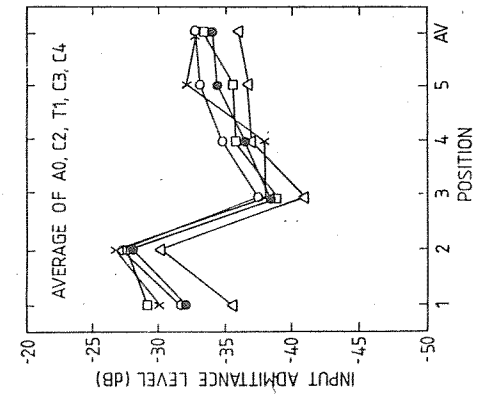
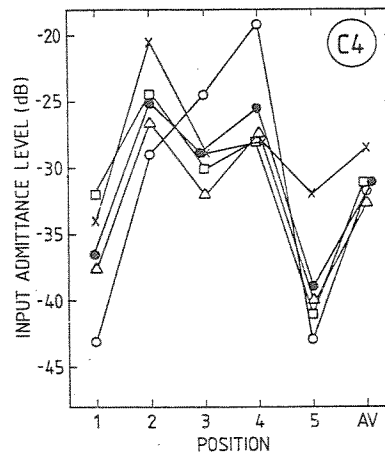
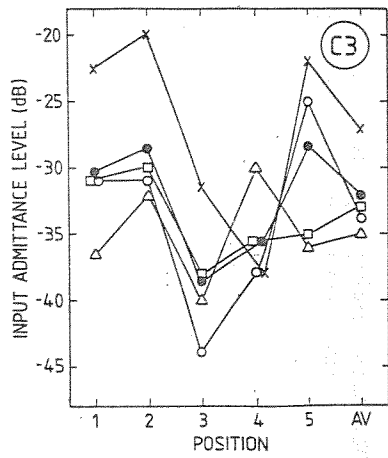
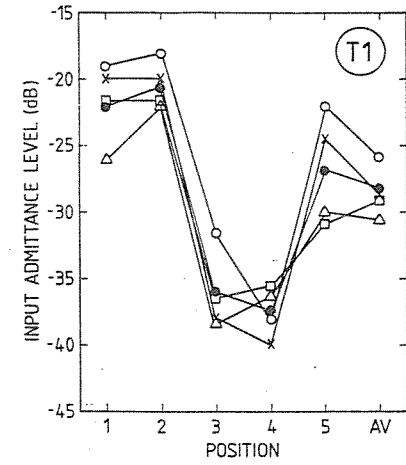
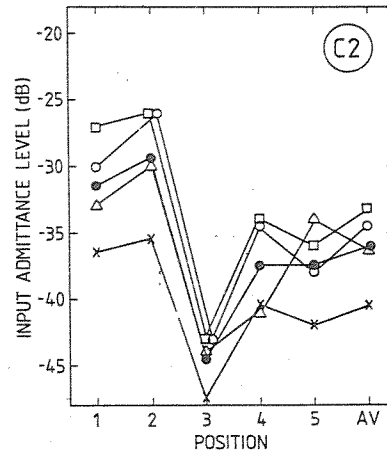
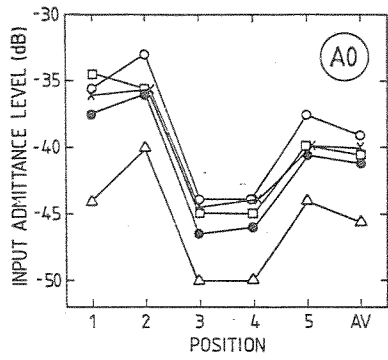


Fig. 3. Input admittance level as function of the position. Violin 1, Violin 2, Violin 3, Violin 4, and average.

Using the magnitude of the input admittance level as criterion on usefulness, the position 2 (that is, outside the G-string, perpendicular to the top plate) gives the best information about the vibrational properties of the violin for all the five resonances.

Furthermore, we can observe in Fig. 3, that: (1) Every resonance has a similar curve as function of the measurement position for all four violins (this suggests that levels in different positions can give a good help to the identification and characterization of resonances). (2) The similarity of the curve course (i.e., with the average level difference removed) of the different violins is higher for the lower frequencies. (3) The level for all the analyzed resonances can vary strongly from a violin to another.

At frequencies between the 8th and the 22nd Bark Band position 4 gives the highest level. Position 2 gives the second highest level in this area of frequencies.

3.4. Selection of a Standard Measurement Position

The input admittance outside the G-string perpendicular to the top plate gives the highest level below the 8th Bark Band. This position gives also the most similar information to the other positions.

From the 8th to the 22nd Bark Band, the input admittance outside the E-string gives the highest level and the most similar information as the other positions.

These two positions proved good for establishing an acoustical quality rating of violins in a previous work (Alonso Moral and Jansson, 1982b).

4. Radiation Properties

This serie represents pilot measurements and should be regarded as preliminary. According to the acoustical reciprocity theorem we can drive

the violin with a loudspeaker and measure the vibrations on the bridge to analyze the sound radiation. The measured transmission corresponds to driving on the bridge and measuring with a microphone. With the reciprocal measures it is good to work. It is easy to drive the violin with a loudspeaker at a fairly large distance.

4.1. Different Measuring Directions

To analyze the radiation level, the violins were driven from six different directions, see Fig. 4. The loudspeaker is placed at a dis-

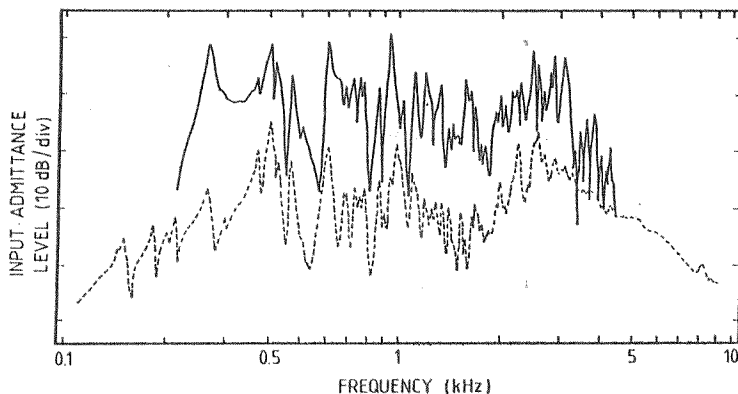


Fig. 4. Definition of the six directions of driving with loudspeaker.

tance of 2 m from the center of the violin body. The bridge vibrations were recorded with the accelerometer in position 2, because this position gave most information about the vibrational properties of the violin.

4.2. Results

An example of a radiation (the full line) and an input admittance

curve (the broken line) are shown in Fig. 5. Generally, the peaks coincide in frequency but there is no simple relation of levels between the

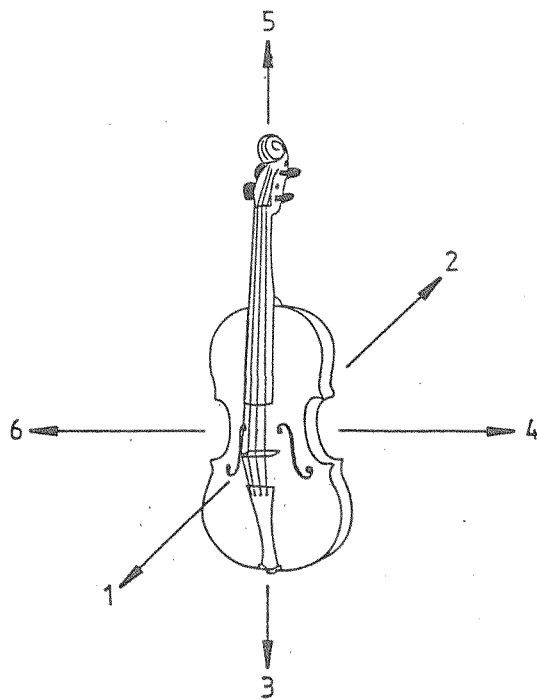


Fig. 5. Radiation level in direction 1 (the full line) and input admittance at position 2 (the broken line) as function of the frequency, for the Czech violin.

two curves. The radiation curve has in addition a more complicated detailed structure.

4.3. Radiation in Different Directions

For directions 1 and 2, the upper diagram in Fig. 6, the violins were free, that is, hung in rubber bands. Thus, we can compare the results of these directions. For resonances below 10 Bark, direction 1 has a tendency to give a higher level than direction 2. This means that the radiation

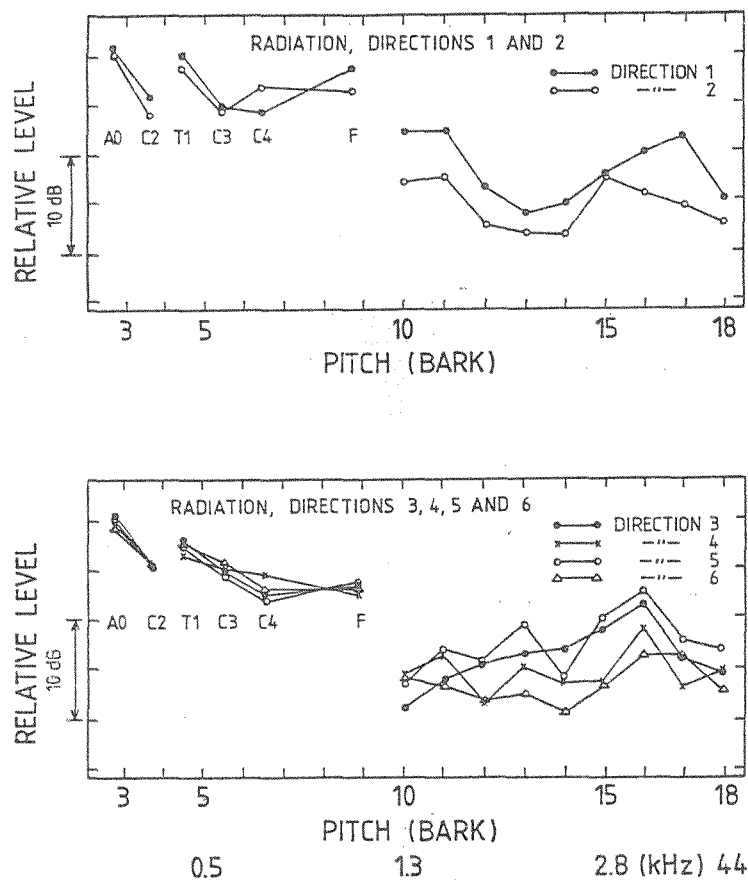


Fig. 6. Sound radiation level for the A0-, C2-, T1-, C3-, and F-resonances and average level from the 10th to the 18th Bark bands. Directions 1 and 2, upper diagram; directions 3 to 6, lower diagram.

perpendicular to the top plate tends to dominate over that of the back plate. Only the C4-resonance has a higher radiation level from the back plate side. Between the 10th and the 18th Bark band, the top plate side has a noticeable higher radiation than the back side (more than 3 dB).

For directions 3, 4, 5, and 6, the lower diagram in Fig. 6, the violins were clamped at the neck. Thus, these results can directly be compared. The radiation levels of the resonances A0, C2, T1, C3, C4, and F are quite independent of direction, but above the 10th Bark band they depend strongly on the direction. There are higher radiation levels for

directions 3 and 5 than for directions 4 and 6, that is, a stronger radiation level along the violin than across it.

The results are in good agreement with Jansson's experiments with played violin (Jansson, 1976).

4.4. Radiation Level

A detailed measure of the total sound radiation of a violin is very difficult to make, but an estimation of how much sound the different resonances radiate is easier to make. The average sound radiation in six directions for the four violins is shown in Fig. 7 for the A0-, C2-, T1-,

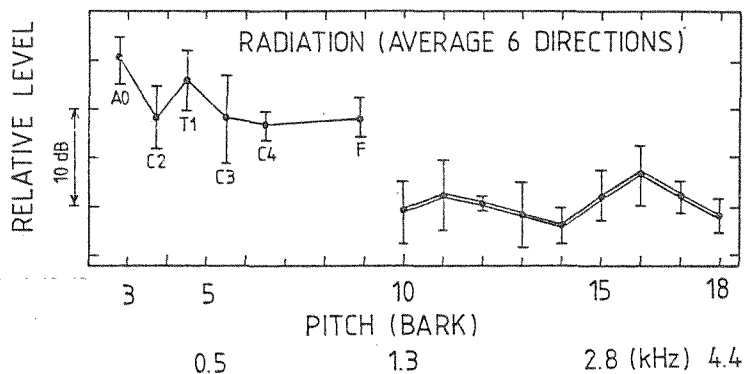


Fig. 7. Sound radiation level for the A0-, C2-, T1-, C3-, C4-, and F-resonances and average level from the 10th to the 18th Bark band.

T1-, C3-, C4-, and F-resonances and the average from the 10th to the 18th Bark band. We can see that the maximal radiation level of the resonances below 10 Bark corresponds to A0 and T1. A somewhat lower level is obtained for the C2-, C3-, C4-, and F-resonances. The values for the different violins vary ± 5 dB for the C3-resonance, and less than ± 3 dB for the other resonances.

Between the 10th and 18th Bark bands, we can observe a prominence

around the 16th Bark band. This prominence is believed to be caused by a resonance of the bridge.

4.5. Radiation and Input Admittance

The ratio sound radiation to input admittance was used as a measure of the radiation effectivity. This ratio is shown in Fig 8. The effectivity

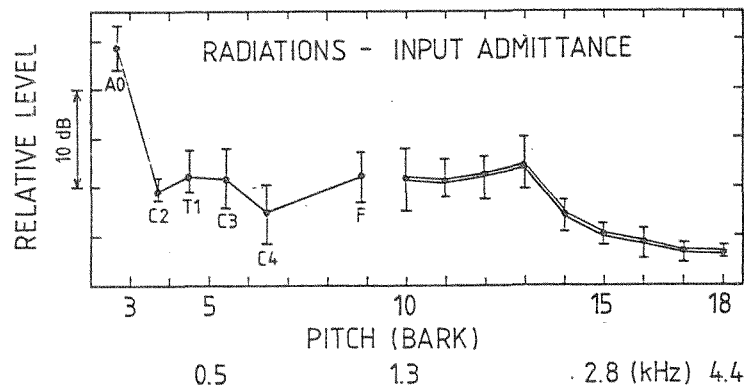


Fig. 8. Ratio of radiation to input admittance levels for the A0-, C2-, C3-, C4-, and F-resonances and average level from the 10th to the 18th Bark band.

is maximum for the Helmholtz's resonance peak, more than 12 dB higher than for the following resonance peaks.

In the frequency range of the first bridge resonance, the radiation effectivity becomes especially low. In this resonance, the bridge vibrates in an eigenmode with a low radiation effectivity which absorbs vibration energy.

The ratio sound radiation to input admittance may vary ± 3 dB from one violin to another. This implies that the sound radiation can be predicted within ± 3 dB from the input admittance measurements.

5. Conclusions

The questions in the introduction were answered by the results in the following way:

- 1) With the admittance at the position 2 only, we can get the essential information about the vibrational properties of the violin.
- 2) The average of the radiation level for the six directions, can be predicted within ± 3 dB with the input admittance at position 2 known.

In addition the following was found:

- 1) The input admittance at the different positions gives a good information for the identification and characterization of the resonances.
- 2) The sound radiation is rather insensitive to the direction for low frequencies but very sensitive on the direction for high frequencies. At high frequencies, the radiation is stronger perpendicular to the top plate than to the back plate and stronger along the violin than across it.
- 3) The ratio sound radiation to input admittance was used as a measure of the radiation effectivity. Thereby it was found that the Helmholtz's resonance is a much more effective sound radiator than the other resonances. The radiation effectivity is especially low in the range of frequencies of the bridge resonance.

References

Alonso Moral, J. and Jansson, E.V. (1982a): "Eigenmodes, input admittance and the function of the violin", *Acustica* 50, 329.

Alonso Moral, J. and Jansson, E.V. (1982b): "Input admittance, eigenmodes, and quality of violins", *STL-QPSR* 2-3/1982, 60.

Jansson, E.V. (1976): "Long-time-average-spectra applied to analysis of music. Part III: A simple method for surveyable analysis of complex sound sources by means of a reverberation chamber", *Acustica* 34, 275.

Jansson, E., Molin, N.E., and Sundin, H. (1970): "Resonances of a violin body studied by hologram interferometry and acoustical methods", *Physica Scripta* 2, 243.

STUDY YOUR BOWING TECHNIQUE!*

Anders G. Askenfelt

Dept. of Speech Communication and Music Acoustics, KTH, Stockholm

Abstract

A simple equipment which makes it possible to simultaneously register the motion of the bow and the downward force on the string exerted by the player ("bow pressure") under normal playing conditions is presented. Some preliminary registrations of various bowing gestures are included.

Introduction

Players of bowed instruments exert a subtle control of the sound source of the instrument, controlling the strings with the left hand and the bow with the right. As regards the control of the bow, three parameters are of primary interest, (1) the motion of the bow transverse to the strings, (2) the force which the player exerts when pressing the bow against the strings, and (3) the distance from the bridge to the contact position of the bow. The equipment described in the following makes it possible to measure the first two of these parameters during playing, essentially without interfering with normal playing conditions.

The following introductory section illuminates the importance of the string player's ability to control and coordinate the three parameters mentioned, the variation of these parameters during play being essentially unaddressed in violin research previously.

* This article will also be published in the Quarterly Progress and Status Report 1/1984, Dept. of Speech Communication & Music Acoustics, Royal Inst. of Technology, Stockholm (in print).

The bow and the string

The normal excitation tool of the instruments of the violin family is the bow. The string is set into vibration as the bow is moved across the string. A sharp, propagating corner is formed on the string in an interactive slip-stick process between bow and string. The corner circulates on the lensshaped envelope of the vibrating string, with an period determined by the fundamental frequency of the note played.

Musically, the motion pattern of the bow is of great importance in the performance of string music, e.g., in phrasing, the motion often being carefully addressed by the composer in the score. Physically, the momentary velocity of the bow is one of the player's chief controls of loudness, the excursion of the string being directionally proportional to the bow velocity. The other available control of loudness is the distance from the bowing point to the bridge, the transverse excursion of the string being inversely proportional to this distance (Cremer, 1981).

According to the basic Helmholtz model of string motion, the bow force does not influence the vibrations of the string as long as the frictional force between bow and string is high enough to maintain the stick-slip process of the string under the bow. However, as familiar to all string players, the bow force does effect the vibrations of the string, an increased bow force giving a more brilliant and carrying tone. As shown by Cremer (1981), a higher bow force than minimum leads to a resharpening of the circulating corner of the string during the passage under the bow, the corner being rounded off at the reflections at the string terminations, mainly at the bridge. This gives a boost of the higher partials with increasing bow force, an effect also available to the player by decreasing the distance between the bow and the bridge. However, this later strategy is accompanied by the increase in loudness earlier mentioned.

In the following the parameter (1) will be referred to as transverse bow motion although the motion takes place in the longitudinal direction

of the bow. This is in order to avoid misunderstandings as the string often is used as a direction of reference in studies of the violin. As regards parameter (2) the correct term bow force will be used instead of the customary term "bow pressure".**

Method

Bow motion

The instantaneous transverse position of the bow was measured by means of the Wheatstone-bridge principle, Fig 1. A thin resistance wire was inserted amongst the bow hairs. This wire is divided in two parts by the string, the ratio of the lengths of these two parts depending on the transverse position of the bow. The two parts of the wire make up one branch of a Wheatstone bridge, the other branch consisting of one fixed and one variable resistor, allowing for offset calibration.

With the midpoint of the bow resting on the string the bridge is in balance. When the bow is moved away from this point a voltage is generated proportional to the distance from the midpoint of the bow. The signal is registered on an ink writer. When the bow is not in contact with the string the ink jet is deflected away from the paper, leaving no trace. The linear relationship between output voltage and transverse bow position is shown in Fig 2.

This simple device makes it possible to register the player's motion of the bow without interfering with normal playing conditions. The player may even use his own instrument as the only preparations needed are made on the bow. The only restriction necessary in conjunction with

** It would be desirable that the correct term "bow force" be used consistently in scientific presentations, as it is a force and not a force per unit area which is being measured. The reason for the persistence of the term "bow pressure" would be that the player has good reasons to associate to pressure, as he actually presses the bow against the string.

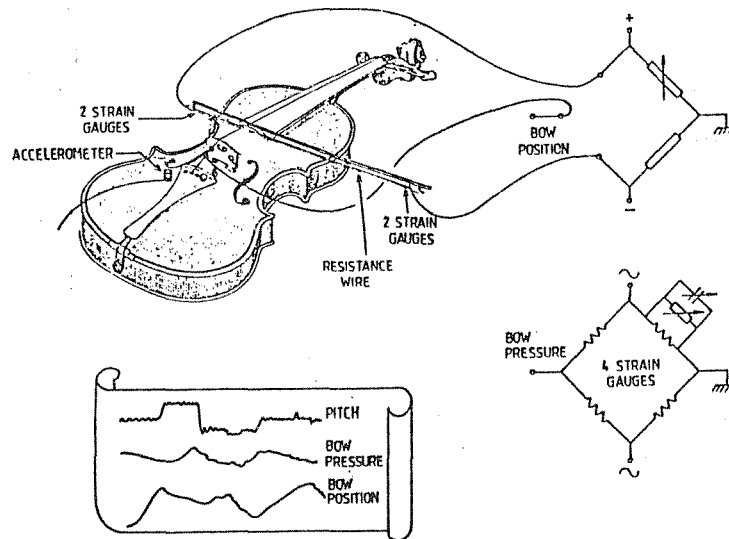


Fig. 1. Sketch of the equipment used for the simultaneous registration of bow motion, bow force, and pitch. The sensor for the transverse bow position is a thin resistance wire inserted among the bow hairs. This wire is divided into two parts by the string, the two wire parts constituting one branch of a Wheatstone bridge. The sensors for the bow force are four strain gauges mounted on thin bronze strips through which the bow hair is fastened to the bow. The strain gauges are connected in another Wheatstone bridge. The pitch is registered by an accelerometer sensing the vibrations of the violin body. All three signals are recorded on an ink writer.

the use of this prepared bow is the moderate use of rosin in order to avoid intermittent electrical contact between bow and string.

Bow force

The instantaneous bow force exerted by the player was registered by the use of another Wheatstone bridge. The bow hair was cut at the frog and the tip and thin strips of phosphorus bronze were glued to the bow hair in both ends. The bow hair was refastened to the bow via these metal strips. Four strain gauges were glued to the strips, one on each side, and connected in a Wheatstone bridge. When the player presses the bow against the string, the metal strips bend and the bridge generates a

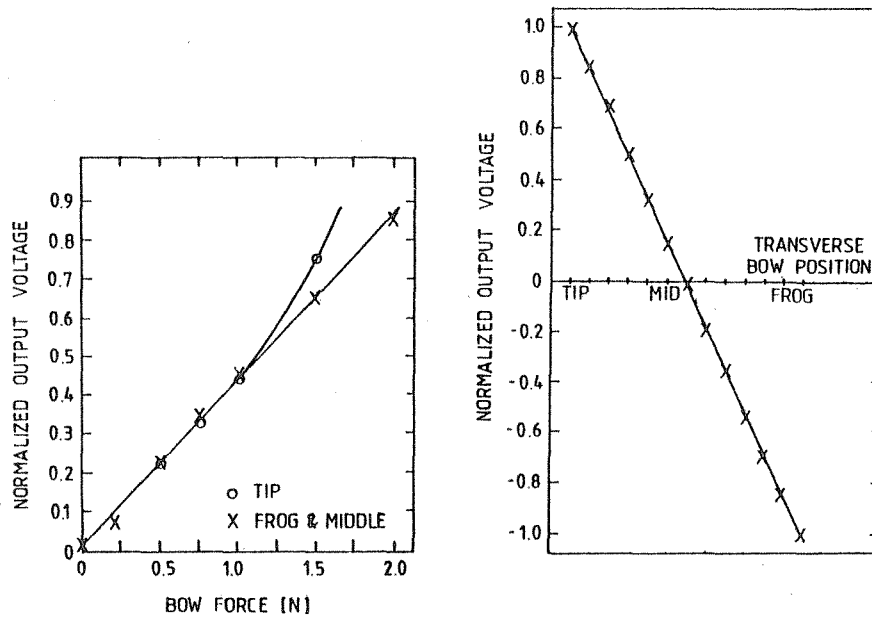


Fig. 2. Calibration charts for the signals representing transverse bow position and bow force.

voltage proportional to the bow force. This signal is recorded on the same paper as the bow motion.

The output voltage is essentially a linear function of the bow force, Fig. 2. The only deviations occur when using very high bow forces near the tip, a combination not used in normal playing.

The preparations of the bow described above did not change the normal playing conditions to any appreciable extent, according to professional violin players. For example, the total weight and the distribution of the weight along the bow are essentially unaltered. The most marked difference when using this prepared bow is the shortening of the accessible bow length by a couple of centimeters, corresponding to less than 10% of the original length. The reduced length of the bow was 0.58 m.

Examples of registrations

The transverse bow motion and the bow force were registered on paper together with other parameters of interest, in these experiments pitch or acceleration level in the top plate of the instrument. The pitch and acceleration were measured with the aid of an accelerometer fastened to the violin top plate close to the bridge on the the bass bar side. The acceleration level was used as an estimate of the excitation of the instrument. Some examples of registrations are shown in Figs. 3-8, displaying different manners of bowing as performed by two professional players.

Typical values of bow force observed during the experiments were between 0.5 and 1 N.*** The lowest bow force which still produced a steady tone was approximately 0.15 N. A bow force of 1.5 N and above is to be considered as high.

Typical values of bow velocity were between 0.6 and 1.3 m/s. The lowest velocity which still produces a steady tone was approximately 0.04 m/s, one full bow stroke lasting about 15 s. The highest bow velocity observed was almost 3 m/s, this high value being reached in sforzandi during closing chords of a movement.

The first example of registrations, Fig. 3, pertains to a rising one octave G-major scale starting on the low G-string. The scale is played legato, detache and staccato, respectively. The differences between these types of bowing are clearly demonstrated in the figure.

The next figure, Fig. 4, shows a sforzando in two different versions, a short version with the bow leaving the string immediately after a rapid bow stroke, and a longer with the bow resting on the string throughout

*** The force unit 1 N (Newton) corresponds to the weight of 100 g within an error of less than 2 %.

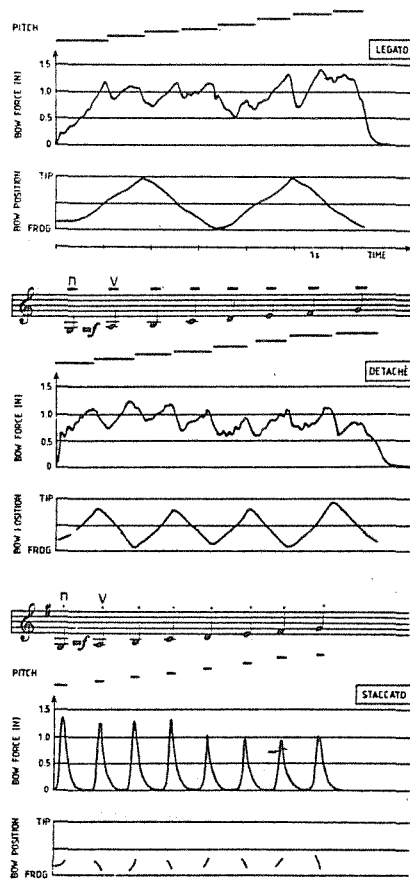


Fig. 3. Registrations of pitch, bow force, and transverse bow position. The example played is a G-major scale in one octave starting from the low G-string, legato (top), detaché (middle), and staccato (bottom).

the bowstroke. Note the differences in the excitation of the instrument as displayed by the acceleration level curves. The long version consists of two portions with different decay slopes, emanating from a corresponding division of the bow stroke in two portions with a high and a slower velocity, respectively.

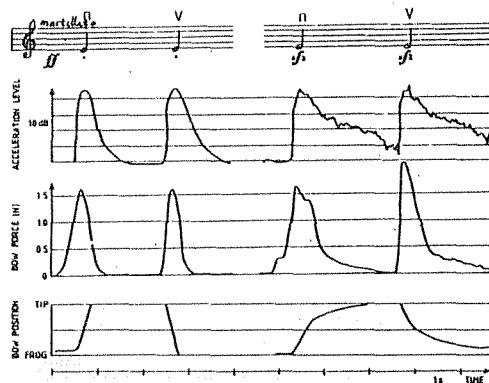


Fig. 4. Registrations of acceleration level, bow force, and bow position. The example played is a sforzando in two different versions, short (left) and long (right).

The registration in Fig. 5 illustrates a crescendo - diminuendo made both the normal way, i.e., upbow - downbow, and also the opposite way, downbow - upbow. Note the coordination of increase in bow force with the increase in bow velocity, i.e., the force increases as the slope of the bow position curve increases. These gestures requires a careful planning by the player as regards the consumption of bow length, in order to achieve a large dynamic span. In this example the span in acceleration level is approximately 25 dB in both versions.

An example of an usual accompaniment in Mozart-style music is displayed in Fig. 6, showing groups of notes played spiccato (eight-notes) and saltelato (sixteenth-notes). Note that the player increases the bow velocity in crescendo by lengthening the bow strokes, the time for a stroke being constant. A matching increase in bow force accompanies the increase in bow velocity.

The registration in Fig. 7 illustrates the typical accompaniment of Vienna-waltz, showing the after-beats played by the second violins. The bar is divided asymmetrically, the time lengths from onset to onset

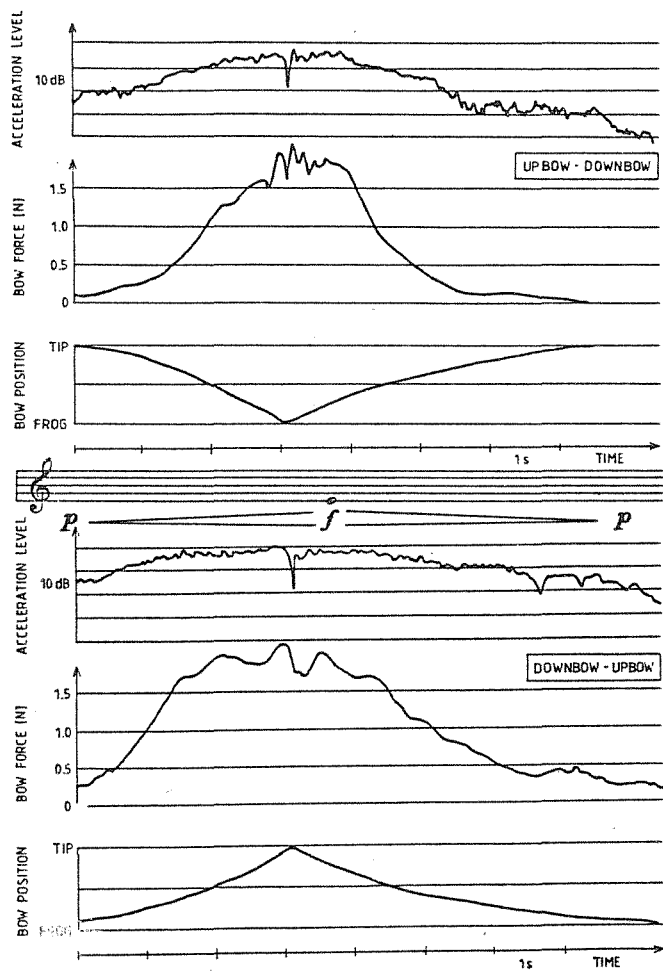


Fig. 5. Registrations of a crescendo - diminuendo played upbow - downbow (top) and downbow - upbow (bottom). The same signals as in Fig. 4.

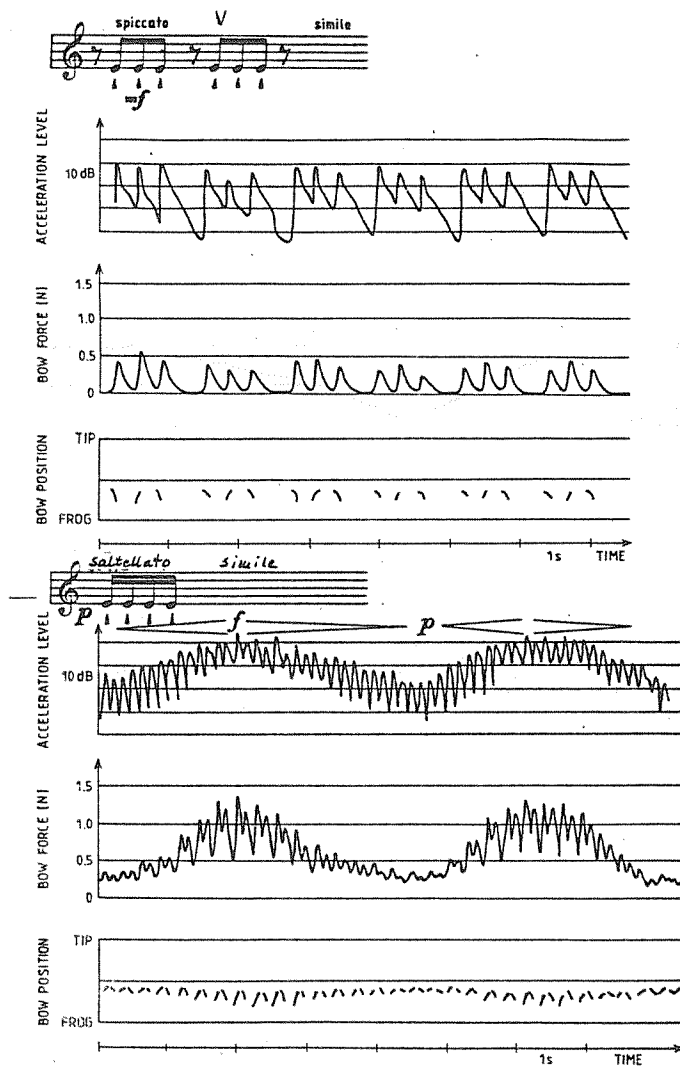


Fig. 6. Example of a Mozart-style accompaniment spiccato (top) and saltellato (bottom) during crescendo - diminuendo. The same signals as in Fig. 4.

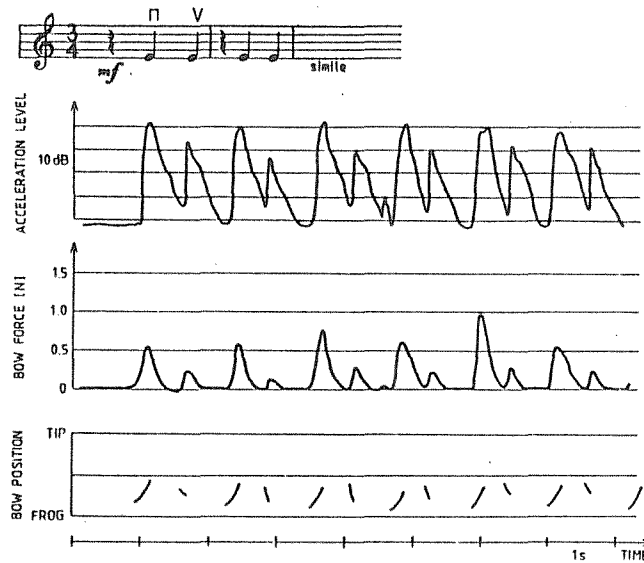


Fig. 7. Example of a Vienna-waltz accompaniment. The bar is subdivided asymmetrically, see text. The same signals as in Fig. 4.

Fig. 7. Example of a Vienna-waltz accompaniment. The bar is subdivided asymmetrically, see text. The same signals as in Fig. 4.

between beats 2-3 occupying 38% of the duration of a bar, leaving 62% for the remaining two beats (cf., Bengtsson and Gabrielsson, 1983). The timing in the first bar deviates from the following bars, indicating that the player adapts to the rhythm gradually.

The last example, Fig 8, shows the opening of the first movement of Beethoven's violin concerto played in two different versions. The player was instructed to render one tender and one aggressive performance, respectively, maintaining an identical tempo and approximately the same loudness. As seen in the figure, the aggressive version is characterized by a higher mean bow force as well as more rapid changes in the force. Also, the player changes the bowing pattern between the versions, apparently in order to afford a faster bowing. The turning points of the bow

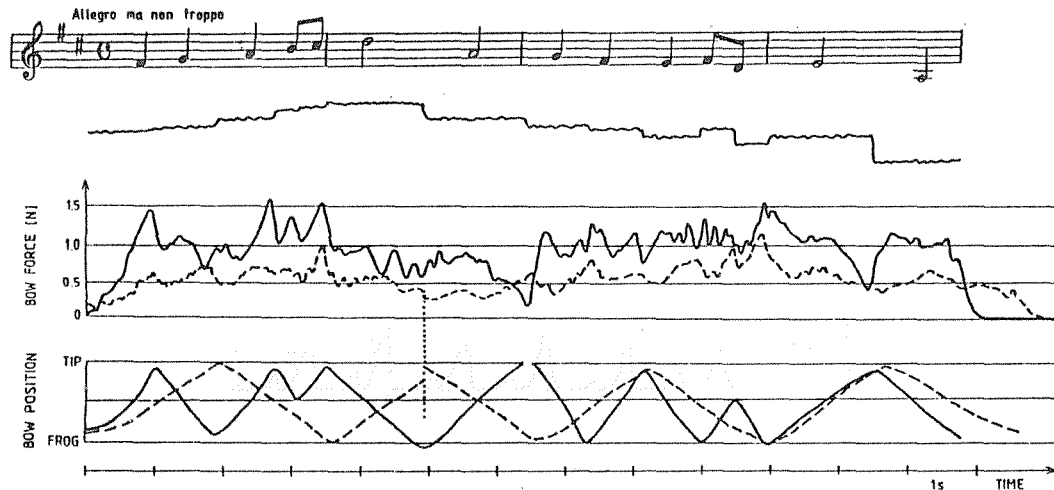


Fig. 8. Registrations of the opening of Beethoven's Violin Concerto played in two versions, tender (broken lines) and aggressive (full lines). The last tone in the second bar has been shortened by a couple of millimeters in the tender version, in order to compensate for a little lengthening of this note. The following half is shifted the same distance to the left as indicated by the short dotted vertical line. The same signals as in Fig. 3.

are made a little sharper in the aggressive version, and at one occasion the player lifts the bow from the string in order to give an extra stress to the following note, starting this note with a sudden increase in bow force.

Concluding remarks

This last example is perhaps the most interesting application of the equipment described, giving insight into the bowing gestures used in playing music in different moods

As indicated in Fig. 8, the level of physical activity in bowing is higher in the aggressive version than in the tender version. Interest-

ingly, similar differences have been revealed between other motion patterns performed under different emotions. For example, Clynes (e.g., 1983), in the studies of human touch expression, found the emotions "hate" and "anger" to be characterized by a stronger touch and, in particular, more abrupt changes in the movements, as compared to the emotions "love" and "reverence". The significance of the changes in the signals apparent both in the touch experiments as well in the registrations in this study, suggest that the derivatives of the parameters registered will offer informative contributions in a continued study of bowing gestures, the derivatives emphasizing the changes in the signals (Askenfelt and Sjölin, 1980).

The results presented in the this study show that the method is capable of visualizing and discriminating well between the intangible differences in bowing patterns associated with differing performances. Furthermore, the method does not disturb the player in his performance to any appreciable extent. These features imply that the equipment offers means to examine the art of the playing of bowed instruments more thoroughly in the future. Hopefully, such a study will give insight into the code used by musicians in order to convey the emotional atmosphere of a piece of music.

Acknowledgements

The author is indebted to violinists Semmy Lazaroff and Bertil Orsin for their kind assistance in the experiments.

References

Askenfelt A. & Sjölin Å.: "Voice analysis in depressed patients: Rate of change of fundamental frequency related to mental state", STL-QPSR 2-3/1980, pp. 71-84.

Bengtsson I. & Gabrielsson A.(1983):"Analysis and synthesis of musical rhythm.", in Studies of Music Performance, Publications issued by the Royal Swedish Academy of Music, No.39, Stockholm.

Clynes M. (1983): "Expressive microstructure in music.",
in Studies of Music Performance,
Publications issued by the Royal Swedish Academy of Music, No.39, Stockholm.

Cremer L. (1981): Physik der Geige, S. Hirzel Verlag, Stuttgart.

PIANO TOUCH, HAMMER ACTION AND STRING MOTION

A. Askenfelt and E. Jansson

Dept. of Speech Communication and Music Acoustics, KTH, Stockholm

Abstract

In this paper we present experimental data on the timing of parts in the grand piano action and on the interaction hammer-string, together with a first interpretation of these data.

Timing in the piano action

Let us start with a brief description of the grand piano action, cf. Fig. 1. With the key in its upper position the hammer rests via its

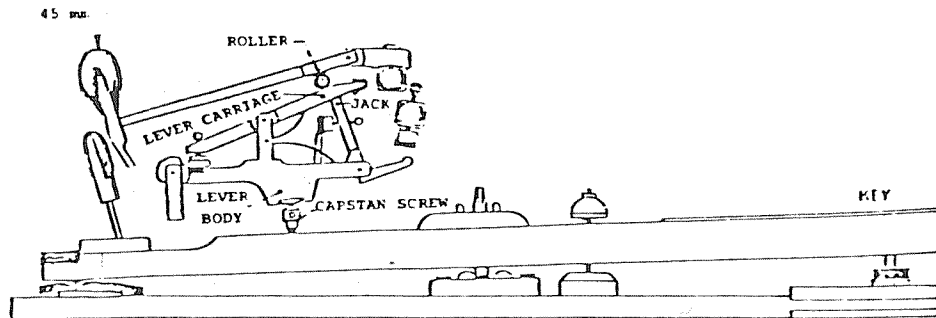


Fig. 1. The grand piano action.

roller on the level carriage and body. The lever body rests on the capstan screw which is joined with the key. When the key is pressed, the entire lever body moves upwards and the jack takes over the support of the hammer roller. The hammer and the lever body move upwards together until the lower end of the jack touches the escapement dolly. Now the

jack starts to move backwards and the hammer gets a final kick when the edge of the jack passes the roller. The hammer flies freely and hits the string, bounces back, and is captured by the check.

We have measured the timing of moving parts in the piano action by means of simple electrical preparations and digital storage oscilloscope. Thin copper wires were applied to different points:

- (1) to the hammer, making it possible to measure the string-hammer contact,
- (2) to the roller and the jack, to record the roller-jack contact, and
- (3) to the key to record the bottom contact of the key.

The contact signals were added by a simple resistor network which condensed these three on-off signals into one trace of the oscilloscope. An example of such a recording is shown in Fig. 2. Starting from the left, there is no voltage signal, which means that the hammer rests on the lever carriage, thereafter contact between roller and jack (the broken line). After a short time, further to the right, the key reaches its bottom position (the dotted line). Thereafter, the upwards step shows that there is no contact between roller and jack, i.e., the hammer moves freely in the air. At the large step downwards (the full line), the hammer is in contact with the string. To make the time relations between the different contact points clear, the stepwise signal is re-plotted with corresponding horizontal lines underneath.

The curve below shows the velocity of the key, when the key was hit from the air above. Starting from the left we see that the key rapidly goes down towards a maximum velocity, at which moment the jack starts lifting the hammer. Then the downward velocity decreases, in this case to zero, whereafter the finger "catches up" with the hammer and a new downward velocity maximum is reached before the key hits the bottom position and the velocity falls to zero. Note that this zero falls close to the moment when the hammer and string make contact.

A crucial part in the piano action is the contact between roller-jack. The jack pushes the roller until the jack hits the escapement dolly. Soon hereafter, the hammer with roller lifts from the jack and the hammer strikes the string. The pushing force on the hammer roller was estimated

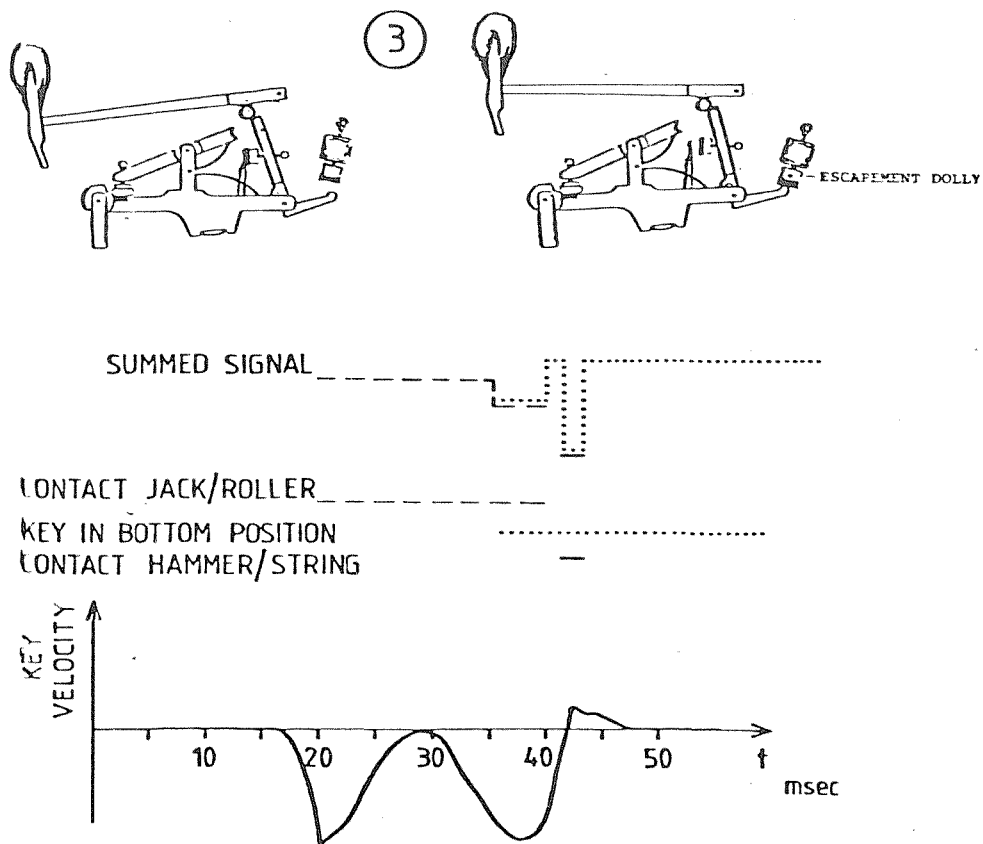


Fig. 2. Timing in the grand piano action (top) and key velocity (bottom), see text. The key was struck with force from above.

by measuring the resistance between roller and jack, which was covered with graphite. In this way, we found that the pushing force rapidly reaches a constant high value after which it suddenly is turned off before the hammer strikes the string. This turning-off point is set by the adjustment of the escapement dolly.

String vibrations and hammer-string interaction

Let us look how the string vibrations differ between different strings, see Fig. 3. The string velocity was measured by applying a magnetic field across the string at a certain point and by recording the

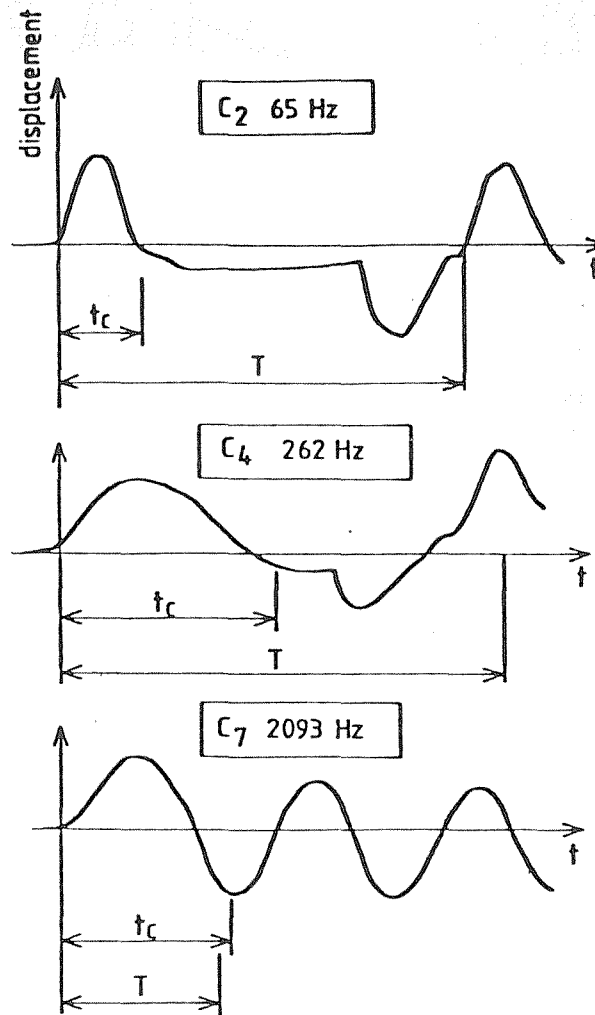


Fig. 3. String displacement versus time for a bass note (top), a middle register note (middle), and a treble note (bottom). The period time is marked with T and the hammer-string contact duration with t_c .

induced voltage from the string vibrations. The corresponding string displacement was obtained by a simple integration. The curve at the top in Fig. 3 shows string displacement versus time for C2=65 Hz, the middle one is the corresponding curve for C4=262 Hz, and at the bottom is C7=2093 Hz. Note that the waveforms are quite different. The displacement curve for C2 consists of two pulses followed by a long portion of zero displacement. For the middle C, C4, there is just a short portion of zero displacement and for the high C there is none.

The hammer-string contact durations are marked in Fig. 3 by t_c . The hammer-string contact durations are long for the lowest note, approximately 4 ms, and short for the highest note, 1 ms. In spite of the long string-hammer contact duration in ms at the lowest note, we obtain a relative duration of only 20% of a period time for this tone, which can be expanded to approximately 30% by extremely soft touch. For the middle C, the hammer-string contact time varies between a half and a full period, and for the high C, the contact time is between one and 2.5 periods. This means that we obtain an inefficient excitation of the C2-note because of a too short excitation pulse and an inefficient excitation of the C7-note because of a too long excitation pulse. Middle C is fairly efficiently excited, the starting pulse being half a period. Note that the C2-note is well described by traveling pulses, while the high C7 rather is a standing wave. The duration of the displacement pulses is closely related to the hammer-string contact duration.

The influence of the hammer weight and shape on the hammer-string interaction was investigated by changing hammers between the keys. The middle C, C4, was fitted with the original hammer, a heavy bass hammer, and a light treble hammer. As expected, we obtained a longer than normal contact duration with the bass hammer and a shorter than normal with the treble hammer. The pulse shapes on the string also changed depending on the size and hardness of the hammer. The treble hammer, for example, was not only lighter but also harder and more pointed than the normal hammer. The shape of the string vibrations did not look very different for different hammers but the sounds they produced were indeed quite different. Especially the treble hammer produced a very different sound, reminding somewhat of a harpsichord.

Let us look a little closer at the hammer-string contact. At the hammer towards the bridge, the velocity signal consisted of one broad pulse during the hammer-string contact duration but on the opposite side of the hammer towards the agraffe there were four short humps. The frequency of these humps turned out to be independent of the hammer properties. This fact proves that the frequency is determined by the short string length between hammer and agraffe. This phenomenon is also illustrated in Fig. 4. The upper diagram shows the velocity of the string and the lower the hammer acceleration. The recording positions for the two signals are shown in the lower half of the figure. The string velocity and hammer acceleration actually recorded are marked with full lines.

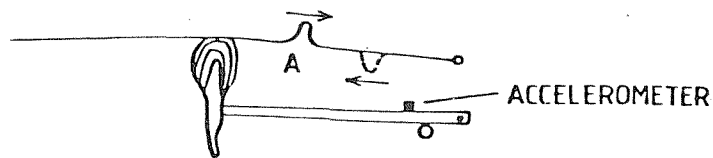
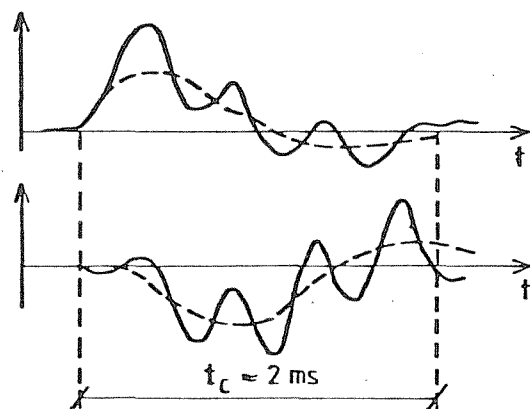


Fig. 4. String velocity at A and hammer acceleration, see text.

Notice that the periodic variation in the two lines is of the same frequency. Notice also that the periodic motion of the two full lines are in phase. In the periodic motions a slower process is included, which is marked with broken lines. The two broken lines represent out of phase motions, in contrast to the higher frequency motions, which are in phase.

We interpret that the "high frequency" in phase "motion" derives from a pulse train on the short string length between hammer-agraffe. The slow out of phase "motions" derive from a small string displacement, similar to plucking. More experimental evidence should, however, be collected before a final interpretation is made.

The influence of pricking the hammer with a piano tuner's needle was also investigated. A normal hammer was softened in steps until it was completely destroyed and the string velocity was recorded after each step. There was no dramatic change in the string waveform going from a normal hammer to the very soft one. However, the hammer produced quite different sounds before and after "torture", ranging from the normal bright piano sound to a rather dull one.

Conclusions

In our experiments we have found that the time for the key-bottom contact coincides closely with the time for the hammer-string contact. The duration in msec of the hammer-string contact is longer for bassnotes than for treble notes. However, expressed in fractions of half a period, the contact duration is short for bass notes but long for treble notes (longer than a full period). In the middle register the contact duration is approximately half a period. The hammer-string action seems to incorporate two processes; a fast periodic process set by the short string length between hammer-agraffe, and a slow pushing type of motion.

TRACKING "ENCLOSED AIR-PLATE" COUPLING WITH INTERIOR GAS EXCHANGE

G. Bissinger and C.M. Hutchins*

East Carolina University, Greenville, NC, USA

*Montclair, NJ, USA

Abstract

By interchanging the interior air in a violin with CO_2 and CCl_2F_2 gases it was possible to drop the air mode frequencies by factors of .81 and .49, respectively. It was found that certain plate vibrations, as measured with accelerometers at various places, "track" these shifts in internal gas oscillations. These tests are strong indicators that air mode oscillations can effectively force significant plate oscillations in the region of the air mode resonance frequencies, and create uncertainty about the assignment of "air", "wood" and "top plate" character to some of the lower resonances of the violin.

The proper identification of the character of a particular vibrational mode in a string instrument is a difficult task due to the complex manner in which the instrument vibrates. It is also an important task since the scaling of string instrument dimensions, such as was done to create the violin octet (Hutchins, 1962), is based on an interpretation of the character of these vibrational modes. Recently we have been investigating how effectively the interior gas oscillations force plate motions in the violin (Bissinger and Hutchins, 1983) by interchanging the interior air (molecular weight = 29) with CO_2 (MW = 44). To extend these investigations further we have here added CCl_2F_2 (MW = 120). These gas exchanges shift all the "enclosed air" resonances lower in frequency by a constant factor which varies with the square root of the molecular weight. For the gases used here the factor is 0.81 (CO_2) and 0.49 (CCl_2F_2).

Using an acoustic driver placed off-center inside the lower bout, we have observed the top plate response, via accelerometers attached to

various parts of the top plate of the violin, to gauge what effect this gas exchange has on the frequency and amplitude of peaks in the top plate response curve. Also, a probe microphone placed in the lower bout, on the side opposite to the acoustic driver, was used to monitor interior gas oscillations. The various exchange gases, all heavier than air, were slowly passed into the instrument to maintain a nearly pure interior gas by displacement. Gas loss or mixing through the f-holes, associated with certain oscillatory modes of the interior gas (particularly those that have an antinode at the f-holes, such as the A0), was generally easily made up with a relatively small gas flow. Initial gas flow was adjusted until the A1 mode fell at the proper frequency relative to that measured with air inside the instrument cavity. Normally there was a small deviation above the expected frequency for the A0 mode due to the mass plug in the f-hole being a mixture of air and interchange gas; this deviation was larger for heavier gases.

Data was collected on a standard violin (SUS #180) as well as on a long pattern Stradivarius copy (SUS #280), a mezzo-violin (SUS #159) and a 16" viola (SUS #213) and within expected variations all showed the same general behaviors. Here we will present only the data for SUS #180, which was suspended horizontally with thin rubber bands from a massive metal fixture, with the gas feed, miniature pickup microphone, and acoustic driver inserted through the f-holes. The acoustic driver was connected to a swept-frequency sine wave generator linked to a strip chart recorder that was used to collect the internal microphone output and the accelerometer output at three different positions versus frequency of the driving signal. The accelerometer was placed in each of three positions successively, viz., in the middle of the upper bout to the left of the fingerboard (bass bar side), at the bridge (centered between the two feet) and on the left in the middle of the lower bout. Except for the accelerometer, all devices were unmoved during gas interchange for the duration of the measurements. Further experimental details can be found in Bissinger and Hutchins (1983).

To analyze the data we started with known modes and frequencies for the A0-A7 internal air oscillations in a violin-shaped cavity from the

work of Jansson (1973; 1977). The frequencies of the two lowest modes, A0 and A1, which were unambiguous in the resonance spectra for SUS#180, were used to normalize this instrument's air mode frequencies to those determined by Jansson for another instrument. With this normalization factor and the frequencies of the A2-A7 modes it was possible to predict the frequencies of the A0-A7 modes for the CO₂ and CCl₂F₂ gas interchanges in this particular violin.

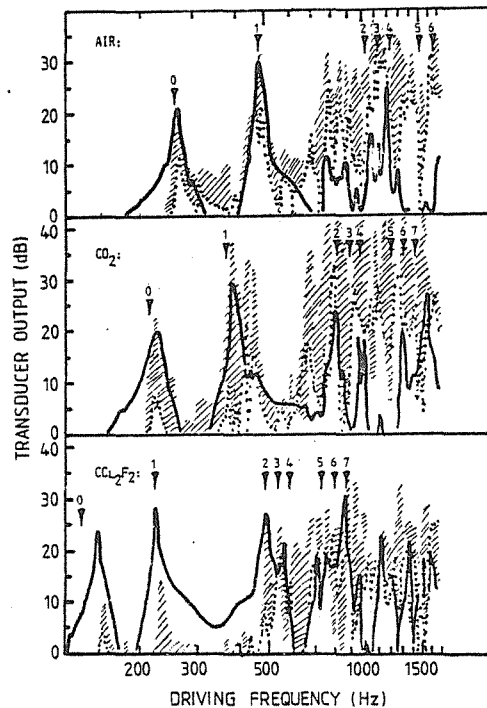


Fig. 1. Transducer output (solid line - microphone in lower bout, dotted line - bridge accelerometer, cross-hatched region - maximum range of accelerometer readings) versus acoustic driver frequency for air, CO₂, and CCl₂F₂ interior gases. Small arrows indicate the predicted positions for interior gas resonance frequencies as calculated from Jansson (1973; 1977) for each exchange gas.

Our experimental results are presented in Fig. 1 for SUS#180 with interchange of CO₂ and CCl₂F₂ with air. Included in the figure are marks that indicate the original (normalized to SUS#180) air mode frequencies

for air and the predicted frequencies for the CO_2 and CCl_2F_2 resonance peaks. It is obvious from the figure that strong plate vibrations are associated with some of the strong interior gas oscillations, particularly so for the A0, A1, and A2 modes. On the other hand, certain of the interior gas modes do not appear to force significant plate vibrations. With such a restricted sample of plate motion as we have here it is difficult to directly associate plate motions with nodal-antinodal patterns of the interior gas modes. However the accelerometer readings for plate motion associated with A0 and A1 modes have relative magnitudes at the three positions quite similar to the respective pressure variations in these modes for all three interior gases, while the CCl_2F_2 resonance spectrum shows good agreement for the A2 mode also. With the large number of closely spaced resonance peaks at frequencies above 700 Hz (air case) it is quite difficult to make an unambiguous assignment to individual peaks in this region. Since the A2 mode occurs about 1000-1100 Hz (air) and about 800-900 Hz (CO_2), only for the CCl_2F_2 case does the frequency drop into a relatively uncluttered portion of the resonance spectrum.

The investigation outlined above, although just in its initial stages, has made it clear that, at least in some cases, the plates of the instrument act as compliant surfaces, capable of being set easily into motion by internal gas pressure oscillations. How significant this compliant motion is in terms of the overall acoustic output of the instrument is not clear. In the case of the A0 mode, interchanging the interior air with CO_2 has been shown to affect the acoustic output of the violin (Bissinger and Hutchins, 1983). How much of the acoustic output of a violin at the A0 mode frequency is associated with compliant plate motion and how much with the gas sloshing back and forth through the f-holes is not known. Further work on these same questions is necessary to clarify the connection between effective "enclosed air-plate" coupling and effective radiation of acoustic energy.

References

Bissinger, G. and Hutchins, C.M. (1983): "Evidence for the coupling between plate and enclosed air vibrations in violins", Catgut Acoust.Soc. Newsletter 39, 7-11.

Hutchins, C.M (1962): "The physics of violins", Sci. Amer., Nov., 78-92.

Jansson, E.V. (1973): "On higher air modes in the violin", Catgut Acoust.Soc. Newsletter 19, 13-15.

Jansson, E.V. (1977): "Acoustical properties of complex cavities. Prediction and measurements of resonance properties of violin-shaped and guitar-shaped cavities", Acustica 37, 211-221.

AN OSCILLATOR MODEL FOR ANALYSIS OF GUITAR SOUND PRESSURE RESPONSE

Ove Christensen

The Panum Institute, University of Copenhagen, Denmark

Abstract

We investigate sound pressure response of classical guitars in the region of frequencies up to 6-800 Hz. In this range, the response spectrum is characterized by resonance peaks corresponding to vibrational modes of the top plate. We model guitar response as a superposition of contributions from single resonances. Each resonance is modelled as a harmonic oscillator, moving a piston and acting as a simple monopole radiator. We find that this simple model adequately describes guitar responses up to 6-800 Hz. Theoretical fits to response curves make it possible to determine for each resonance (oscillator) the ratio A/m (piston area to oscillator mass). The net sound radiated from the oscillator is proportional to this ratio. Data for five good classical guitars are presented. The implication of this work is, that guitar responses up to 6-800 Hz can be characterized by three parameters for four to six resonances instead of by raw data points.

Introduction

The sound radiated from the guitar is mainly generated by the vibrating top plate. One way to characterize a guitar is by measuring the sound pressure response for a sinusoidal constant-force excitation, usually applied to the bridge. The sound pressure response shows well-defined resonance peaks at frequencies from approx. 100 Hz up to about 6-800 Hz, depending on the individual instrument. Hologram-interferometric studies of the top plate have shown (Jansson, 1971) that the resonances correspond to characteristic modes of vibration of the top plate. For the lower resonances, the top plate vibrates in modes with few nodal lines as shown in Fig. 1. At higher frequencies, the sound pressure response from many overlapping resonances forms a 'resonance continuum' (Caldersmith, 1981) with a multitude of peaks and antiresonances. At these frequencies, the top plate vibrates in increasingly smaller subdivisions.

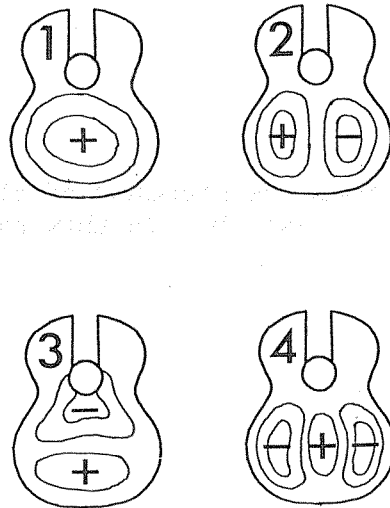


Fig. 1. The vibrational configurations of the four lowest top plate modes found in most classical guitars. Typical resonance frequencies are 200, 300, 400, and 500-550 Hz. Contours of the same vibrational amplitude are indicated. The relative direction of vibration (up/down) is indicated with plus and minus. The second resonance in the figure is a pure dipole. The third and fourth resonances contain both monopole and multipole radiation.

The purpose of this paper is to give an understanding of guitar sound pressure response in the region of frequencies up to 6-800 Hz where the response is characterized by resonance peaks.

We shall assume here, that each vibratory mode can be represented as a simple harmonic oscillator. The lowest top-plate mode is a pure monopole source of radiation. Modes with more nodal lines in general produce both multipole and net monopole radiation. Since multipole radiation is inefficient at lower frequencies, we only consider the monopole part of the radiation from each oscillator.

The first top-plate is a pure monopole source and is coupled to the Helmholtz resonance of the air cavity. We have earlier (Christensen and Vistisen, 1980) given a quantitative description of this system. In this paper, we focus on the response over a broader frequency range and sacrifice the more detailed description of the two lowest resonances. Thus, the lowest resonance at around 100 Hz is omitted and the second resonance at around 200 Hz is treated as if it is due entirely to the first top-plate resonance.

We present a simplified model of guitar response at frequencies up to 6-800 Hz. The theoretical concepts employed are the harmonic oscillator combined with the sound pressure response from a simple monopole source of acoustical radiation. We explore to which extent the frequency response from a classic guitar can be described by a superposition of responses from harmonic oscillators, each of which acts as a simple source of monopole radiation. Each oscillator is characterized by its resonance frequency and Q-factor together with the ratio of its effective piston area to effective mass as seen from the driving point.

Theory

The harmonic oscillator

The basic theoretical element in this paper is the simple harmonic oscillator which moves a piston and, hence, gives rise to acoustic monopole radiation. The oscillator might be thought of as a loudspeaker enclosed in a cabinet. Let x denote the distance of the piston from its equilibrium position. The oscillator, of mass m and with stiffness constant k , is acted upon by a force F according to Newtons second law:

$$m\ddot{x} = F - kx - R\dot{x}$$

where R is the resistance to motion. For a sinusoidally varying force,

the motion is also sinusoidal and the above equation can be solved for the oscillator velocity u

$$u = \frac{F}{m} \frac{i\omega}{(\omega_0^2 - \omega^2) + i\gamma\omega} \quad (1)$$

Here, the resonance frequency f_0 is given by $\omega_0 = 2\pi f_0$, $\omega_0^2 = k/m$ and γ equals R/m . In terms of the Q-factor $\gamma = 2\pi f_0/Q$.

The moving piston acts as a source of monopole radiation. At a distance r from the source, the magnitude of sound pressure is given by

$$p = - \frac{i\omega\rho}{4\pi r} uA \quad (2)$$

where ρ is the density of air (1.205 kg/m^3). The variation of phase with distance from the source is not important for the present purpose. Using the piston velocity from Eq. (1) we obtain for the sound pressure:

$$p = F \frac{A}{m} \frac{\rho}{4\pi r} \frac{\omega^2}{(\omega_0^2 - \omega^2) + i\gamma\omega} \quad (3)$$

At a given distance, the sound pressure is proportional to the ratio of piston area to mass A/m . The last factor accounts for the frequency variation. The pressure is positive for $f \ll f_0$ and negative for $f \gg f_0$. For low frequencies, the magnitude of the sound pressure is proportional to f^2 whereas at high frequencies, the response becomes constant, proportional to A/m .

The real guitar

The guitar is a vibratory system characterized by many resonances. The lowest resonances typical for most classic guitars are shown in Fig. 1. In the measurements presented here, the guitar was excited by a

constant force transducer at the center of the bridge. Each of the resonances may be characterized by an effective piston area and an effective mass. For the more complicated vibrational configurations as, for instance, modes no. 3 and 4 in Fig. 1, some parts of the top plate move 180 degrees out of phase with the point of excitation. In such cases, the effective monopole piston area is defined as the area which, when moving with the velocity of the point of excitation, produces the actual net volume displacement of the source. Mathematically speaking, this relation may be formulated as:

$$A_i u_{exc} = \int_{\text{guitar face}} u_i(x,y) da \quad (4)$$

where $u_i(x,y)$ is the velocity of the point (x,y) of the guitar top plate for the i 'th resonance and where u_{exc} is the velocity at the point of excitation.

It follows that the effective piston area can be negative, i.e., that the net volume displacement takes place at a phase opposite to that of the point of excitation. Indeed we shall show that the great variability in guitar response curves for different guitars is due to various combinations of positive and negative piston areas.

The effective mass of a particular mode depends upon the position of the exciter. If the exciter is placed close to a nodal line, the effective mass of that mode becomes large. The ratio A/m may therefore change drastically when the point of excitation is changed.

The sound pressure from the i 'th resonance is a function of A_i/m_i , f_{oi} , and Q_i , i.e., $p = p(f, A_i/m_i, f_{oi}, Q_i)$. Therefore the total sound pressure from the guitar - not counting multipole radiation - is given as

$$P_{tot}(f) = \sum_i p(f, A_i/m_i, f_{oi}, Q_i) \quad (5)$$

Since the contribution from one oscillator grows as f^2 and reaches a constant level above resonance, it follows that at any frequency f , the sound pressure is mainly determined by oscillators for which $f_{oi} \leq f$. In

fitting a series of oscillators to describe a measured sound pressure response, one can start by fitting the first oscillator, then the second oscillator etc. because the contribution from oscillators at higher frequencies is marginal due to the f^2 -dependence of response below resonance.

Theoretical examples

In the following we will give some theoretical examples on sound pressure response curves resulting from the superposition of two and three oscillators. The first resonance, at the lowest frequency, represents the first top plate mode of the guitar which corresponds to the second resonance of the guitar. The ratio of the effective top plate area to mass has been chosen to be largest for this resonance, in accordance with the experimental findings presented later.

The two-oscillator case

The contribution to sound pressure from a resonance is positive below resonance and negative above resonance. Thus, for two resonances with the same sign of the piston area, the contributions of the oscillators tend to cancel each other between resonances, leading to an antiresonance between the two resonances, as shown in Fig. 2. The antiresonance occurs close to the cross-over frequency of the individual response curves. Above the highest resonance the two modes vibrate in phase and, therefore, reinforce each other.

If the two oscillators have the opposite sign of the piston area, the response is increased between the resonances since the phase of both oscillators is the same here. Above the highest resonance, the contributions from the two oscillators tend to make them cancel each other and an antiresonance occurs close to the cross-over frequency of the individual response curves. If, however, the two oscillators have opposite sign of

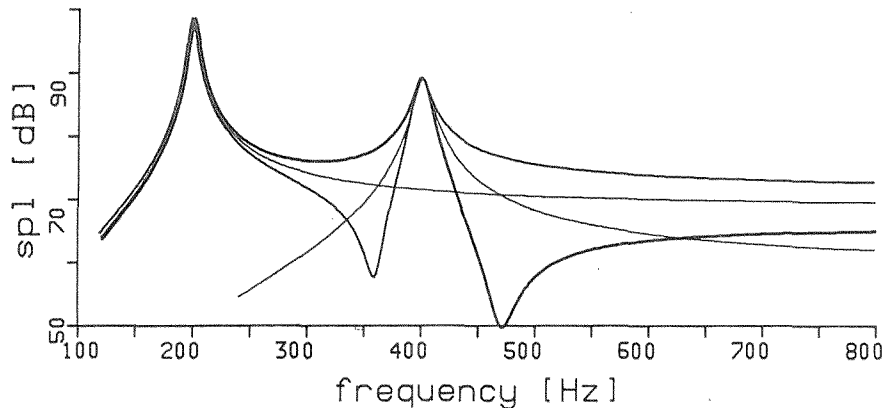


Fig. 2. Sound pressure response from two superposed oscillators. The oscillators have resonance frequencies of 200 and 400 Hz and A/m values of 6 and 2 cm^2/g . The Q -factors of both oscillators are 30. The thin lines give the contributions of the individual oscillators. The medium-heavy line (antiresonance between resonances) shows the response when both piston areas are positive. The heavy line (antiresonance after second resonance) shows the response when the second piston area is negative. The sound pressure is calculated at a distance of 1 m with an exciting force of 1 N.

piston area and if the A/m -ratio of the first one is sufficiently small, there is no antiresonance after the second resonance. Such a case is seen if one tries to fit the two first resonances of a guitar, i.e., the coupled Helmholtz and first top plate resonances.

The three-oscillator case

In Fig. 3 the sound pressure response is shown for a system of three oscillators. There are four possible nonidentical combinations of signs of the piston areas. The individual curves of Fig. 3 can all be understood from the previous two-oscillator case. The piston area of the first resonance at 200 Hz is chosen positive. The structure around the second resonance at 400 Hz is understood from the position of the antiresonance which occurs before the peak if the piston area is positive and after the peak if the piston area is negative. At 600 Hz, the combined

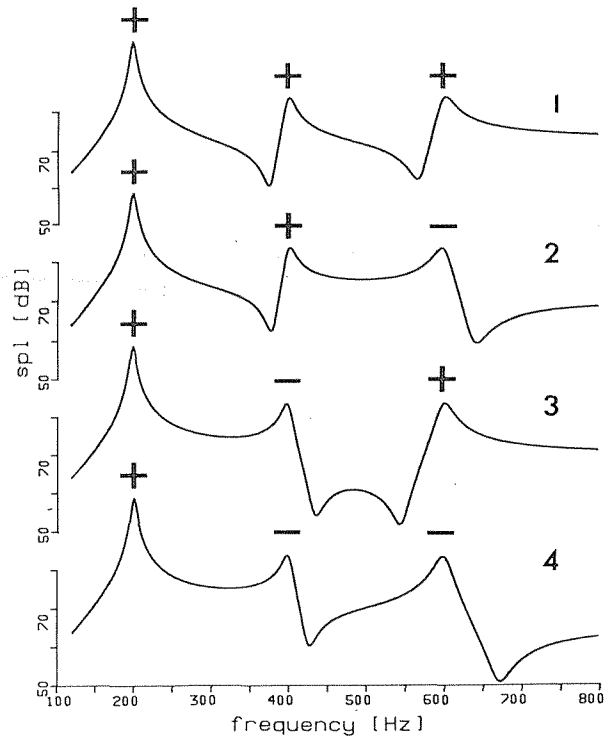


Fig. 3. Sound pressure response from three superposed oscillators. The oscillators have resonance frequencies at 200, 400, and 600 Hz. The Q -factors of all oscillators are 30 and the A/m -ratios of the oscillators are 6, 1 and 1 cm^2/g . The four response curves represent situations with different combinations of the signs of the three piston areas, as indicated above each resonance peak. The sound pressure is calculated at a distance of 1 m with an exciting force of 1 N.

two first resonances act roughly as one piston, since the response of an oscillator approaches a constant level at frequencies well above resonance. The structure around the third resonance is, thus, again explained by the position of the antiresonance.

The situation represented by the top curve in Fig. 3 has - to the author's knowledge - never been seen in a guitar. The situation in the

second curve from the top is found in guitars with a pronounced second resonance, cf. Fig. 1. The three peaks in the curve represent then the first, second, and third top plate modes. The third curve from the top represents a rather undesirable situation in which two antiresonances fall in-between two neighbouring resonances and create a region of poor acoustical response. The bottom curve shows a situation found in guitars with a second top-plate resonance which not is excited when the exciter is positioned at the center nodal line of this mode, see Fig. 1. The resonances in this curve correspond to the first, third, and fourth top plate modes in most classic guitars.

Thus, many qualitative features of guitar response curves may be understood from this simple model of superimposed harmonic oscillators. The variability of response curves is brought about by the combinations of different signs of piston area of the individual resonances.

Experimental details

Measurements

The sound pressure response curves for the five guitars studied here were measured as described earlier (Christensen and Vistisen, 1980) in an anechoic chamber. The sound pressure level was measured 2 m above the guitar top plate. The exciting force of approximately 0.2 N was applied to the center of the bridge. Response curves for the five guitars are shown in Fig. 4. In order to facilitate comparisons with theoretical calculations, the sound pressure response curves were scaled to represent values at 1 m distance from the guitar for an exciting force of 1N.

The instruments

The guitars used in this study were all handcrafted instruments with spruce top plates. All guitars have rosewood back and sides with the exception of no. 3, which has cypress back and sides. Further details of the instruments are listed below.

- 1) Ramirez: The bracing has a diagonal bar crossing the transverse bar below the soundhole and running down on the treble side of the top plate; serial no. 4.952, Madrid, 1971.
- 2) Ibanez: This is essentially a Japanese version of a Ramirez guitar; bracing as described on guitar 1.
- 3) Taurus: Traditional Torres bracing; serial no. 56, Barcelona, 1967.
- 4) Contreras: Flamenco guitar with traditional Torres bracing; Madrid, ca. 1977.
- 5) Romanillos: Torres bracing with transverse thin plate about the size of the bridge plated below the bridge; serial no. 224, England, 1978.

Results and discussion

Theoretical response curves from superposed harmonic oscillators were fitted to experimental response curves as shown in Fig. 4. The initial data used in theoretical calculations were the resonance frequencies from the experimental response curves together with tentative estimates of their Q -factors. The signs on the piston areas of the resonance peaks were initially chosen from a judgement of the position of the antiresonances as described in the preceding chapter. The magnitudes of the A/m -ratio for the resonances and the final Q -factors were adjusted to obtain the visually best fit of the calculated response to the experimental one as judged from a plot of these curves.

The calculated response curves are shown in Fig. 4 together with the measured responses. The data used in the calculations are shown in Table 1.

In general, there is a good agreement between calculated response curves and measured ones over a large part of the frequency region studied. The oscillator model explains the structure of the response curves and even provides a good quantitative agreement. No fit was attempted

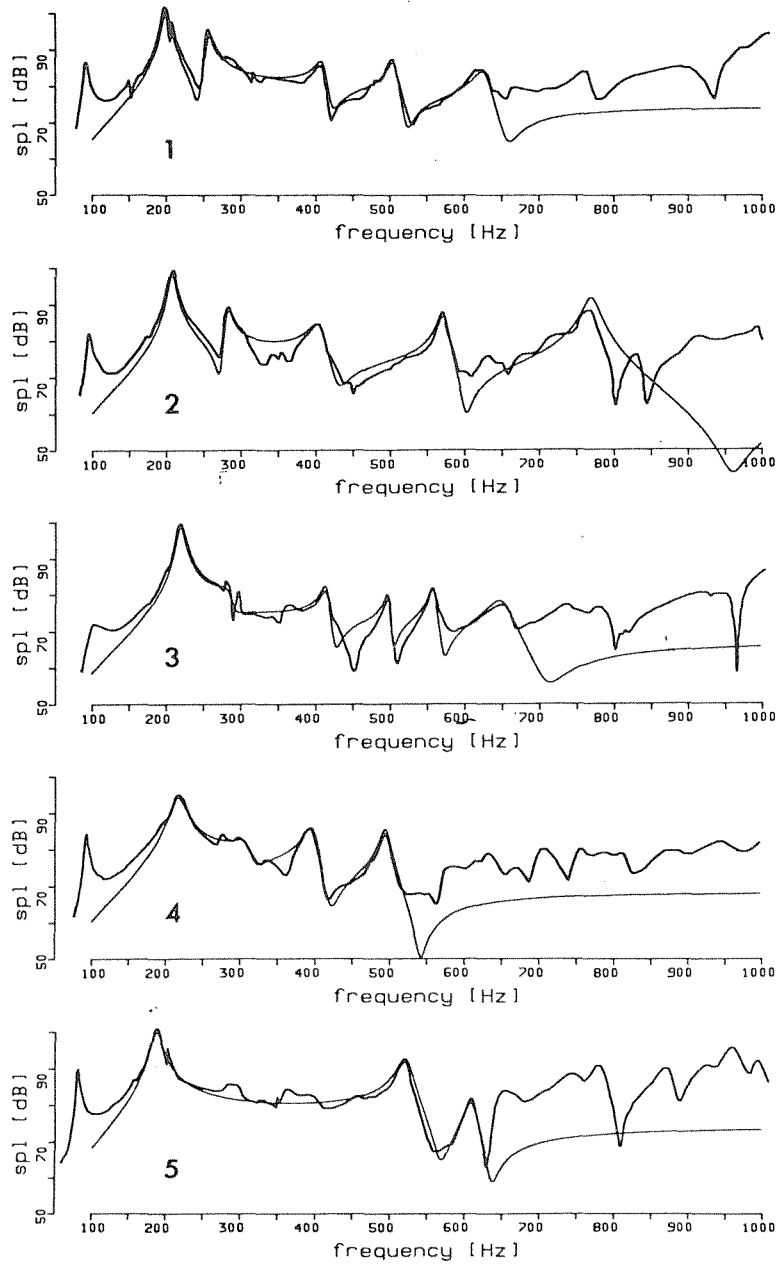


Fig. 4. Comparison between measured sound pressure responses and calculated ones for five guitars. Thin lines are calculated responses and heavy lines are experimental ones. All curves are scaled to apply for an exciting force of 1 N at a distance of 1 m from the guitar top plate. The oscillator parameters used in the calculation are shown in Table 1.

Table 1. Oscillator parameters used in calculating the theoretical response curves in Fig. 4.

Guitar	f_0 (Hz)	Q	A/m (cm^2/g)	top-plate mode
1:Ramirez	200	25	10.	1
-	257	25	4.	2
-	410	30	-1.2	3
-	506	40	-1.0	4
-	627	30	-1.0	?
2:Ibanez	208	25	7.	1
-	282	35	1.5	2
-	405	20	-1.5	3
-	572	50	-1.0	4
-	770	40	-2.0	?
3:Taurus	220	25	7.5	1
-	285	15	-0.8	2
-	415	40	-0.6	3
-	498	70	-0.25	4
-	559	60	-0.4	?
-	650	20	-0.8	?
4:Contreras	216	12	9.0	1
-	310	15	-1.	2
-	395	25	-1.5	3
-	495	40	-1.0	4
5:Romanillos	187	15	14.0	1
-	522	30	-3.0	4
-	610	50	-0.5	?

below 150 Hz because the structure of the two first resonances - at approximately 100 and 200 Hz - has already been explained quantitatively as a result of a coupling between the Helmholtz and first top plate resonances (Christensen and Vistisen, 1980). Only the highest of these resonances is taken into account because the aim of this work is to test if response curves may be fitted to the superposed oscillator model rather than to give a detailed account of the nature of each resonance.

Above 600-800 Hz it was not possible to fit the sound pressure response by superposed oscillators. At these 'high' frequencies there is no structure characteristic of resonances. It is known from hologram-interferometric studies (Jansson, 1971; Firth, 1977) that resonances at high frequencies still may be characterized by simple geometric patterns, as the ones in Fig. 1, but with an increasing number of nodal lines on the guitar top plate. The net monopole radiation from such resonances decreases while at the same time multipole radiation becomes more efficient. Caldersmith (1981) has characterized this region of guitar response as a 'resonance continuum' with a strong directional dependence of the radiated sound.

In contrast, the region of frequencies studied here (up to 6-800 Hz) is characterized by strong sources of net monopole radiation - air 'pumping' modes - with little directional dependence.

Table 1 gives a list of the parameters used in the fitting to the measured response curves. Each resonance is given a tentative assignment to a corresponding top plate mode. Such an assignment is based on the author's investigation of the mode structure at resonance of many guitars. No such specific assignment was undertaken of these instruments. For the low-order top plate modes assigned here, there is little doubt of the correctness of the assignment which follows the one observed in a number of hologram-interferometric studies (Jansson, 1971; Firth, 1977; Schwab, 1975).

Comments to Table 1

The first top-plate mode at around 200 Hz has piston area to mass ratios ranging from 7 to 14 cm²/g. These values are slightly higher than the ones found from an analysis of the two lowest resonances (Christensen

and Vistisen, 1980) because we have not accounted for the Helmholtz resonance. The A/m -ratio for the first top-plate mode is almost one order of magnitude larger than for the higher resonances. The contribution to sound pressure from one oscillator approaches a constant at high frequencies. Therefore, the magnitude of the A/m -ratio for the first top-plate mode is important for the behaviour at high frequencies too. If $(A/m)_1$ is reduced by a factor of two, the sound pressure level is reduced by about 3 dB between the higher resonances. The sound pressure level between the resonances is rather important. The partials of a tone which fall in-between the resonances have a longer sustain, because the energy of the vibrating string is drained very fast in the vicinity of the resonances.

The second top-plate mode at 260-310 Hz is usually a pure dipole in guitars with a symmetrical bracing (see Fig. 1) but it can be turned into a strong monopole source if the bracing is nonsymmetrical. Guitars no. 3 and 4 have symmetrical bracing and, accordingly, we find that the second top-plate mode is characterized by a rather small negative A/m -ratio and a poor Q -factor, probably because this mode is excited very close to the center nodal line. As seen from Fig. 4, this mode is rather insignificant and for guitars no. 3 and 4 it has only been accounted for because it gives a small 'cosmetic' improvement of the fit to the measured response. On the contrary, guitars no. 1 and 2 with nonsymmetrical bracing show a strong monopole contribution from the second top-plate mode with a relatively large positive A/m -ratio and a fairly high Q -factor.

The third top-plate mode occurs close to 400 Hz and is probably coupled to the half-wave longitudinal resonance in the air cavity. For all instruments studied, this resonance had a negative A/m -ratio. This is also the case for all of the higher-order resonances. A probable reason for this is, that for the higher-order modes, most of the motion takes place at the outer lobes of the top plate because the center is made stiff by the presence of the bridge.

The fourth top-plate resonance can be identified in all guitars studied. It occurs at 500 to 570 Hz. For all but one guitar, it was possible to identify at least one additional resonance at higher frequencies before the sound pressure response approaches a resonance continuum with no characteristic resonance peaks.

In conclusion, we find that the first four top-plate resonances account for the sound pressure response up to about 600 Hz. In addition, there might be higher air-pumping resonances up to about 800 Hz. At still higher frequencies - in the 'resonance continuum' - it is not possible to fit guitar sound pressures by the present model.

Conclusion

The purpose of this paper was to explain the sound pressure response curves for the classical guitar. This aim has been reached to the extent that we now have a qualitative understanding of response curves. The simple principles outlined in the sections on 'the two-oscillator case' and 'the three-oscillator case' show that the behavior between resonances can be explained from an understanding of the harmonic oscillator piston. The very different behavior obtained between the resonances (see Figs. 2 and 3) is due to the different combinations of the signs and the magnitudes of piston areas for different vibrational modes and are, hence, related to the vibrational structure of the top-plate modes.

Qualitatively we have shown that guitar response curves may be accounted for up to 6-800 Hz by superimposing responses from harmonic oscillators, each of which acts as a simple source of monopole radiation. Each oscillator corresponds to a resonance peak in the response curve. The correspondence obtained between measured response curves and model calculations implies that the response up to 6-800 Hz is dominated by monopole radiation, mainly contributed by the first four top-plate resonances.

Recently we have found (Christensen, 1983) that most of the acoustical energy present in long-time-average spectra of played classical guitar music originates from the frequency region 200 to 800 Hz. It follows that the region, which contributes mostly to the radiated acoustical energy, is dominated by radiation from monopole sources. Further progress in guitar making may, thus, be achieved by devising practical methods to tune the top plate to provide good responses at the first four top plate modes.

Understanding sound pressure response curves have some implications:

It is much easier to characterize a guitar by the parameters of some four to six harmonic oscillators than by the frequency response curves. This is particularly useful in comparing different instruments because the subjective impression of quality may be correlated to oscillator parameters. One can in this way gain an understanding of the physical characteristics that are desirable from a subjective impression of instrument quality.

It is interesting to note that in principle the mode frequencies and vibration amplitudes of a given top plate may be computed theoretically (Schwab, 1976). Except for Q-factors, such a computation could give information about the A/m-ratios and resonance frequencies for a given top-plate design. The present model could then be used to calculate the sound pressure response curve. This would be particularly fruitful if one at the same time had a subjective quality evaluation based on oscillator parameters.

Acknowledgments

The author is grateful to Graham Caldersmith for drawing his attention to the occurrence of negative piston areas.

References

- Caldersmith, G. (1981): "Physics at the workbench of the luthier", Catgut Acoust.Soc. Newsletter No. 35, 15,
- Christensen, O. (1983): "The response of played guitars at middle frequencies", *Acustica* 52,
- Christensen, O. and Vistisen, B.B. (1980): "Simple model for low-frequency guitar function", *J.Acoust.Soc.Am.* 68, 758.
- Firth, I. (1977): "Physics of the guitar at the Helmholtz and the first top-plate resonances", *J.Acoust.Soc.Am.* 61, 588.
- Jansson, E.V. (1971): "A study of acoustical and hologram interferometric measurements of the top plate vibrations of a guitar", *Acustica* 25, 96.
- Schwab, H.L. (1975): "Finite element analysis of a Guitar Soundboard", Catgut Acoust.Soc. Newsletter No. 24, 13.
- Schwab, H.L. (1976): "Finite element analysis of a Guitar Soundboard - Part II", Catgut Acoust.Soc. Newsletter No. 25, 13.

ON THE ACOUSTICS OF THE CONCERT HARP'S SOUNDBOARD AND SOUNDBOX
I.M. Firth and A.J. Bell
University of St. Andrews, St. Andrews, Fife, Scotland

Abstract

The complete concert harp soundboard comprises of the actual tapering spruce plate with two central beech "supporting" bars and two spruce "harmonic" bars placed on either side. Measurements will be presented to show how the dimensions of the plates affect the primary resonances. For the free plate, families of planar and torsional modes can be distinguished. With the plate clamped to the soundbox the modes are monopole, dipole etc. and their exact shape and frequency can be influenced by the dimensions of the board.

The acoustics of the harp is a relatively new field of research. Firth produced the first paper in 1977; though his work was on the clarsach, the small harp native to Scotland. It has only been since 1981 that the concert harp has been studied (Bell, 1981).

There are four main parts to the concert harp (Fig. 1) - the soundbox, the string arm, the forepillar and the base. This model, the Salvi "Orchestra" harp, has forty-six strings ranging in pitch from 34 Hz to 3136 Hz. The pedals in the base are part of the tuning mechanism. Depressing one moves a complex system of rods inside the forepillar and the string arm. The rods twist studded brass plates onto particular strings thereby shortening its vibrating length and raising its pitch. Two discs to each string ensure that any string's pitch can be raised by one or two semi-tones. This flexibility enables the harp to be tuned to any chromatic key (Rensch, 1969).

The soundbox should be considered like a guitar or violin body. There is a series of taught strings vibrating into a flexible soundboard, fastened to a fairly rigid box that encloses an air volume. There are apertures in the soundbox; these are at the rear of the box; their original purpose was to help to string the instrument - they do, however, act as Helmholtz resonators.

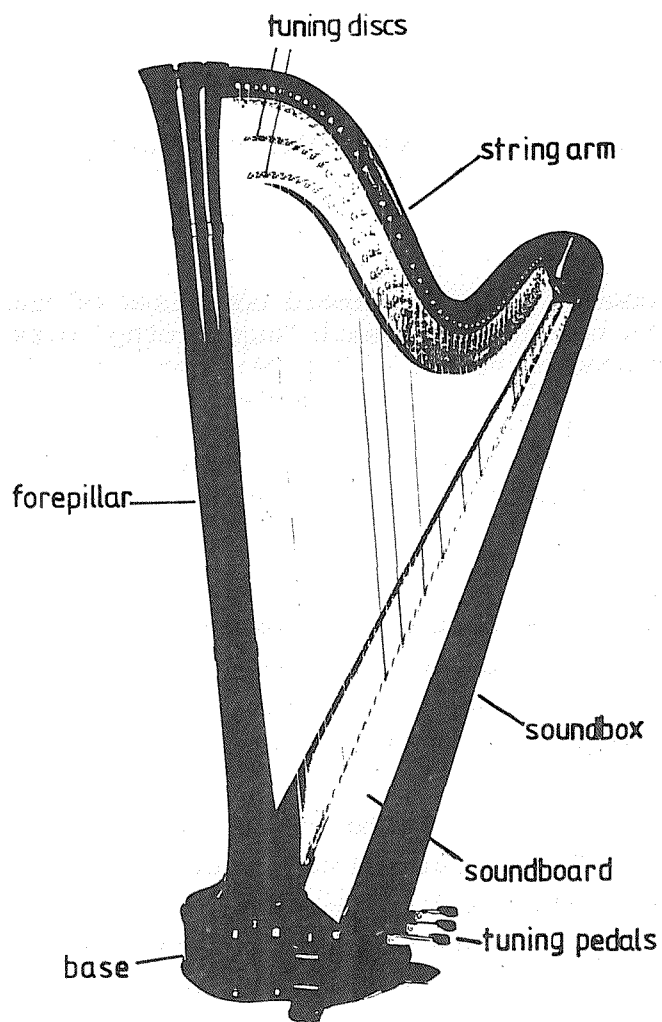


Fig. 1. Main parts of the concert harp.

The soundboard is usually of European spruce (*Picea Excelsis*) quarter-sawn with the wood grain running across the board (Fig. 2). The front of the board has a thin veneer, again of spruce. The board narrows from the bass end to the treble, it also thins in the same direction.

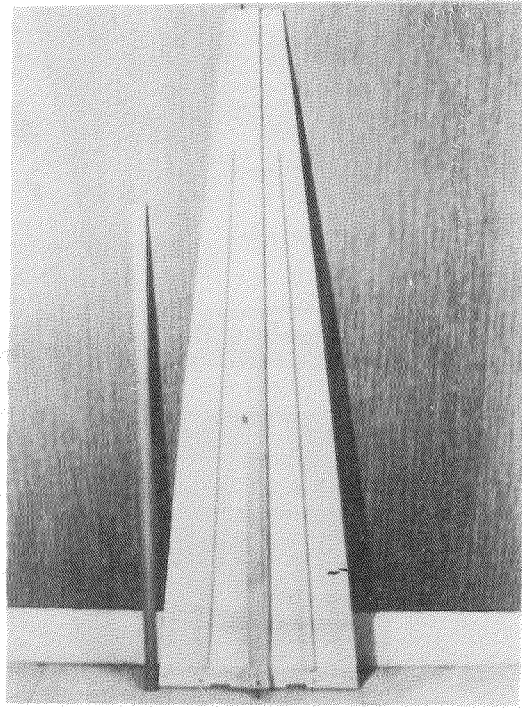


Fig. 2. The harp soundboard. Typical dimensions are
length 136 cm
width (at bass) 44 cm thickness (at bass) 12 mm
width (at treble) 12 cm thickness (at treble) 2 mm

There are two central bars on the board; these are made from beech wood. On the front is the cover bar, while on the back is the larger reinforcing bar.

There are two other bars on this side of the board; these are the harmonic bars. These are small, light and positioned on either side of the reinforcing bar. They bear little of the tension from the strings. We will return to their effect on the harp's performance later.

We should begin our acoustical study by considering the free sound-

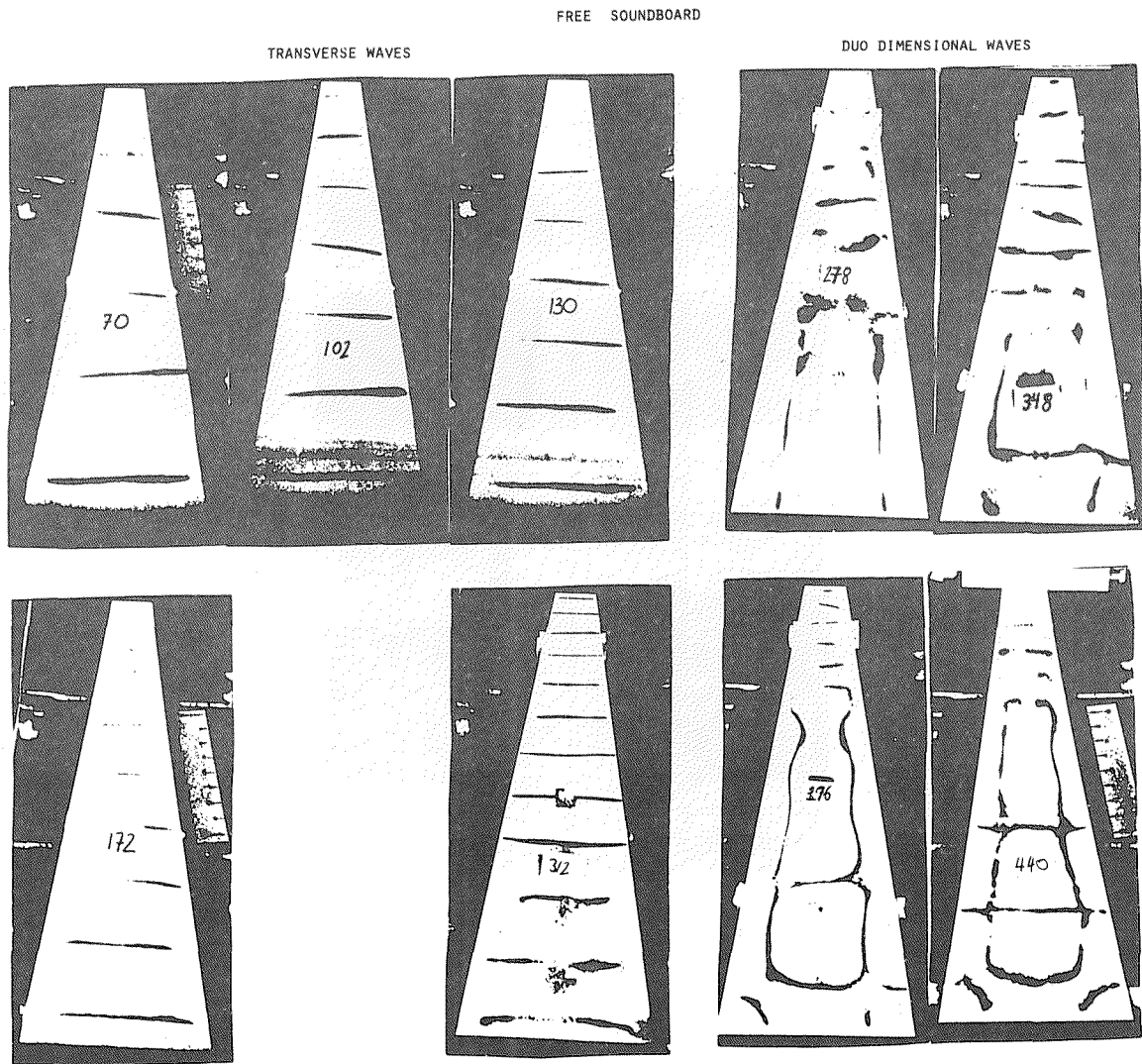


Fig. 3. Chladni patterns of free unbarred tree soundboard plate.

board's vibration characteristics. Fig. 3 shows some Chladni patterns for the unbarred plate. At the lowest frequencies the board bends only along one direction so the nodal lines are across the board. As a group these are referred to as the transverse modes. At higher frequencies the vibrations are along and across the board and the net effects are these round nodal patterns, which become more complex with increasing frequency.

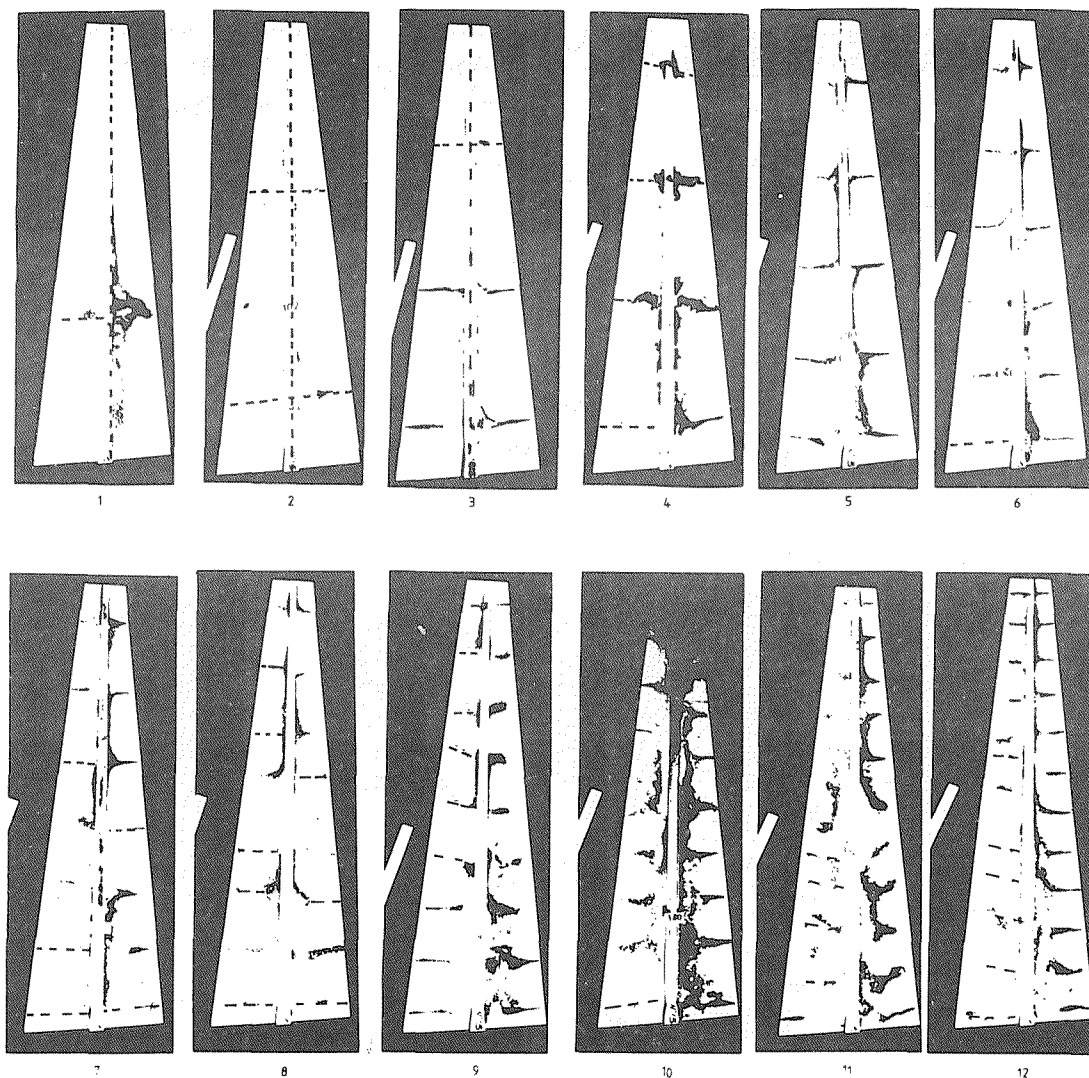


Fig. 4. Chladni patterns of free soundboard plate with central bars - torsional modes.

The frequencies are at the modes

no. 1	65 Hz;	no. 5	210 Hz;	no. 9	341 Hz;
no. 2	102 Hz;	no. 6	245 Hz;	no. 10	380 Hz;
no. 3	135 Hz;	no. 7	277 Hz;	no. 11	422 Hz;
no. 4	176 Hz;	no. 8	310 Hz;	no. 12	457 Hz.

With the central bars fitted to the soundboard the resonant patterns change (Fig. 4). This is one important group of resonances, called the

torsional modes, which all have a nodal line at the central bars. Of the first twenty resonances on the barred soundboard thirteen of them are torsional. An important point is that these resonances are harmonic. This can be seen more clearly if we consider a graph of resonant frequency against resonance number; the line joining these points is straight (Fig. 5).

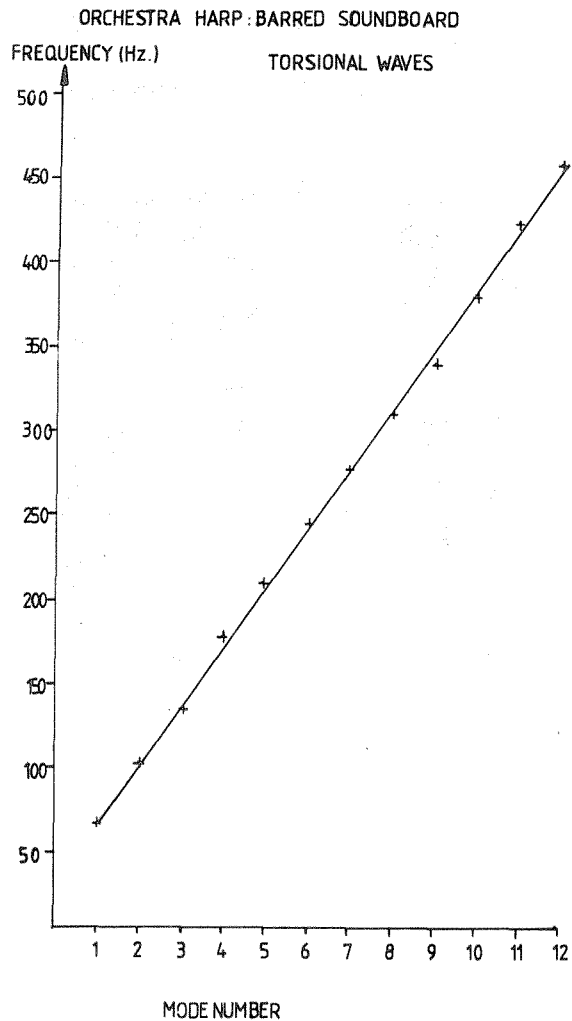


Fig. 5. Resonance frequencies of barred soundboard - torsional modes.

Apart from the torsional modes there are other families of resonances (Fig. 6). The first group occurs on low frequencies and are a combination of the transverse modes, which we have seen before on the unbarred board and the torsional modes. The next group of patterns show resonances with vibration both along and across the board; the central bars

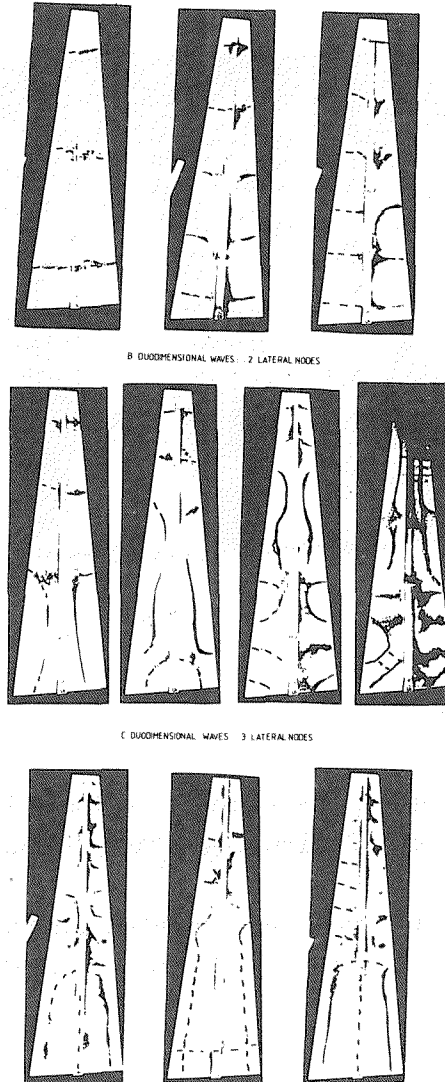


Fig. 6. Chladni patterns of free soundboard plate with central bars - transverse mode. Frequencies are
 A: 122 Hz, 227 Hz, 267 Hz
 B: 200 Hz, 285 Hz, 366 Hz, 410 Hz
 C: 505 Hz, 655 Hz, 527 Hz

being at a position of antinode. With increasing frequency the vibration across the board "creeps" up the soundboard. This last row of patterns shows resonances with three nodal lines across the board.

The next stage is to attach the soundboard onto the soundbox. Fig. 7

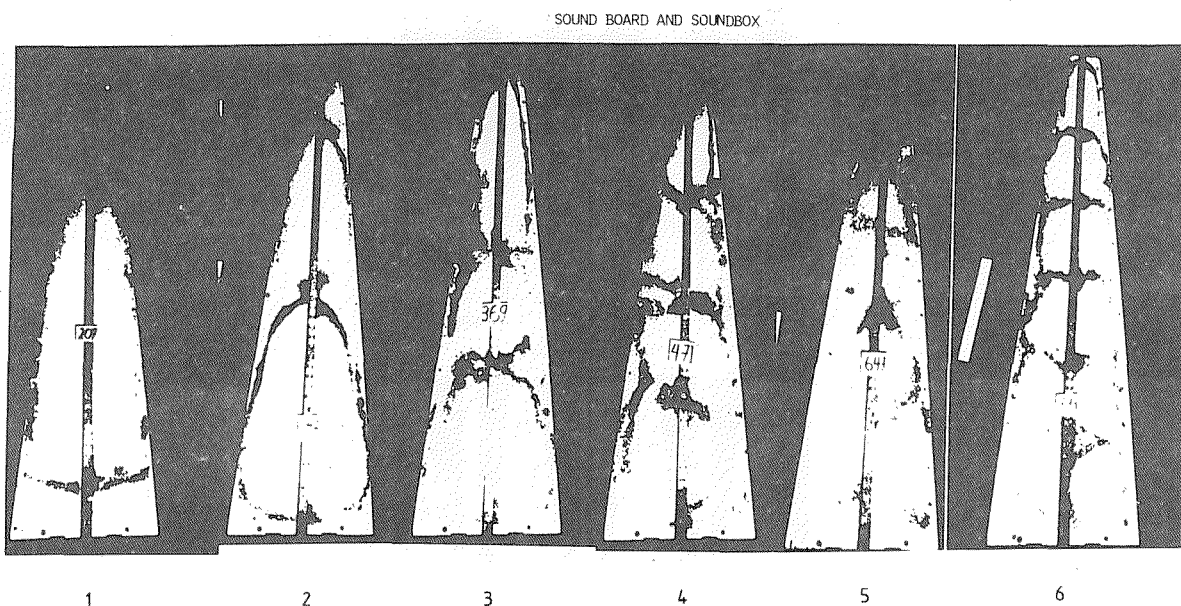


Fig. 7. Chladni patterns of soundboard on soundbox.

shows the resonant modes of the fixed soundboard; its edges are almost nodal and we have a series of diaphragmatic resonant patterns.

These Chladni patterns serve as a useful introduction to harp acoustics but the results are limited. The next stage is to determine the harp's input admittance.

In Fig. 8 we see our equipment set up to do this. The soundboard has been clamped to a heavy wooden jig to simulate the effects of being fitted to the soundbox. The shaker with an impedance head are fixed to a slide on this heavy, sand-filled, iron bar and can be moved along the length of the soundboard. Using the signal generator and compressor circuits of the Heterodyne analyser (B+K2010) we can ensure a constant

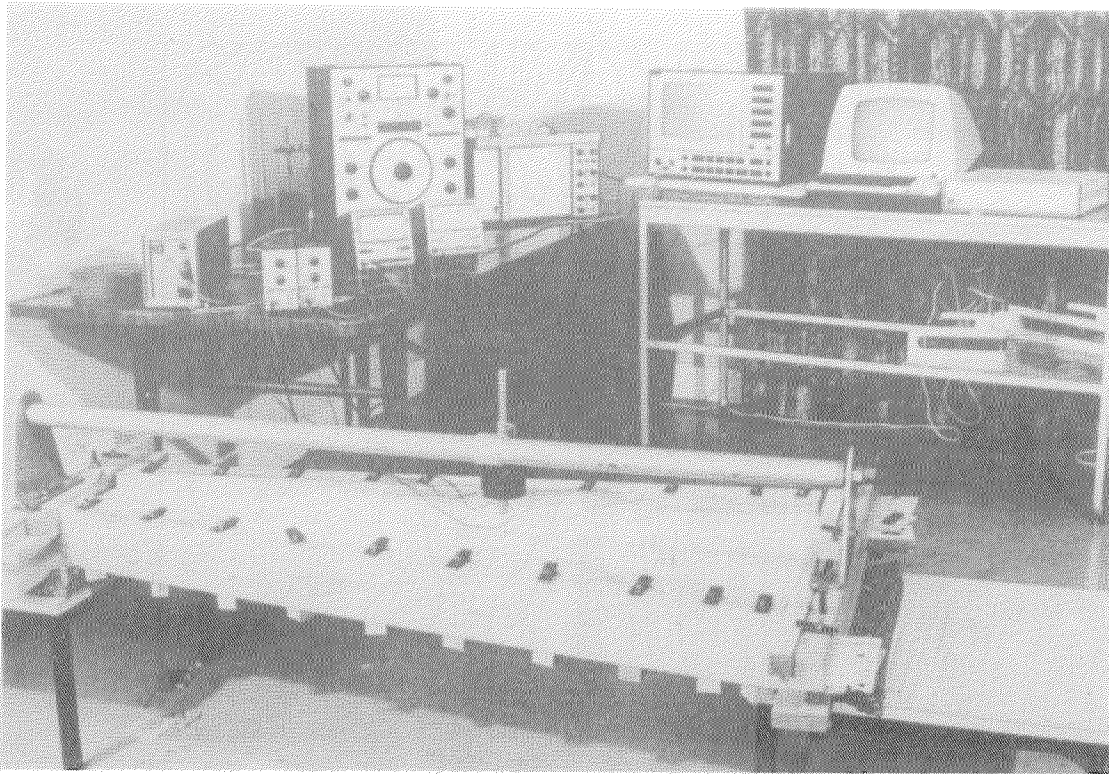


Fig. 8. Experimental equipment for recording of input admittance.

excitation force as the shaker is swept through a frequency range. As we sweep, the board's velocity is measured and recorded, in a digital form, on a High resolution frequency analyser (B+K2033). Any number of admittance measurements can be transferred to a computer for storage and processing (B&K, 1980). Normally the shaker is positioned on the central bar of the soundboard. By conducting twenty of these tests one can determine the soundboard's admittance along its length.

In order to present our data in a simple clear form we have found that the best method is in the form of a contour map (Fig. 9): the Y-component of the map is in position along the soundboard from bass at the lower end to treble at the top. The X-component is frequency from 50 Hz to 500 Hz, and the contour lines link points with the same admittance value (in dB). The first, second, third, fourth and part of the fifth soundboard resonances can be clearly seen as ranges of well-defined peaks on the admittance plot.

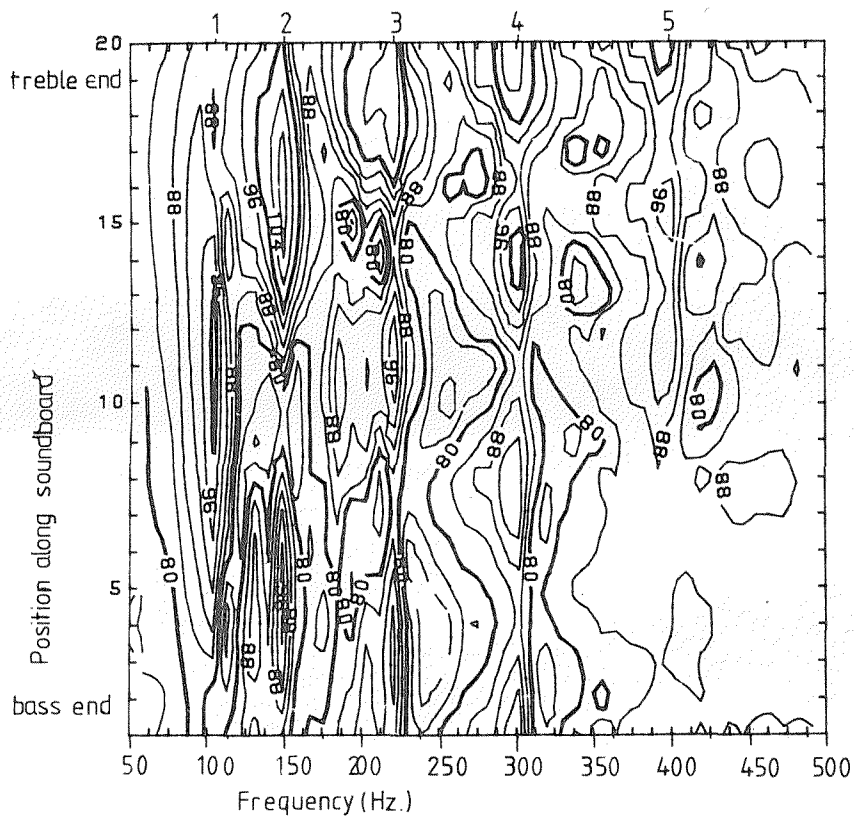


Fig. 9. An example of admittance contour maps of an orchestra soundboard. 110 dB = 1 s/kg.

Having introduced the harp and two techniques used to study it, we should go on to discuss some of our experiments. These deal with the effect the dimensions of the soundboard have on the harp's resonant format.

When the harp was introduced it was mentioned that the harp soundboard thins from the bass end to the treble. We wanted to ascertain how the resonant vibrations of the soundboard changed as the soundboard's thickness was increasingly tapered.

We began with an almost uniformly thick soundboard and conducted admittance tests as the board's thickness was gradually tapered; the results are shown in Fig. 10. By considering the last contour map first, one can see the characteristic resonant patterns of a normal soundboard with its edges held. But in the first admittance map the pattern is quite different. Resonances occur, but each occurs at only one partic-

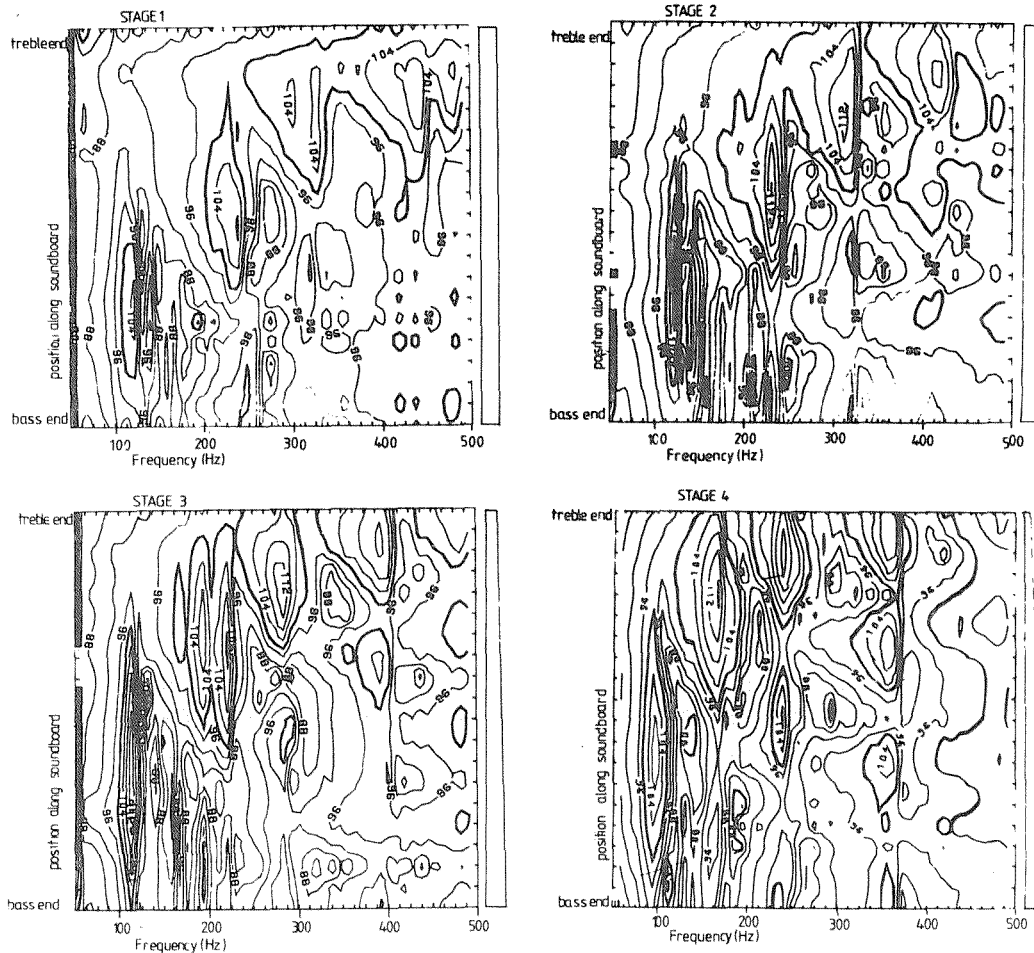


Fig. 10. Results of thickness tapering experiments. Admittance contour maps at stage 1 = 12 mm all over, stage 2 = 12 mm (bass) tapering to 9 mm (treble), stage 3 = 12 mm tapering to 5 mm, and stage 4 = 12 mm tapering to 2 mm.

ular region in position and frequency. For example, the lower three oscillatory regions of the fourth resonance, which can be seen quite clearly on the final plot, are invisible on the first. To exaggerate this change one could say that the soundboard changes from vibrating like a stiff bar to vibrating like an elastic membrane.

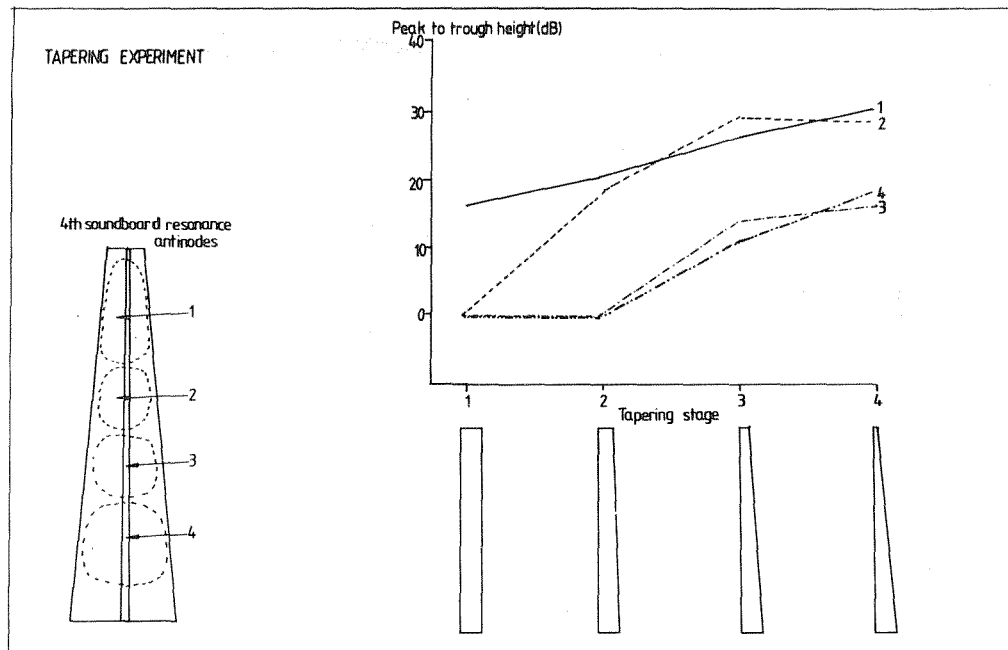


Fig. 11. Thickness tapering experiment. Peak to Trough heights of antinodes of 4th soundboard resonance against tapering stage. Tapering stages 1 through 4.

One way of representing this emergence is to plot the peak to trough height of one of the resonance antinodes. Here is such a plot for the fourth soundboard resonance (Fig. 11). Initially the lowest three antinodes have a Peak to Trough height of zero; they cannot be seen. But as the board's thickness is tapered, the antinodes emerge and the Peak to Trough heights can be measured. In a similar experiment to this we

wanted to discover how the soundboard's resonances were dependent on the board's width. We began with a very wide soundboard - its thickness had the usual tapering and took admittance measurements as it was narrowed. Fig. 12 shows the initial size of the soundboard, and the final size; a

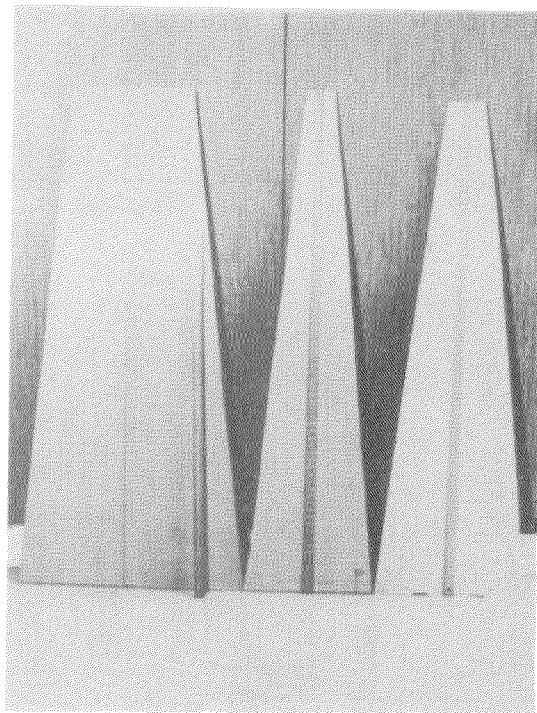


Fig. 12. Width of experimental soundboard, initial (70 cm at the bass and 38 cm at the treble) and final (36 cm at the bass and 4 cm at the treble) and a normal soundboard.

normal soundboard is also shown for comparison. Some of the admittance plots are shown in Fig. 13. With the very wide board the resonances are situated at the low frequency end of the map. Narrowing the board makes it stiffer and the resonant frequencies increase; we gain a board with a wide frequency distribution of resonances. This distribution can be shown on a graph of resonant frequency against soundboard width (Fig. 14). The fourth resonance's frequency increases more than the first resonance; the result is a wide distribution of resonances. On the harp with its wide string pitch range, a wide frequency distribution of resonances is an

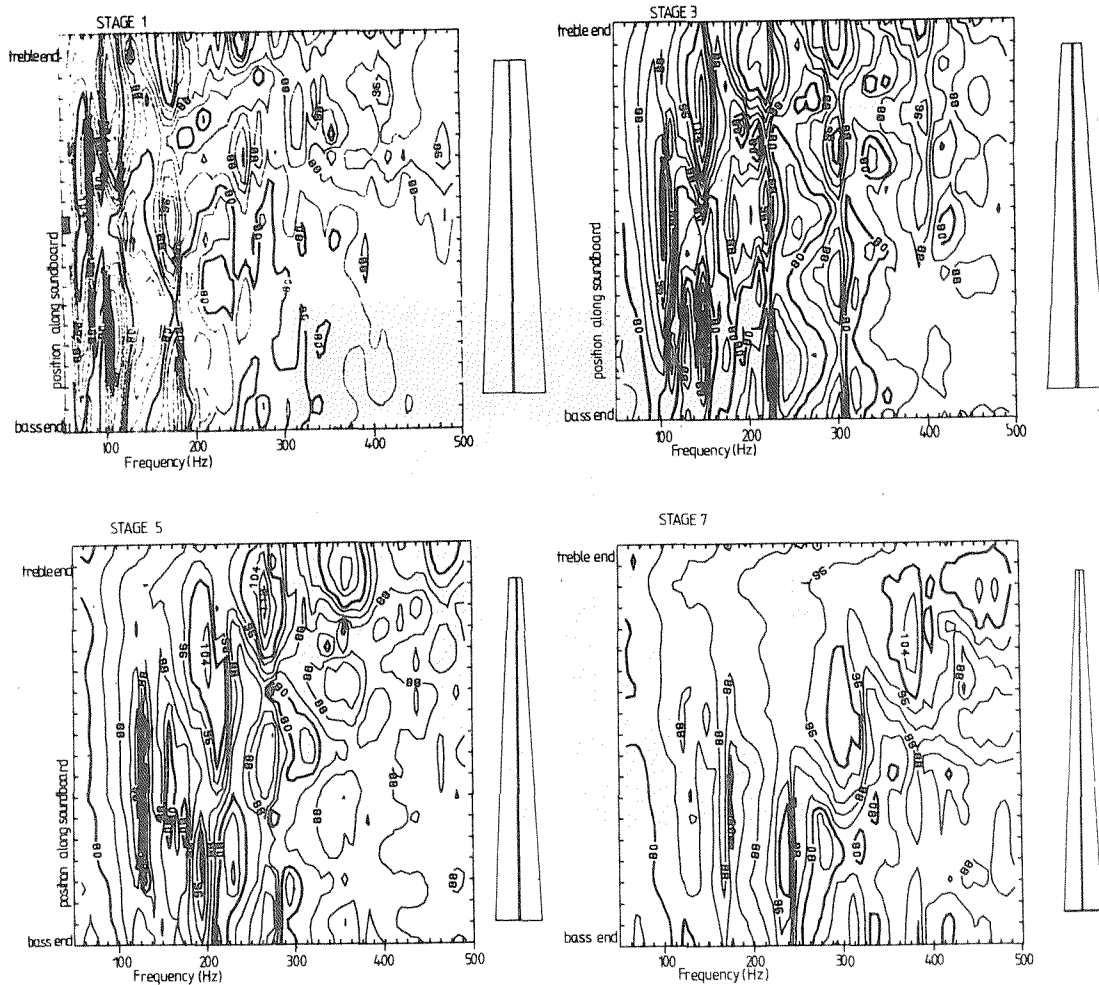


Fig. 13. Soundboard with narrowing experiment.
Admittance contour maps at four stages.

advantage. There is a limit as to how far one can narrow the board as it becomes too rigid. With dimensions just two cm thinner than a normal soundboard the resonant pattern becomes like that of a rigid bar.

To conclude, we should return to the subject of the harmonic bars (Fig. 15). These two plots show the resonant formats without and then with the harmonic bars fitted to the board. Two small changes can be seen. The bars have added stiffness to the board so the resonant fre-

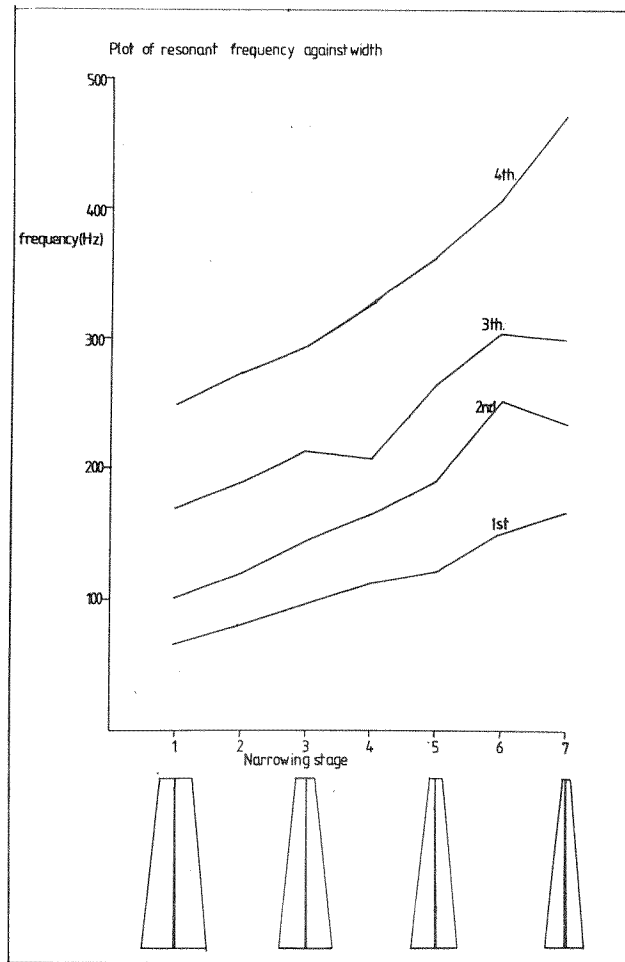


Fig. 14. Soundboard with narrowing experiment. Resonance frequencies.

quencies have all increased slightly (by about a semitone). The other difference is that the first resonance does not extend so far into the treble end of the board. This can be seen by following the 100 dB contour; in the first plot it extends from 4 - 15, in the second it extends from 4 - 12. However, these effects are quite small and one finds oneself asking why the harmonic bars are placed on the soundboard. One explanation could be that early harps had no veneer and the boards tended to split along the wood grains. The harmonic bars may thus prevent this splitting.

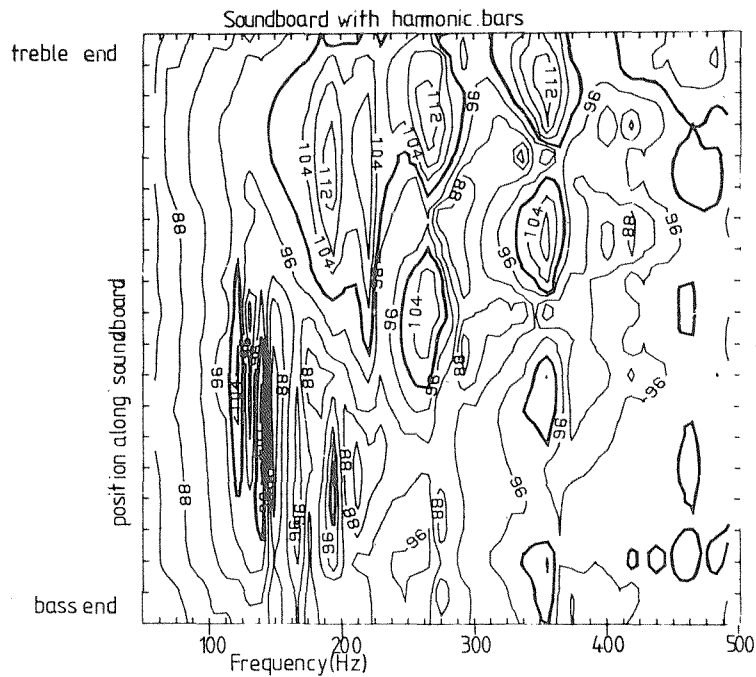
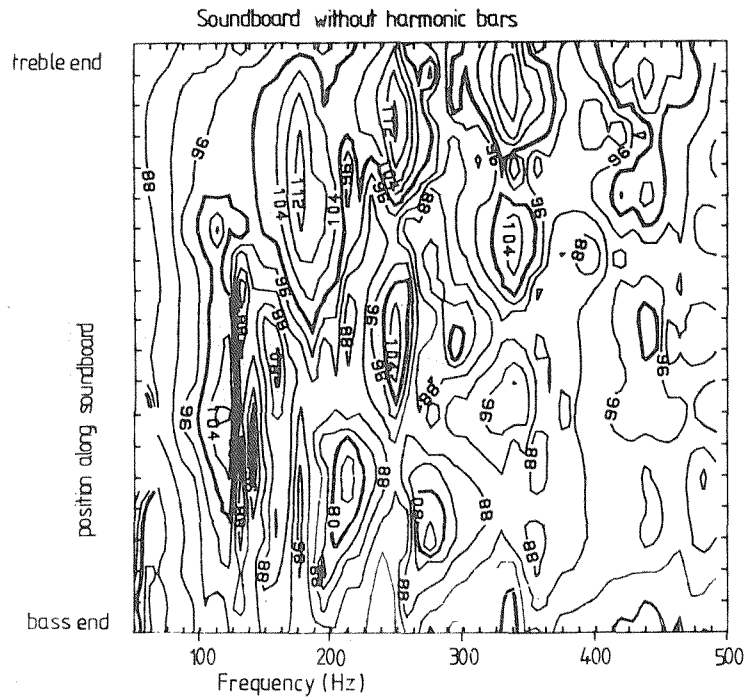


Fig. 15. The effect of the harmonic bars on soundboard admittance.

In this paper we have presented an introduction to the harp and our research to date. Work is continuing on the vibrations of the soundboard and also on the air resonances in the soundbox.

Acknowledgements

We wish to thank Mr. Victor Salvi of Salvi Harps Italia for his interest and support in our work and for his grant which enabled us to present this paper.

References

Firth, I.M. (1977): "On the acoustics of the harp", *Acustica* 37, 148-154.

Bell, A.J. (1981): "An investigation of directivity, and wood and air resonances of the concert harp", Report presented to Physics Dept., University of St. Andrews.

Rensch, R. (1969): The Harp, Duckworth, London, pp. 97-102; 166-173.

B&K (1980): "Instruction Manual for High Resolution Frequency Analyser", Bruel and Kjaer, Naerum, Chapter 9.

SOME ANALYSES OF VIOLA TONE

S. Fredin, G. Hammel, J.A. Strain, P.D. Townsend, and L. Wilzen
School of Mathematical and Physical Sciences, University of Sussex
Brighton, Sussex, England

Abstract

By use of a mechanical bowing system and a spectrum analyser the harmonic content of notes from several violins and violas have been recorded. Variations in harmonic content were noted under changing conditions of bow speed, bow pressure, bow position and fundamental. A comparison of loudness curves and harmonic content was particularly instructive and in several cases dips in the loudness curves were correlated to power absorption by sympathetic excitation of unbowed strings via higher harmonics of string and bowed note.

Introduction

In analysis of the tone quality of an instrument there is always a problem of how to generate the sound, both in a reproducible fashion and in a manner which is representative of the normal playing condition. Excitation with a sine wave source coupled to a viola can be done mechanically or electromagnetically and because of the simplicity of the excitation signal the measured response may be readily analysed. However, under normal playing conditions the slip-stick action of the bow produces a more complex string motion which feeds a wide range of harmonic frequencies into the instrument. Since the relative amplitude of these notes will depend on bowing conditions such as pressure, bow position, rosin etc. the real tone quality of a viola during performance may not be well represented by the laboratory excitation with sine waves.

To minimise this difficulty we use an automatic bowing system with a violin bow driven at constant speed and controlled in position and bow pressure. Notes are "fingered" on the string by pressing with a rubber tipped rod held in a frame. The apparatus is in a small room which has carpeting on the walls and ceiling to reduce extraneous sounds. Microphone detection gives reproducible signals and no resonances associated with the room or framework have been noted.

Signals from the microphone are analysed by a spectrum analyser and the data are stored in a computer. Having played a series of notes on a string the computer record can be presented as an isometric projection of the intensity versus the harmonic content of each note that was played (e.g., Fig. 1). One can visually appreciate some of the more gross features in the response of the instrument. For example the fundamental is the strongest harmonic for the lower and higher notes but in the

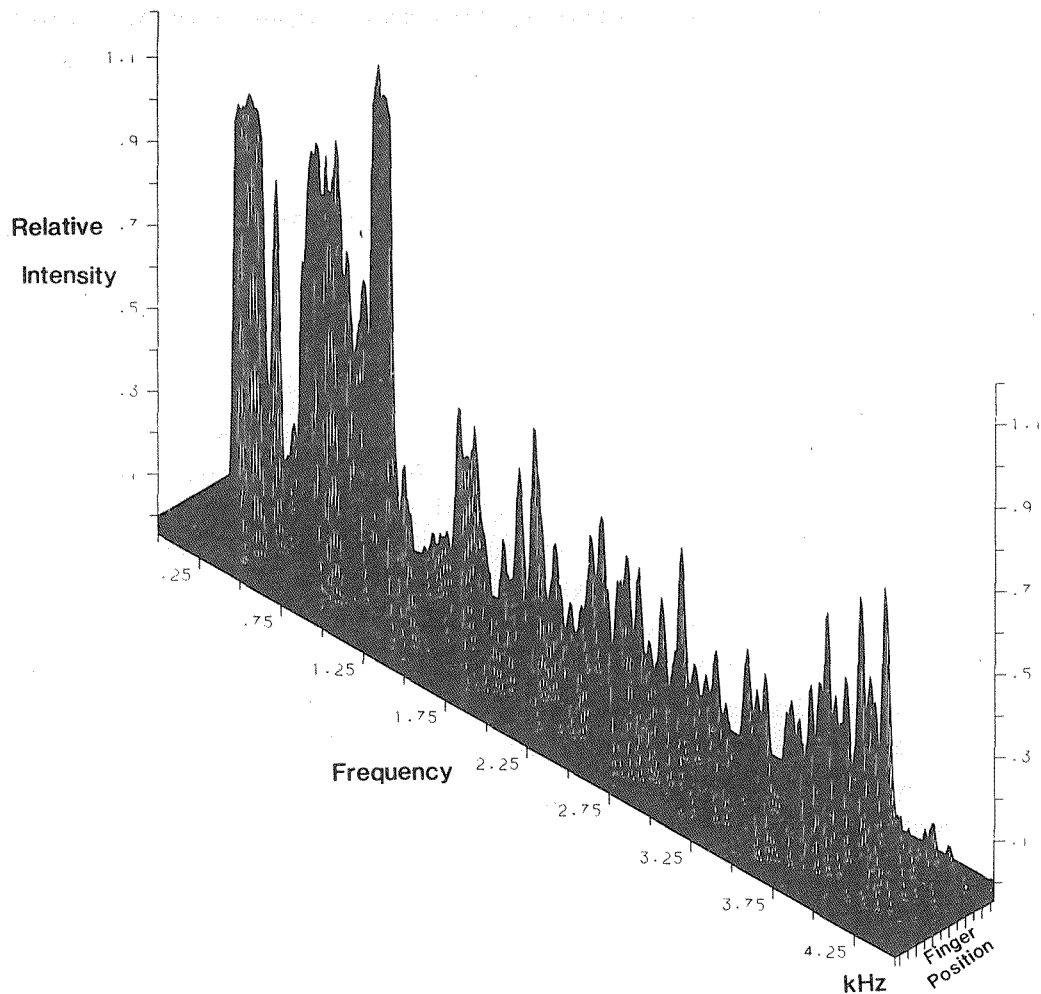


Fig. 1. An intensity plot of the harmonics for a series of notes played on a viola (L) made by D. Mills. The fingering on the A string covers the region from A_4 (400 Hz) to F_5^\sharp (740 Hz).

middle range near $C_5^\#$ (554 Hz) the fundamental is suppressed. An alternative presentation is in the form of a contour map of the isometric projection (Fig. 2). The areas of strong and weak response are clearly delineated as are the relative intensities of the harmonics. Additionally some lower frequency sound appears for the higher notes which is not obviously a sub-harmonic but appears, in this case, near 375 Hz.

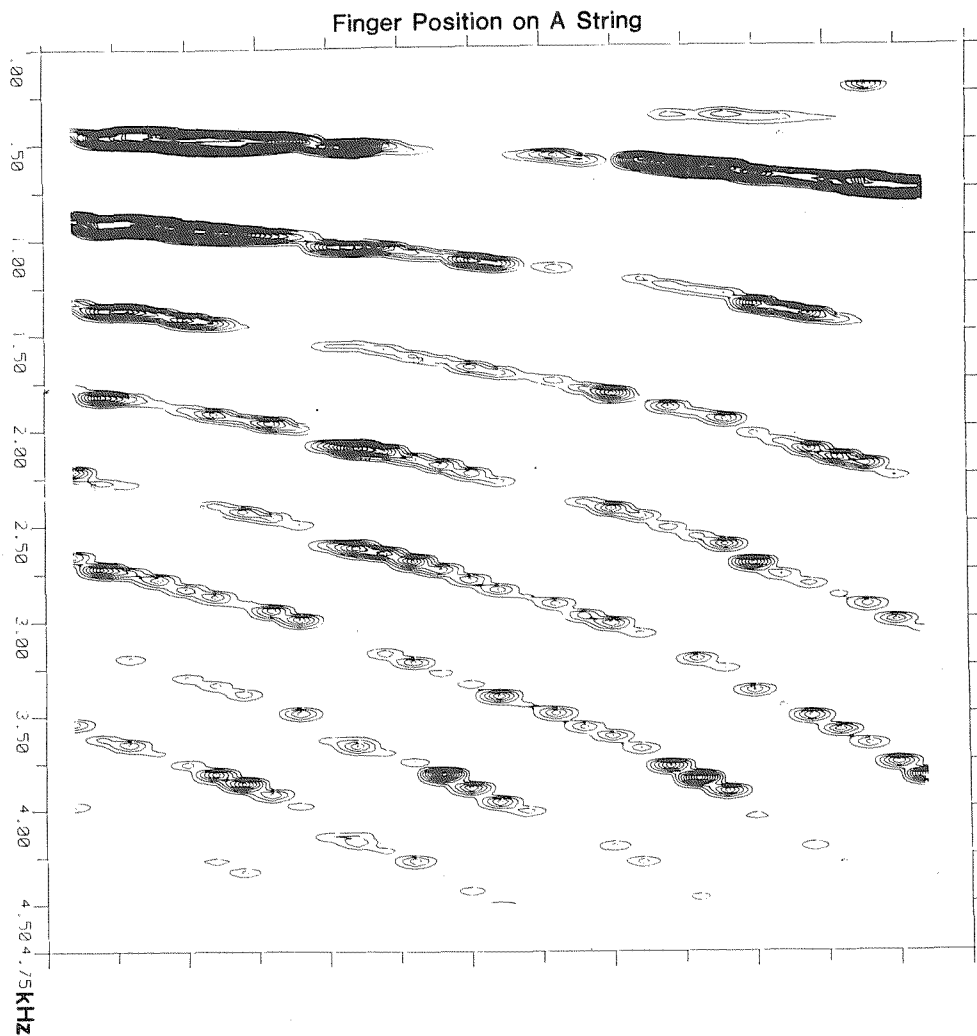
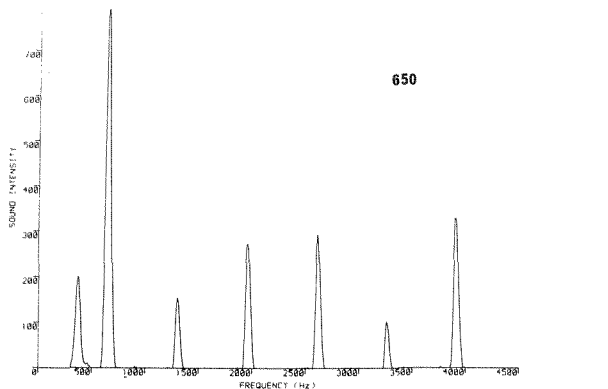
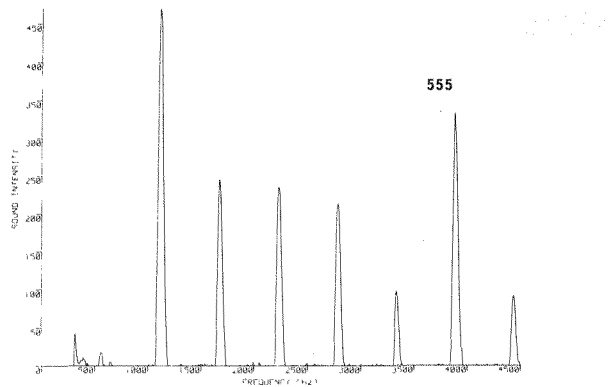
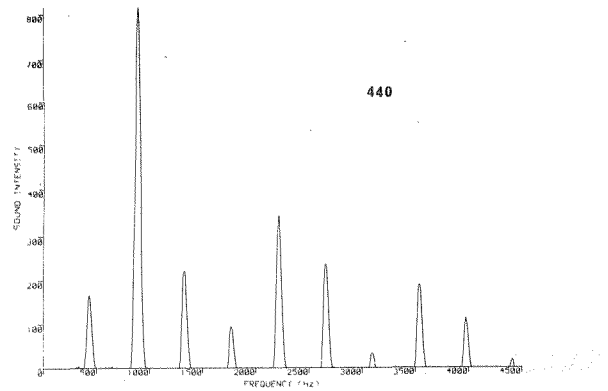


Fig. 2. A contour map of data shown in Fig. 1.



Harmonic analysis for three fundamentals on a viola A string.

Fig. 3. Harmonic analyses for the signals of notes played at 440, 555 and 650 Hz (i.e. near A_4 , C_5^\sharp and E_5).

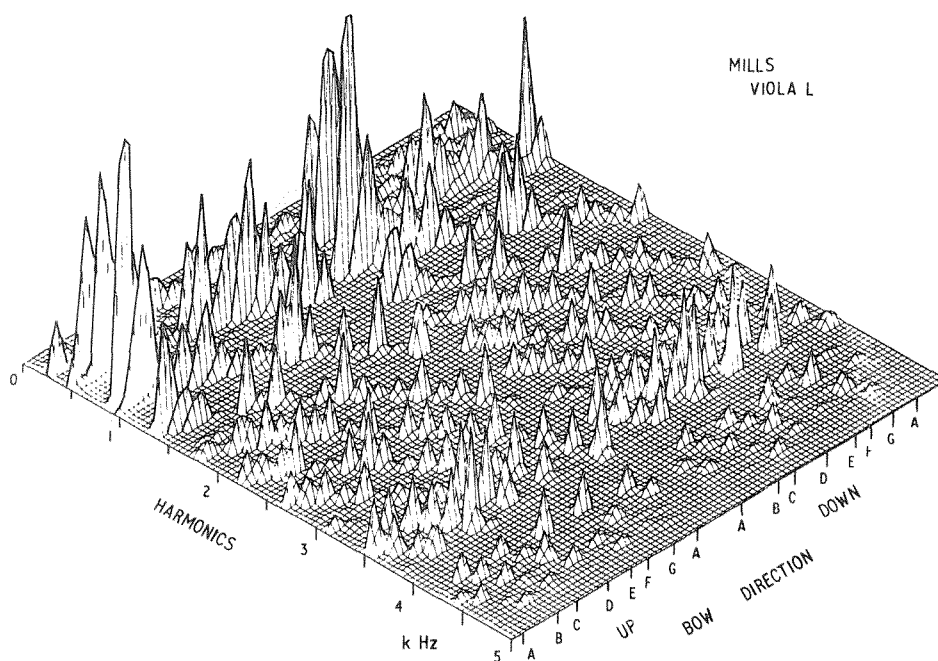


Fig. 4. Isometric plots of notes played on the Mills viola (L) showing differences in response between up and down bow strokes.

One may present the simple harmonic content of a single note and Fig. 3 describes spectra selected for fingered frequencies of 440, 555 and 650 Hz. In principle the alternative section through the map of intensity at a fixed frequency is available but this must be used with caution as the pressure applied to the string is changed if a wide range of notes are played on a single string. The instrument is bowed at less than maximum loudness and some studies of changes in spectrum with loudness have been made but these do not have a major effect for the loudness range used.

As examples of the data obtainable we shall briefly present:

- (i) Differences resulting from bow direction
- (ii) The influence of changing string type
- (iii) A test of the cavity resonance for a large viola
- (iv) Examples of weak harmonics corresponding to power transfer to other strings.

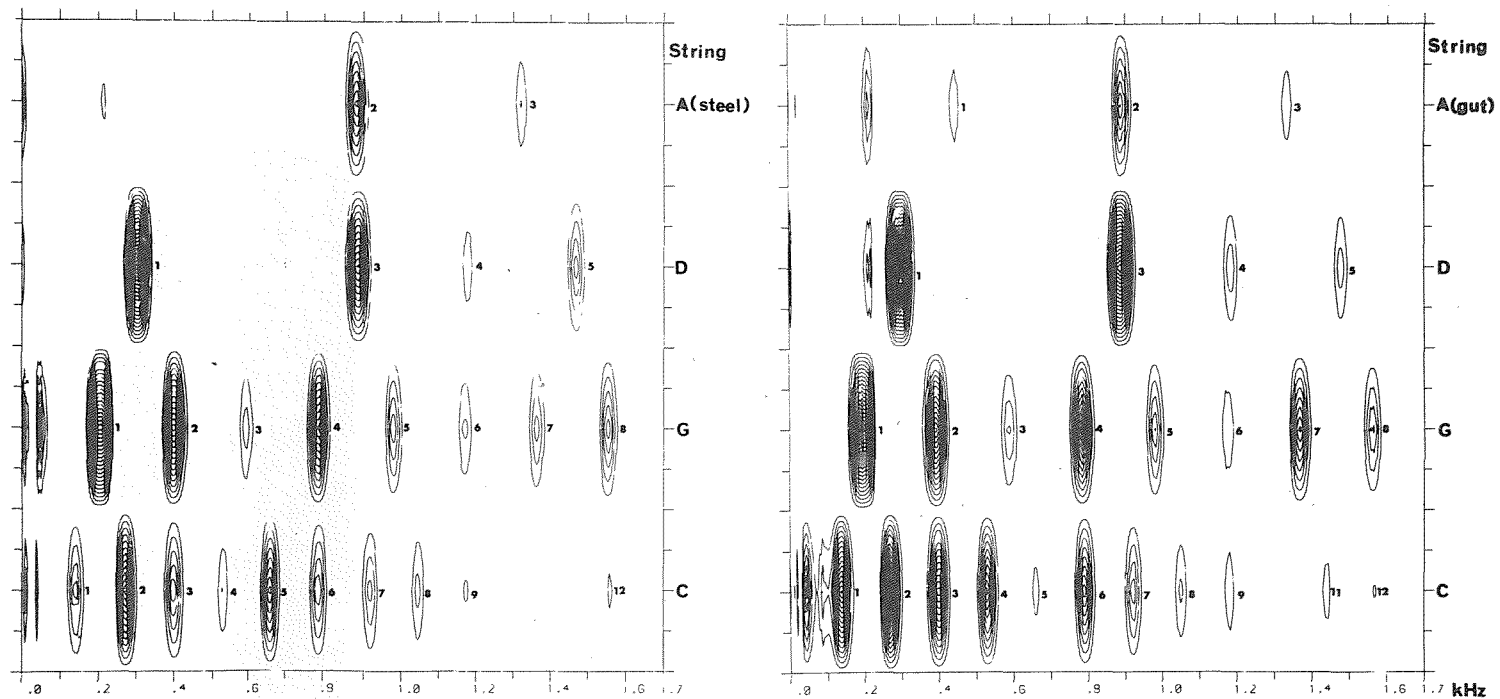


Fig. 5. The open string contour maps for the 20 inch viola with (a) a metal A string and (b) a gut A string.

Results

(i) Fig. 4 gives a pair of isometric plots for the same viola in which one set of data were recorded for up bow strokes and one set for down bows. There is an obvious difference in the relative intensities of the harmonics between the two halves of the figure. The bow itself does not contribute to this as the results were similar with the bow reversed. Directional dependence of the bow stroke on viola tone is not unexpected as internally the instrument is highly asymmetric with central differences of a sound post and bass bar. Musically the changes are small but detectable. The example indicates a feature which is not measurable by the simpler sine wave excitation methods.

(ii) For this work a 20 inch viola was made by Mr. D. Mills of Hove in Sussex to the C.A.S. pattern. Although it had a strong and pleasing tone on the lower three strings of C, G and D the original A string was relatively weak.

There is a difficulty in finding suitable strings for this large viola and originally we used a light gauge plated steel guitar string for the A but this was replaced with a heavier, gut, string from a viola da Gamba. There was an improvement both in total power and tone quality from the new A string. For comparison the intensity contours of the 4 open strings are shown in Figs. 5a and 5b for the original and revised set of strings. As expected the heavier string is more powerful but it is apparent that the new string has significantly altered the sound production from the other 3 strings as well.

Also note that in both cases the A string gives some sub-harmonic signal at 220 Hz. With the heavier A string there is a strong increase in the fundamental of the C at 131 Hz together with lower frequency noise.

(iii) In the design of the large C.A.S. viola the intent was to place major resonances near the C, D and G frequencies. Indeed the big Mills viola seems to fulfill this design. A test of the cavity resonance was to monitor the total power emitted as a function of the fingered note and to compare this with the power curve for the viola with the cavity damped by a light foam filling of the f holes. Fig. 6 shows a major drop in the

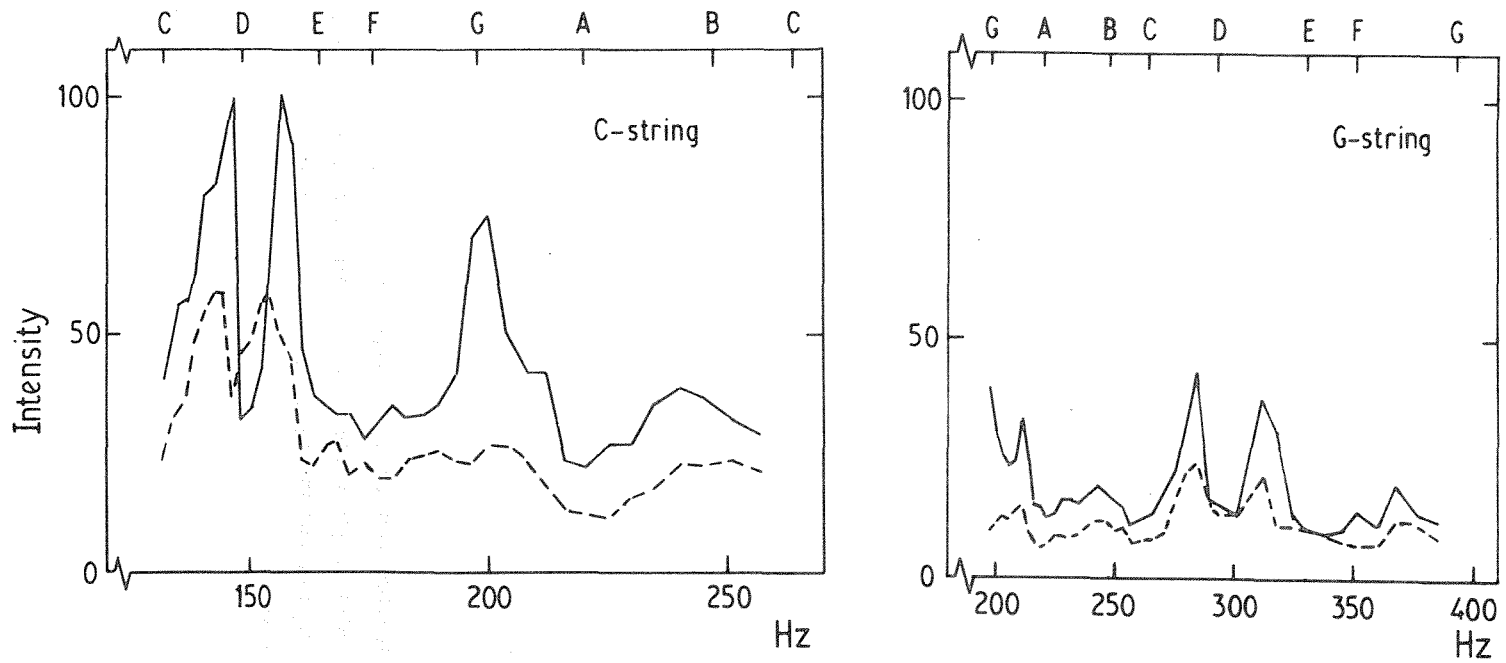


Fig. 6. Power measurements of notes played on the C and G strings of the 20 inch viola. Dashed lines are foam filled f holes.

This is in part due to frequency pulling of the instrument by the strong air resonance near 225 Hz ($\sim A_3$). There is a shoulder in the resonance curve at 235 Hz. One consequence of this strong resonance was noted when a fundamental of 222 Hz was bowed. The recorded signal showed a triple peaked "fundamental" with components at 200, 222 and 236 Hz.

(iv) The comparison of harmonic content with total power has been made for each string (e.g., as shown in Fig. 7 for a standard size viola C string).

The powerful notes of the total power curve can be directly related to the harmonic content shown by the contour plots and one is immediately aware that not all the power corresponds to emission in strong fundamentals. Within the contour plots there are frequencies which always correspond to weak emission, no matter which harmonic or fundamental produces the frequency.

Such frequencies correspond to harmonics of the other undamped open strings and the weakness is most pronounced when harmonics of two strings coincide. For example, with the viola A string (Fig. 2) there are lines of weakness at 587, 1173, 1564 and 2347 which correspond to harmonics of the other strings. Table I lists the possible coincidences of harmonics of the C, D and G strings with notes generated on the A string and it is immediately apparent that these select the contour dips of Fig. 2. Similar features are apparent for the contour plots of other strings. To test this possible explanation we have remeasured the viola response with the C, D and G strings damped with a strip of foam threaded through the strings.

Surprisingly this did not change the major features of the contour map but on closer inspection the dips at frequencies listed above were seen to be more pronounced. Our interpretation is that initially there is a loss of sound intensity by power transfer through the matching harmonics of the bowed and open strings. Some of this lost energy is re-emitted by the open strings but once they are damped this secondary source is inhibited, hence damping open strings further reduces the total sound level at these critical frequencies.

Table 1. Coincident open string harmonics of the viola strings. Note that interaction of the open strings (e.g. C, D, G) will interfere most strongly with notes bowed on the other string (e.g. A) when several harmonics coincide. Frequencies in Hz have been taken from a tempered scale.

C string (131)	G string (196)	D string (294)	A string (440)
393	392		
	588	588	
786	784		
		882	880
1178	1176	1176	
1568	1568		
	1764	1764	1760
1961	1960		
2368	2352	2352	
		2640	2640

Summary

Acoustic measurements of bowed instruments are inevitably very complex because of the wide range of parameters which control the sound. The present attempts to limit the number of variables are encouraging as at least a few of the features of the harmonic content and instrument loudness are interpretable, although the present work is still limited to a diagnostic role.

Acknowledgements

It is a pleasure to mention the enthusiasm and stimulation of discussions with Dr. P.J. Chandler and we are most fortunate to have had the violas made for us by Mr. D. Mills who is both a physicist and a highly skilled instrument maker.

ACOUSTIC RESONANT SCATTERING - A POSSIBLE NEW METHOD
FOR STUDYING MUSICAL INSTRUMENTS

Colin Gough

Dept. of Physics, University of Birmingham, England

Abstract

An account will be given of some preliminary experiments in which we have measured the sound re-radiated by musical instruments when they are themselves excited by sound. When the frequency of incident sound is such that an acoustically important resonance is excited, the intensity of re-radiated sound is large and is determined by the acoustic radiation efficiency of the excited mode. In principle, therefore, such measurements can provide valuable information on the parameters that characterise an instrument's tone. The method has been tested using Helmholtz resonators and preliminary work has begun using violins of various quality. In these measurements the violin is suspended in an anechoic chamber and the sound field is monitored using a single microphone as the sound produced by a single loudspeaker is swept in frequency over a range of interest. Although a complete analysis would require a more sophisticated experimental arrangement, it is hoped that the strong acoustic resonances from the open-strings and their harmonics will provide useful information about the radiation efficiency of the violin as a function of frequency, and hence help to characterise the quality of instruments.

Weinreich (1983) has recently described a very powerful technique for studying the acoustics of the violin, in which the various resonances of the instrument are excited by a carefully characterised sound field. In addition to providing the usual spectroscopic information on the positions and widths of the acoustically important vibrational modes of an instrument, the directionality and magnitude of sound radiated by such modes are also obtained. In this paper we outline a variant of this technique in which we measure the sound re-radiated by an instrument when it is acoustically excited. From such measurements absolute values for the acoustic efficiency, ϵ , of resonantly excited modes can be derived.

We define the acoustic efficiency as the fraction of stored vibrational energy ultimately converted into useful sound radiation. The tonal quality of an instrument will clearly be strongly influenced by the acoustic efficiency of the various structural resonances excited under normal playing conditions.

Although the resonant scattering of electromagnetic waves is a widely used and powerful spectroscopic technique in atomic and nuclear physics, we are not aware of any spectroscopic applications of resonant scattering in acoustics. We therefore decided to undertake this preliminary investigation to test the practicality and validity of the technique by making a series of measurements on a set of Helmholtz resonators for which the radiation efficiency can be evaluated independently. In this paper we briefly outline the theoretical background of the experiment and describe the results obtained for the Helmholtz resonators. We then give a couple of examples of the kind of measurements that might usefully be made on the violin.

The theory for the absorption and re-radiation of sound by an acoustically excited mechanical resonator is given by Rayleigh (1945). Assuming that the resonator acts as a monopole source of sound and is small in comparison with the acoustic wavelength, λ , the energy absorbed and re-radiated at resonance is equal to the energy flux of the incident, uniform sound wave crossing an area λ^2/π . At a distance d from the resonator the pressure of the scattered wave, P_s , as a fraction of the incident sound pressure, P_0 , is therefore given by $\lambda/2\pi d$.

This simple, yet remarkable, result shows that, at a given distance, the amplitude of scattered sound is independent of the size of the scattering object and depends only on the acoustic wavelength. It is also independent of the nature of the resonantly excited mechanical system - it could be the oscillating air column of a wind instrument or the cavity, string or structural resonance of a stringed instrument. It does assume, however, that the damping of the resonating system is by acoustic radiation alone. If there are additional viscous or internal friction losses the mechanical resonances will not be so strongly excited. The pressure of the scattered wave will therefore be reduced by the radiation efficiency, ϵ , defined above, so that

$$\frac{P_S}{P_O} = \epsilon \frac{\lambda}{2\pi d} \quad (1)$$

By measuring this quantity and comparing it with the theoretical expression, an absolute and rather direct determination of the radiation efficiency can in principle be obtained.

A schematic representation of the experimental arrangement is shown in Fig. 1. The measurements were made in an anechoic chamber of modest quality. A large QUAD electrostatic speaker was used as the source of sound, and the frequency was swept over the range of interest using a voltage-controlled oscillator (VCO) to drive the loudspeaker amplifier. The resonator or musical instrument to be studied was placed at a central distance of about 2 m from the loudspeaker with the microphone at a distance of typically between .25 m and 1 m from the source of re-radiated sound.

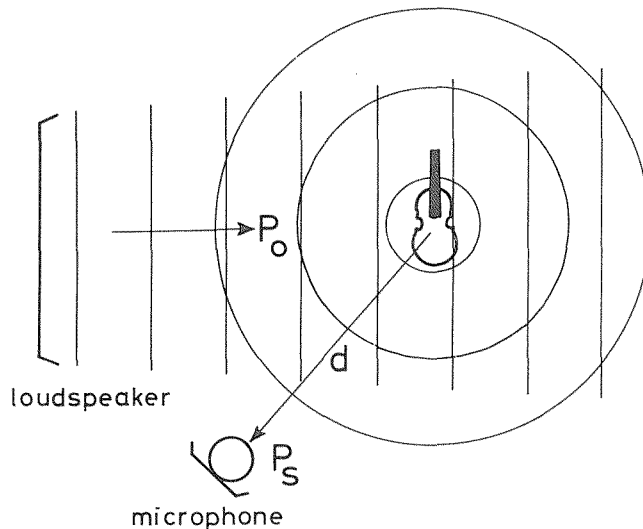


Fig. 1. Experimental arrangement to measure re-radiated sound.

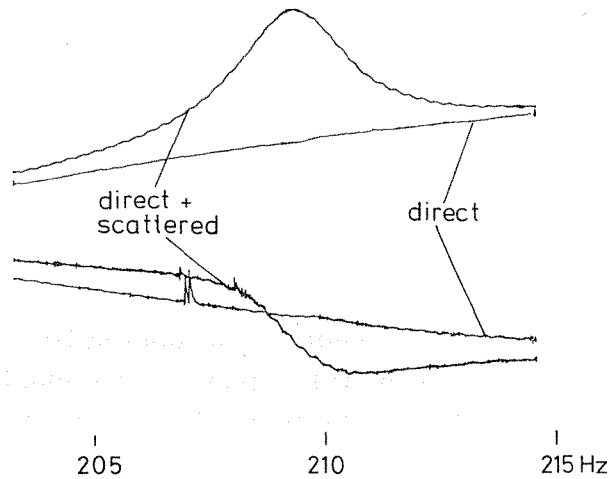


Fig. 2. Typical measurements showing the components of pressure in phase and phase quadrature before and after scattering object (a milk-bottle) is placed in position.

The microphone receives sound direct from the loudspeaker in addition to any sound re-radiated by the scattering object. To distinguish between the direct and re-radiated sound we have to measure the components of the sound pressure in-phase and in phase quadrature with the output of the VCO both before and after the scattering object is placed in position. A typical set of measurements for our "standard musical instrument" - a milk bottle - is shown in Fig. 2. The distances and, therefore, relative phases have been adjusted to give difference signals with the familiar absorption and dispersion curves of a simple resonator.

We measure the sound pressure at the position of the scattering object before the resonator is placed in position so that we can normalise the re-radiated sound pressure to the incident sound pressure. In Fig. 3 we show some normalised measurements for the scattering amplitude as a function of scattering distance, d , plotted in such a way to allow comparison with Eq. (1). The predicted inverse dependence on distance is confirmed and a value for the radiation efficiency of order 20% is obtained for the milk bottle.

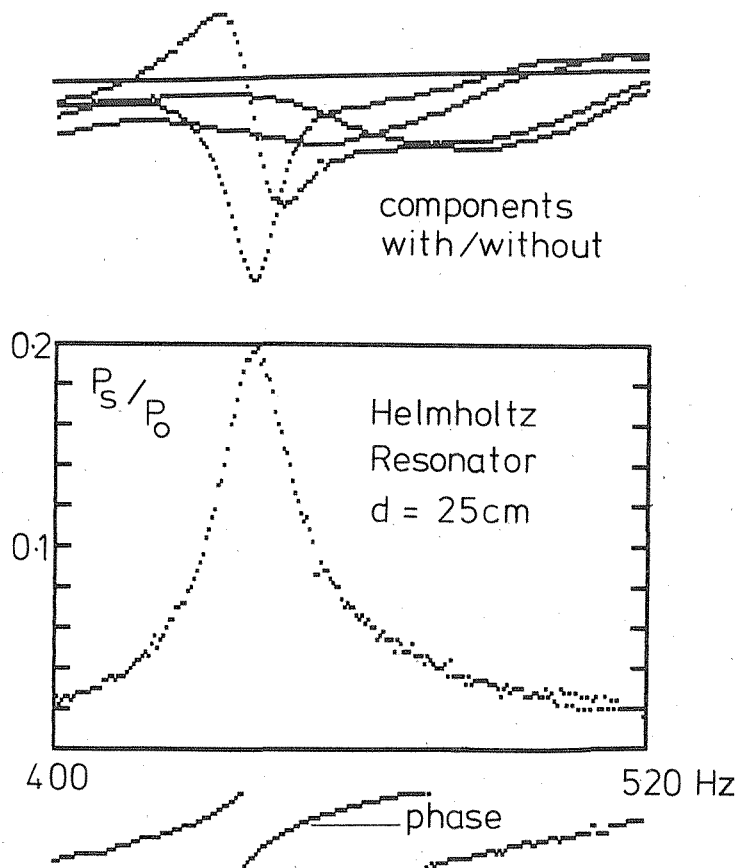


Fig. 3. Output from microcomputer-input signals, re-radiation pressure amplitude and phase.

As an independent check on the validity of this method for determining radiation efficiencies, we undertook a series of measurements on a collection of Helmholtz resonators used in the earlier years of this century for scientific measurements. For radiation damping alone, the Q-value, Q_R , of a Helmholtz resonator of volume V is given by $Q_R = \frac{1}{2\pi^2} \frac{\lambda^3}{V}$ (Rayleigh, 1945). The measured Q-value, Q_M , will be reduced by additional viscous and thermal damping. We can, therefore, make an independent determination of the radiation efficiency of a Helmholtz resonator simply by comparing the measured Q-value with the radiation limited value, $\epsilon = Q_M/Q_R$. Weinreich has pointed out that for an optimally designed Helmholtz resonator viscous losses will equal those from radiation, so that

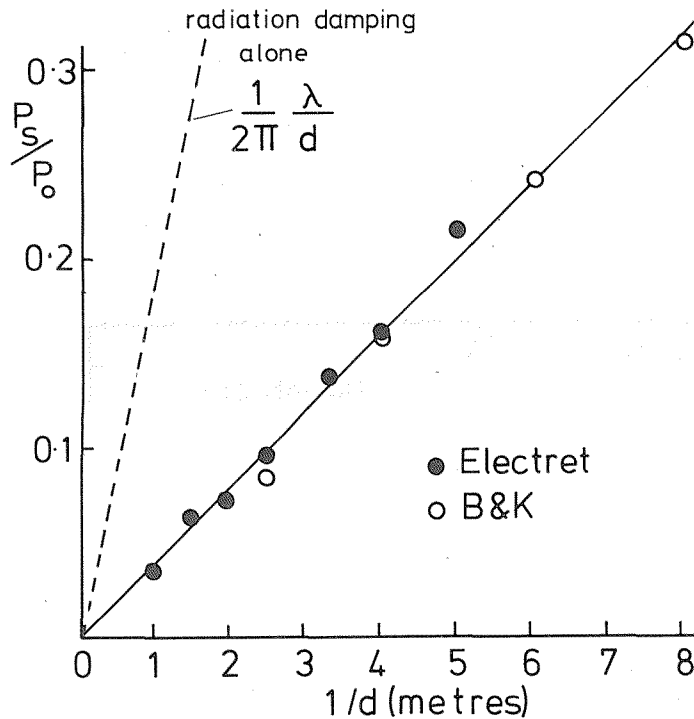


Fig. 4. Scattering amplitude as a function of scattering distance.

when thermal losses are included the acoustic efficiency of a Helmholtz resonator will always be less than 50%.

Fig. 4 shows an example of measurements made with the aid of a small microcomputer, which records data via an 8-bit A/D converter and performs the necessary algebra to display the amplitude of the scattered sound as a function of frequency. From such measurements it is straightforward to derive Q-values, which can be used to derive values for the radiation efficiency, as described above. In the following table we compare values of radiation efficiencies obtained from measurements of the amplitude of resonantly re-radiated sound and from Q-values.

Frequency	192	256	320	440	512	576	640	704	768
ϵ scatt.	.39	.30	.27	.39	.39	.35	.48	.37	.48
ϵ Q-val.	.40	.25	.19	.33	.38	.41	.39	.39	.55

With one exception, these values are consistent with Weinreich's (private communication) prediction that the acoustic efficiency of a Helmholtz resonator will always be less than 50%. The general level of agreement between these two quite independent determinations of radiation efficiencies encourages us to believe that acoustic resonant scattering could indeed provide reliable values for the acoustic efficiency of resonant modes in systems for which no independent theoretical estimate of the natural line widths (radiation limited) can be obtained - as, for example, the structural modes of vibration of the violin.

In the acoustically important range of the violin it is never a very good approximation to assume that the size of the violin is much less than the acoustic wavelength involved in exciting structural resonances. Consequently, even in the absence of excited resonances, the violin will scatter a significant amount of the incident sound giving a background signal that will vary slowly with frequency. Moreover, the sound radiated by the violin will also include non-negligible contributions from dipole and higher-order components, which will complicate the interpretation of any measurements. Nevertheless, it seemed worthwhile to investigate the resonantly scattered radiation from a violin, if for no other reason than to test the limitations of this technique for locating resonances and for determining their radiation efficiencies.

In an attempt to overcome the background problem of non-resonantly scattered radiation arising from the finite size of the violin, we measure the difference in scattered radiation with the violin first in its natural state and then modified in some way to remove the resonant modes of interest. The difference between such measurements gives information on the resonant modes that have been removed, with contributions from non-resonantly scattered radiation and radiation from unchanged resonances automatically subtracted from the result. Fig. 5 shows the difference in scattered sound from a Vuillaume violin before and after its strings were damped, its f-holes covered and its table heavily loaded, which removes the air and main mechanical resonances from the frequency range of interest. The measured difference should, therefore, provide information on the principal acoustic resonances of the violin with any non-resonant background scattering automatically subtracted. A number of resonances of the strings, air and structure can be identified from these measurements. In future we anticipate measuring the difference in

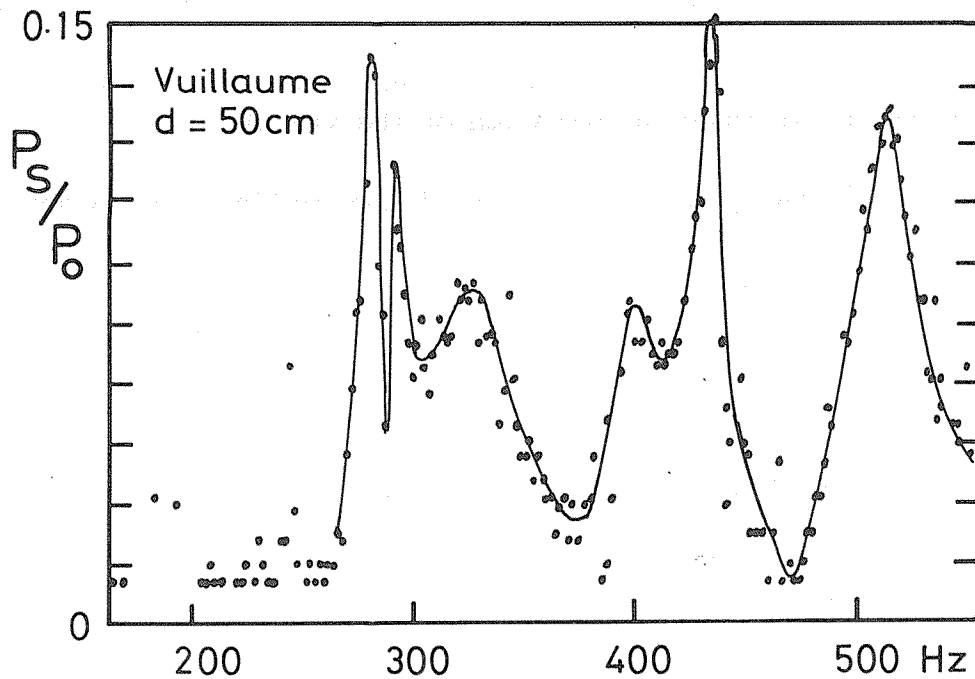


Fig. 5. Resonant scattering from a Vuillaume violin (see text).

scattering between violins in their natural playing state and a solid violin with no internal resonances to avoid artificial modification of the instrument being studied.

If this technique can be shown to give reproducible results, it could be useful for comparing instruments in different laboratories, since nothing has to be attached to the violin which might otherwise change its properties. Moreover, the method relies only on comparison of sound amplitudes to give absolute values for "the radiation efficiency". Even if such measurements turn out to be difficult to interpret, especially at the higher frequencies, the method is potentially valuable since it is free from problems of calibration.

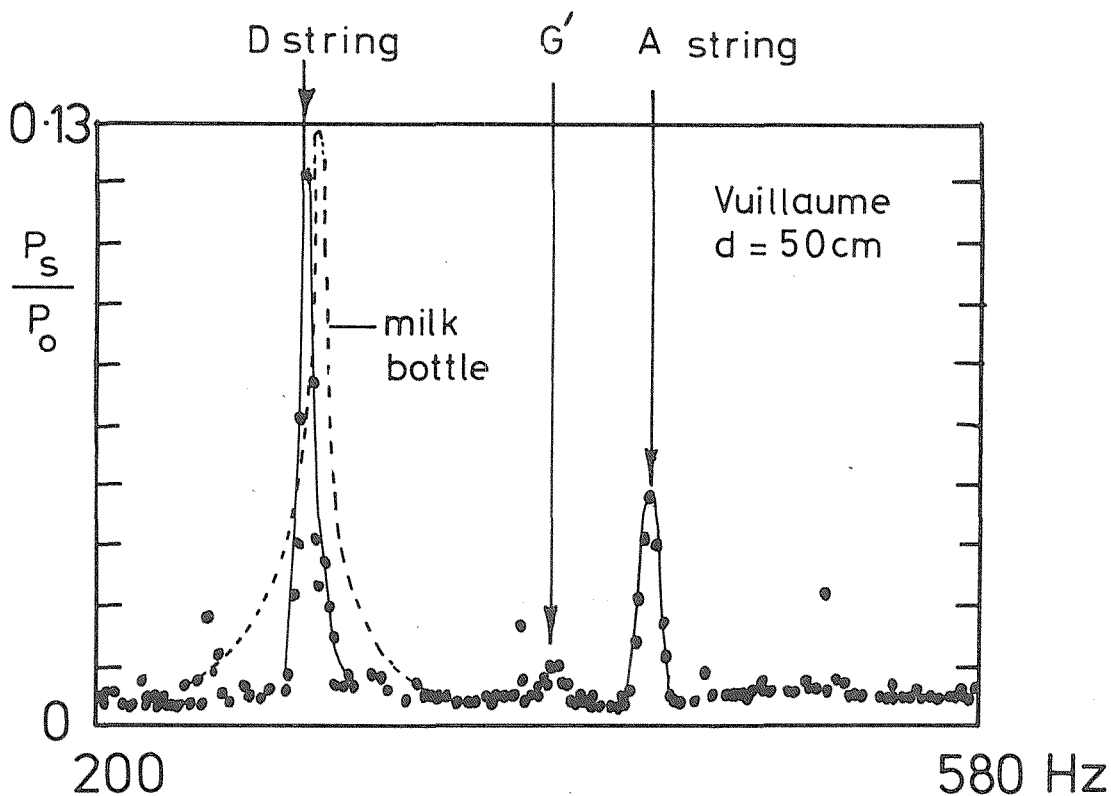


Fig. 6. Resonant scattering from strings of violin compared with scattering from milk-bottle.

Fig. 6 shows measurements of the difference in scattering before and after the violin strings were heavily damped. The difference gives the sound resonantly scattered from the freely vibrating strings alone - we assume that damping the strings has no significant effect on any of the other resonances of the instrument. For comparison, we have superimposed the sound scattered by our standard milk-bottle. Although the D-string resonance is much narrower, the amplitude of the scattered sound is almost the same indicating that, within the approximations referred to above, the acoustic efficiency of the string is of order 20%. The string, of course, radiates very little of its energy directly but relies on coupling through the bridge to the acoustically important vibrational modes of the body of the instrument. The amplitude of sound scattered by the resonantly excited string, therefore, provides a measure of the

radiation efficiency of the instrument as a whole at this frequency (i.e., 20%), which will in general involve interference effects between the various resonant modes of the instrument excited. For the D-string resonance it is probably only the air resonance that is strongly excited.

It should be emphasised that all the measurements reported here are of a very preliminary nature and will be repeated with higher accuracy (12-bit resolution) and better frequency resolution in the near future. However, we are already encouraged by these preliminary measurements and believe that acoustic resonance spectroscopy is a technique that should be investigated further, as it can, in principle provide rather interesting spectroscopic information that would be difficult to determine by other methods.

Resonances

Rayleigh, J.W.S. (1945): The Theory of Sound, Voll, 1894; reprinted by Dover, New York, 1945.

Weinreich, G., private communication.

Weinreich, G. (1983): "Violin radiativity: Concepts and measurements", invited paper to SMAC 1983, Stockholm; to be publ. in the Proc., Vol. II.

CHARACTERISTICS OF DYNAMIC POSSIBILITIES OF SOUND
IN CONTEMPORARY BOWED INSTRUMENTS

Helena Harajda

Acoustics Department of Experimental Physics Institute
Pedagogical University (WSP), Zielona Góra
Union of Luthery Masters (ZPAL), Warsaw, Poland

Abstract

The aim of the research has been to determine how the dynamic characteristics of the sound of the contemporary master bowed instruments are formed. A group of features subjectively felt as changes in the volume, connected with forming and the shape of the change in the intensity level, has been chosen. The following points have been taken into consideration: 1. the dynamic range, 2. the carrying of sound in respect to volume, 3. the leveling of volume (the difference of intensity level in the transition from one sound to another in the stable conditions of excitement), 4. the efficiency of achieving the optimum sound volume. The instruments tested were the violins of normal size submitted to the 6th International H. Weiniawski Violinmakers' Competition in Poznan, violins and cellos of 3/4 size submitted to the Polish National Wide Violinmakers' Competition as well as violas and cellos of normal size manufactured by Polish luthiers included in the prize-winning group of the International Luthieri Competition in Cremona. Measured characteristics have been compared with the subjective sound evaluation.

Introduction

Contemporary bowed instruments come from factories or are made by amateur violin makers and highly qualified violin making artists. The sound quality of instruments produced both in factories and by amateur violin makers happens to be, to a large extent, casual. In the artists' workshops, instruments are manufactured with great competence where material properties resulting in the sound quality as well as the awareness of the sound quality required by concert artists are taken into account. In Poland, these violin making artists are properly educated in music schools where they get thoroughly acquainted with acoustics. The instruments which are presented at competitions for violin makers and are highly evaluated by a jury are classified as masterly instruments. The

acoustical parameters that characterize their sound are within the established requirements of the sound model (Harajda, 1976). It may thus be assumed that statistical limits of variations in these parameters mark the impassable zones within which the qualities of the sound model in masterly instruments can vary.

Aim and method

The purpose of this study is the analytic presentation of dynamic characteristics of sound in contemporary bowed instruments which are classified at competitions for violin makers as masterly instruments. They happen to differ a lot in size.

The basic measures of the group of violin instruments under consideration are presented in Table 1.

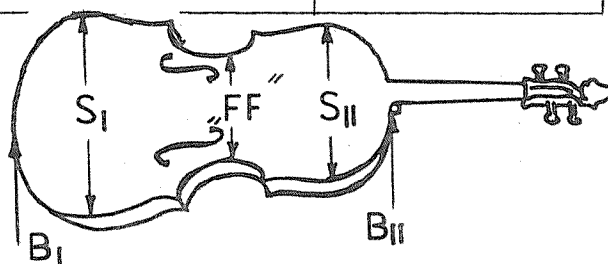
Research has been carried out to analyze the variations of those properties of sound in bowed instruments which are generally acknowledged by specialists on violin making to be essential (Leonhardt, 1969). They often become the core of subjective aural evaluation since they affect the intensity level of sound. These properties are as follows:

- 1) the intensity level of sound,
- 2) the dynamic range from "p" to "f",
- 3) the range of carrying the sound intensity,
- 4) the equality of intensity level while passing from one tone to the other on the same strings; and the equality of sound level between different strings,
- 5) the capability of proper attaining the maximum intensity level of sound for a given sound corresponding to the optimum sound volume.

The natural way of exciting the sound has been used, since the use of mechanic or electromagnetic means of sound excitation always with the same force - quite indispensable in some investigations on properties of the bulk of the instrument - does not guarantee the presentation of optimum sound possibilities of the instrument as a result of the scheme

Table 1. Measures of violin instruments entering for the 6th Wieniawski International Competition for Violin Makers in Poznań.

Measure	mean value in mm	limits of changeability in mm	standard deviations in mm	coefficient of changeability in %
length	357	352 - 363	2.09	0.59
width SI	208	204 - 213	2.18	1.05
SII	168	161 - 173	2.13	1.27
"FF"	110	106 - 118	2.35	2.14
height "FF"	61.5	58.0 - 66.5	1.64	2.68
BI	31	29 - 33	0.80	2.67
BII	30	28 - 32	0.80	2.67
BI - BII	1.0	0 - 2.5	0.64	64.00



"violinist - bow - instrument". Proper bowing allows to treat each case in an individual way. A good and properly trained violinist is capable of repeating any sound with such accuracy so as to retain the statistical distribution of parameters determining the detailed infrastructure of a given sound. For violin teachers and violin makers such abilities are well known.

An example of changes in the detailed structure during tonal stability is shown in Table 2.

Table 2. Fragment of detailed structure of a violin tone during stability of the fundamental.

tone g^1 (392Hz) for case S6

t (ms)	A0 (dB)	F0 (Hz)
1600	* 86	* 388.34
	* 86	* 388.34
	* 86	* 388.34
	* 86	* 392.15
1625	* 86	* 388.34
	* 86	* 392.15
	* 86	* 392.15
	* 86	* 392.15
1650	* 86	* 392.15
	* 86	* 388.34
	* 86	* 388.34
	* 86	* 388.34
1675	* 86	* 392.15
	* 86	* 392.15
	* 86	* 392.15
	* 86	* 388.34
1700	* 86	* 392.15
	* 86	* 392.15
	* 86	* 392.15
	* 86	* 388.34
1725	* 85	* 392.15
	* 85	* 388.34
	* 85	* 388.34
	* 85	* 384.61
1750	* 85	* 392.15
	* 85	* 388.34
	* 86	* 388.34
	* 86	* 388.34
1775	* 85	* 392.15
	* 85	* 392.15
	* 85	* 388.34
	* 85	* 388.34
1800	* 85	* 388.34
	* 85	* 392.15
	* 85	* 392.15

While recording, the conditions under which the instruments were evaluated at competitions for violin makers were retained (Harajda, 1980). The recording took place in a good chamber concert hall (Fig. 1), where the distribution of sound volume was uniform. The sound was recorded at two places, half a meter and four meters from the sound source.

The performers were violinists from Poznan Academy of Music.

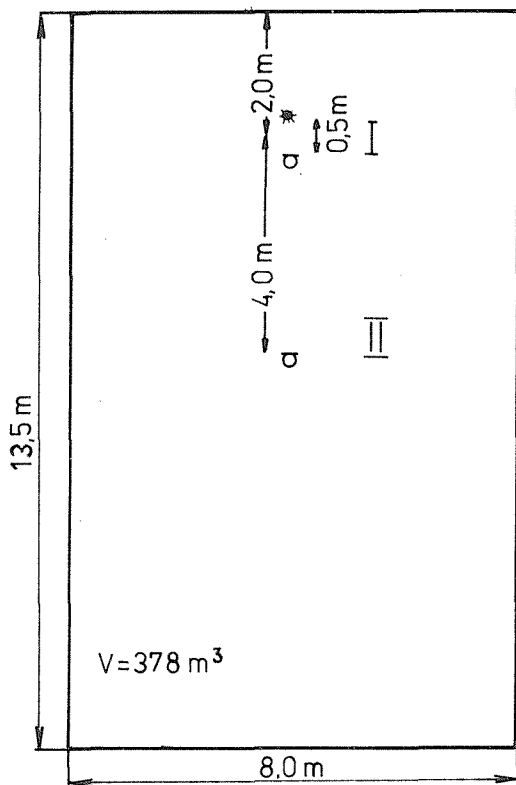


Fig. 1. Scheme of placing the measurement points.

Research material

Investigated were the sound properties of those instruments of standard size which in competitions for violin makers were specified as good

as well as the sound properties of all instruments of 3/4 size presented at a violin makers' competition (Table 3).

Table 3. Instruments under investigation.

Instrument	Size	Number	Event
Violin	standard	81	6th International H. Wieniawski Violin-makers Competition, Poznań, Poland 1981
Viola	standard	3	International Competition for Violin Makers, Cremona, 1982
Cello	standard	5	
Violin	3/4	30	All-Poland Z. Szulz Competition for Violin Makers, Poznań, 1979
Cello	3/4	3	

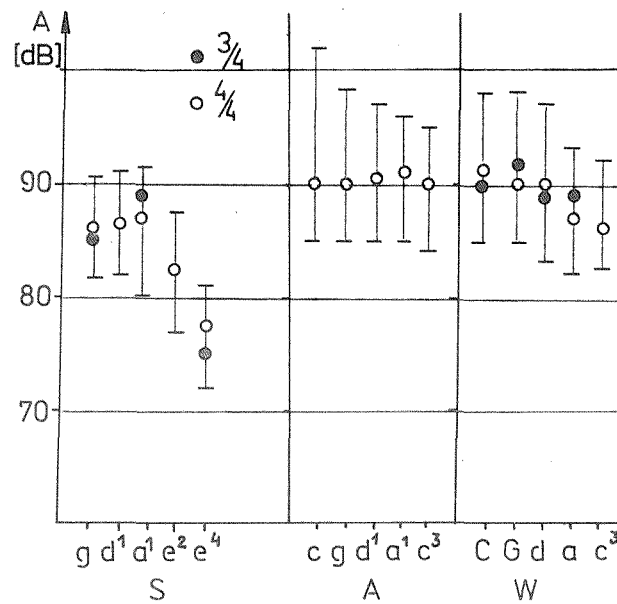


Fig. 2. Sound intensity levels (A [dB]) in violins (S), violas (A), cellos (W) at measurement point I.

Isolated tones (6 times each), a scale, and short melodies were performed (Table 4).

The dynamics of playing was specified as "p", "mf", and "f". The tuning of the instruments was controlled all the time. By means of commonly used electroacoustical equipment, an oscillographic analysis was carried out.

Results

The intensity level of basic tones for violin, viola, and cello is presented in Fig. 2.

Measured at a short distance $/I/$ from the source, the mean values and variation limits have been marked. The largest variations of mean values have been found for violin. Worth mentioning is also the fact that variations in the level of sound intensity among the different violin strings are remarkably similar, quite unlike the other bowed instruments. The upper limit undergoes most changes.

The present research supports the results obtained in investigations carried out previously (Harajda, 1976), i.e., to testify that the intensity level is not the very property to determine in the sound quality of a given instrument (Fig. 3).

The dynamic range from "p" to "f", the distance from the sound source being that of half a meter, is shown in Fig. 4. For violins of standard size, the dynamics was averaged for all scale tones; for the other string instruments the dynamics has been given separately for each separate instrument. Differences in dynamic range for the same group of instruments are remarkable.

Comparison between the place won by a violin at the competition for violin makers and the evaluation of the dynamic range of the tones allow us to assume that it is an important, though not the only, criterion of sound quality.

Table 4. Test material

Instrument	Size	Musical material	
		isolated tones	scale/melody
Violin	standard	g, d^1, a^1, e^2, e^4	g to a^2 scale ($a^1=400$ Hz)
Viola	standard	c, g, d^1, a^1, c^3	$g-e-a-g$ melody $g^1-e^1-a^1-g^1$ " $g^3-e^3-a^3-g^3$ "
Cello	standard	C, G, d, a, e^3	melody
Violin	3/4	g, d^1, a^1, e^4	$g e^4$ scale
Cello	3/4	C, a, e^3	$C c^2$ scale

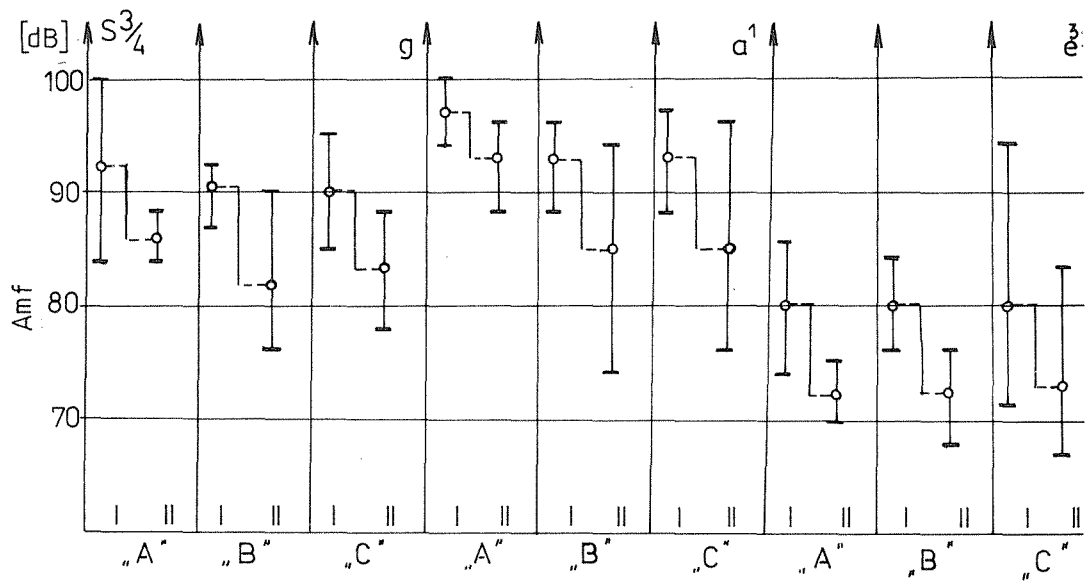


Fig. 3. Sound intensity levels (A mf [dB]) in 3/4-violins for three groups of quality (A,B,C) at the two measurement points (I,II).

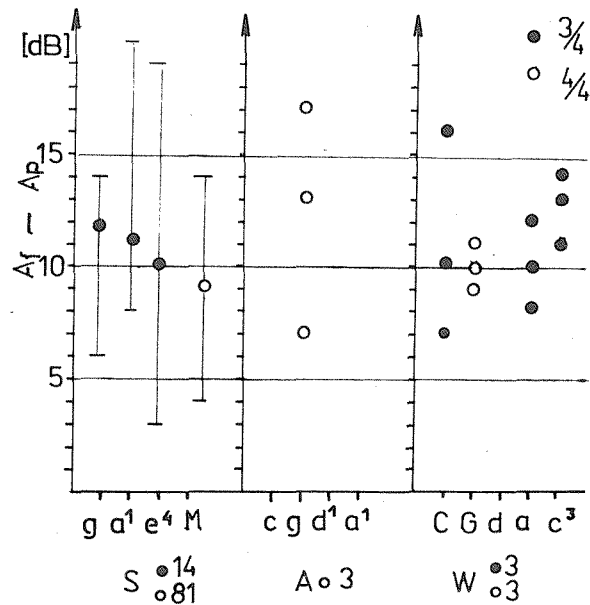


Fig. 4. Dynamic range ($A_f - A_p$) of isolated sounds (letters corresponding to the played notes) and melodies (M) for violins (S), violas (A), and cellos (W) at measurement point I.

In the group of the violins of the 3/4 size, a correlation between the place won by the instrument and the dynamic range was evident in the highest tones only at the distance of four meters from the sound source (Fig. 5).

The range of carrying the sound in the instruments under consideration evaluated in a small chamber concert hall was satisfactory. The decline in the intensity level for violins of standard size amounted to ca 5 dB. The instruments for children proved to be of a lesser carrying sound range. In individual cases there are great differences in carrying sound range, till 15 dB (Fig. 6).

In the group of instruments for children, when the intensity level

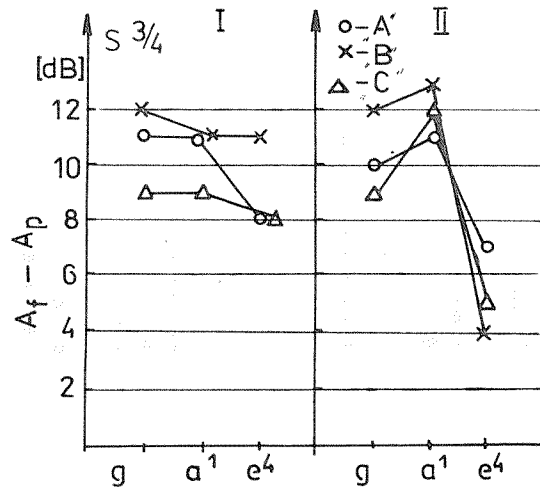


Fig. 5. Dynamic range ($A_I - A_P$) of 3/4-violins for three groups of quality (A,B,C) at the two measurement points (I,II) and the tones g, a¹, and e⁴.

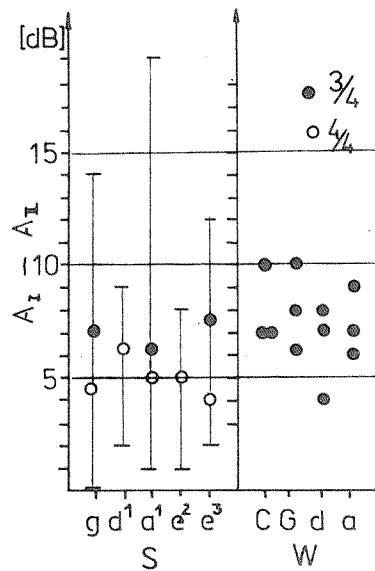


Fig. 6. Range of carrying the sound ($A_I - A_{II}$) in full size and 3/4-violins (S) and 3/4-cellos (W) or marked single tones.

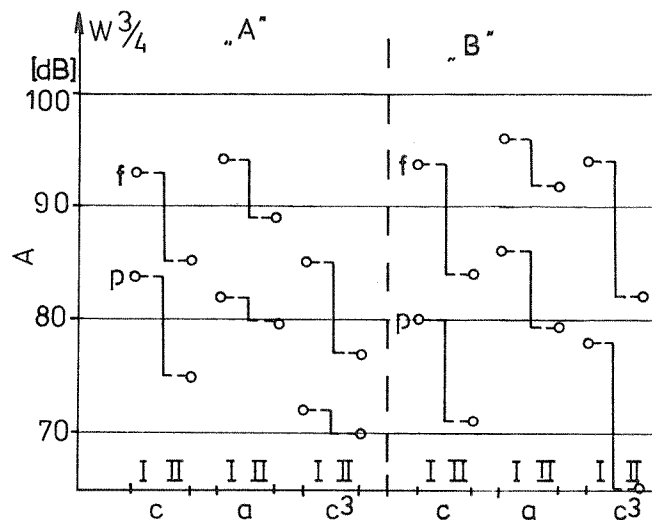


Fig. 7. Changes of sound intensity level (f and p) at the two measurement points in 3/4-cellos of different quality (A,B) for the marked single tones.

declined with the growing distance, the instruments were low evaluated, particularly evident in the cello sound (Fig. 7).

The difference of the intensity level when passing from one tone to the other on the same string is lowest for the standardized violin and amounts, on the average, to 4-6 dB (Fig. 8).

Individual differences are, however, high. The tones of the 3/4-violins are less uniform (5-10 dB). In the group of cello instruments, since the number of investigated instruments was rather small, the results are presented for each instrument separately. Along with the growth of this instrument size, the possibility to attain a uniform sound proves to be more difficult.

The possibilities to attain a sound equality on different strings of both the violin and the cello (of the size 3/4) are more limited, as compared to the sounds performed on the same string. The high level of sound equability is to be found in violas and cellos of standard size;

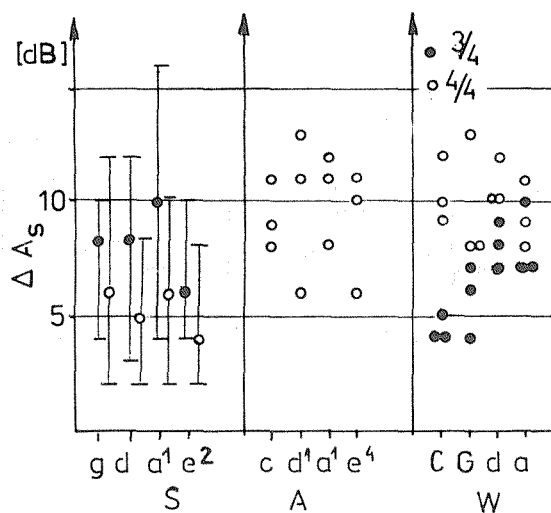


Fig. 8. Equality of sound intensity level (ΔA_s) within the same strings of violins (S), violas (A), and cellos (W).

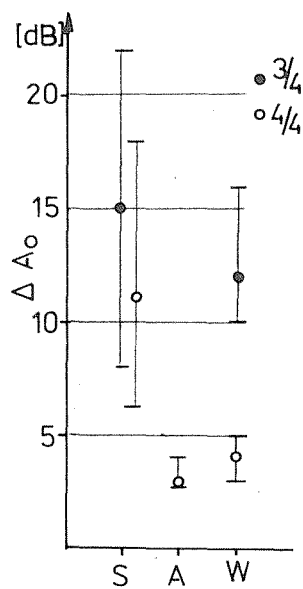


Fig. 9. Equality of the sound intensity level (ΔA_0) for all strings of violins (S), violas (A), and cellos (W).

the differences in the intensity level among sounds produced on different strings are lower than 5 dB (Fig. 9).

A characteristic property for particular instruments is the way in which the changes in the intensity level of sound occur when, after excitation that recurs several times, the sound tends to attain its

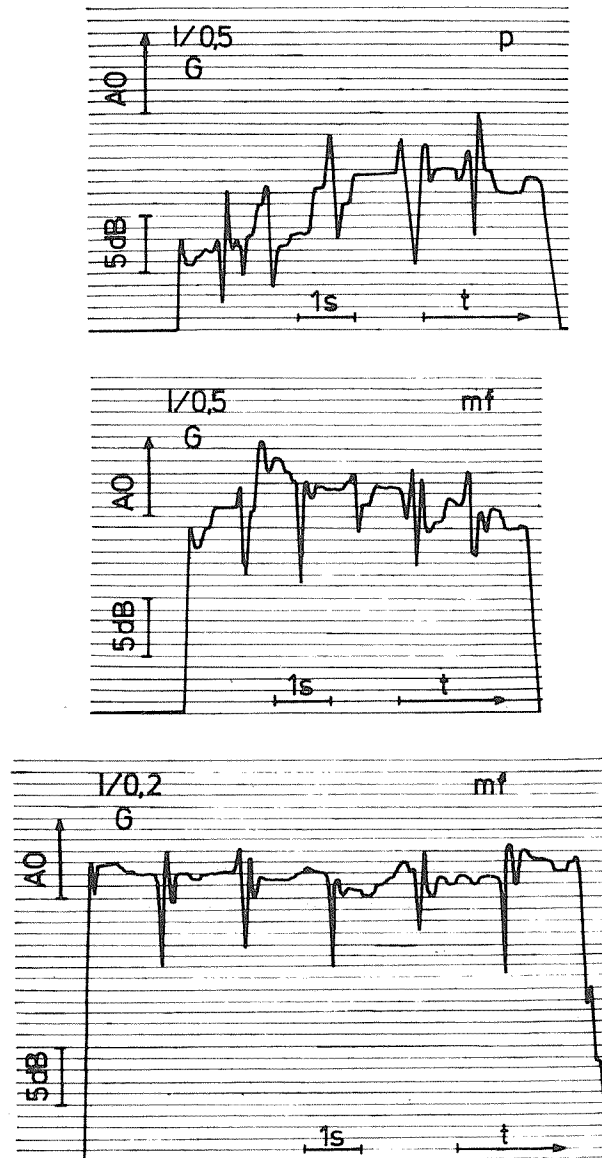


Fig. 10. Changes of sound intensity level while trying to attain the optimum sound volume (6 bow movements).

optimum volume. We can come across some instruments which, after the first bow movement, attain the optimum level of sound intensity as well as such instruments in which that level is attained after several attempts at sound excitation (Fig. 10).

The differences of that kind is to be found almost exclusively when the dynamics of playing is that of "p" and "mf". The sounds performed with the strength of "f", in 85 per cent, attain the maximum amplitude almost at once. There is no correlation between the place won by the instrument at the competition and the speed with which the optimum level of the sound volume is formed. Some violinists appreciate those instruments in which the excitation comes easier while others prefer such instruments which make a certain resistance to the excitation.

Conclusions

The results of the investigation presented in this paper on the characteristic properties of played tones and in particular their intensity levels allow us to establish the limits for permissible variations. To be contained within those limits gives a chance for an instrument to be classified as one of high quality, although the quality cannot be assured in this way apart from the above mentioned properties, some other features determine in the quality as well. The fall outside the established limits is closely related to the lowering of the instrument quality. The dynamic range and the range of carrying the sound are the parameters with a strong bearing on the instrument quality.

In the group of violas and cellos the equality of sound intensity level between the strings is high enough, while the violins are always characterized by fairly great differences in that level. Within the tones produced on the same string, the equality for the violin may amount to the value of 2 dB, and for the remaining types of bowed instruments - to 6 dB.

The property to make differences among particular bowed instruments is, no doubt, the easiness to attain a full sound volume, especially when the dynamics is that of "p". It does not mean, however, that this property should be considered as the very criterion of the quality of the instrument because the violinists are not uniform in their opinions on whether, and to what extent, this is or is not a positive characteristic of the instrument.

References

Harajda, H. (1976): "Research of the amplitude system of sounds of contemporary masters' violins" (in Polish), Ann. of AR, Poznan XC, pp. 59-71.

Harajda, H. (1980): "Changes in amplitude of violin sounds in a concert hall", The Catgut Ac.Soc. Newsletter, 33, pp. 13-17.

Leonhardt, K. (1969): Geigenbau und Klangfarbe, Verlag Das Musikinstrument, Frankfurt am Main.

THE FUNCTION OF THE VIOLIN BODY -- WHAT THE PHYSICIST DOES NOT KNOW!

Erik V. Jansson

Department of Speech Communication and Music Acoustics, KTH

Abstract

The physicist needs measures that are reproducible and interpretable for his investigations. To investigate the function of the violin, these measures must be calibrated regarding their importance and sensitivity for the violin as musical instrument. In our investigations we have adopted the input admittance as method, i.e., the resulting velocity for a given force as function of frequency. Thereby we can measure frequencies, Q-factors, and "driving levels" of the resonances of the violin body, i.e., acoustical fundamental measures possible to interpret. A first calibration of these measures suggests that the peak level of three resonances at approximately 400, 500, and 700 are most important for the quality. Experiments show that these resonances are somewhat sensitive to properties of the chinrest and to the holding of the violin. The "vibration patterns" of the three resonances show rather interesting similarities of the second and the fifth mode of the free plates. Therefore, we are presently investigating relations between these properties of the free plates and of the assembled instrument.

We feel that we are working with measures with a fair reproducibility, with meaningful interpretation, and with a first calibration of their importance. It is not known, however, why the physical measures are important (a confirmation of the importance is needed), and what the physical scale of sensitivity is (the necessary resolution for measurements). This confirmed and sufficiently detailed calibration must be related to wanted spectral and temporal properties of played tones. The calibration is necessary for systematic investigations of, for instance, where in the production chain the important properties are set and how much can they be readjusted.

(The investigations are conducted together with J. Alonso Moral and Carleen Hutchins.)

Introduction

The physicist needs measures that are reproducible for his investigations. The measures must be possible to interpret in physically

meaningful terms. To investigate the function of the violin as a musical instrument, the measures must be calibrated. To begin with, a qualitative calibration is necessary, i.e., which measures are the important ones for the musical quality of a violin. Secondly, a quantitative calibration of the important measures is necessary, i.e., how sensitive is the musical quality to the magnitude of the different important measures? In this my paper I shall point out what I know and what I do not know. The material for the presentation is taken from investigations in cooperation with Jesús Alonso Moral and Carleen Hutchins.

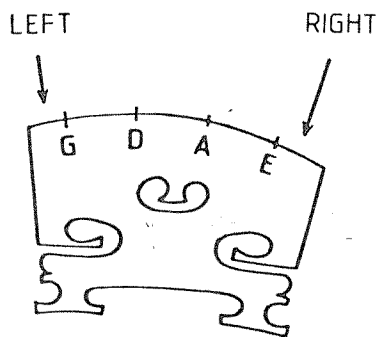


Fig. 1. Positions and directions for recording of input admittance.

Reproducibility of Measurements

At KTH we have adopted a method of recording the input admittance. Thereby, we record the resulting velocity from a force of constant magnitude but with slowly increasing frequency, Fig. 1. We have selected two positions as standard for measurements, both with the force applied on top of the bridge and in perpendicular to the top plate. The first position is outside the G-string, i.e., at the bassbar side, and the second position is outside the E-string, i.e., at the sound post side.

A result of such a recording of input admittance is shown for driving at the bassbar side. The input admittance curve is reproducible with a fair accuracy. Below 1 kHz it is reproduced within ± 1 dB, if reasonable care is taken in the setting up. For higher frequencies, say from 1 kHz to 5 kHz, it is somewhat less good. Great care is needed in the attachment of the driving-recording transducer, otherwise large discrepancies may occur around 2 kHz.

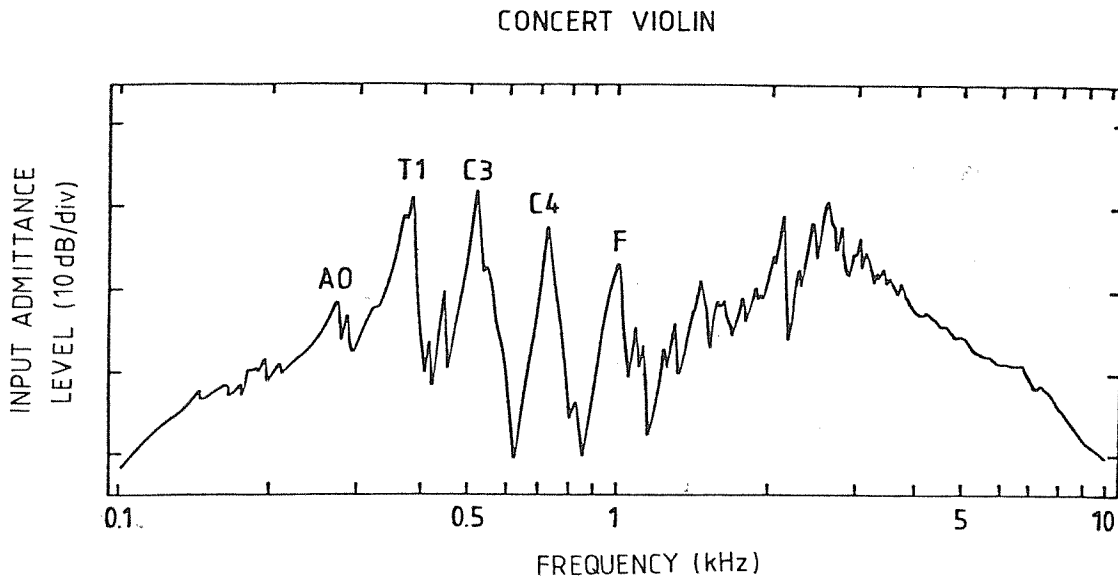


Fig. 2. An example of an input admittance curve.

Interpretation of the Input Admittance Curve

The input admittance curve can be interpreted in physically meaningful terms. The peaks represent a mapping of the resonances, i.e., the acoustical bricks of which the violin is built. The four peaks labelled A0, T1, C3, and C4 correspond to four resonances, eigenmodes, whose typical vibration patterns are known. The fifth peak F has yet to be explained. From the diagram the frequencies, the width, and the height (the level) of the peaks can be measured. Thus, measures are obtained of resonance frequencies, Q-factors, and "driving level". It should be pointed out

that it is the peaks that are the meaningful measures. Between 1 and 5 kHz there is a broad hill with its maximum at 2.5 kHz. This hill is introduced by properties of the bridge, but seems to be supplemented by the top plate construction, i.e., cutting the centrum of the top plate free from the edges by means of the f-holes (the hill is somewhat influenced by the mass of the driving transducer, approximately 1 g).

Qualitative Calibration of Measures

An analysis of 24 violins of different musical qualities suggests that the levels of the peaks T1, C3, and C4 are the most important for the tonal quality of the violin (Alonso Moral and Jansson, 1982). Furthermore, the bridge properties are important. A confirmation of this calibration is, however, badly needed, as we do not know why these measures should be important. An analysis by synthesis procedure seems to be the best approach to really solve this problem.

Naturally, even less is known about the sensitivity scale, i.e., we are far off from being able to give quantitative calibrations of the important acoustical measures of a violin. Again, this seems to be best solved by an analysis by synthesis procedure. But by starting from the hypothesis that the five peaks A0, C2, T1, C3, and C4 and the "bridge-hill" maximum are the important measures, we can attack the problem.

Identification of Resonance Peaks

The frequencies of the lowest resonance peaks give a fairly safe indication for a correct labelling of peaks. This is exemplified in Fig. 3. The three horizontal bars marked "4", along the lowest line, mark the range of resonances for four violins. The resonances were identified by means of optical recordings of their vibration patterns. The "24 bar-line" and the "6 bar-line" mark ranges of interpreted T1, C3, and C4 resonances for 24 and 6 new violins. The peaks are in this case assumed to fall in the same order as for the "4-violins". Thereby, it is found that the ranges of the three resonances are approximately the same -- a good old Italian violin, the crosses, falls within the same ranges. Observe that there is hardly any overlap between the ranges of the T1 and the C3 resonances.

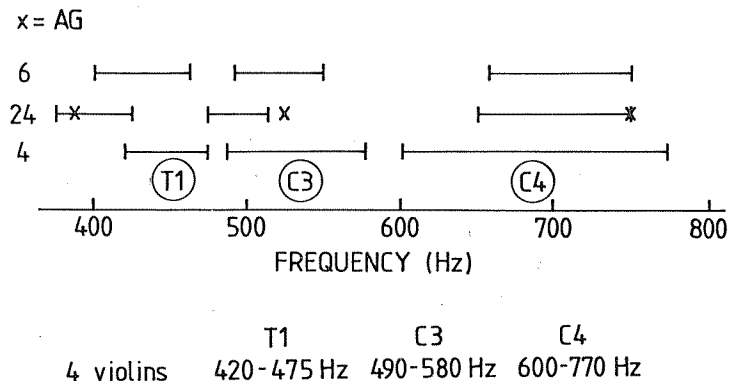


Fig. 3. Frequency ranges of resonance peaks.

Sensitivity of Properties to External Perturbations

As indicated, the calibration needs to be set by some kind of analysis by synthesis procedure. The sensitivity of the violin to external perturbations may, however, give an idea of magnitudes at least. Furthermore, it will give the accuracy with which the real properties of a violin can be determined. That should open ways to determine the sensitivity calibration by playing the violin under different conditions.

Influence of Chinrest

Let us start to look at the influence of the chinrest. This is demonstrated in Fig. 4. Along the horizontal axis the five investigated peaks and the "bridge hill" are marked A0, C2, T1, C3, C4, and BRIDGE. The

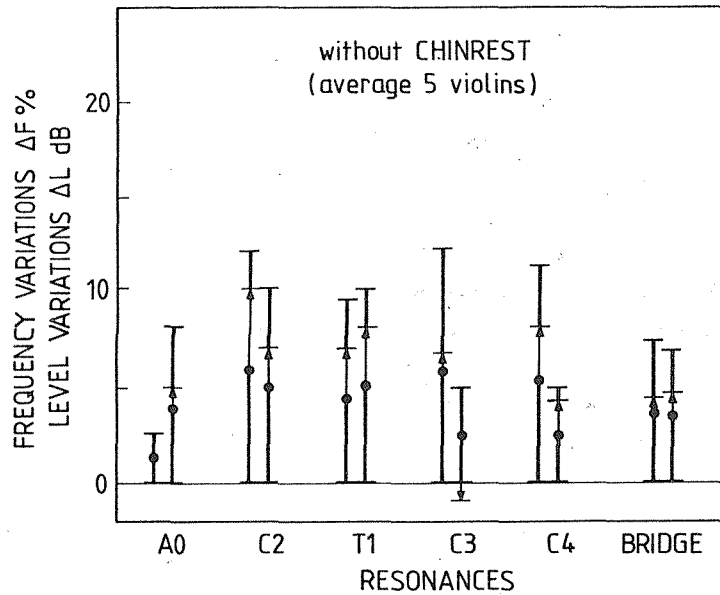


Fig. 4. Frequency (left) and level ranges (right) of resonance peaks. The arrows from the dots mark the shift of the mean by removal of chinrest.

left vertical bar of each pair marks the frequency range in percent, i.e., the frequency variations of the peak. The mean value is marked with a dot on the middle of the bar. The right bar of each pair marks in the same way the level variations and mean values of each peak in dB. The arrows pointing from the mean values (the dots) mark the shift of the mean values by the studied perturbation.

This first case shows the effect of removing the chinrest of the violin. The recordings were made with approximately free boundaries, i.e., the violin was hung in the standard way Carleen Hutchins uses. The removal of the chinrest gives small but significant changes of the peak measures. The classification "small" is used as the average shifts are considerably smaller than half the variation width in measures, i.e., the average shift is well within the ranges of variations. Different peaks, resonances, are somewhat differently influenced. The average frequency shift is 2%, i.e., a fifth of the 10% frequency variation range. The average level shift is 2 dB and the range of level variations 8 dB.

Damping of Strings

An important question is: Can the strings be damped during measurements to remove the influence of string resonances? It is easily seen that the damping of strings gives rather small perturbations of the properties, Fig. 5. The average frequency shift is 0.5% and the average level shift 1 dB. Without string damping, three double peaks give interpretation difficulties. The influence of the string damping is small compared with that of the chinrest, for instance.

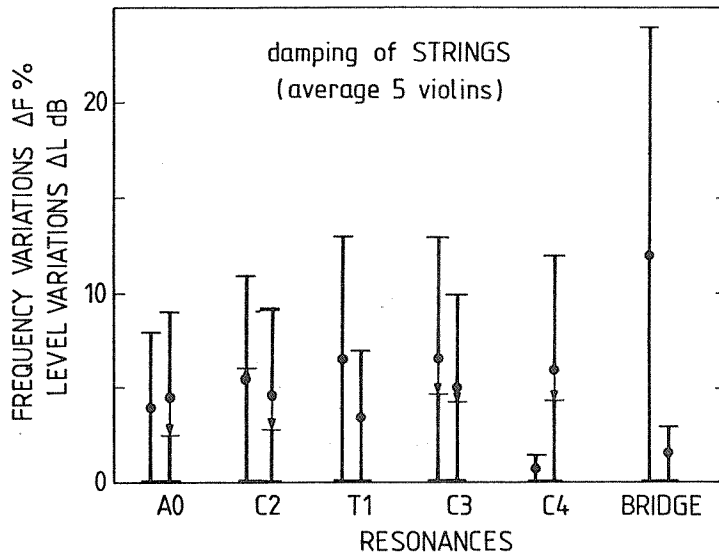


Fig. 5. As for Fig. 4. but the shift of average by damping of strings.

Holding of the Violin

The holding of the violin in playing is likely to perturb the measures obtained with free boundaries. The recorded perturbations of holding for one violin is shown in Fig. 6. The groups of three bars display frequency measures (left), level measures (middle), and Q-factor measures (the

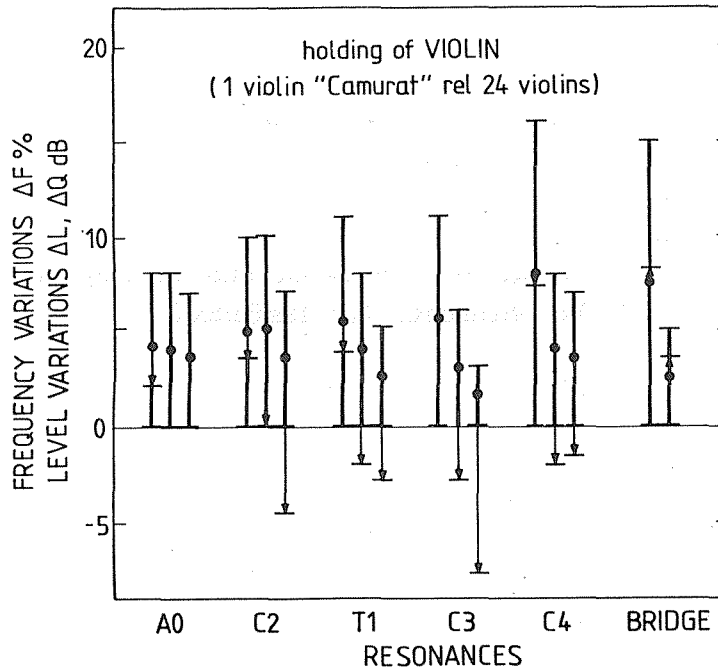


Fig. 6. Frequency (left), level (middle), and Q-factor ranges of resonance peaks. The arrows from the dots mark the shift of the mean from free to holding of the violin.

right bar calculated as level measures in dB). The frequency shifts are small (-1.5% on the average), but the level and Q-factor shifts are large. The decrease in level and Q-factor is on the average 50% with the small shifts of the "bridge hill" excluded. This indicates that the holding of the violin causes mainly losses. The losses measured with free boundaries are likely to give a large underestimation of the losses for the violin under playing conditions.

Without Strings and Bridge

A natural question is: How much are the measured properties influenced by the stringing and its accessories? The differences between measurements with and without strings, bridge etc. are given in Fig. 7. The measurements were made on top of the bridge at the bass bar side and at the position of the corresponding bridge foot without bridge. The frequency shifts are small, on the average 1% except for the 7% of the C4 resonance. The level shifts are moderate, say -3 dB for the A0, C2, and

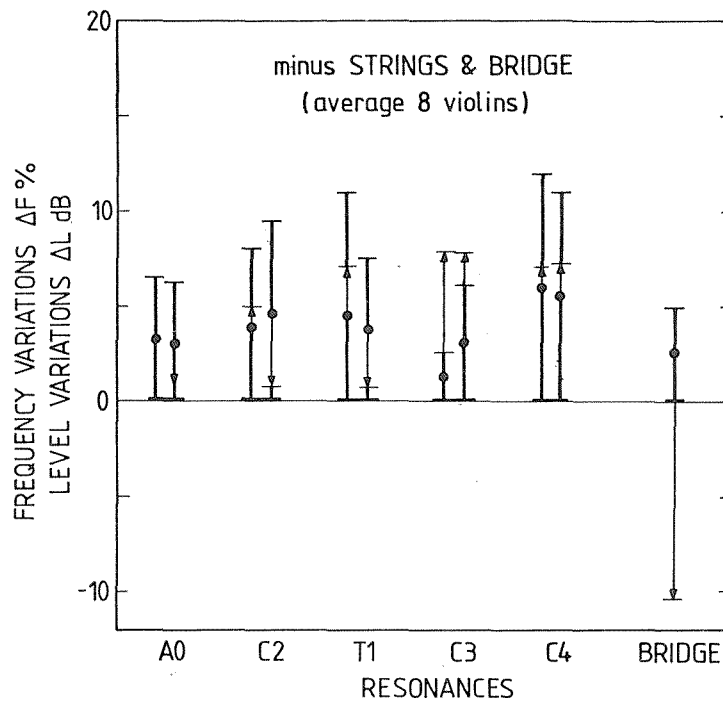


Fig. 7. As for Fig. 4 but shift of the mean by removal of strings and bridge.

T1 resonances and +3 dB for the C3 and C4 resonances. The level decrease is large for the "bridge-hill", -13 dB. The large shift is interpreted to prove that the influence of the first bridge resonance is large in this frequency region.

Conclusions of Accuracy and Sensitivity

We have found that the standard way of recording properties, i.e., with free boundaries, gives a reasonable approximation of the violin in playing except for a large underestimation of losses. Damping of strings gives minor influence; the losses increase approximately 1 dB and the resonance frequencies shift 0.5%. The chinrest gives a somewhat larger influence; an average decrease of 2% and 2 dB respectively. The holding for playing gives a 6 dB (50% decrease in level and Q-factors). Knowledge of the perturbations seems to open ways to systematically change the

acoustical properties and compare those with changes in musical qualities of a violin. Thereby, one should first aim at a qualitative calibration, i.e., which properties are the most important ones, and, secondly, aim at a quantitative calibrations, i.e., how sensitive is the tonal quality of the violin to variations in the physical properties.

There seems to be a large uncertainty on needed accuracy in measurements. A high accuracy is generally wanted but the chinrest and, especially, the holding change properties of a violin considerably. Furthermore, if the high levels of the T1, C3, and C4 are favorable, why do the players hold the violin the way they do? Or perhaps the holding is not as disastrous as our measurements imply?

Free Plates and Assembled Violins

Another point of great interest is that of the maker: How do you make a high quality violin? As we do not know for sure what properties the high quality violin should have, there are naturally some difficulties for the physicist to specify how to make such a one. But again, starting from a hypothesis what the properties should be, a problem is defined and can be attacked. Let us assume that the resonances T1, C3, and C4 are the important ones. The problem that can be attacked is: How do we achieve these resonances and how can they be adjusted? This is equivalent to attacking the question of calibration.

The vibration modes, i.e., the vibration patterns, look typically as sketched in the upper row of Fig. 8. Mode T1 has its main vibrations between the f-holes, and two curved vertical nodal lines. Mode C3 has similar nodal lines, but the main vibrations are at the edges and the plates move in phase. Typical vibration patterns of free violin plates are shown in the lower row. The free plate vibration pattern reflects the stiffness-mass distribution of the plates. These vibration patterns, the second and the fifth eigenmodes of free violin plates, show astonishing similarities with those of the assembled violin. The arrows between the vibration patterns of the lower row and those of the upper row indicate, how the vibration patterns of the free plates can be combined into those

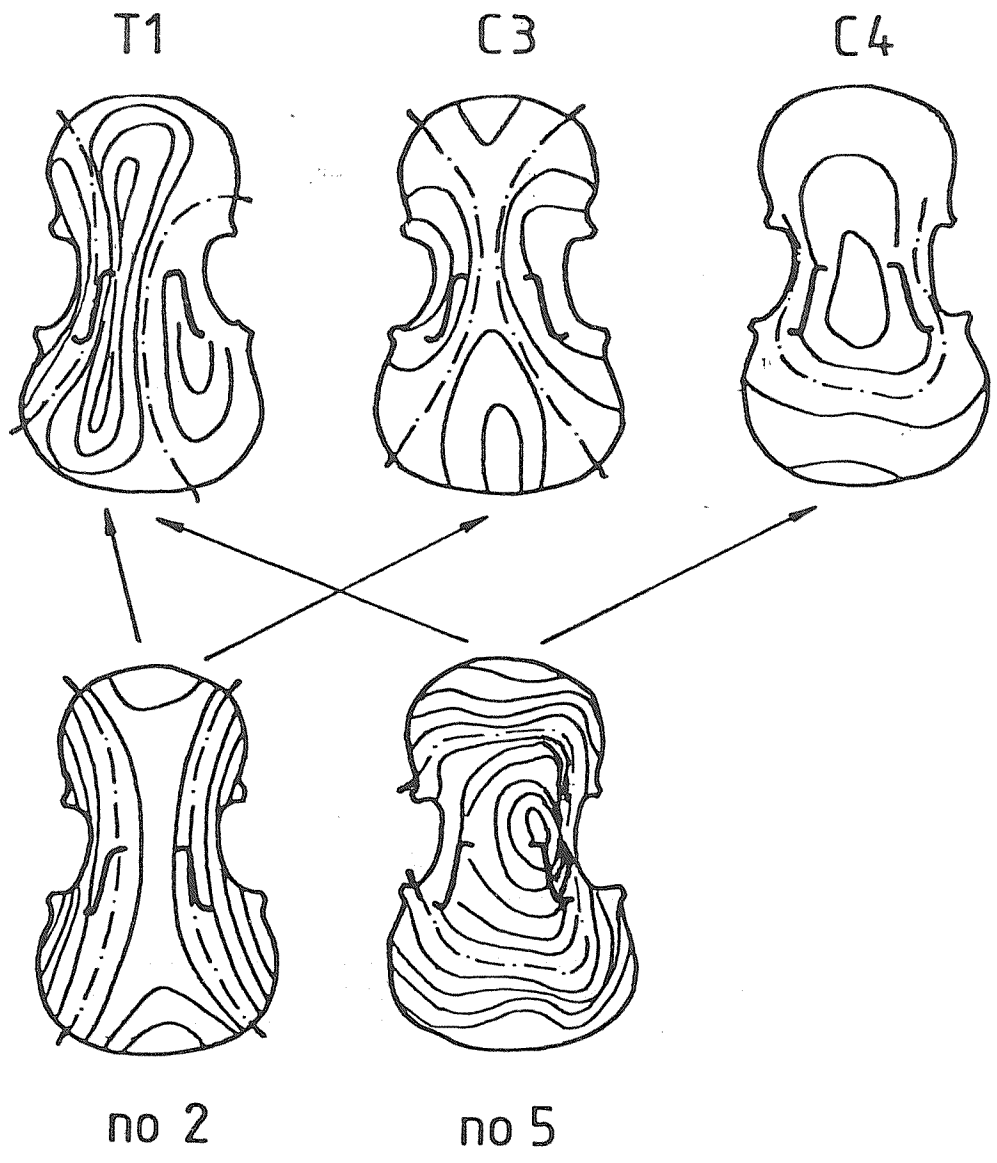


Fig. 8. Vibration patterns of assembled (upper row) and free (lower row) violin plates. Thin lines mark equal vibration lines and (-.-.-) mark nodal lines.

of the assembled violin. The assembling of the violin is, however, a rather large change of boundaries and we can not assume that slightly perturbed free plate modes are transformed into the modes of the assembled violin. The similarities can not safely be assumed to be more than accidental without further evidence. As a matter of fact, from a physic-

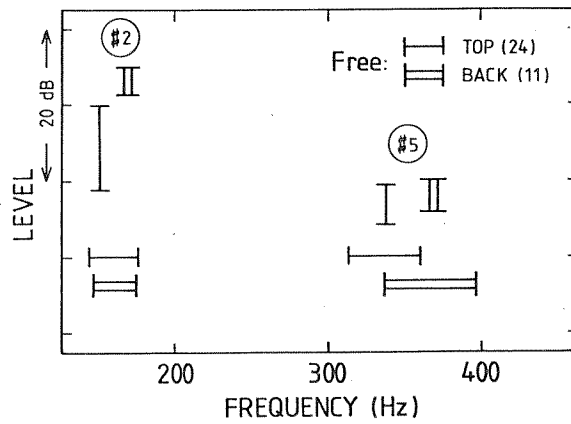
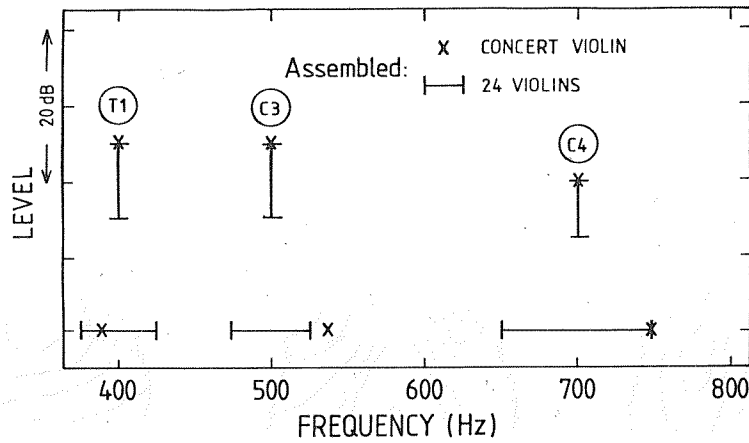


Fig. 9. Variations of levels and frequencies at resonance of three modes of assembled violins (upper diagram) and of two modes of free plates (lower diagram).

al standpoint, the perturbations in the assembling are so large that the presented properties of the free plates cannot fully predict the presented properties of the assembled violin.

Frequencies and Levels at Resonance

In order to study relations between free plates and assembled violins, we have started a larger investigation. In one part, we are collecting

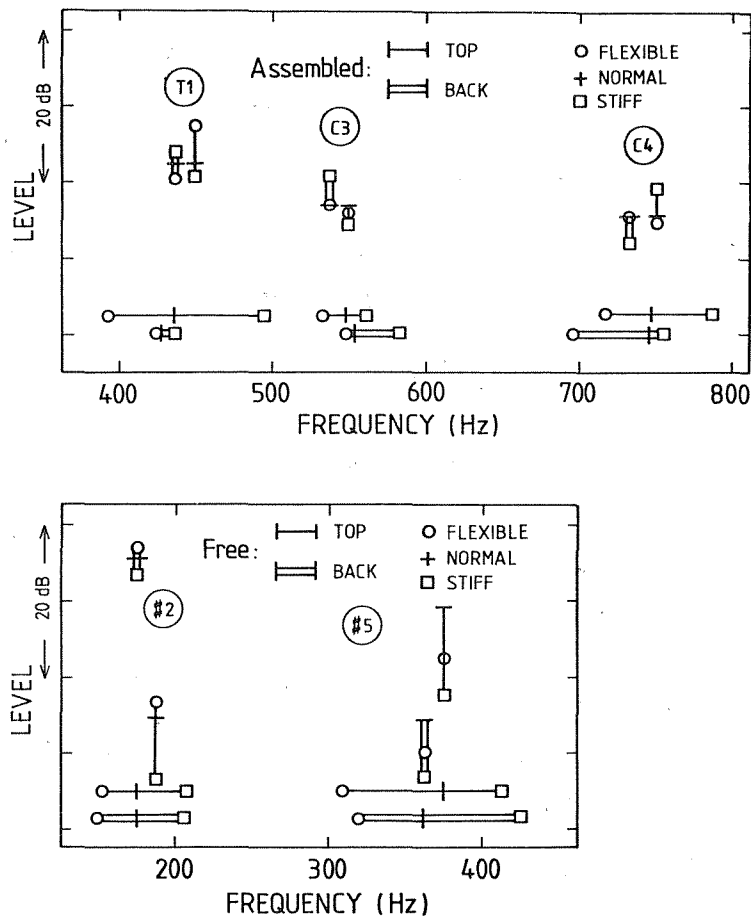


Fig. 10. Variations of levels and frequencies at resonance of three modes of assembled model violins (upper diagram) and of two modes of the corresponding free plates (lower diagram).

data on violins under construction. Our first interest is to find the typical properties and their range of variations. Presently, we have a too limited number of violins for general conclusions, but let me use our present results to point out possible relations.

In the lower frame of Fig. 9, the ranges of variations are sketched for levels and frequencies at resonances of some free top and back

plates. In the upper frame the same data are sketched for 25 assembled violins.

In a second part, we are modelling properties into violins. In the first step of the laboratory experiments, Alonso Moral in cooperation with Carleen Hutchins made a pilot test to measure relations between free plates and assembled violins. The plates were selected to contain three top plates and three back plates one normal, one flexible, and one stiff as given by their resonance frequencies, Fig. 10 lower frame. A comparison of the lower parts of Figs. 10 and 11 shows that the range of frequency variations is well covered by the six selected plates. The level variations are also well covered (absolute levels cannot be compared because of different ways of measuring). The vibration levels of the fifth mode are somewhat astonishing though, the flexible plate gives lower vibration level than the normal (this may reflect the maker's way of working to find the best compromise).

The interesting question is: Does the range of variations covered for the free plates result in a covered range for the assembled violins? A comparison of the upper parts of Figs. 9 and 10 shows that the frequency ranges are reasonably well covered. The crosses are close for the case of normal-normal plates. The variations of vibration levels with the six plates are, however, smaller. Thus, it seems that we must include additional parameters to cover the full range of vibration levels.

Another interesting question is: Does the top or the back plate give a dominating influence on any of the modes of the assembled violin? By looking at the upper part of the last figure, we find that only in the case of the T1 mode, there is a clear dominance for one mode, the top plate mode. This is especially true for the frequencies. An intriguing point is that the levels for the different combinations tend to be the opposite for the T1 and the C4 modes.

Correlation of Eigenfrequencies Free and Assembled Plate Modes

An even more detailed question for the maker is: Does a specific mode of the back or the top plate give a dominating influence on a specific mode of the assembled violin? As a very preliminary test of possible

relations, the correlation was calculated between the resonance frequencies of modes 1, 2, and 5 of the free plates and the T1, C3, and C4 modes of the assembled violins, see Table I. The results suggest that the top plate modes are most important for the assembled T1-mode, but the back plate modes are most important for C3 and C4. Somewhat surprisingly the correlations also suggest that the free plate modes no 1 of both the top and the back plate are the most important. Only the free back plate mode no 5 has a large correlation with the C3-mode. Whether the surprising result is "accidental" or significant remains to prove with a larger and more representative number of violins.

Table I. Correlations between the resonance frequencies of the free plate modes and the modes of the assembled violins (6 violins).

		ASSEMBLED	VIOLIN	MODES
		T1	C3	C4
FREE PLATE MODES				
no. 1	Top/Back	.79/-.42	.29/.98	.63/.91
no. 2	Top/Back	.47/ .14	.49/.42	.49/.71
no. 5	Top/Back	.25/-.47	.51/.95	.63/.75

Conclusions on Free and Assembled Plates

Our first analysis of experiments on free plates and assembled violins indicates that we really cannot explain very much, i.e., we can obtain reproducible measures but we can hardly give even a qualitative calibration of their importance. We can monitor frequencies in the assembled violins, but presently not levels. Possibly, this can be done by including all measures, such as a separation in Q-factors and the vibration patterns. But that we do not know. So let me end with a question: Is it only the complexity of the violin that hides the solution of the physical problem or does our investigations not include the parameters of major importance?

Reference

Alonso Moral, J. and Jansson, E.V. (1982): "Input admittance, Eigenmodes and quality of violins", STL-QPSR 2-3/1982, pp. 60-75.

EVIDENCE OF BRIDGE AND SOUNDBOARD CONTRIBUTIONS
TO KEYBOARD INHARMONICITY

Cary Karp
SMS-Musikmuseet
Stockholm, Sweden

The "stiff string" equation as given by Shankland, Coltman, Morse and others allows the calculation of the partial frequencies of vibration of a string as functions of several of its physical parameters, including the conditions at its end supports. Many authors report observations made on the strings of the contemporary piano to be in good agreement with values calculated assuming the strings to be hinged at their supports. In the present study one modern grand piano, two harpsichords, and one early 19th-century wooden frame grand piano were examined. The modern piano and one of the harpsichords behaved as expected on the basis of results reported in the literature. The other two instruments yielded inharmonicity data which could not be explained at all satisfactorily in terms of string stiffness. The deviations from expected values were large and of clear musical significance. Severely limiting the motion of the bridges and soundboards of all four instruments brought measured values into good agreement with values calculated assuming the strings to be clamped at their supports. There is reason to believe that the differences between the two pairs of instruments may be explained in terms of the rotation of the bridges about their longitudinal axes.

The fundamental frequency of vibration of a string under tension between rigid supports can be calculated to a satisfactory degree of accuracy as a function of the string's length, diameter, density, and the stress applied to it. Since, however, no string is perfectly flexible higher partial frequencies of vibration will not be integral multiples of the fundamental frequency. In order to calculate higher partials additional parameters must be considered. The most commonly used algebraic "stiff string" equation uses the parameters listed above and allows for string stiffness by using its modulus of elasticity. The equation con-

tains terms to allow for explicit solution in the two cases where the string is either clamped or hinged at both its supports.

Several authors have investigated modern pianos and have shown that the positions of its inharmonic partials are generally in good agreement with values calculated assuming the strings to be hinged at their supports. The conclusion drawn has been that it would appear likely that piano strings, indeed, are hinged at their supports and that piano inharmonicity can be explained solely in terms of string stiffness.

Since the bridge on a piano soundboard is obviously not a rigid support, the present study was intended to determine the effect of eliminating the motion of the bridge and soundboard at the point of string support. Although it did not prove possible to eliminate all such motion, substantial reductions were effected. Fig. 1 shows a clear frequency shift for all partials on a modern piano string when bridge motion was reduced. On the basis of this and other similar observations it may be suggested that the strings of a modern piano are clamped at their supports, and that bridge and soundboard motion shift all partial frequencies to positions very near those predicted by calculations assuming the strings to be hinged at their supports. Keyboard inharmonicity can, therefore, not be explained solely in terms of string stiffness.

On an 1811 wooden frame grand piano what presumably were bridge and soundboard effects generated the data given in Fig. 2. Here it is clearly seen that inharmonicity is negative for a large number of lower partials, rendering the stiff string equation virtually inapplicable in this case. The implications of this negative inharmonicity for the subjective experience of sound quality and pitch cannot be ignored. On another string on the same instrument (data given in Fig. 3) inharmonicity is held quite close to zero for most of the lower partials. It would appear possible that certain aspects of bridge and soundboard design can deliberately be utilized to reduce the effects of string inharmonicity, and that the attempt to do so may cause partial frequencies to lie below strictly harmonic positions.

Two harpsichords were also examined. One was a modern factory built instrument with a relatively thick soundboard, built more according to modern piano design criteria than in any traditional harpsichord style.

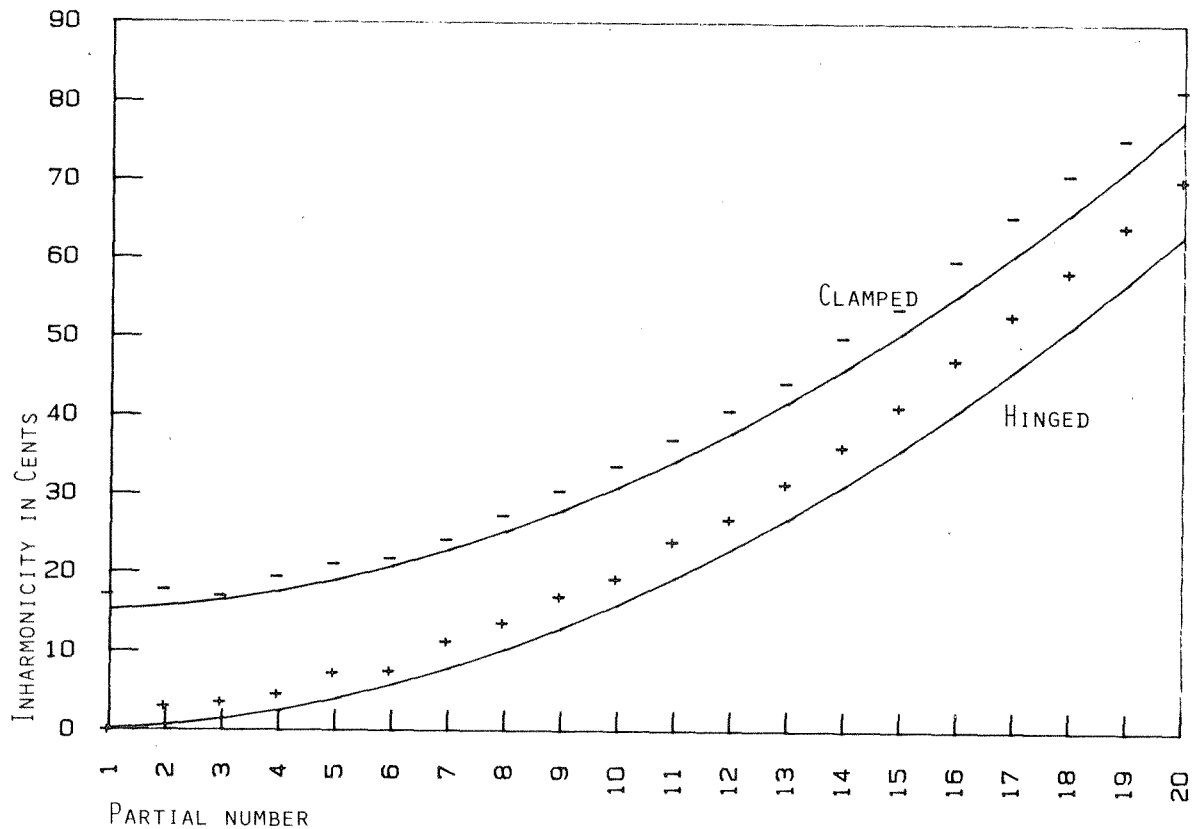


Fig. 1. + = MEASURED VALUES WITH NORMAL BRIDGE AND SOUNDBOARD MOTION
 - = MEASURED VALUES WITH REDUCED BRIDGE AND SOUNDBOARD MOTION
 SOLID CURVES = CALCULATED VALUES

The other was patterned after an 18th century prototype. In analogy to the modern piano, the inharmonic behavior of the first harpsichord appeared to be explainable in terms of hinged stiff strings, although reduction of bridge and soundboard motion revealed the strings to be clamped. The second harpsichord behaved similarly to the wooden frame piano, displaying both "zero" and negative inharmonicity. Immobilizing the bridge on this instrument also caused predictable clamped string behavior. (The nature of the older piano precluded the mechanical action necessary to make similar conclusive measurements on it.)

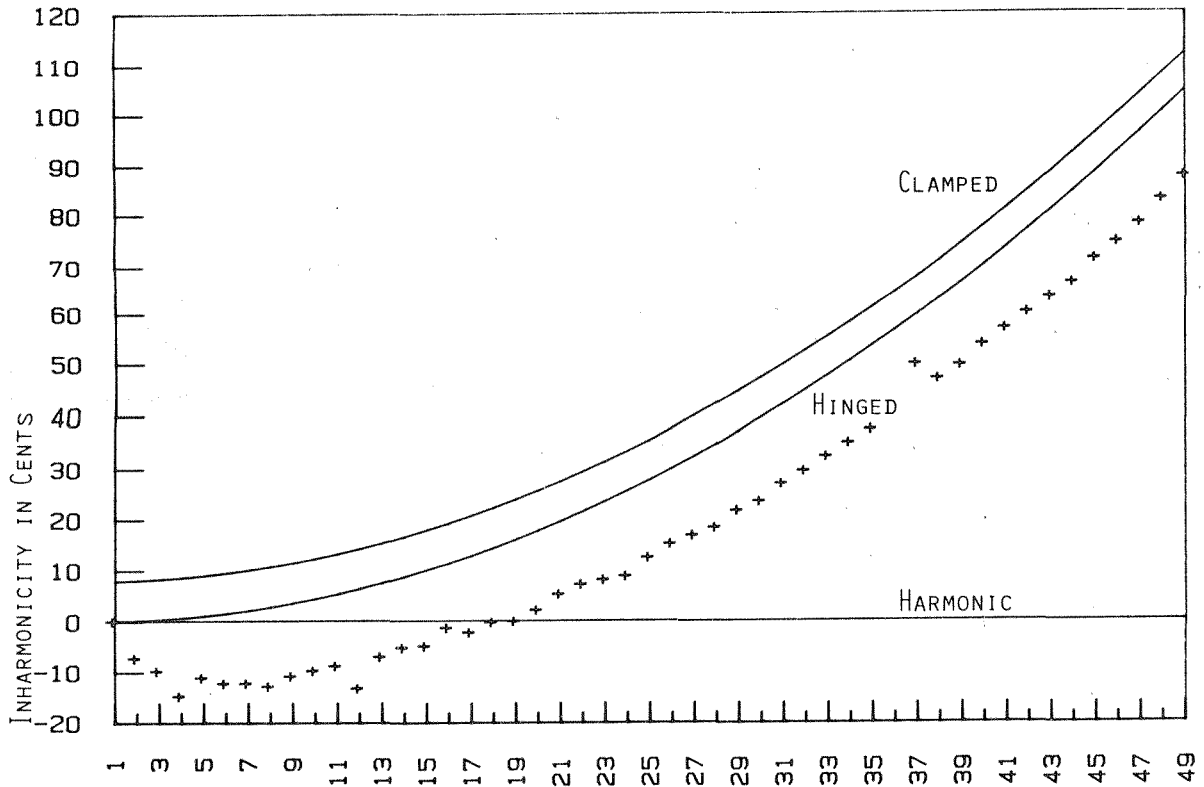


Fig. 2. PARTIAL NUMBER
 + = MEASURED VALUES
 SOLID CURVES = CALCULATED VALUES

The two pairs of instruments, "old" and "modern", differ in that the former display design features which clearly reduce the net effects of inharmonicity. Although no direct evidence was found which enables this to be related to makers' intent, the following observations may still be of interest: The soundboards of the modern instruments are thick and flat, whereas on the older instruments they are thin, much less rigid, and inclined to "dish" at the bridge. The motion of the bridges on the modern instruments could be reduced simply by loading them from above and below perpendicular to the plane of the soundboard. On the older type

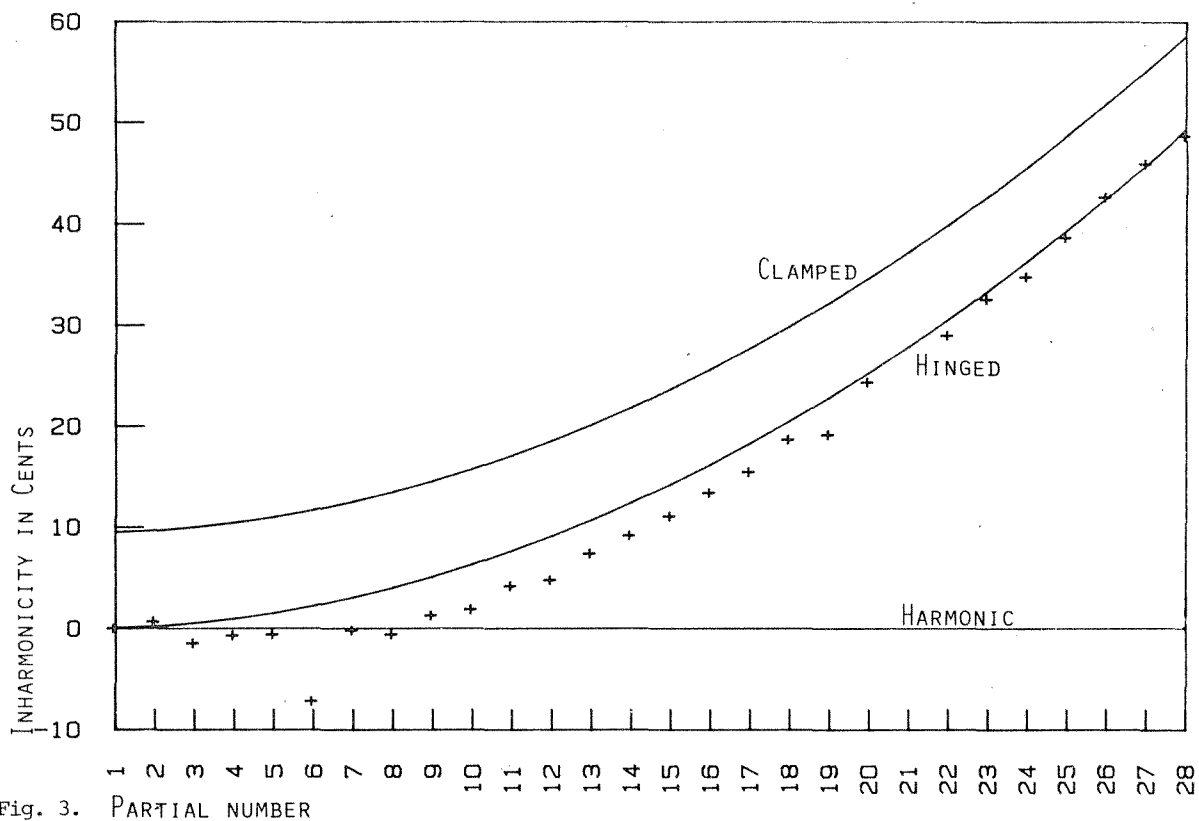


Fig. 3. PARTIAL NUMBER
 + = MEASURED VALUES
 SOLID CURVES = CALCULATED VALUES

harpsichord it was also necessary to prevent the bridge from twisting forward. Clear evidence of longitudinal modes of vibration was found only in the sound spectrum of this instrument.

It would, therefore, seem possible that the difference between the inharmonic behavior of modern and older strung keyboard instruments may correlate to the lack of preoccupation with producing absolutely flat soundboards which appears to characterize earlier schools of keyboard making. The student of modern piano design who speculates about the possibility of reducing inharmonicity may benefit from a study of older types of pianos and other strung keyboard instruments.

A NEW IDENTIFICATION EXPRESSION OF HELMHOLTZIAN WAVES
AND THEIR FORMATION MECHANISM
Masao Kondo and Hidemi Kubota
Gakushuin University, Tokyo, Japan

On finding the fact that there are always coexisting on a string the plural number of Helmholtzian waves instead of a single wave, two new concepts are introduced for understanding the "Helmholtz Motion". One is an identification expression of Helmholtzian waves in terms of acceleration, and the other is a special reference frame of the laminar flow type.

(1) The former is found to be very useful, especially when one deals with the plural number of Helmholtzian waves coexisting on a string, and the same expression is also applied, without any alteration, to a simple bend travelling on a string. Here the introduction of the latter frame serves to convince us that the simple travelling bends and the Helmholtzian waves are physically the same.

(2) In the bowing process, each "stick" or each "slip" makes a pair of small bends on a string at the bowing point, which start their travel toward ends at which they reflect back. All these pairs of bends which are generated successively in the course of bowing are integrated on the limited length of the string; some are summed up to larger bends, some remain separately as small bends, and some in other ways. The results of integration are largely influenced by the location of the bowing point as well as by the bowing speed and the bowing force.

The integrated state being reduced by the inherent damping makes the whole motion of a bowed string, in which, of course, a single Helmholtzian wave is predominantly observed in normal playing.

Introduction

One stream of our study has been the observation of bowed strings with anamorphic cameras and a bowing machine of the endless belt type. Although a number of results have been reported piece by piece at ICA conferences since 1968 (*), the structure of the bowed strings has not been understood completely until now.

The key for solving this problem is the finding of the fact that there are always -- yes! always -- a number of Helmholtzian waves coexisting on a string, both clockwise and counterclockwise, strong and weak, each with its own phase difference(**). In order to describe and understand such string movements, we have needed a new identification symbol or expression for a Helmholtzian wave.

The typical wave motion generated by bowing a string has a specific shape and a specific velocity distribution, which are designated as a "Helmholtzian wave" (in a limited sense) and a "Raman wave", respectively. These two kinds of waves are essential and (seem to be) enough to understand the kinematics of a single Helmholtzian wave. But when we have to deal with a number of Helmholtzian waves existing simultaneously on a string, another new wave concept becomes a powerful tool in order to understand the situation, that is, the "Acceleration wave".

- (*)
- | | |
|---|----------------------------------|
| A. Kuni and M. Kondo: - - - - - | 6th ICA Report 1968 |
| M. Kondo and A. Kuni: - - - - - | 8th ICA Report 1974 |
| M. Kondo, A. Kuni, and H. Kubota: - - - - - | 9th ICA Report 1977 |
| M. Kondo and five students, 2 papers: } | |
| H. Kubota and M. Kondo: - - - - - | } - - - - - 10th ICA Report 1980 |
| M. Hirota and M. Kondo: - - - - - | |
| H. Kubota and M. Kondo: - - - - - | 11th ICA Report 1983 |

All papers in the session of Musical Instruments

(**)

Doctorial thesis of Hidemi KUBOTA (submitted to the Gakushin University in 1983). A part of his thesis was reported at the 11th ICA (in the poster session), July 1983, entitled "Tables of Numbers of the Helmholtzian waves on a bowed String" (which shows the possible number of Helmholtzian waves coexisting on a bowed string. This number depends on the bowing position.)

The experiences of treating many examples with the aid of this acceleration wave have led us to understand the build-up mechanism of the wave motion of a string generated by the bowing action.

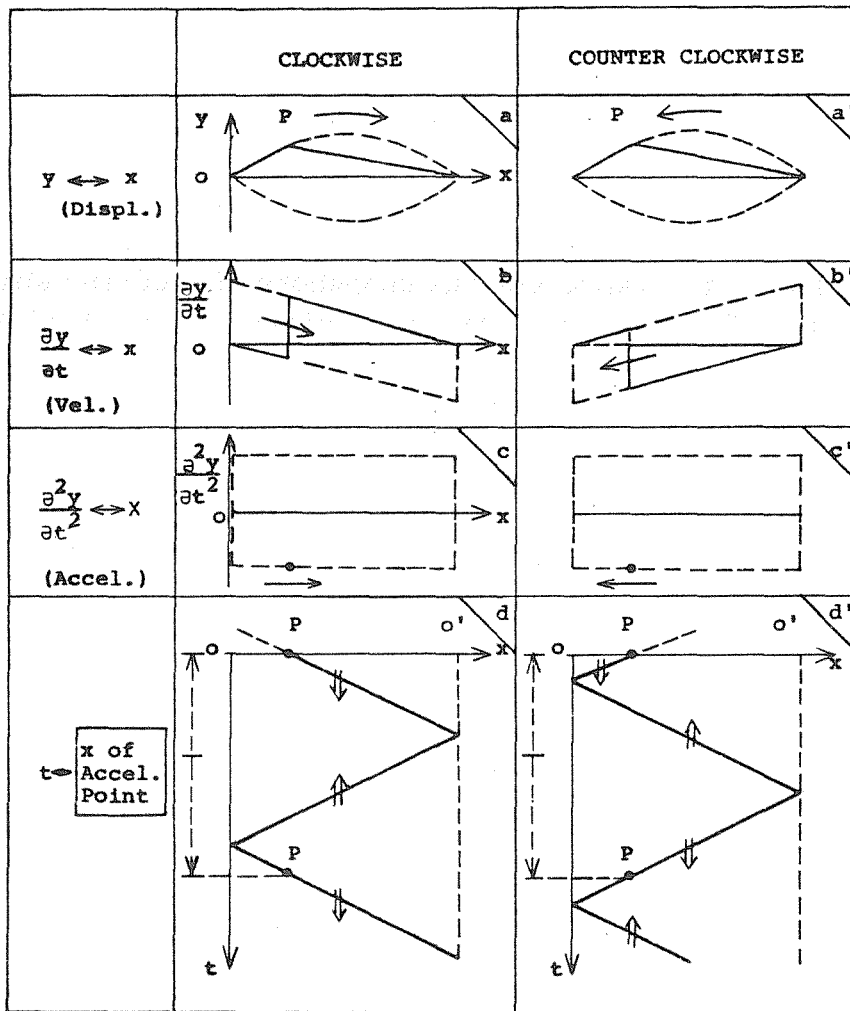
PART I. A NEW IDENTIFICATION EXPRESSION OF HELMHOLTZIAN WAVES

Helmholtzian Waves - clockwise and counterclockwise

(a) and (a') in Fig. 1 represent the snapshots of a string which is in "Helmholtz motion". The string shape consists of two straight lines connected at P where it makes a bend. The bend travels with the propagation velocity of transverse waves along two parabolic curves successively, thus making round trips between the two fixed ends. Whether this round trip is clockwise or counterclockwise is not known from the snapshots, because (a) and (a') look just the same. Suppose that we assume the motion in (a) to be clockwise and the motion in (a') to be counterclockwise, and indicate this by the thin arrows.

(b) and (b') in Fig. 1 express the velocity distributions of the moving strings (a) and (a') respectively. It is an important property of this type of motion that the velocity of the string element jumps an equal amount wherever a bend passes through the element.

The two kinds of diagrams mentioned above are essential and seem to be enough to understand the kinematics of a single Helmholtzian wave. By partially differentiating with time the velocities of the string elements in (b) and (b'), one gets the acceleration distribution along the whole length of the string as seen in (c) and (c'). At the bend, the acceleration has a definite non-zero value (with positive or negative sign), but elsewhere on the string the acceleration is zero. We will call the point which expresses the non-zero definite value of acceleration at a bend the "acceleration point". As the height of the acceleration point does not change when it moves with the bend, the locus of the acceleration point describes the four sides of a rectangle (shown by dotted lines in (c) and (c')); it moves along the upper and lower sides at the speed of the bend.



(\rightarrow) or (\leftarrow) shows a moving direction.
 (\uparrow) or (\downarrow) shows the direction of acceleration.

Fig. 1.

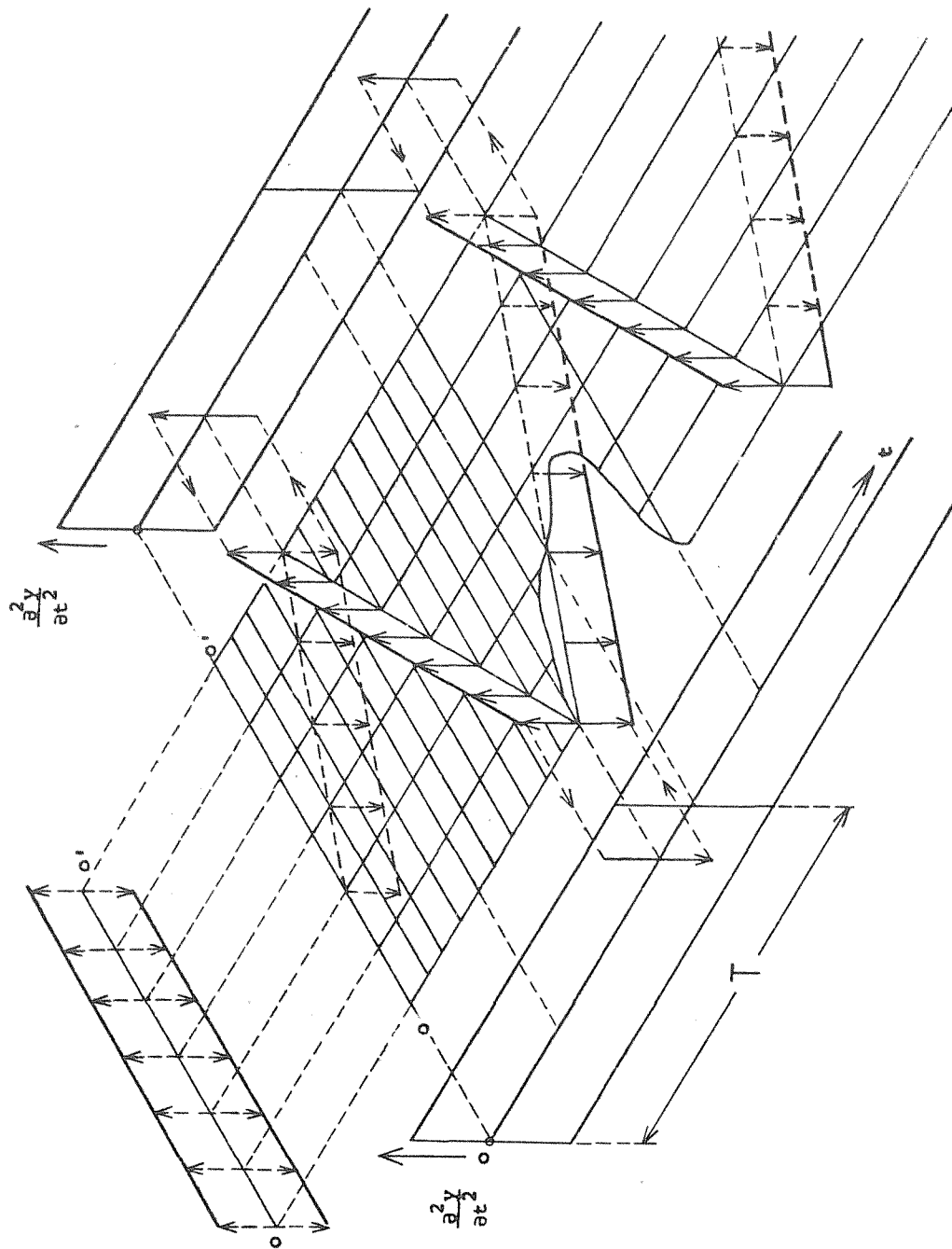


Fig. 2. Three dimensional model of the passage of the acceleration point.

Expressing the height, the location, and the direction of motion of the acceleration point identifies a particular Helmholtzian wave. To see the time change of a Helmholtzian wave, it is convenient to draw a graph of its inherent acceleration point with coordinates (x,t), as in (d) and (d'). By adding to the path of the acceleration point a thick arrow which shows the sense of acceleration, (d) and (d') of Fig. 1 become complete, in that they tell us also the rotational modes of the bend. As a thick arrow changes its sign at both fixed ends of the string, we can conclude the following:

The passage $\frac{dx}{dt} > 0$ with \Downarrow } means the clockwise round trip
 and $\frac{dx}{dt} < 0$ with \Uparrow } of the bend, and
 the passage $\frac{dx}{dt} > 0$ with \Uparrow } means the counterclockwise round trip
 and $\frac{dx}{dt} < 0$ with \Downarrow } of the bend

If we combine (c) and (d), we get a three dimensional model of the passage of the acceleration point, as shown in Fig. 2, where the thick arrows are no longer necessary.

The simplicity of the passage of the acceleration point -- always straight and parallel to the x-t plane -- makes this diagram very useful, especially when a number of Helmholtzian waves are coexisting on a string.

"Stick" bends and "slip" bends

The interaction between bow and string consists of a "stick" duration and a "slip" duration, during the "slip" duration, it is hoped that the string is as much free as possible from the bow. In the following we assume that no friction exists during a "slip" duration. At the moment of transition both from "slip" to "stick" and "stick" to "slip" (i.e., at

the beginning and at the release of the "stick"), the string element at the contact point receives a transverse shock of minus and plus signs, respectively. These transverse shocks generate on the string a pair of bends which start their travels toward ends.

In Fig. 3, a long string is stretched along the x-axis, and is bowed in the (-y) direction at P_0 . At the stick point P_0 , twin bends +B and -B are born; and +B travels as $+B_1 \rightarrow +B_2 \rightarrow \dots +B_n \rightarrow +B_{n+1} \rightarrow \dots \infty$ to the right, and -B as $-B_1 \rightarrow -B_2 \rightarrow \dots -B_n \rightarrow \dots -\infty$ to the left. When the contact point of the string and the bow comes to the point P_n , the string has moved down to the position given by the dashed line $(-B_n)(P_n)(+B_n)$; the whole depression is moving downward at the same speed as that of the bow. Now, release the bow at this moment, by any means; another pair of bends $-B'_{n+1}$ and $+B'_{n+1}$ are born, and they proceed in opposite directions. Let us call the bends generated at the beginning of "stick" stick bends, and the ones at the release of "stick" slip bends. Stick bends and slip bends have opposite shapes; one is convex, the other concave in this figure. The string element at a stick bend (+B or -B) has a downward acceleration (\Downarrow) and the one at a slip bend ($+B'$ or $-B'$) an upward acceleration (\Uparrow), and all the other parts of the string have no acceleration at all. These bends propagate to both sides with the wave velocity of the string, keeping their shapes unaltered if both damping and dispersion are negligible.

Focussing our attention on these bends, and disregarding the shape and the velocity of the string, we can draw a (x,t) diagram of bends as in Fig. 4. Here, $\pm \tan \theta = \frac{dx}{dt}$ = propagation velocity of the bend.

Bends and Helmholtzian waves

Now we will see how the propagation of the bends examined above leads to the bends of the Helmholtzian waves.

(1) Shape Relation: The upper right half of Fig. 3 is shown magnified in Fig. 5(a), where Q is the right fixed end of the string and P is

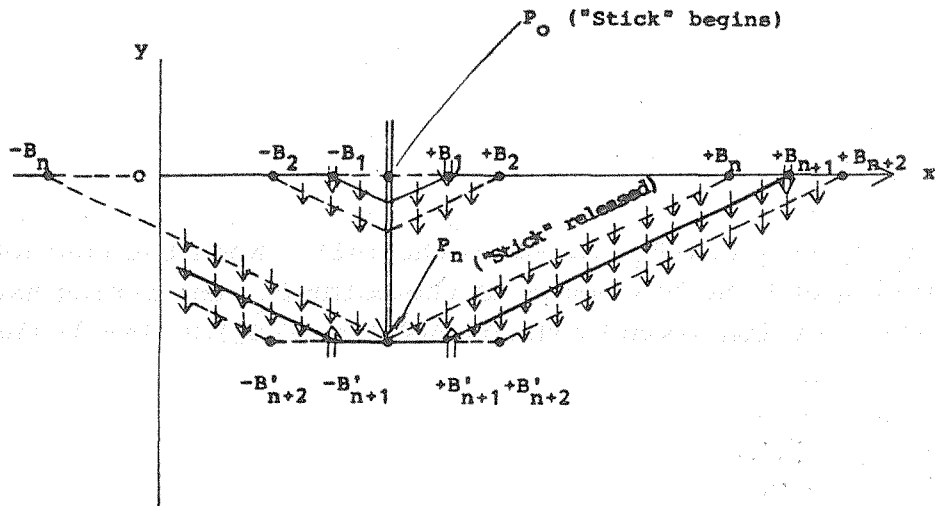


Fig. 3. Stick bends and slip bends.

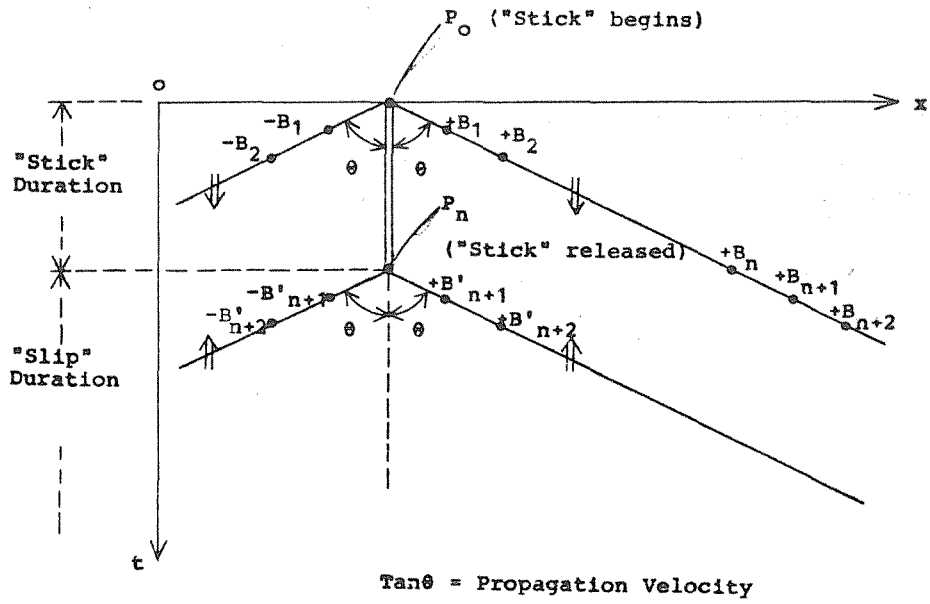


Fig. 4.

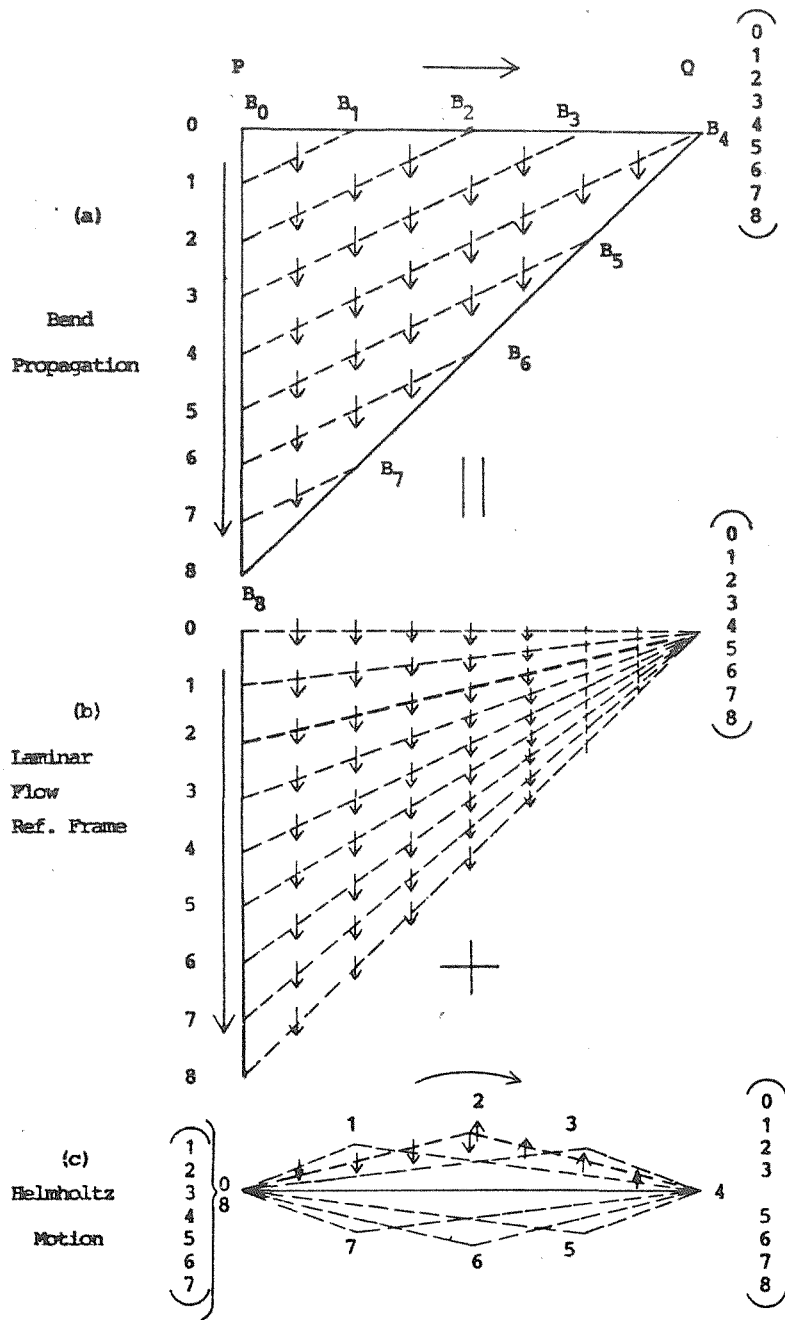


Fig. 5. Displacement.

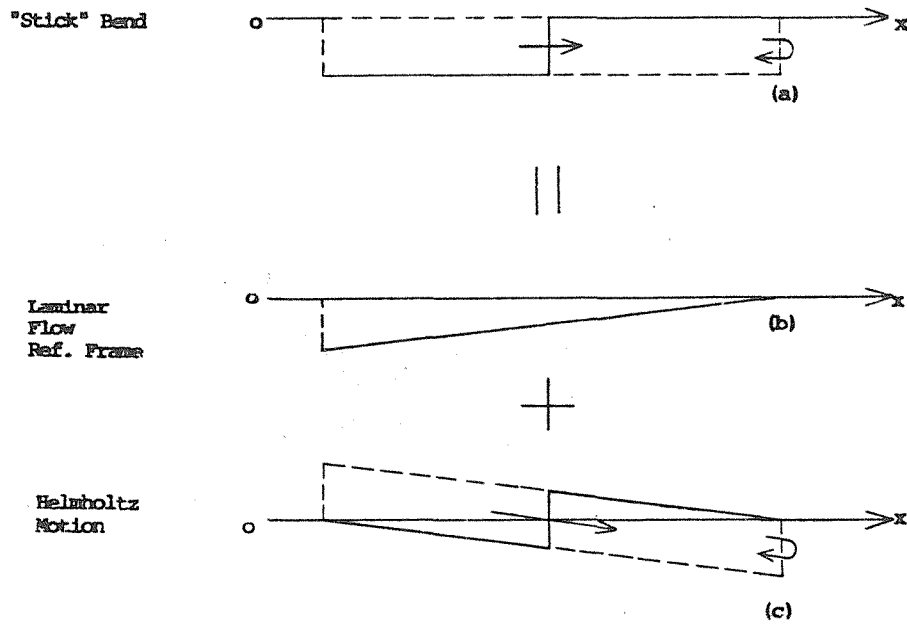


Fig. 6. Velocity.

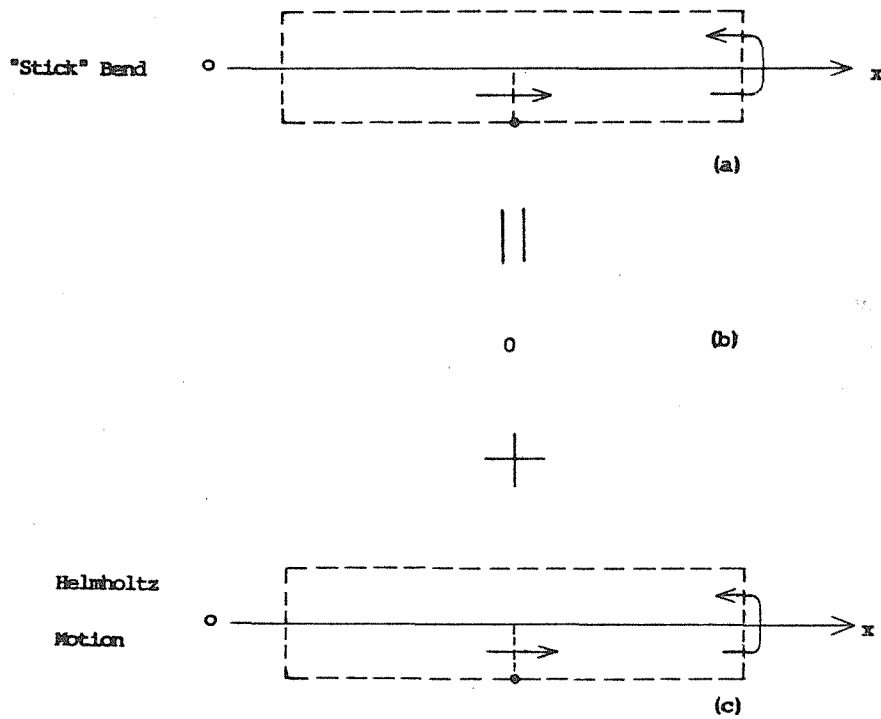


Fig. 7. Acceleration.

the bowing point moving downward with a uniform speed. If the string motion of (a) is seen from the reference frame (b), the string motion appears as (c) which we recognize as a Helmholtzian wave. The frame (b) is a special reference frame in which the whole area is moving in the $-y$ direction with uniform speed as in a laminar flow.

The above discussion is safely applied to the real phenomena when range of y is small compared to the length PQ . The propagation of a bend is composed of two components, one a laminar flow motion, the other a Helmholtzian wave.

(2) Velocity Relation: Fig. 6 shows the velocity relation, which is simpler than the shape relation and more easily understood.

(3) Acceleration Relation: As the laminar flow reference frame has no acceleration, the acceleration relation becomes very simple; it tells us that a "bend" and a "Helmholtzian wave" are just the same when seen through the window of acceleration (Fig. 7). So the acceleration points discussed in the first section of Part I are the identifications of both "Helmholtzian waves" and the newly born "stick and slip" bends.

PART II. FORMATION MECHANISM OF HELMHOLTZIAN WAVES

Passages of "stick" and "slip" bends

When a string has a limited length L and "stick" continues for a while (Fig. 8), each stick bend reflects back at a fixed end and also again at the contact point of the string and the bow. The contact point acts just as a fixed end, as long as the bow holds the string firmly. Thus twin bends make two different zigzag passages, depending upon the distances the bends have to pass between two successive reflections.

Fig. 9 shows the case in which the release of stick occurs at P_R (at time t_R). Here the twin "slip" bends are born and they follow the dashed lines, while the former "stick" bends follow the solid lines. The four waves have no obstacles between two fixed ends.

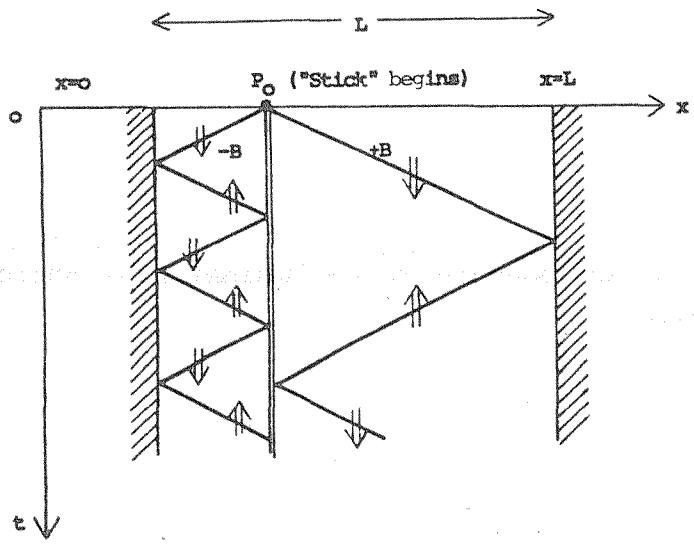


Fig. 8.

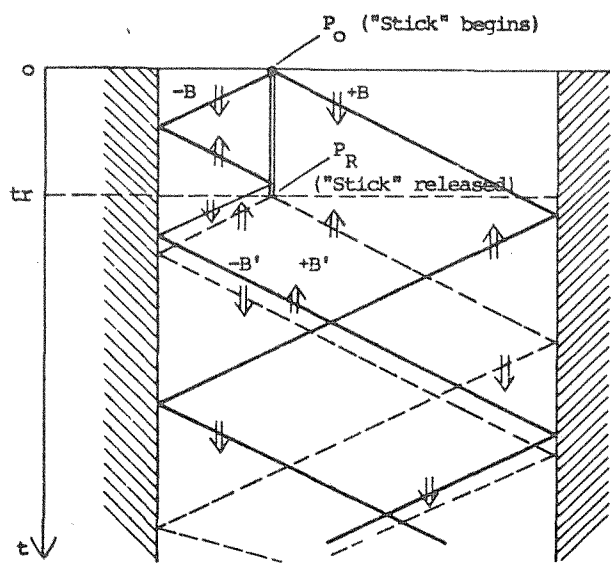


Fig. 9.

Trigger to release "stick"

Next we consider the problem: "What is the trigger to release the "stick"?"

Fig. 10(a) shows the stroboscopic shapes of a bowed string, in its "stick" duration. The string is stretched between $x=0$ and L , and is bowed downward at P (i.e., in the $-y$ direction). This drawing of the string in a (x,y) frame corresponds to Fig. 8 where the movements of the two stick bends are shown in a (x,t) frame. (The scale of x is just half of that in Fig. 10(a).) Dashed lines are the parts of the string moving downward with the same speed (\downarrow) as that of the bow, and thick solid lines are the parts at rest. It should be noticed that the angle of the bend under the bow does not change continuously, but decreases stepwise every time when a stick bend arrives there.

This angle determines the pulling force of the bow. To see the stepwise change of this angle, it is convenient to divide the angle into two components; the left component is the angle between the bow and the left part of the string, and the right component the angle between the bow and the right part of the string. The pulling force F_L due to the left component is schematically shown in (c) and the pulling force F_R due to the right component is shown in (b), and the total pulling force F_L+F_R is also shown in (b).

If the frictional force between bow and string is α the slip occurs at the $[L-2]$ step, and in case of β at the $[R-1]$ step, and in case of ν at the $[L-3]$ step, as shown at (b) in Fig. 10.

In this example, the bowing point is at $2/7 L$ from the left end. By changing the bowing point, a player can bring the $[L]$ step and the $[R]$ step the same location, thus getting a double size step which will give him larger tolerance of bowing forces than a single size step can give.

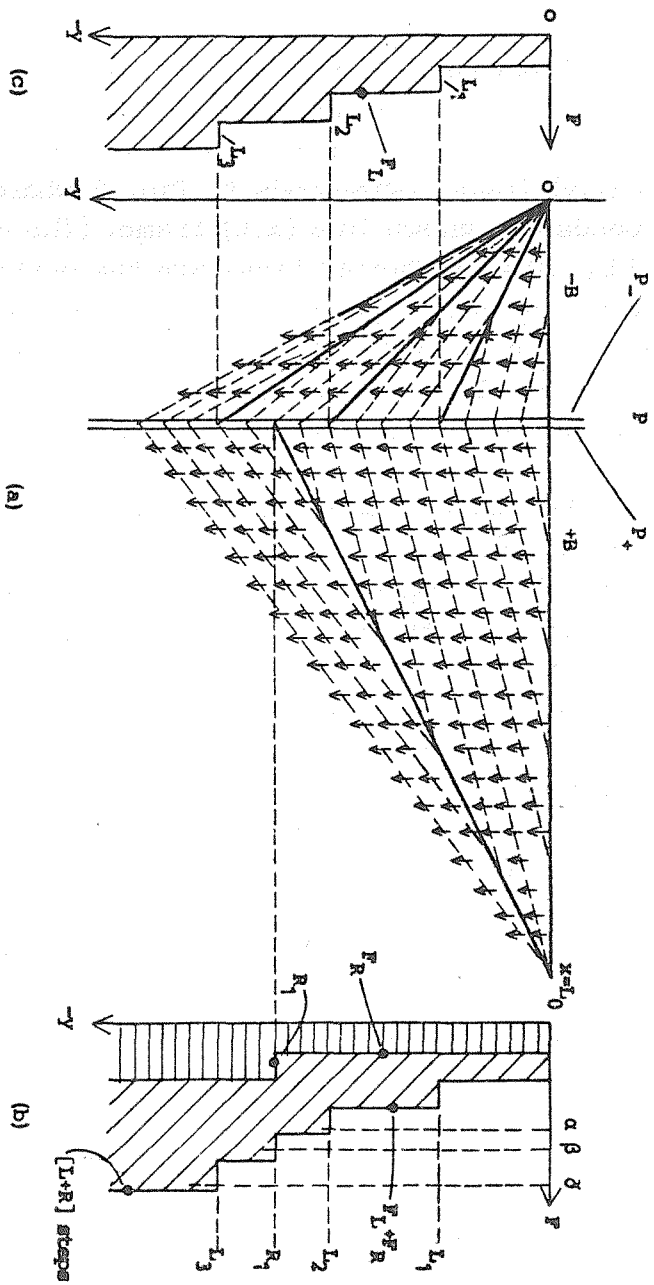


Fig. 10.

Summation of stick bends and slip bends

Take a simple example in which the bowing is performed at a point $1/3$ L from the left end, and see how bends add together. Every column of Fig. 11 is a (x,t) diagram; the horizontal line is the length of the string L and time axis is vertically downward. At the point 1 of the first column, the first "stick" begins, which sends twin bends to both sides. At time $2/3$ T after the point 1, these bends meet again at the bowing point, and make a force rise of double size which is likely to exceed the frictional force between the bow and the string. Suppose a "slip" does occur at this moment. The moment is the point 1 of the second column, from where a twin slip bends spring out for both sides. The left bound bend follows the passage of solid lines, between the left and right ends (for five times in the figure). The right bound bend follows a more complicated passage of dashed lines, as shown.

When the left bound bend comes back for the first time to the bowing point, the second "stick" occurs at a time which corresponds to the point 2 of the first column. Then the same sequence as that of the first follows and the second "slip" occurs. The third column shows the passages of the twin slip bends continuing for four periods; for the left bound bend solid lines are used as before, and for the right bound bend chain lines are used to be distinguished from the second column.

Adding the second and third columns together, we get the fourth column. It is interesting to see the left-bound bends generated both at 1 and 2 coincide in the same passage, while right-bound bends generated at 1 and 2 help each other to make the complete two zigzag courses equally spaced between the doubled zigzag course of the left-bound bends.

Examining the fourth column more deeply seems to be suggestive to understand the building-up process of the multiple Helmholtzian waves on a string. Look at the points surrounded by small squares along the bowing line where slip-bends come from both sides and meet under the bow and

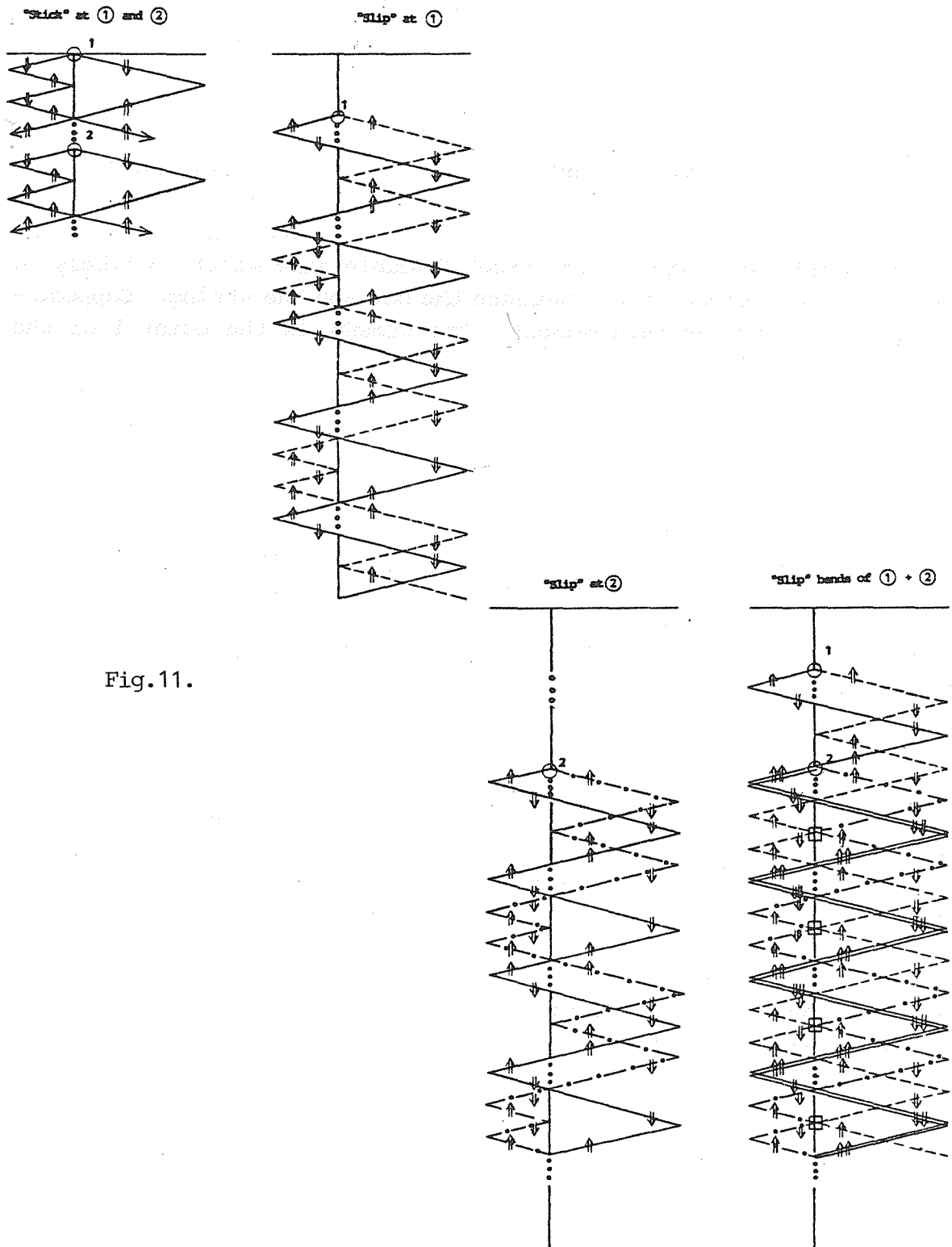


Fig.11.

reflect back to their own sides. As the bends have the opposite signs, they cancel their effect of reflection if they are of an equal magnitude. Consequently, these simultaneous reflections have no influence on the bow and the string. This situation is equivalent to the one in which each bend coming from both sides passes straight and freely to the other side through the bowing point, without giving any influence to the bowing action.

Finally, when we add the first column to the fourth, we get the complete wave motion of the string generated by two successive units of "stick" and "slip" disregarding the damping. Here, of course, the wave motion of the string is expressed in terms of "acceleration symbol".

Although the work is still in progress, we have found that applying this method to several cases with different bowing positions has led to plausible and reasonable results, and we expect this method will clarify the building up of waves and the long-range order of the cycles, and also reveal many complicated cases corresponding to the performances of real bowing.

AUTOMATIC TRANSCRIPTION OF POLYPHONIC MUSIC
BY LINEAR PREDICTIVE ANALYSIS
J.E. Philipp
Institut für Phonetik, Universität Köln, BRD

Abstract

A FORTRAN program has been designed which performs automatic transcription of polyphonic music by means of bandpass filtering with a digital polyphase filterbank and subsequent LPC analysis. Frequency resolution is a quartertone for sounds stationary for times > 50 ms.

The Problem: Frequency Resolution

The notation of recorded music is a fundamental task in ethnomusicological research. The 'traditional' method of listening to the music and trying one's best at writing it into the western system of staff lines can be very cumbersome. Therefore many attempts have been made to design devices or programs for automatic transcription. With monophonic music, such efforts have been fairly successful. This has been demonstrated by the early Grützmacher-Lottermoser 'Tonhörensreiber' (1937), the Serger 'Melograph' (1974), and the Askenfelt 'Trio Detector' (1976) and a host of algorithms designed for speech processing applications. Polyphonic music analysis has been tried by several authors (Moorer, 1977; Piszczalski and Galler, 1977; Tove et al., 1967) by means of Fourier and adaptive bandpass filtering techniques. One of the main problems in this approach arises from musical sounds being stationary often for no longer than 50 ms. Such a time window is insufficient for discrimination of spectral lines less than 20 Hz apart. So half-tone intervals below e' (≈ 330 Hz) will not be resolved.

Linear Predictive analysis can in principle do much better. Unlike LPC speech analysis, however, which involves modelling the few resonances of the vocal tract only, polyphonic music analysis requires the representation of each partial by a pair of zeros of the predictor polynomial. The generally large number of partials in the relevant frequency range

from 0 to 2500 Hz leads to predictor orders too high to render possible application of LPC analysis to the signal directly. Therefore, preparatory bandpass filtering is a necessity.

The Realized Approach to a Solution: Polyphase Filterbank + LPC

To test the applicability of LPC to polyphonic music analysis, a program for automatic transcription has been designed which processes the digitized music signal (12 bit, rate 8 kHz) according to the following scheme:

1. bandpass-filtering by means of a Polyphase filterbank (channel width 260 Hz, lowpass channel width 125 Hz) with a simultaneous rate reduction to 1 kHz;
2. LPC analysis of the channel signals in portions of 40 samples, corresponding to 40 ms-frames overlapping by 20 ms; each frame may contain up to 9 partials;
3. elimination of spurious results by comparison of successive frames;
4. display of detected partials in a semilog frequency-vs-time print-plot with superimposed staff lines.

The digital Polyphase network used consists of 4 groups and 8 recursive subfilters with a subsequent 32-point FFT. The subfilters are derived from an elliptical prototype lowpass filter of order 6 by means of the closed solution for the subfilter transfer functions given by Vary (1979), who also pointed out how to elegantly reduce the sample rate by integer fractions of the number of filter channels. The prototype lowpass filter (passband edge 125 Hz, stopband att. 50 dB) has been designed with the aid of several modules of Dehner's 'Doredi'-program (1979).

The channel outputs are fed into an LPC routine, where proper choice of predictor order plays a crucial part. Orders less than the number of

complex exponentials needed to represent the signal will merge partials, orders higher will split them. Therefore, the number of predictor coefficients is adapted to each analysis frame as follows. 20 predictor equations with 18 coefficients are set up, using 40 samples. The system of equations is recursively solved by means of Householder transformations; the n -th transformation yields a system of equations from which that predictor of order n can be determined which minimizes the squared prediction error summed over the 20 primary equations. If this error drops below some empirical threshold, the recursion is stopped. Let n be the predictor order thus obtained. Whenever n is less than the maximum of 18, which is usually the case, the system of predictor equations is reformulated as a system of $40-n$ equations with n coefficients, which in turn is solved by n Householder transformations. Thus a predictor minimizing the prediction error over $40-n > 20$ equations is obtained, which contributes to the achieved spectral resolution.

Frequencies and damping factors are computed by rooting the predictor polynomials with the aid of the IMSL routine ZRPOLY; finally, amplitudes of the spectral components are computed by least-squares-fitting the model signal consisting of the sum of n damped complex exponentials to the original bandpass frame.

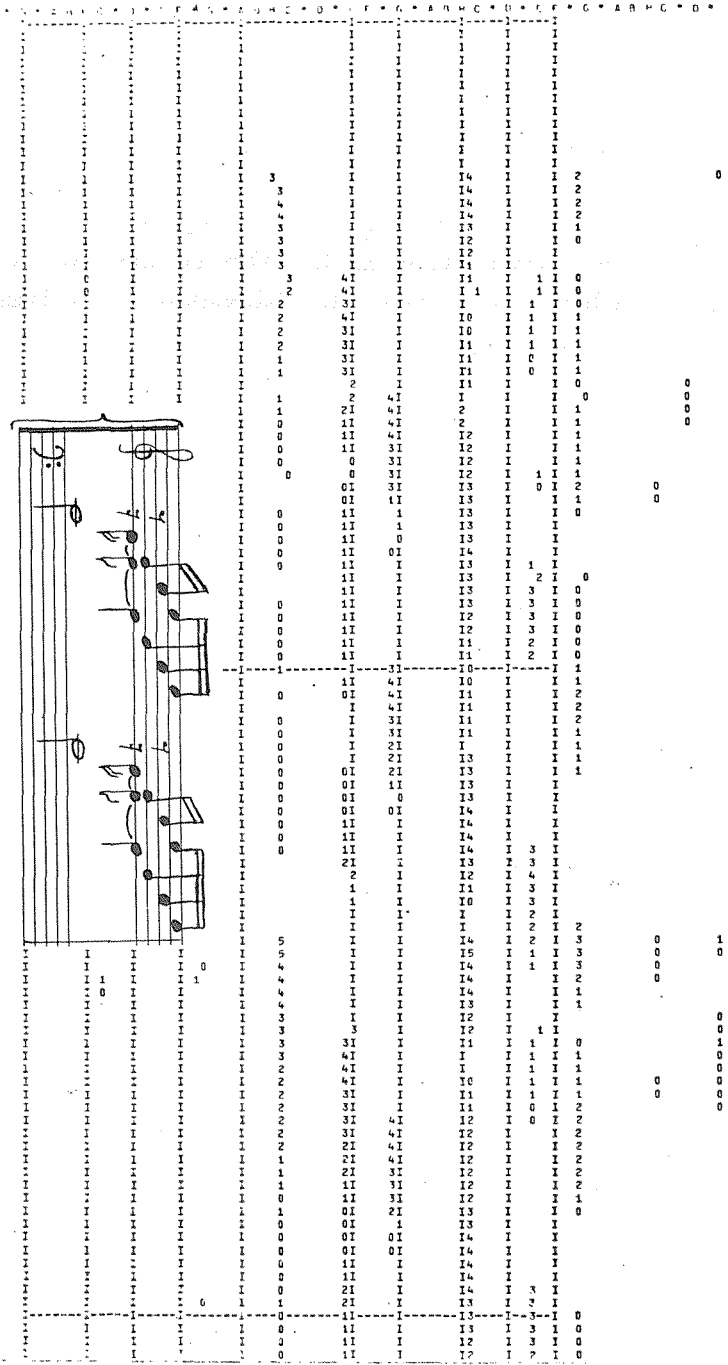
Spurious 'lines' are eliminated by:

- a. discarding all lines weaker than -40 dB (0 dB $\hat{=}$ max. single-tone ADC drive level), and
- b. discarding all those lines which do not appear in at least two overlapping frames (modulo slight frequency differences).

The Results

The overall performance of the procedure is characterized by a frequency resolution of a quarter tone for stationary sounds, provided the intensities of the components are of about the same order of magnitude. Attacks can lead to frequency errors up to a quarter tone, and of course no means exist for separating coincident partials as, for example, the

Fig. 1. Transcription of J.S. Bach's prelude in C major (BWV 846), played on piano. Numbers printed indicate intensity of respective partial averaged over one frame time, in steps of 5 dB.



fundamental of c' and the first harmonic of c" sounding together in the example given in Fig. 1.

So far, the program has been tested with music for piano, violin (monophonic), wind ensemble, and choir (2 parts), respectively. As could be expected, the greatest practical problem turned out to be the confusing diversity of partials in the printouts. Another problem arises from the amount of computation time needed: 5 minutes are used by the CYBER 76 at the computation center of the University of Köln to analyze 10 s of music, while the same task on the PDP 11/10 of the Phonetics Department takes a whole night.

References

- Askenfelt, A. (1976): STL-QPSR 1/1976, pp. 1-11.
- Dehner, G.F. (1979): 'DOREDI', in Programs for Digital Signal Processing, IEEE Press.
- Grützmacher, M. and Lottermoser, W. (1937): Akustische Zeitschrift 2, pp. 242-248.
- Moore, M. (1974): Selected Reports of Ethnomusicology, II, 1, UCLA, Los Angeles, CA.
- Moorer, J.A. (1977): Computer Music Journal, Nov., pp. 32-38.
- Piszczałski, M. and Galler, B.A. (1977): Computer Music Journal, Nov., pp. 24-31.
- Tove, P.A., Ejdesjö, L., and Svärdström, A. (1967): J.Acoust.Soc.Am. 41, pp. 1265-1271.
- Vary, P. (1979): Archiv für Elektrische Übertragungstechnik (AEÜ) 33, pp. 293-300.

FAST DECAY OF LONGITUDINAL VIBRATIONS IN VIOLIN STRINGS
M.P. Rafferty and A.R. Lee*
University College, Cardiff, Wales, Great Britain

Abstract

Measurements have been made of the decay rates of longitudinal vibrations in violin strings excited by bowing. Using photoelectric devices these vibrations are detected from the rocking motion of the top of the bridge in two orthogonal directions. It is found that the longitudinal oscillations decay with rates of ~ 500 dB/sec. In contrast, the transverse vibrations excited by plucking the violin string are found to have much slower decay rates of ~ 50 dB/sec.

Introduction

The vibrations normally excited in violins are predominantly transverse. Both 'arco' and 'pizzicato' playing create transverse vibrations which are coupled to the violin body through the rocking action of the bridge and finally radiated as sound. In the case of the longitudinal and torsional modes, it is usually assumed that such oscillations are of only minor importance compared to the transverse modes and that they do not couple strongly to the violin body. We have undertaken our initial work on the longitudinal vibrations (Lee and Rafferty, 1983) in order to locate the frequencies of these modes. Here we present measurements of the decay rates of such modes to gain insight into their possible importance in the transient regions of violin tones.

Indirect excitations and 'squeaks'

Longitudinal oscillations in violin strings can be divided into two categories. Indirect excitations (Benade, 1976) are second order oscil-

* On leave from Physics Dept., La Trobe University, Victoria, Australia

lations produced when a string vibrates with large transverse amplitude. They arise as a result of changes in tension along the string and have a frequency of twice that of the 'source' transverse modes (Morse and Ingard, 1968). Such oscillations are always present in normal violin tones but will not be discussed here. Our measurements are made on the second type of oscillation or 'squeak'. These pure longitudinal oscillations can be excited by bowing along the string. (They are occasionally excited accidentally during normal violin playing but do not form a part of standard violin technique!)

Experiment

We monitor the motion of the bridge-top using photoelectric devices which are attached to the fingerboard. These devices consist of an infrared source facing a photosensitive receiver. A small light plastic flag is stuck to the top of the bridge to intercept the infrared beam as shown in Fig. 1. As the flag moves in and out, the output from the device varies in proportion to the displacement. We record the electrical signals on tape and later feed them to a PDP11 computer via an antialiasing filter and ADC at sampling rates of up to 40,000 Hz. The stored wave forms are then either displayed in a time domain form or

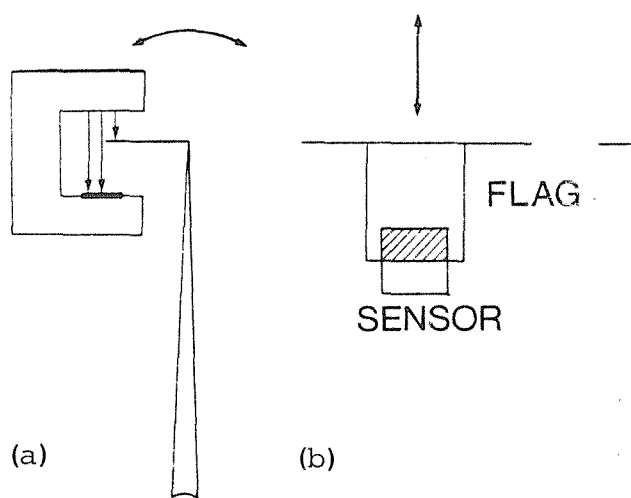


Fig. 1.
Experimental arrangement for
monitoring the motion of the
bridge-top.
(a) Side view.
(b) Top view.

Fourier transformed into a spectrum in the frequency domain. The photoelectric devices are arranged to monitor the motion of the bridge-top in two orthogonal directions which are shown in Fig. 2. Our two chosen

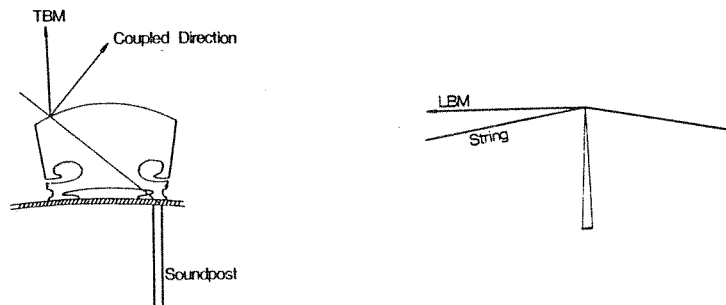


Fig. 2. The two orthogonal directions of monitoring the motion of the bridge-top. (a) Longitudinal bridge motion (LBM) and (b) Transverse bridge motion (TBM).

directions are those of the longitudinal bridge motion (LBM) which is perpendicular to the plane of the bridge, and of the transverse bridge motion (TBM) which is perpendicular to the violin belly. The LBM detector is mounted between the G and D strings and the TBM detector is mounted on the outside edge of the bridge adjacent to the G string. Fig. 3 shows a photograph of the apparatus mounted on the instrument in which the plastic flags are just visible.

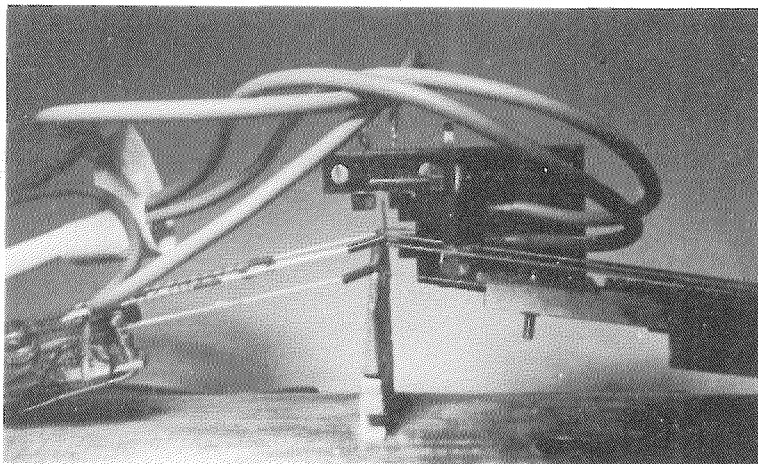


Fig. 3. Photograph of the photoelectric detectors mounted on the instrument.

Results and discussion

In Fig. 4(a) we show the waveform detected in the longitudinal direction for pure longitudinal excitation on the open D string. Its Fourier spectrum shown in Fig. 4(b) has two components at 2617 Hz and 5234 Hz. Fig. 5 shows how these two components decay with time. The first partial decays at a rate of ~ 500 dB/sec whilst the second partial decays at ~ 300

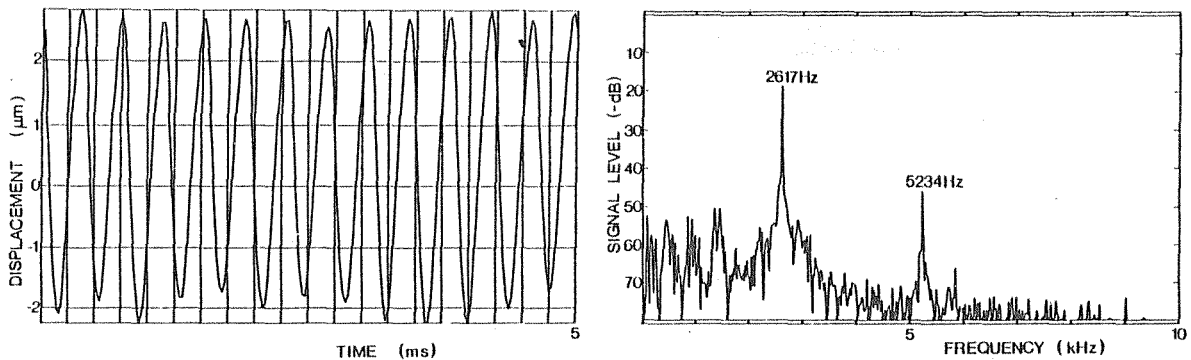


Fig. 4. (a) Waveform of a longitudinal excitation produced on the open D string.
(b) Corresponding Fourier spectrum.

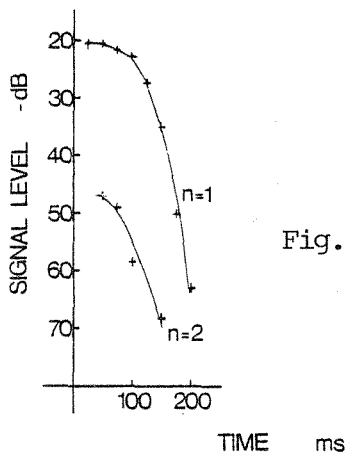


Fig. 5. The decay of the longitudinal excitation on the D string shown in Fig. 4.

dB/sec. In comparison, Fig. 6 shows the decay of a pizzicato tone played normally on the open G string. Here the decay of the first seven par-

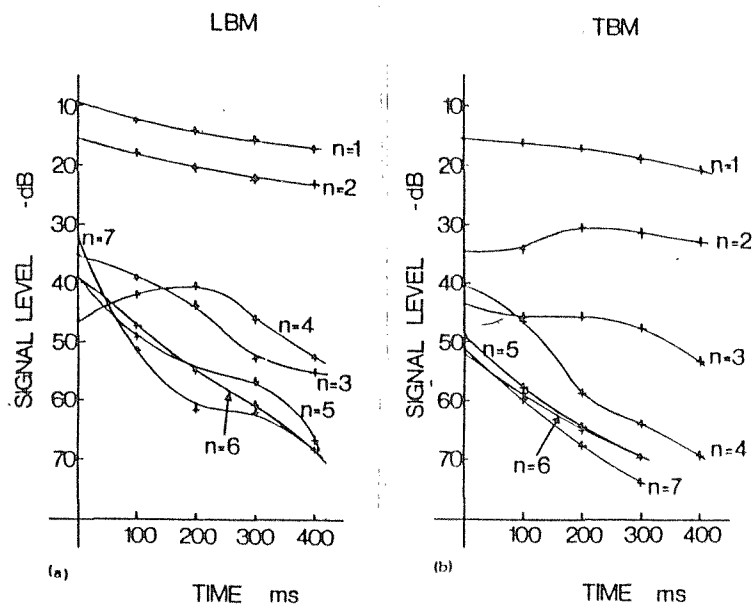


Fig. 6. The decay of partials 1 to 7 for a normally played pizzicato note on the G string. (a) shows the LBM recorded simultaneously with (b), the TBM.

tials of the transverse modes obtained by taking successive FFT's is plotted. Figs. 6(a) and 6(b) are simultaneous recordings of the LBM and TBM respectively during one pizzicato note. In both the LBM and TBM directions, the decay rates are ~ 30 - 80 dB/sec which are much slower than those found for the longitudinal excitations. Although the signal levels are not normalised, the seventh partial (frequency 1365 Hz) has a somewhat higher initial level in the LBM direction than in the TBM direction and decays with a rate of ~ 2000 dB/sec. Since the frequency of the fundamental of the longitudinal series for the G string is 1347 Hz, this may be due to excitation of the longitudinal mode in the initial transient.

Conclusion

Our measurements of the decay rates of longitudinal excitations in violin strings indicate that should these modes be excited in normal violin tones, we might only expect them to last roughly 100 msec into the initial transient. We have found some evidence for excitation of these modes in pizzicato tones but not in bowed tones. We now plan more controlled experiments using single frequency excitation in order to assess the coupling between the longitudinal direction of bridge motion and the body of the instrument. This should lead to a better understanding of the contributions of indirect excitations to the structure of normal violin tones.

Acknowledgements

We are grateful to Professor Charles Taylor for his continual encouragement and to Drs. Michael Greenhough and Bernard Richardson for advice and many useful discussions. MPR held a University of Wales Faculty of Science Bursary during these investigations.

References

Benade, A.H. (1976): Fundamentals of Musical Acoustics, Oxford University Press, New York.

Lee, A.R. and Rafferty, M.P. (1983): "Longitudinal vibrations in violin strings", J.Acoust.Soc.Am., 73, pp. 1361-1365.

Morse, P.M. and Ingard, K.U. (1968): Theoretical Acoustics, McGraw Hill, New York, Chapter 14.

JITTER IN VIOLIN TONES
Rudolf A. Rasch
Institute of Musicology, University of Utrecht
Utrecht, the Netherlands

Abstract

Musical tones like those of the singing voice and the stringed instruments are not a sequence of exactly repeated waveforms with constant frequency, amplitude, and spectrum. Instead, the mentioned characteristics are constantly varying. Frequency variations can be classified as jitter (random variation from period-to-period), vibrato (periodic variations with a frequency of 4-7 Hz), and tense (slow, long-term variations). We have investigated a number of musical tones as to these features and will present the results of various types of measurements, like period-to-period-times-differences, standard deviation of periods, autocorrelation of periods, etc. Special attention will be paid to the consequences of these frequency variations for the building-up of beats in mistuned consonant intervals of musical tones and the significance of all this for the frequency intonation of musical tones.

Introduction

In general, frequency variations are always present in musical tones which, as a rule, pretend to realize a single frequency value indicated by the pitch of the note in the score. These frequency variations can be grouped into three categories: (1) trend (slow, gradual changes of frequency), (2) vibrato (periodical frequency variations with a frequency of 5 to 6 Hz and a depth of 1 to 5%), and (3) jitter, to be defined as small-scale period-to-period fluctuations with a random or pseudo-random character. The vibrato of musical tones has been studied extensively,

beginning with Seashore (1932; later important studies include those by Fletcher and Sanders, 1967; Sundberg, 1972 and Klein and Hartmann, 1979), but this is not the case with jitter. Jitter has been studied in connection with pathological speech (i.a., Lieberman, 1963) and from the point of view of hearing theory (i.a., Pollack, 1968 and Cardozo and Ritsma, 1968). Only a few studies are available that deal with the jitter of musical tones, and they are concerned with the tones of stringed instruments only: Cardozo and Van Noorden, 1968 (cello), Cremer, 1973 (violin), and McIntyre et al., 1981 (violin). Still, jitter is present in all musical tones, often in significant amounts. We studied the jitter of several types of musical instruments. Results concerning the singing voice will be presented elsewhere (Rasch, 1983). On this occasion, focus will be upon the jitter in violin tones.

Jitter (s_j) will be quantified here as the standard deviation of period durations (s_p) when there is no vibrato or trend:

$$s_j = s_p = (\sum (p_i - \bar{p})^2 / n)^{\frac{1}{2}},$$

in which p_i is the duration of the i -th period, \bar{p} the mean period duration, and n the number of periods. This measure can be made more meaningful in a musical context by interpreting the standard deviation as a musical interval which can be expressed in cents:

$$J = 1200 \log_2 (1 + s_j / \bar{p}) \text{ cents,}$$

which measure we will use throughout this paper. J will be called the amount of jitter.

When there is no vibrato or trend, the above given measure can be calculated directly from measured period durations. When also vibrato and/or trend are present, the situation is a bit more complicated. It can be shown that the amount of jitter (s_j , now defined as the standard deviation of period durations as far as due to jitter) can be derived from the variances of period durations (s_p^2) and of period difference

times (s_d^2) in the following way:

$$s_j = \frac{(1-r_v)s_p^2 - \frac{1}{2}s_d^2}{r_j - r_v} ,$$

in which r_j and r_v are the autocorrelations of period durations due to jitter and vibrato/jitter, respectively. For a vibrato, this autocorrelation equals $\cos(2\pi f_v/\bar{f})$, in which f_v is the vibrato frequency and \bar{f} the mean signal frequency. When vibrato/trend is sufficiently slow compared to the period durations and the variance due to these factors is not too large, then the amount of jitter is well approximated by:

$$s_j = \frac{s_d^2}{2 - 2r_j} ,$$

which means that, when r_j can be assumed to be constant, jitter is about proportional to the standard deviation of the time differences of successive periods. For violin tones, r_j seems to be about zero for the lowest octave and in the order of magnitude of -0.5 for the higher octaves.

Measurement procedure

For the measurement of jitter, we needed accurate measurements of single period durations. Violin tones were played in a low-reverberation room. From the microphone signal the fundamental component was filtered out and fed to a Schmitt trigger that produced pulses at every positive zero crossing. The onset times of the pulses were measured by a 10 MHz clock and stored in computer memory. Further analyses were done with help of computer programs. Diagrams with instantaneous frequency (as the

reciprocal of period duration) could be plotted on a graphic terminal (see Fig. 1).

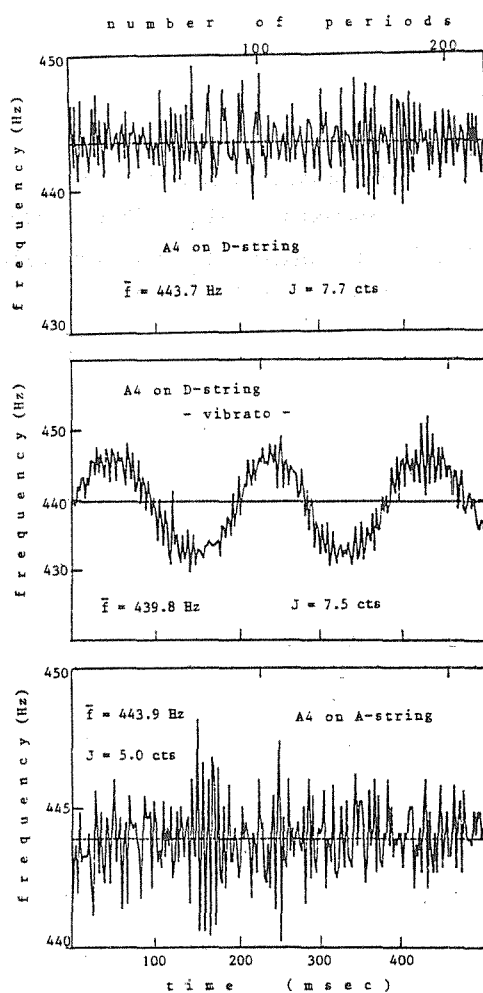


Fig. 1. Frequency-per-period as a function of time, for three A4 tones played on a violin. The dashed horizontal line is the mean frequency, J is the amount of jitter. The vibrato has a depth of about 18 cents.

Results and discussion

The results of the measurements of the amounts of jitter in a number

of tones played by a professional violinist are presented in Fig. 2. First of all, it is clear that the amount of jitter differs from note to note, but there is no general trend of frequency dependence. Non-vibrato and vibrato tones show about the same amounts of jitter. The open G-string had a fundamental that was too weak for reliable measurements.

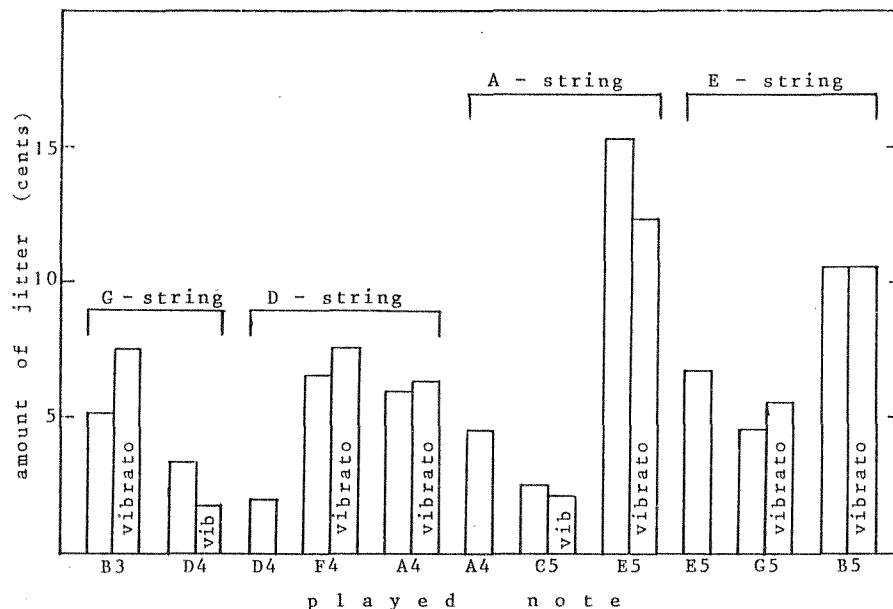


Fig. 2. Amount of jitter for several played notes on the violin. The amounts indicated are means of two to five measurements of 1 sec from repeatedly played notes. When there are two bars for the same note, the left one is for the notes senza vibrato, the right one for the notes con vibrato.

With some reservations, three minima can be discerned in the jitter-against-frequency curve, viz., at D4, C5, and G5. These minima could have to do with some of the major resonances of the violin, viz., the main air resonance (D4), the main wood resonance (C5), and a second wood resonance (G5). I want to propose here the hypothesis that the differences shown have to do with the mutual coupling between the strings, as primary oscillators, and the sounding body (top plate, air cavity) of the violin, as resonators. That this coupling must exist, is evident from

the observation that not only the strings can drive the top plate, but also a string can be driven by the top plate when it is vibrating with the resonance frequency of the string. When an oscillator is driven by another one, the phase lag ϑ of its oscillation relative to the driver's is most simply given by $\cot \vartheta = Q(f_1/f_0 - f_0/f_1)$, in which Q refers to the damping of the driven oscillator, f_0 to the signal frequency of the driving oscillator, and f_1 to the resonance frequency of the driven oscillator. Now, when an oscillator is driven at its resonance frequency, its phase lag is a quarter of a cycle. But the phase lag of the feedback oscillation in the driver is again a quarter of a cycle, adding up to a phase lag a half a cycle. When the damping of driving and driven systems is sufficiently unequal, the feedback oscillation will not have any other effect than a slight attenuation. However, when an oscillator is driven with another than its resonance frequency, its phase lag will be less, or more, than a quarter cycle, so that the feedback oscillation will be less, or more, than half a cycle behind the primary oscillation. It seems plausible that the phase conflict between original and returning wave can cause small phase instabilities which become, as a matter of fact, apparent in the sounding signal as small frequency instabilities, or, in other words, jitter. These instabilities should be stronger the further away the resonator is driven from its own resonance frequency, so that one expects minimal jitter at the resonances of the violin body.

For the singing voice, we found the same relation between jitter and the separation between signal and resonance frequency (Rasch, 1983).

As part of the measurements of period durations and the calculations of statistical measures based on these durations, we calculated autocorrelation functions of period durations, for a lag of one to six periods. These functions show very typical alternations of positive maxima and negative minima, which were per note highly reproducible (see Fig. 3). For A4 and higher notes, the first minimum is about -0.5 at a lag of one period, followed by a maximum of about $+0.5$ at a lag of two to four periods. These autocorrelation patterns point to a compensatory process: longer periods are followed by shorter ones and vice versa with a rough periodicity of a few periods. This is in line with our feedback hypothe-

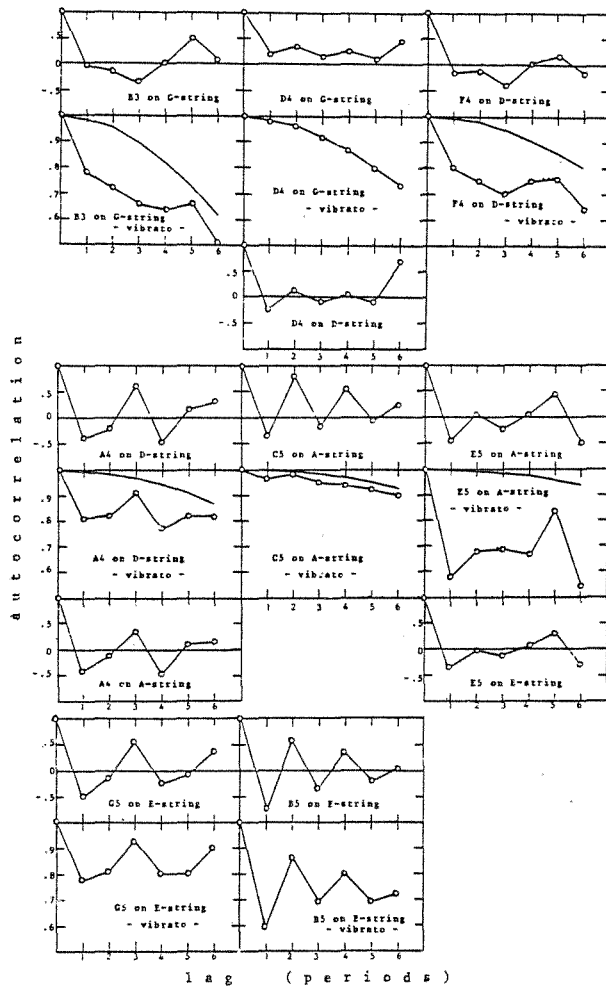


Fig. 3. Autocorrelation as a function of the lag, measured in periods. The functions inserted in the diagrams for several vibrato tones indicate the autocorrelation of an 'ideal' vibrato tone, without any jitter. The autocorrelation function of the D4 vibrato tone is almost equal to such a cosine. For G5 and B5, it is almost one even for a lag of 6 periods.

sis. The returning oscillation causes a small phase shift in the primary oscillation but, since the frequency of the primary oscillation is dominated by the characteristics of the string, this shift has to be compensated at one time, earlier or later. That the autocorrelation patterns

have to do something with the returning oscillation is confirmed by the observation that the patterns are similar for the same notes played on a different string, even when the amounts of jitter differ widely.

For the lower tones of the violin (B3 and D4), the autocorrelation patterns are a little different. The first minimum is less outspoken (about zero), while it is followed by a clear maximum of +0.5 or higher after five or six periods. This may have to do with the fact that the most important resonance here is the main air resonance, while the higher tones pass wood resonances. The F4 has an intermediary pattern.

Other violins tested, but not presented here, showed similar autocorrelation patterns.

The autocorrelation function of period durations of a tone with vibrato and without jitter is a cosine with the vibrato period as periodicity ($\cos 2\pi f_v t = \cos 2\pi k f_v / \bar{f}$, in which k is the lag in periods). In the vibrato tones studied by us, autocorrelations were in fact composites of a cosine and the autocorrelation of the non-vibrato tone. The stronger the jitter was in the non-vibrato tone, the larger was the deviation of the autocorrelation curve of the vibrato tone from the pure cosine. So, it seems that the autocorrelation of period durations is a rather stable property of tones of a certain pitch.

Our measured amounts of jitter are larger than the ones reported by McIntyre et al. (1981), but they correspond more or less to the observations of Cardozo and Van Noorden (1968) and Cremer (1973). As already indicated by McIntyre, their small observed amounts of jitter may be due to the fact that they used the bridge-force wave form, while we as well as the other authors mentioned used the microphone signal of radiated sound. It is quite possible that a part of the jitter does not arise in the strings but somewhere in the resonating system of the violins, e.g., the bridge-to-top-plate transfer. Since it is our intention to complement our physical measurements with psychophysical experiments on the perception of jitter (and vibrato), we prefer the measurements from radiated sound even when there is jitter from different origins contaminated in it.

Conclusions

The data presented about the amounts of jitter present in violin tones must be seen as preliminary. However, they are encouraging further research. Jitter is a noisy phenomenon, which can vary with player, playing mode, frequency, employed string, but also with attention and concentration, fitness and fatigue, exercise and mood, so that really smooth, nice data should never be expected. However, jitter seems to be a rather fundamental property of musical sounds in general and as such it deserves to be investigated into detail. In part it may be caused by the imperfections of systems which produce musical tones, but the coupling between 'oscillator' and 'resonator' may well be an important origin of jitter as well. These couplings typically occur in all acoustical musical instruments as that jitter should be expected to be present about everywhere. It may well be one of the features of tones that makes possible a distinction between the dead sounds of electronic frequency generators and the live sounds of musical instruments.

Acknowledgements

I want to thank the Audiology Department of the Institute of Perception TNO in Soesterberg, The Netherlands, for their kindness to allow me to use their computer and attached audio-apparatus.

References

Cardozo, B.L. and Noorden, L.P.A.S. van. (1968): "Imperfect periodicity in the bowed string", Inst.Perc. Res., Eindhoven NL, Annual Progr.Rep. 3, pp. 23-28.

Cardozo, B.L. and Ritsma, R.J. (1968): "On the perception of imperfect periodicity", IEEE Trans.Audio Electroacoust. 16, pp. 159-164.

Cremer, L. (1974): "Der Einfluss des "Bogendruckes" auf die selbsterregten Schwingungen der gestrichenen Saite", Acustica 30, pp. 119-136.

Fletcher, H. and Sanders, L.C. (1967): "Quality of violin vibrato tones", JAcoust.Soc.Am. 41, pp. 1534-1544.

Klein, M.A. and Hartmann, W.M. (1979): "Perception of vibrato width", Proc. Res.Symp.Psychol.Acoust.Music, Lawrence, KA, pp. 155-172.

Pollack, I. (1968): "Detection and relative discrimination of auditory jitter", JAcoust.Soc.Am. 43, pp. 308-315.

Rasch, R.A. (1983): "Jitter in the singing voice", submitted to the Proc. 10th Internat. Congr. Phonetics Utrecht 1983.

Seashore, C.E. (ed.) (1932): The Vibrato. Studies Psychol. Music 1, Iowa City, Iowa Univ.

Sundberg, J. (1932): "Pitch of synthetic sung vowels", STL-QPSR 1/1972, pp. 34-44.

THE ADJUSTMENT OF MODE FREQUENCIES IN GUITARS:
A STUDY BY MEANS OF HOLOGRAPHIC INTERFEROMETRY
AND FINITE ELEMENT ANALYSIS
B.E. Richardson and G.W. Roberts
University College, Cardiff, Wales, UK

Abstract

The tone quality of a guitar is largely governed by the normal modes of vibration of the body, the coupling between the strings and the body, and the initial excitation of the strings. We have made physical measurements on guitars to establish the influence of these parameters on the tone and playing qualities of the instrument.

Introduction

The tone quality of a guitar is largely governed by the modes of vibration of the body, the coupling between the strings and the body, and the initial excitation of the strings. We have made physical measurements on guitars to establish the influence of these parameters on the tone and playing qualities of the instrument.

We have used holographic interferometry, speckle interferometry and acoustic measurements to perform mode analysis on completed guitars and on guitars at various stages of construction. These studies have identified the important stages of guitar construction and the typical frequency position of modes, and they have led us to propose a new criterion of resonance placement for the guitar which we believe would provide good playing qualities and an even tone in the instrument's lowest two octaves (Richardson and Taylor, 1983).

Mode frequencies may be adjusted by means of variations in parameters such as the thickness of the plates, the strutting design, the choice of wood (variation in the density and elasticity of the wood), and the shape of the plates. We are currently using finite element analysis to investigate how these parameters may be used to control the mode frequencies in both free and fixed plates. Our main aims of the work are: (a) to establish any relationships between mode frequencies and q -values of the body of the guitar and its sound quality, and (b) to investigate how the maker can adjust the plates to produce an instrument of the desired quality.

Experiments on completed guitars

Mode analysis involves the measurement of the resonant frequency, q -value and amplitude distribution (the geometrical distribution of the vibrational amplitude) of each mode. We have used holographic interferometry, speckle interferometry and acoustical measurements to determine these three quantities (for details of the methods, see Jansson, 1971; Vest, 1979). We present results made on one guitar, which incorporates the general characteristics of all the guitars we have investigated.

Figs. 1 to 3 show time-averaged interferograms of the modes of vibration of a guitar (Guitar BR11). Note that the instrument was clamped by the neck only so that the body was completely free. The instrument was excited electromagnetically at a single frequency from an audio oscillator. The frequency of excitation was varied and individual modes were identified by means of speckle interferometry and then recorded holographically. We measured resonance frequencies and Q -values using an accelerometer attached to the plate. In some cases it was necessary to use two drivers so that combination modes could be eliminated (Stetson and Taylor, 1971); the positions of the drivers can be seen in each interferogram. In the following discussions we have categorised modes as $T(m,n)$ or $B(m,n)$ by counting half-waves across each plate (m) and half-waves along each plate (n); top-plate modes and back-plate modes are distinguished by the letters T and B .

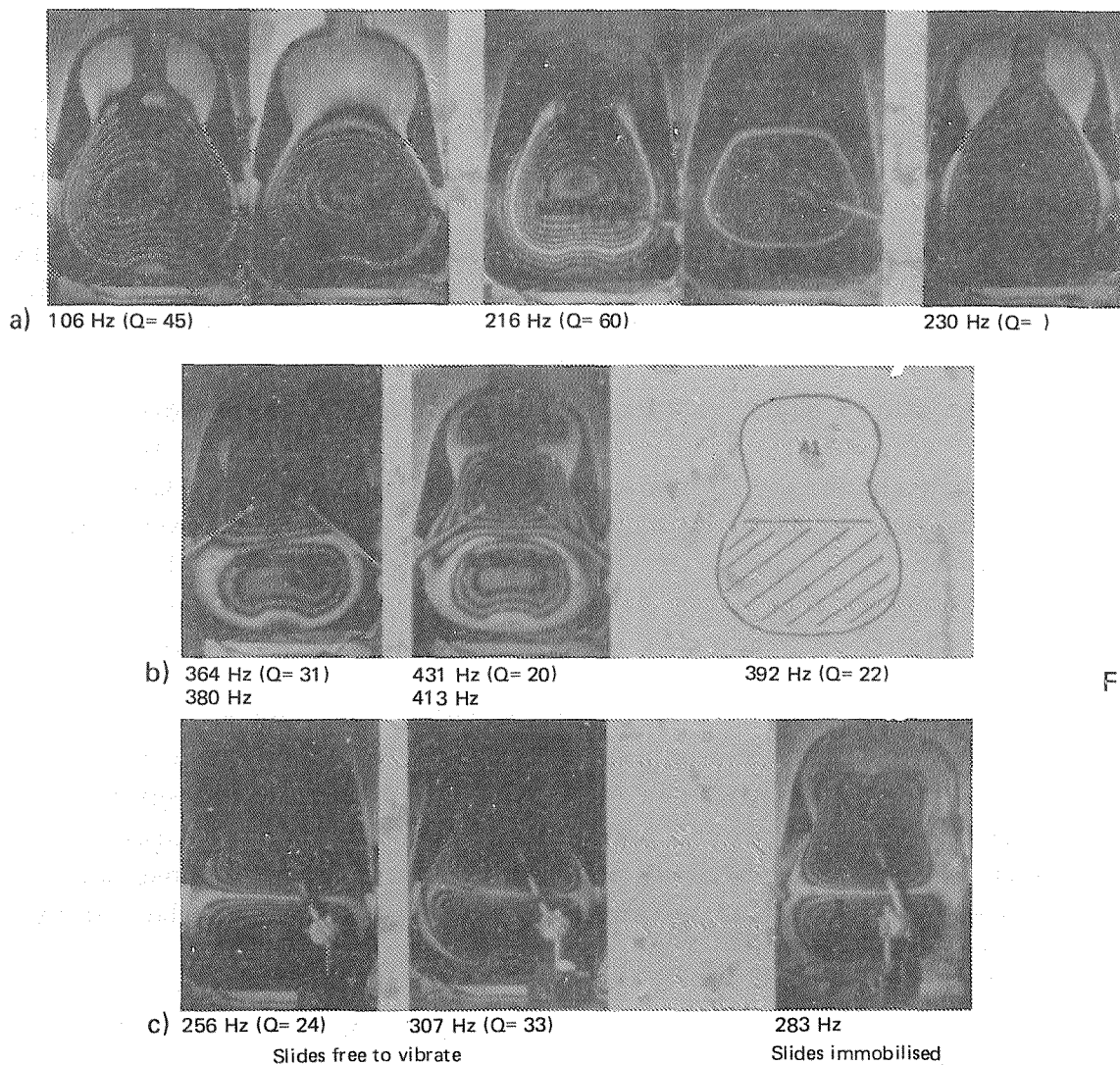


Fig 1

Fig. 1. Time-averaged holographic interferograms of coupled modes of a guitar (Guitar BR11). The resonant frequencies and Q -values of each mode are shown below the interferograms.

- (a) Low-frequency resonance triplet; coupling between the top plate, the back plate and the air cavity (Helmholtz resonance).
- (b) Resonance doublet; coupling between the T(1,2) mode and the first internal air mode (A1).
- (c) Resonance doublet; coupling between the B(1,2) mode and a structural element, possibly the sides or the neck.

Fig. 1a shows the action of Guitar BR11 in its low-frequency range. Coupling between the fundamental modes of the top and back plates and the body cavity form a coupled resonance system which displays three resonances. At the lowest resonance the plates move in phase (with respect to the centre of the body) so that the whole body swells and contracts. This mode of vibration is often referred to as the 'air resonance' (AO). At the middle resonance the plates move out of phase. The nodal lines, the brightest fringes in the interferograms, are inset on both plates indicating that the edges of the plate are in motion; the whole body is vibrating rather like a thick, freely-supported plate. At the upper resonance the plates again vibrate in phase, but this phase relationship is sometimes affected by coupling to other plate modes. The back-plate motion at this resonance (not shown) was similar to that at the lowest resonance. In most guitars the middle resonance is the strongest, but in this instrument the velocity of the top plate in its antinodal region at the middle resonance was about five times greater than at the other two resonances. The back plate was more active than the top plate at all three resonances. However, we have investigated one guitar (Guitar BR9) in which the upper resonance of this triplet was the most dominant (Richardson, 1982). Recent research (Dickens, 1981) has shown that this action is obtained by tuning the (decoupled) fundamental back-plate mode to a lower frequency than the (decoupled) fundamental top-plate mode. Guitar BR9 was preferred by some players, though it is not clear whether the improved playing qualities arose as a direct result of the relative tuning of the plates.

The plates sometimes couple to other air modes. Fig. 1b shows the effect of coupling between one of the higher top-plate modes and an internal air mode which involves air being exchanged between the upper and lower bouts (Jansson, 1977). The doublet frequencies were modified by filling the body with carbon dioxide rather than air. We isolated the air mode itself by immobilising the body with sand bags. This coupling seems to be desirable because it raised the position of the nodal line, which, for this mode, usually lies on a line across the bridge saddle. As the nodal line moves up the body, coupling of transverse string motion to this mode enhanced.

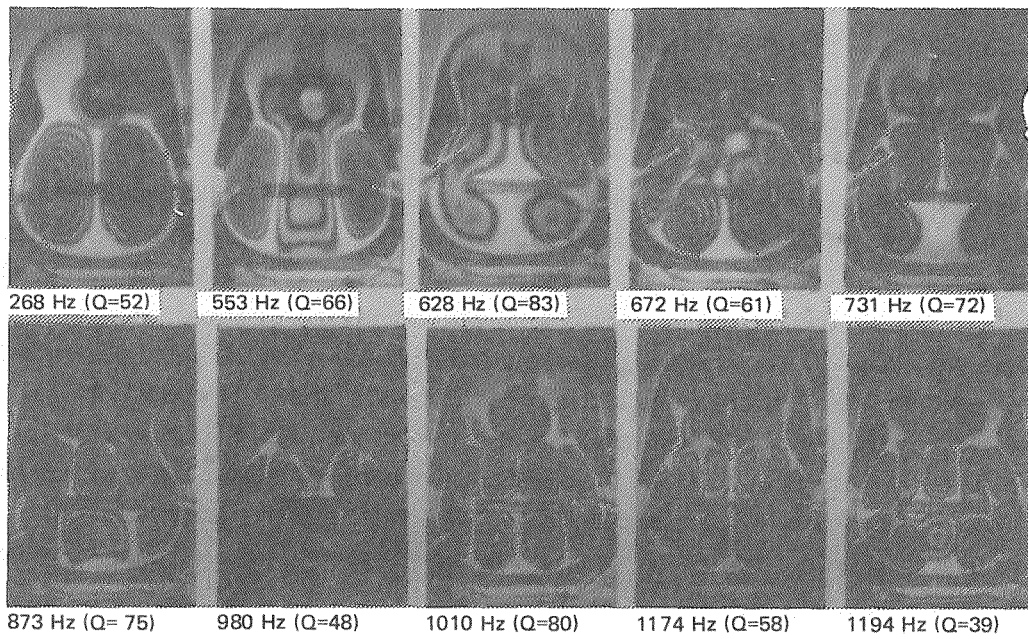


Fig 2

Fig. 2. Time-averaged holographic interferograms of top-plate modes of a guitar (Guitar BR11), The resonant frequencies and Q-values of each mode are shown below the interferograms.

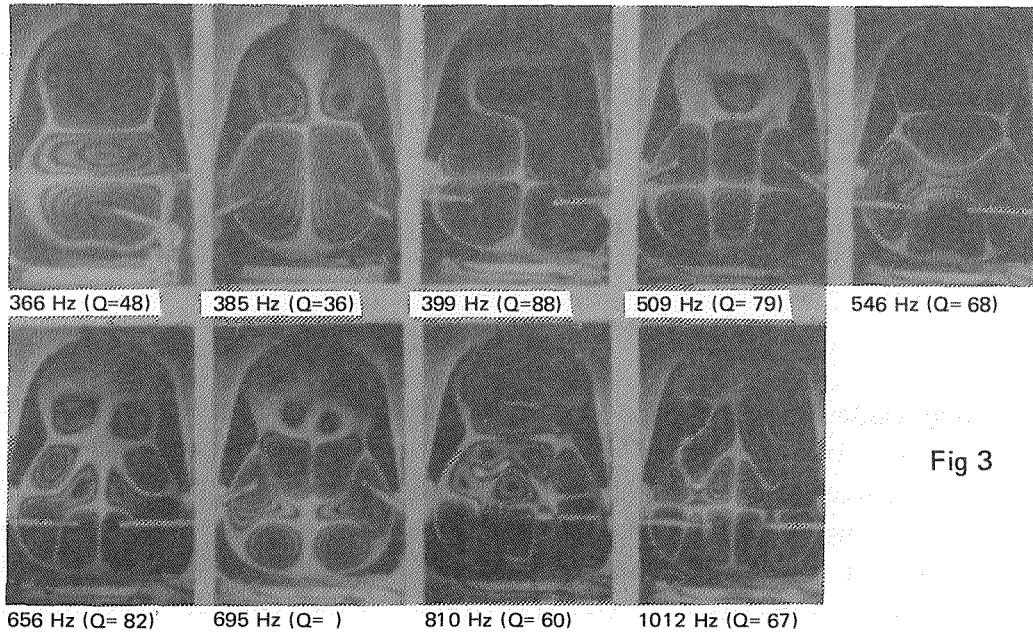


Fig 3

Fig. 3. Time-averaged holographic interferograms of back-plate modes of a guitar (Guitar BR11). The resonant frequencies and Q-values of each mode are shown below the interferograms.

Resonances can be split because of coupling to structural motion. The resonance doublet shown in Fig. 1c is thought to be the result of coupling between a back-plate mode and motion of the sides or the neck; the splitting is eliminated when the sides are immobilised.

Figs. 2 and 3 show higher modes of Guitar BR11. Our experiments have shown that there is little coupling between the top and back plates or between the plates and higher-frequency internal air modes, and we therefore feel justified in referring to these modes as 'plate' modes. Most of the higher top-plate modes have nodal lines at the periphery of the plate, and the lower cross strut (located just below the soundhole) tends to inhibit motion of the plate in that region. On the back plate, the cross struts (three in all) tend to act as the localisation of either nodes or antinodes. The back plate does not always have a node at the periphery of the plate, and modifications to the sides would probably affect the frequencies of these modes.

Only the lowest two or three back-plate modes have an appreciable affect on the response of the instrument when it is driven from the top plate. However, the presence of this 'resonant system' in the sound field of the vibrating top plate modifies the sound radiation from the instrument. Back-plate motion can be seen through the soundhole in some of the interferograms of the top-plate modes.

Experiments on incomplete guitars

We have made measurements on free guitar plates (using Chladni patterns) and on instruments at various stages of construction. The most important changes in mode shapes and frequencies occur when the plates are fixed to the sides and when the bridge is added. Fig. 4 shows that the addition of the bindings, fret board, strings or polish had little affect on the frequencies of the top-plate modes, but the addition of the bridge increased the frequencies of some of the modes by more than 50%. The addition of the bridge mainly affected the frequencies of $T(n,1)$ -type modes for $n > 2$. The frequencies of the $T(1,1)$ and $T(2,1)$ modes were not

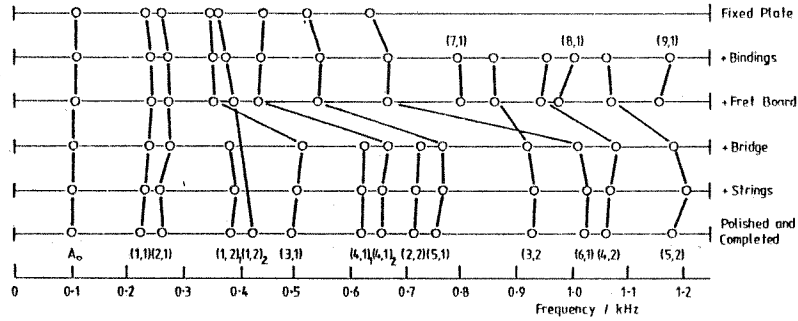


Fig. 4. A mapping of the top-plate-mode frequencies of a guitar (Guitar BR9) during its construction. The T(1,2) mode was split by coupling to the A1 internal air mode. There were two T(4,1) modes as found in Guitar BR11 (see Fig. 2).

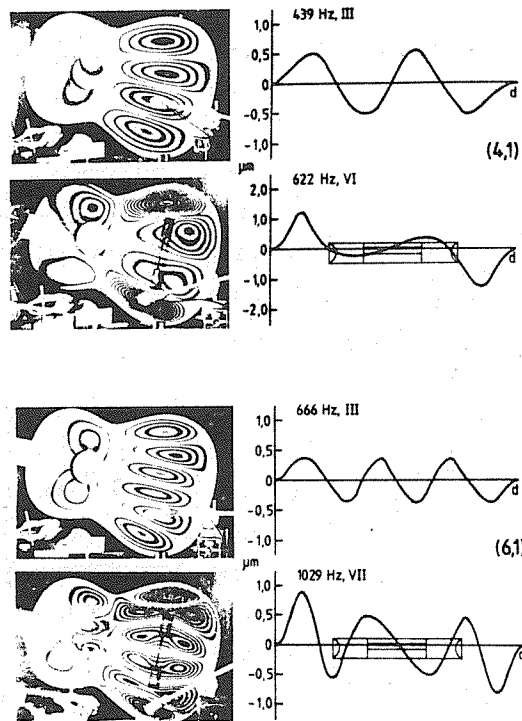


Fig. 5. Time-averaged holographic interferograms of two top-plate modes before and after the addition of the bridge (Guitar BR9). The graphs show the bending experienced by the top plate along a line drawn across the bridge saddle.

affected by the addition of the bridge, and other mechanisms must be sought for 'tuning' these two modes.

The bridge is clearly an important part of the strutting system of a guitar and the maker can use it to selectively tune some of the higher modes. Fig. 5 shows interferograms of two modes of the top plate before and after adding the bridge. Bending of the plate tends to occur at preferred points, and alterations to the length of the bridge tie block or bridge wings could be used to tune the modes relative to one another.

Finite element analysis

Finite element analysis is a mathematical technique which may be used to predict the amplitude distributions and frequencies of the normal modes of complex vibrating structures (Zienkiewicz, 1977). Only the dimensions and material properties of the structure need be known. We are using a commercially-available finite element package called ASAS, which we run on the 'Batch Computers' at the Rutherford and Appleton Laboratories, Didcot, England (computing facilities are provided by the Science and Engineering Research Council of Great Britain).

At present, we are modelling only the top plate of the guitar. The absence of the air activity, back or sides means that neither the low-frequency resonance triplet (see Fig. 1a) nor any other plate-internal air mode interactions (e.g., Fig. 1b) will be predicted. If required, the low-frequency response could be obtained from one of the many analytical models now available for predicting the low-frequency resonance triplet (e.g., Christensen, 1982), in which typical data could be substituted for the fundamental back-plate resonance and for the Helmholtz air resonance. Similar models could be developed to describe the other types of air-plate coupling. The method allows us to have only one of three boundary conditions: 'free', 'fixed' or 'hinged'. Because nearly all top-plate modes have a nodal line at the periphery of the plate and because the bending in this region has zero slope (Fig. 5), we chose the 'fixed' boundary to model the top plate of the completed instrument. Comparisons

between the theoretical predictions and measured values for mode frequencies and shapes show that this is a reasonable assumption. We therefore contend that the model presented here provides an adequate description of the guitar's mechanical action above 200 Hz. Finally, we can determine the free-plate modes using the 'free' boundary condition, and we can therefore attempt to establish any relationships which exist between the modes of the free plate and the modes of the completed instrument.

The structure to be analysed is first divided by the imaginary lines of a mesh into a finite number of elements (Fig. 6). The vibration

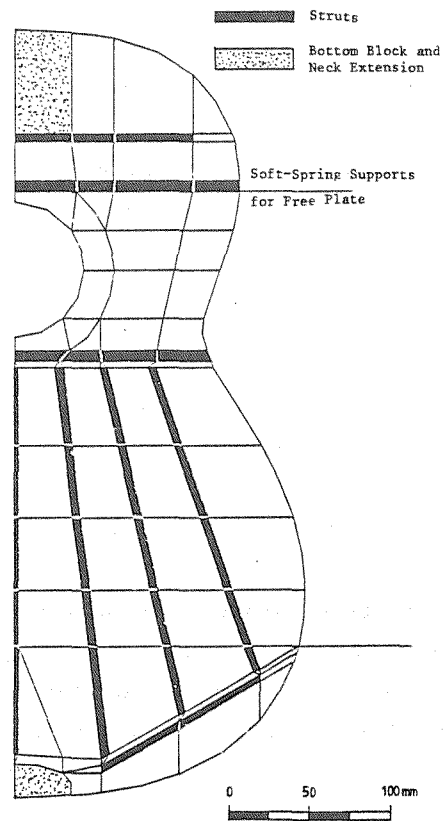


Fig. 6. Finite element mesh of a guitar plate, built to a design by Romanillos (1979). The soft-spring supports eliminate rigid-body modes of the free plate. For the calculation of the fixed-plate modes, the plate was fixed at its edges, the bottom block and the neck extension.

problem is then formulated in terms of a system of equations which can be produced one element at a time within a computer to give approximations to the shapes and frequencies of the vibrational modes. The accuracy of the predictions can be increased by using a finer mesh, but the mesh shown here was found to be sufficiently fine for the frequency range presented.

We encountered two major problems, both of which we solved by a process of trial and error. Firstly, we had to use 'thick-plate theory' rather than 'thin-plate theory'. The former requires an additional two shear moduli, the effects of which are known to be important only at high frequencies. Secondly, we had to model the cross struts and fan struts using stacked plate elements rather than using 'beam' elements. We have not been able to obtain information about the assumptions used in formulating the finite element package and we cannot, therefore, assess the origin of these problems. We do not know whether the use of other finite element packages would involve similar problems. Our solution to these problems are perfectly valid, but both involve an increase in computing time.

In order to ensure that the finite element predictions were correct, we modelled an actual plate for which we had experimental data of mode frequencies and shapes. Material properties used for the calculations are shown in Table 1. The finished plate was 2.9 mm thick. All struts were made from quarter-sawn spruce and were 5 mm wide. Cross struts were 14 mm high (maximum) and fan struts were 4 or 5 mm high (maximum), and both were shaped according to conventional guitar-making principles (McLeod and Welford, 1971). The free plate was modelled at various stages of construction from the flat board to the finished plate. Strut arching and cross-sectional shapes were included in the final set. Finally, the theoretical predictions of the fixed-plate modes were compared with those of the real plate fixed to the sides. Figs. 7 and 8 show the computed modes of the free and fixed plate. The amplitude distributions of the modes are shown in the form of 'contour' plots. We have not yet modelled the plate including the bridge, though we intend to do so in the near future. However, the plate we were modelling was the one used in the

Table 1. Material properties of the quarter-cut spruce plate and spruce strutting used in the finite element model. The following conventions are used: y is along the grain, x is across the grain and z is through the grain; E is the Young modulus; G is the shear modulus.

Quantity	Value	Unit
E_y (plate)	9225	MPa
E_y (struts)	15000	MPa
E_x	852	MPa
G_{xy}	850	MPa
G_{yz}	850	MPa
G_{xz}	44	MPa
Poisson Ratio	0.37	
Density (plate)	420	Kg m ⁻³
Density (struts)	480	Kg m ⁻³

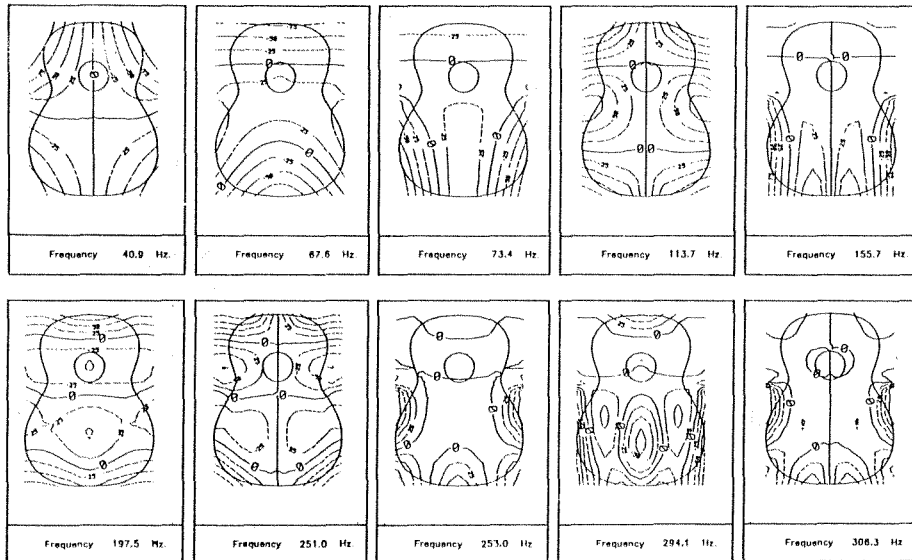


Fig. 7. The first ten modes of a freely-supported guitar top plate computed by finite element analysis.

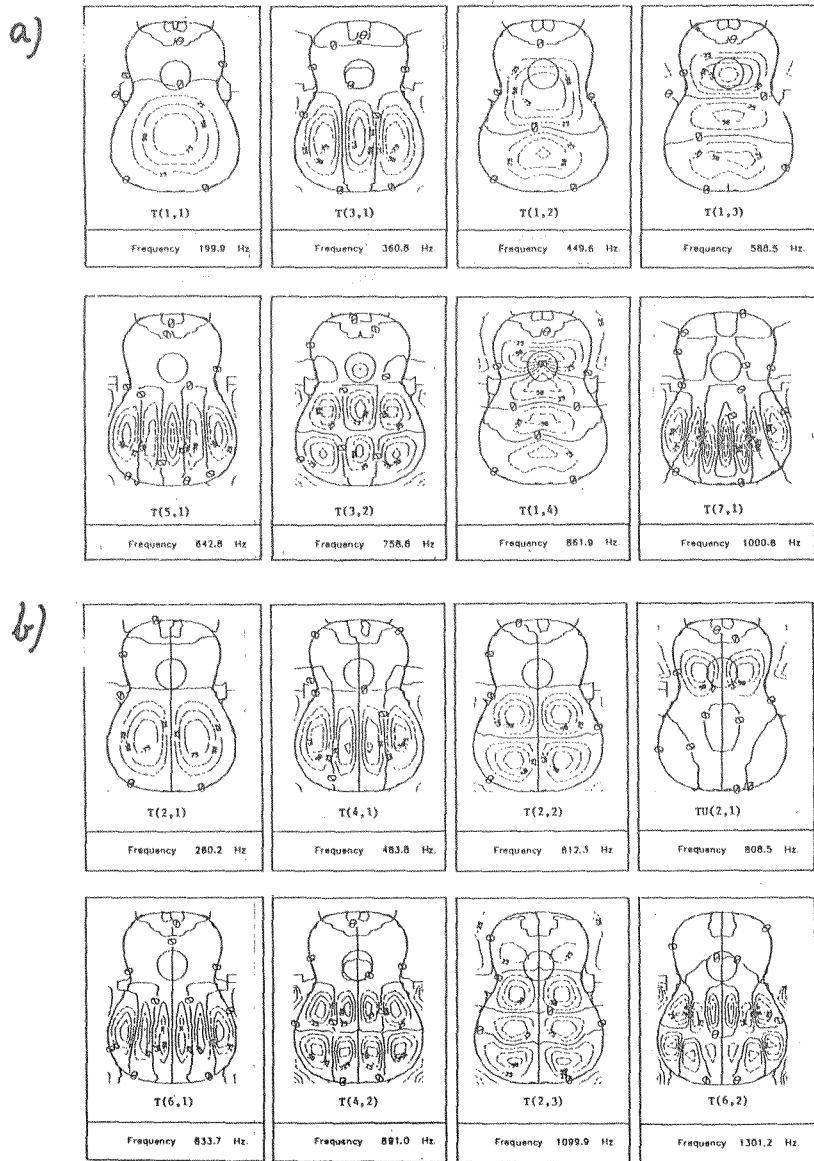


Fig. 8. Fixed-plate modes of a guitar top plate computed by finite element analysis.

(a) The first eight symmetric modes.

(b) The first eight antisymmetric modes.

construction of the guitar shown in Figs. 1 to 3 (Guitar BR11), so a comparison of the mode frequencies shown in these figures with those obtained from the model (Fig. 8) will indicate the affect of the addition of the bridge on this instrument.

The theoretical and experimental results were in good agreement. For the unstrutted plate and the fixed, completed plate the agreement was better than 5%. For the free, strutted plate the errors were larger, some modes being 10% out. Some of these errors were the result of inaccurate modelling of the fan struts which run across the grain at the bottom of the lower bout. We know from experimental experience that the free-plate modes which exhibit bending in these areas are very sensitive to small changes in the height of these fan struts, but the influence of the struts is greatly reduced when the plate is glued to the sides.

Using this plate as a 'standard' we then introduced changes in the plate's dimensions and material properties. After each modification we computed modes of the free and fixed plate, but we restrict the results presented here to those of the fixed plate. Fig. 9 shows how the mode frequencies depend on the thickness of the plate (like many guitar top plates, this plate has a constant thickness); the strutting configuration and strut heights were kept constant. Mode frequencies are approximately linear functions of the thickness of the plate. Some modes are seen to cross over, especially if the 'antisymmetric' and 'symmetric' graphs are combined. Thus, the maker is able to modify the relative tuning of modes by altering the thickness of the plate. We should note here that the mode frequencies of a flat, unstrutted plate are proportional to the thickness of the plate and that they have a fixed relationship which is governed by the shape of the plate. Where modes cross on either Fig. 9a or 9b, inter-modal coupling occurs. This is the same type of coupling which generates the 'ring' and 'X' modes from the two simple beam modes of a rectangular spruce plate (Caldersmith and Rossing, 1983). Such coupling can only occur between symmetric or antisymmetric modes. Fig. 10 shows the affect of reducing the heights of all the fan struts by 75%, 50% and 25% of their heights in the 'standard' plate (100% case). The thickness of the plate was kept constant at 2.9 mm. Reduction of the heights of the fan

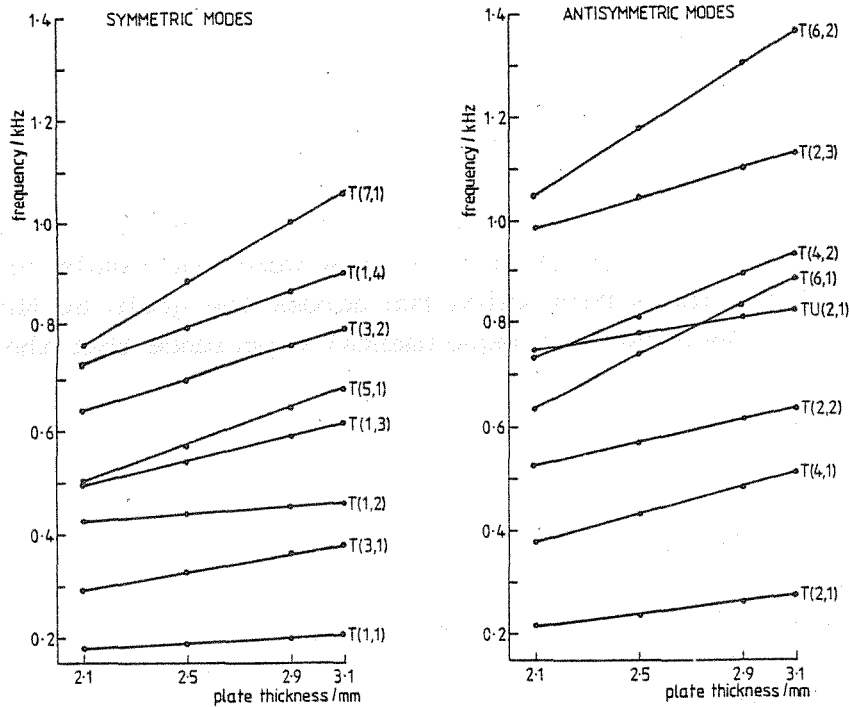


Fig. 9. Top-plate mode frequencies as a function of the thickness of the plate. (a) Symmetric modes. (b) Antisymmetric modes.

struts increases or decreases the frequencies of modes depending on whether it is the reduction in mass or stiffness of the struts which is the more important. It appears that the mode frequencies are more sensitive to changes in the thickness of the plate rather than to changes in the heights of the fan struts. We also computed the affect of reducing the heights of all the cross struts (heights of the fan struts constant). Table 2 shows that fewer modes are then affected, because most modes have nodal lines running across these cross struts (Fig. 2). The maker can change the heights of the cross struts to tune the T(1,2) mode, but this will also alter the frequency of the T(1,1) mode. As the heights of the cross struts are reduced, the motion of the T(1,1) mode spreads into the upper bout, and the resulting increase in wavelength lowers the frequency of the mode. Inter-modal coupling between the T(1,2) and T(3,1) modes

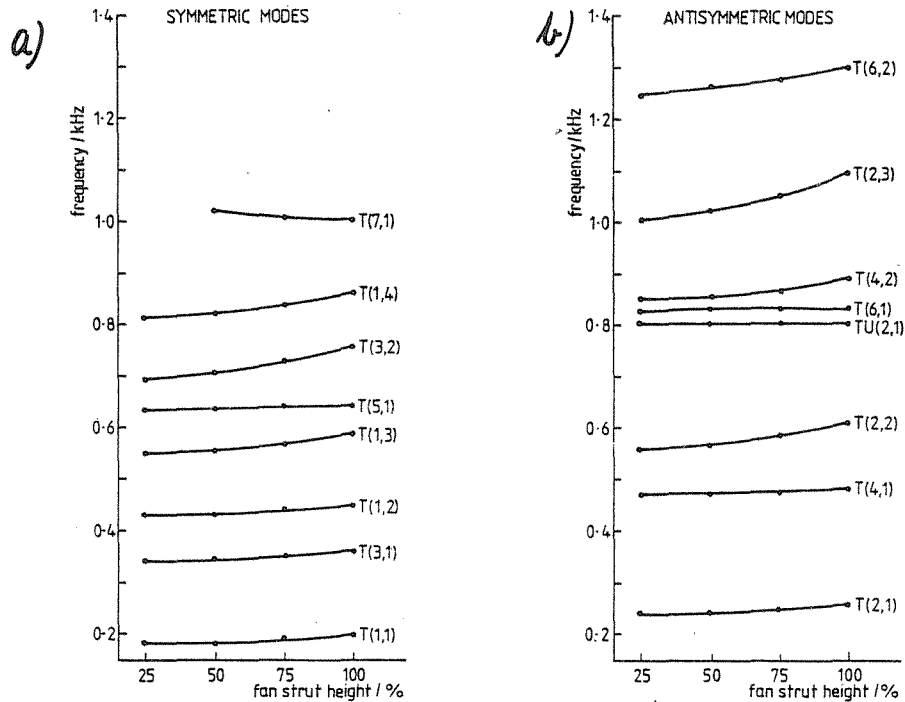


Fig. 10. Top-plate mode frequencies as a function of the heights of the fan struts (relative to the heights of the struts used in the 'standard' plate). The thickness of the plate was constant at 2.9 mm. (a) Symmetric modes. (b) Anti-symmetric modes.

generates a family of pairs of modes having shapes which can be formed by combinations of their shapes shown in Fig. 8. Mode mixing increases as the frequency separation between the modes decreases. We have observed this phenomenon in real guitars. Similar coupling occurs in the completed instrument where the addition of the bridge often raises the frequency of the T(3,1) mode to a similar frequency to that of the T(1,2) mode, again producing mixed mode shapes.

One of the most interesting aspects of the finite element work is that it allows us to 'build' identically-sized instruments from wood of different material properties. The final column of Table 2 shows the mode frequencies of a plate built to the same dimensions as our 'standard'

Table 2. Mode frequencies of the 'standard' plate compared with those of the same plate in which (a) the heights of the cross struts have been reduced by 50%, and (b) the cross-grain stiffness has been reduced by 50%.

Mode	Frequency, Hz		
	'Standard' Plate	50% Cross-Strut Height	50% E _x Plate
T(1,1)	199.9	170.0	196.8
T(3,1)	360.8	341.9	330.2
T(1,2)	449.6	362.2	445.3
T(1,3)	588.5	581.2	583.2
T(5,1)	642.8	639.6	548.7
T(3,2)	758.8	731.8	735.0
T(1,4)	861.9	841.1	855.1
T(7,1)	1000.6	999.8	825.5
T(2,1)	260.2	249.5	248.0
T(4,1)	483.8	479.7	424.1
T(2,2)	612.3	544.6	601.2
TU(2,1)	808.5	638.0	793.6
T(6,1)	833.7	830.8	701.1
T(4,2)	891.0	871.5	843.5
T(2,3)	1099.9	955.4	1085.6
T(6,2)	1301.2	-*	1159.1

* Not computed.

plate but in which the cross-grain stiffness has been reduced to half its original value (426 MPa). The cross-grain stiffness of spruce is one of the most variable parameters that the guitar maker has to cope with. This variation is generally the result of poor cutting, i.e., the wood is not quarter sawn. The reduced value used in this experiment is not unduly low and such a piece of spruce would be used by a guitar maker. We see from a comparison of Fig. 9 and Table 2 that a 2.9 mm thick plate made from this wood would have, apart from a few exceptions, the same mode frequencies as the 'standard' plate reduced to a thickness of 2.4 mm.

Conclusions

We have shown that finite element analysis can be used to model accurately the top-plate modes of a guitar. The model is not able to predict interactions between the top and back plates or between the top plate and the air cavity, but analytical models exist to compute the resonance frequencies of coupled modes of this type. The theoretical work is at an early stage. Our next step will be to include the bridge in our model. We will then investigate thoroughly the affect of changing parameters such as plate thickness, strut height, strutting configuration, bridge design and plate shape. We are also interested in the importance of changes in the wood's material properties on the mechanical action of the instrument.

Finally, we note that it is possible to evaluate the effective mass of the plate at any point using the finite element method. We can, therefore, predict the degree of coupling between the strings and individual modes of the body according to the methods of Gough (1981) and thus predict the type of decay and the decay rates for 'typical' strings mounted on our model. We are also looking into the possibility of evaluating the 'piston area' of the vibrating top plate, from which we should be able to predict the monopole component of the sound radiation from the instrument. Using these techniques, we hope to synthesise guitar tones so that we are able to 'play' our model. Only in this way can we truly assess the importance of changes in the structure of the instrument.

Acknowledgements

The authors would like to thank Thomas Rossing and Ove Christensen for useful discussions concerning plate-air coupling and the calculation of monopole radiation from guitars. This work is supported by grants from the Science and Engineering Research Council of Great Britain and the Royal Society for which we are grateful.

References

- Caldersmith, G. and Rossing, T.D. (1983): "Ring modes, X-modes and Poisson coupling", *Catgut Acoust.Soc. Newsletter* 39, pp. 12-14.
- Christensen, O. (1982): "Quantitative models for low-frequency guitar function", *J. Guitar Acoust.* 6, pp. 10-25.
- Dickens, F.T. (1981): "Analysis of the first and second vibration modes in a guitar using an equivalent electrical circuit", *Catgut Acoust.Soc. Newsletter* 35, pp. 18-21.
- Gough, C.E. (1981): "The theory of string resonances on musical instruments", *Acustica* 49, pp. 124-141.
- Jansson, E.V. (1971): "A study of acoustical and hologram interferometric measurements of the top plate vibrations of a guitar", *Acustica* 25, pp. 95-100.
- Jansson, E.V. (1977): "Acoustical properties of complex cavities. Predictions and measurements of resonance properties of violin-shaped and guitar-shaped cavities", *Acustica* 37, pp.211-221.
- McLeod, D. and Welford, R. (1971): The Classical Guitar, Design and Construction, The Dryad Press.
- Richardson, B.E. (1982): "A physical investigation into some factors affecting the musical performance of the guitar", Ph.D. Thesis, University of Wales.
- Richardson, B.E. and Taylor, C.A. (1983): "Resonance placement in guitars", Proceedings of the 11th ICA, Vol. 4, pp. 381-384.
- Romanillos, J. (1979): "The classical guitar", in Making Musical Instruments (Ford, C. ed.), pp. 101-129, Faber and Faber, London and Amsterdam.
- Stetson, K.A. and Taylor, P.A. (1971): "The use of normal mode theory in holographic vibration analysis with application to an asymmetrical circular disc", *J.Sci.Instru. (J. Phys. E)* 4, pp. 1009-1015.
- Vest, M.C. (1979): Holographic Interferometry, John Wiley and Sons.
- Zienkiewicz, O.C. (1977): The Finite Element Method, 3rd ed., McGraw-Hill.

PLATE VIBRATIONS AND RESPONSE OF CLASSICAL AND FOLK GUITARS

Richard E. Ross* and Thomas D. Rossing
Northern Illinois University, DeKalb, IL, USA

Abstract

Many of the acoustical differences between classical and folk guitars result from differences in the way the plates are braced with struts in the two types of instruments. We find good agreement between the vibrational modes observed in the top plates in the two types of instruments and those calculated for equivalent rectangular plates simply supported at their edges. For the fan-braced classical guitar, the struts are considered to affect only the longitudinal stiffness, whereas in the X-braced folk guitar the struts increase the stiffness both along and across the grain. Classical guitars generally show a greater sound output at low frequency, for a given driving force, than the more stiffly braced folk guitars.

Introduction

Most research on the acoustical behavior of guitars has focused on classical guitars. Much less work has been done on other types of guitars, such as the American folk guitar. It is the purpose of this paper to discuss some of the acoustical and vibrational properties of this popular instrument, and to compare them to the classical guitar.

Folk guitars have steel strings, which are normally played with a plectrum rather than the fingers, and the strings carry a much greater tension than the strings of a classical guitar. Thus the top plate of a folk guitar is usually braced by diagonal struts arranged in a pattern commonly referred to as cross- or X-bracing. The bridge is placed near the center of the lower bout, and a flat brace or bridge-liner appears on

* present address: Scott Community College, Bettendorf, IA, USA

the underside of the plate at this same location. Folk guitars are commonly larger in size than classical guitars.

In this paper we compare the vibrational frequencies of the main modes of vibration of guitar top plates with those calculated using a simple rectangular plate model.

Vibrations of wood plates

The equation of motion for flexural vibrations of a wood plate having flexural rigidity D_y along the grain and D_x across the grain is

$$\frac{\partial^2 w}{\partial t^2} + \frac{1}{\rho h} (D_x \frac{\partial^4 w}{\partial x^4} + 2D_{xy} \frac{\partial^4 w}{\partial x^2 \partial y^2} + D_y \frac{\partial^4 w}{\partial y^4}) = 0 \quad (1)$$

where w is the displacement perpendicular to the middle surface, ρ is the density, h is the thickness of the plate, and D_{xy} is the torsional rigidity. The expressions for the flexural and torsional rigidities can be written in terms of the Young's moduli E_x and E_y , the shear modulus G , and the Poisson's ratios ν_x and ν_y :

$$D_x = \frac{E_x h^3}{12(1-\nu_x \nu_y)}, \quad D_y = \frac{E_y h^3}{12(1-\nu_x \nu_y)}, \quad D_{xy} = \frac{E_y h^3 \nu_x}{12(1-\nu_x \nu_y)} + \frac{Gh^3}{6} \quad (2)$$

For an isotropic plate $G = \frac{E}{2(1+\nu)}$. For an orthotropic plate, G can be estimated from an analogous expression which uses the geometrical mean values for E and ν :

$$G \approx \frac{\sqrt{E_x E_y}}{2(1 + \sqrt{\nu_x \nu_y})}$$

We further note that $\nu_x E_y = \nu_y E_x = \sqrt{\nu_x \nu_y E_x E_y}$, so that

$$D_{xy} \approx \frac{h^3 \sqrt{v_x v_y E_x E_y}}{12(1-v_x v_y)} + \frac{h^3 \sqrt{E_x E_y}}{12(1+\sqrt{v_x v_y})} = \frac{h^3 \sqrt{E_x E_y}}{12(1-v_x v_y)} = \sqrt{D_x D_y} \quad (3)$$

For a rectangular plate with dimensions a and b, simply-supported at its edges, the normal mode solutions can be written:

$$w_{m,n} = \sin \frac{(m+1)\pi x}{a} \sin \frac{(n+1)\pi y}{b} (A \cos \omega t + B \sin \omega t),$$

and the normal mode frequencies are

$$f_{m,n} = \frac{\pi}{2\sqrt{h\rho}} \left[D_x \left(\frac{m+1}{a}\right)^4 + 2 D_{xy} \left[\frac{(m+1)(n+1)}{ab}\right]^4 + D_y \left(\frac{n+1}{b}\right)^4 \right]^{\frac{1}{2}} \quad (4)$$

The effect of adding transverse struts can be included by adding a

term $\frac{E_y t^3 w_y}{d_y}$ to D_x , and the effect of longitudinal struts by adding a term

$\frac{E_y t^3 w_x}{d_x d}$ to D_y , where w and t are the width and thickness of the struts, and d is their spacing. (The ratio w_x/d_x indicates what portion of the plate is effectively stiffened by struts running along the grain, for example.) E_y appears in both terms for additional stiffness, since all struts are assumed to be cut along the grain of the wood. Thus the rigidities of the braced plate are:

$$D'_x = D_x \left(1 + \frac{E_y t^3 w_y}{E_x h^3 d_y}\right), \quad D'_y = D_y \left(1 + \frac{t^3 w_x}{h^3 d_x}\right), \quad \text{and } D'_{xy} = \sqrt{D'_x D'_y} \quad (5)$$

A guitar plate model

In this study we compare the lowest modes of vibration of a guitar top plate with those calculated for an equivalent rectangular plate simply supported at its edges. The dimensions of the equivalent plate are estimated from hologram interferograms of the particular vibrational mode of interest.

For the Torres- or fan-braced classical guitar, the struts are considered to affect only the longitudinal stiffness, whereas in the X-braced folk guitar the struts are considered to increase the stiffness along and across the grain by roughly equal amounts.

The first four modes of a guitar top plate are shown schematically in Fig. 1. The frequencies of these modes, especially the (0,0) mode, depend upon the conditions under which they are measured (Rossing, Popp, and Polstein, 1984). To measure the correct modal frequencies in the top plate, the back should be removed and the ribs fixed (Jansson, 1971). Since this is often not convenient to do, the modal frequencies can be measured with the back plate and ribs immobilized in sand and the sound hole covered. Under these conditions the (0,0) mode is raised in frequency by the effective restoring force of the enclosed air, which can easily be calculated from the equation

$$f_{00}^2 = f_p^2 - \frac{1}{4\pi^2 C_v M_p} \quad (6)$$

where f_p is the frequency of the plate backed by the enclosed air cavity, M_p is the effective mass of the top plate, and C_v is the compliance of the enclosed air.

Other modes are affected much less by the enclosed air. Vibration in the (1,0) mode does not change the volume of the enclosed air, and vibration in the (0,1) or (2,0) modes changes it only slightly.

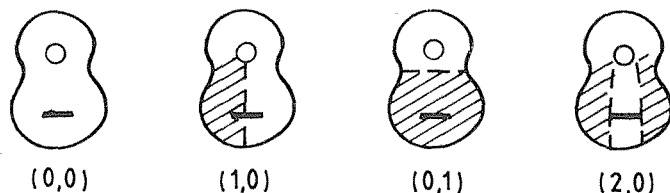


Fig. 1. First four modes of vibration of a guitar top plate.

Guitar response measurements

We have used several methods to measure the frequency response of free plates and guitars (see Ross, 1979). Most often the plates were driven by a small coil of wire attached to the bridge or plate and supplied with an alternating current from an audio amplifier. When a small permanent magnet is inserted into the coil, a sinusoidal driving force results. The motion of the plate was detected by using an accelerometer, a velocity-sensitive phonograph pickup, and/or a small probe microphone within a millimeter or two of the plate. Scanning the plate surface indicated the positions of the nodes and antinodes for each vibrational mode of interest.

Another technique was to attach an accelerometer to some point on the plate and to tap the plate at various other points while analyzing the signal from the accelerometer on a real-time spectrum analyzer. Usually adding up the spectra from eight taps sufficed to determine the frequencies of the main plate resonances.

The radiation response was determined by driving the guitar with the coil driver in an anechoic room and recording the sound pressure level one meter in front of the center of the bridge. Usually the sound pressure directly in front of the sound hole was recorded at the same time.

Results and discussion

The radiation response spectra of a fan-braced classical guitar (Epiphone) and an X-braced folk guitar (Lyle) are shown in Fig. 2. Both guitars have spruce top plates, and the strength of the applied driving force is approximately the same in both. In both cases the driving force was applied to the bridge by a coil driven by an audio amplifier. Sound pressure levels were recorded in an anechoic chamber with a microphone one meter in front of the center of the bridge.

The low-frequency response of the classical guitar is substantially greater than that of the stiffly-braced folk guitar for the same driving force. (The steel strings used on folk guitars provide a greater driving force than the nylon strings of a classical guitar, however, so the sound

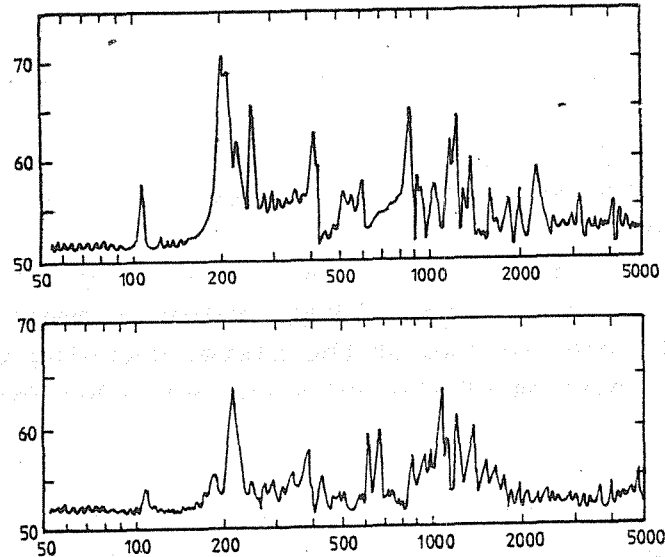


Fig. 2. Sound pressure spectra from two guitars driven with approximately the same force; (a) fan-braced classical guitar; (b) an X-braced folk guitar. Each guitar was driven by a coil attached to the bridge, and the sound pressures were recorded one meter in front of the top plate in an anechoic room (from Ross, 1979).

output is at least as great when it is played.) Several resonances occur at substantially greater frequencies in the folk guitar, especially the one due to the (1,0) mode in the top plate, which is sensitive to transverse stiffness.

The measured and calculated frequencies of the first four modes of four guitar top plates are given in Table 1. The frequencies of the (0,0) modes ((0,0) meas) were calculated from equation (6). For the other modes, the frequencies measured in the complete guitar are used.

For each mode, the frequency was calculated from the rectangular plate model described in an earlier section. Dimensions and areas of the equivalent rectangular plates to be used in the calculations were estimated from holographic interferograms of "typical" guitar plates. Rigidities of the braced plate were estimated from equation (5).

The agreement between the measured and calculated frequencies for these modes is quite good.

Table 1. Measured and calculated frequencies of the first four top plate modes in fan-braced and X-braced guitars.

Wood	fan-braced		X-braced	
	Epiphone	Garcia	Guild	Martin
	spruce	pine	mahogany	spruce
Thickness (mm)	2.7	2.5	3.0	3.0
Mode frequencies (Hz)				
(0,0) calc	182	170	178	192
(0,0) meas	187	212	190	185
(1,0) calc	280	263	392	393
(1,0) meas	242	283	400	365
(0,1) calc	451	420	446	492
(0,1) meas	420	426	430	426
(2,0) calc	499	463	597	588
(2,0) meas	530	560	588	580

Material constants used in calculations:

	E_x (N/m ²)	E_y (N/m ²)	ν_x	ν_y	ρ (kg/m ³)
spruce	1.0×10^{10}	0.69×10^9	0.37	0.02	390
pine	1.66×10^{10}	1.12×10^9	0.46	0.03	540
mahogany	1.16×10^{10}	1.24×10^9	0.31	0.033	500

Conclusions

The results of this study indicate that the frequencies of the vibrational modes of guitar plates (and thus the frequencies of the guitar resonances) can be predicted, with some success, by calculations based on a simple rectangular plate model. Much of this work was done several years ago (Ross, 1979), and meanwhile the work of other investigators has confirmed this (see, for example, Meyer, 1982; Richardson, 1982; Calder-smith, 1981).

There continues to be considerable support for the feeling that the first four top plate resonances largely determine the quality of the guitar sound in the important low- and mid-frequency ranges (Meyer, 1983; Caldersmith, 1982; Christensen, 1983; Jansson, 1982; Richardson and Taylor, 1983).

The authors thank John Popp, Ove Christensen, Graham Caldersmith, and Bernard Richardson for many enlightening comments and discussions.

References

Caldersmith, G. (1981): "Plate and fundamental coupling and its musical importance", *Catgut Acoust. Soc. Newsletter* 36, 21-27.

Caldersmith, G. (1982): "The guitar frequency response", *J.Guitar Acoust.* No. 6, 1-9.

Christensen, O. (1983): "The response of played guitars at middle frequencies", *Acustica* 53, 45-48.

Jansson, E.V. (1982): "Fundamentals of the guitar tone", *J.Guitar Acoust.* No. 6, 26-41.

Meyer, J. (1982): "Relationships between the tonal quality and construction of guitars", *Das Musikinstrument* 31, 1292 and 1440. (This paper first appeared in German in *Das Musikinstrument* 30, 990 and 1110 (1981).)

Meyer, J. (1983): "Quality aspects of the guitar tone", in Function, Construction and Quality of the Guitar, ed. E.V. Jansson, Publ. 38 of the Royal Swedish Academy of Music, Stockholm.

Richardson, B.E. and Taylor, C.A. (1983): "Resonance placement in guitars", Paper 91-16, 11th ICA, Paris.

Ross, R.E. (1979): "The Acoustics of the guitar: an analysis of the effect of bracing stiffness on resonance placement", M.S. Thesis, Northern Illinois University.

Rossing, T.D., Popp, J., and Polstein, D. (1984): "Acoustical response of guitars", Stockholm Music Acoustic Conference, Vol. I.

ACOUSTICAL RESPONSE OF GUITARS
Thomas D. Rossing, John Popp*, and David Polstein**
Northern Illinois University, DeKalb, IL, USA

Abstract

We have studied the most important resonances of several classical and steel-string folk guitars. These resonances are related to the normal modes of vibration of the top plate, the back plate, and the enclosed air. The resonances at low frequency can be understood by considering two-mass and three-mass models. Coupling between the top and back plates takes place through motion of the ribs and/or acoustic waves in the enclosed air. We will discuss the normal modes and resonances of two classical and two folk guitars in details.

Introduction

A number of investigators have studied the acoustical response of guitars. In order to determine the vibrational configuration of the guitar at each of its major resonances, the instrument is usually driven sinusoidally at one or more points, and its motion is observed optically, acoustically, electrically, or mechanically. Optical sensing techniques include holographic interferometry (Stetson, 1981) and laser velocimetry (Boullosa, 1981). For the most part these techniques have been applied to various parts of guitars (especially top plates) rather than to complete guitars, however. Acoustical detection techniques have included using an array of microphones (Strong et al., 1982) and scanning the near field with a single microphone (Ross and Rossing, 1979; see also Ross, 1979). An electrical pickup relies on variation in capacitance as the instrument vibrates, and a mechanical pickup consists of an accelerometer

* Permanent address: Moraine Valley Community College, Palos Hills, IL.

** Student intern from Hampshire College, Amherst, MA, USA.

or velocity transducer of very small mass (a phonograph cartridge can be used).

Frequencies at which the mobility of the instrument (velocity divided by force) is maximum are called resonances, and frequencies at which it is a minimum are called anti-resonances. The configurations in which it vibrates at each of its resonances are often called "modes of vibration", but they are not necessarily the normal modes of vibration or eigenmodes of the system. A mobility maximum or resonance may result from the excitation of two or more normal modes. Only when the spacing of the normal modes is large compared with their natural widths does the vibration pattern at a resonance closely resemble that of a normal mode of vibration (Arnold and Weinreich, 1982).

In this paper we will describe studies of the acoustical response of various parts of the guitar and discuss the way in which they interact as coupled oscillators. Various boundary conditions have been used in order to observe the responses of individual components. Most of the observations were made by using one or more accelerometers in conjunction with a microphone at the soundhole.

The response function

The response function of a guitar is a function of the frequency f and the coordinates of the driving point P and the point Q at which the motion is observed. Mathematically, it can be written as a sum over the normal modes of the free system (Morse and Ingard, 1968). The contribution of each normal mode consists of a product of three factors: the amplitude of the normal mode at P , its amplitude at Q , and a resonance factor which is proportional to $(f^2 - f_i^2)^{-1}$, where f_i is the frequency of the normal mode (Arnold and Weinreich, 1982). In general the response function remains the same when P and Q are interchanged.

If P and Q are the same point, the response function gives the driving point mobility. Since both the magnitude and the phase of the velocity are of interest, it is customary to write the force, the velocity, and

the mobility as complex functions, with the actual physical quantities being represented by the real parts. The response when P and Q are different points is generally called the "transfer mobility" (or transfer admittance).

Each normal mode can be described as a combination of "elementary" motions of the top plate, back plate, ribs, neck, and the air inside the guitar. The normal modes depend upon the acoustical environment of the guitar and especially on how the instrument is supported (that is, on the boundary conditions of the various parts). Thus it is not surprising to find differences in the response curves recorded by various investigators.

Coupling of the top and back plates

Since the top plate and the back plate are the most massive parts of the guitar, one approach to understanding the guitar is to consider the top and back as separate multimode oscillators coupled together by the motion of the ribs and the enclosed air. If the two plates were identical, one would expect the normal modes to occur in pairs, the plates moving in the same direction in one mode and in opposite directions in the other mode. In the anti-phase mode the ribs would move very little. In the in-phase mode, the ribs would move opposite to the main part of each plate, with a node occurring some distance in from the rib.

Stetson (1981) studied this type of motion in a box with square top and back plates and with perforated ribs to minimize air coupling. He found that the anti-phase modes occurred at nearly the same frequencies as those of a single plate, whereas the in-phase modes were higher in frequency. Although the motion of the ribs was not reported, one would expect an up and down motion in the in-phase mode and an in and out bending motion in the anti-phase mode, as indicated in Fig. 1 for the mode pair of lowest frequency.

Clearly, the vibrations of Stetson's box would have been quite differ-



Fig. 1. Two lowest vibrational modes of a box with identical top and bottom plates and perforated sides. (a) Top and bottom move in anti-phase; (b) Main part of top and bottom move in phase but opposite to sides. The in-phase mode will have the higher frequency.

ent had the sides not been perforated. The "stiffness" of the enclosed air would have raised the frequency of the anti-phase mode by a considerable amount. In a guitar, air flows freely in and out of the soundhole, so the stiffness of the enclosed air is considerably smaller than in an airtight box. However, the air flowing in and out of the soundhole has momentum, so it must be included as one of the "elementary motions" that determine the normal modes.

Low frequency modes and equivalent circuits

Several authors have constructed models to illustrate the motion of the top plate, the back plate, and the air in the soundhole at low frequency. A two-mass model that ignores the motion of the back (see Caldersmith, 1978; Firth, 1977; Christensen and Vistisen, 1980) is shown in Fig. 2a, and a three-mass model that includes back motion (see Caldersmith, 1981; Christensen, 1982) is shown in Fig. 2b. The following

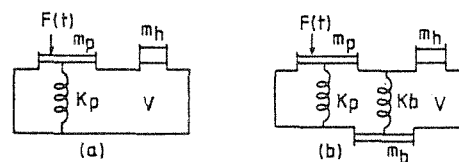


Fig. 2. Models of the guitar: (a) Two-mass model (rigid back); (b) Three-mass model (flexible back).

symbols are used:

- m_p = mass of top plate
- m_h = mass of air in soundhole
- m_b = mass of back
- K_p = stiffness of top plate
- V = volume of enclosed air
- K_b = stiffness of back
- $F(t)$ = force applied to top plate (by the strings)

It is helpful to represent the various components in Fig. 2 as circuit elements in equivalent circuits (Cox, 1980). Of the several choices available, we have chosen the acoustical impedance representation (Beranek, 1954) shown in Fig. 3. The equivalent voltage is the force ap-

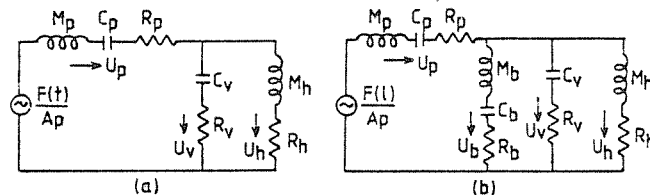


Fig. 3. Equivalent circuits corresponding to models shown in Fig. 2:
 (a) Two-mass model; (b) Three-mass model.

plied to the top plate (by the strings) divided by the top plate area. The equivalent currents are volume velocities (in m^3/s). The following symbols are used:

- $M_p = m_p/A_p^2$ = inertance (mass/area) of top plate (kg/m^4)
- $M_h = m_h/A_h^2$ = inertance of air in sound hole (kg/m^4)
- $M_b = m_b/A_b^2$ = inertance of back plate (kg/m^4)
- $C_p = A^2/K_p$ = compliance of top plate (N/m^5)
- $C_b = A^2/K_b$ = compliance of back plate (N/m^5)
- $C_v = V/\rho c^2$ = compliance of enclosed air (N/m^5)
- U_p = volume velocity of top plate (m^3/s)
- U_h = volume velocity of air in sound hole (m^3/s)
- U_b = volume velocity of back plate (m^3/s)
- R_p = loss (mechanical and radiative) in top plate

R_p = loss (mechanical and radiative) in back plate
 R_h = loss due to radiation by sound hole
 R_v = loss in the enclosure

The two-mass model in Fig. 2a has two resonances with an anti-resonance between them. At the lower resonance, air flows out of the sound hole in phase with the inward-moving top plate. In the equivalent circuit in Fig. 3a this corresponds to U_p and U_v being essentially in phase (they would be exactly in phase if $R_h = R_v = 0$). At the upper resonance, U_p and U_h are essentially opposite in phase; that is air moves into the soundhole when the top plate moves inward. The anti-resonance represents the Helmholtz resonance of the enclosure; U_v and U_p are equal and opposite, and thus U_p in a minimum.

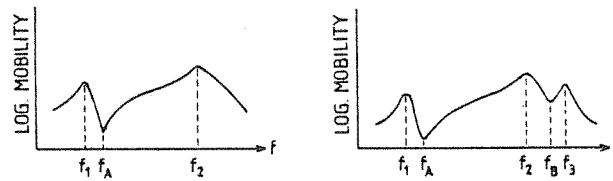


Fig. 4. Top plate mobilities obtained from guitar models: (a) Two-mass (rigid back) model; (b) Three-mass (flexible back) model.

A graph of mobility vs frequency for the two-mass guitar model is shown in Fig. 4a. The two resonances occur at f_1 and f_2 , and the anti-resonance occurs at f_A . (This curve is a familiar one because of its similarity to the mobility of a loudspeaker in a bass-reflex enclosure, see Rossing, 1981). The two resonances f_1 and f_2 will span the lowest top plate mode f_p and the Helmholtz resonance f_A ; that is, f_A and f_p will lie between f_1 and f_2 . In fact it can be shown that $f_1^2 + f_2^2 = f_A^2$ (Ross and Rossing, 1979; Christensen and Vistisen, 1980). If $f_p > f_A$ (as it does in most guitars), f_A will lie closer to f_1 than to f_2 (Meyer, 1974).

The top plate mobility in the three-mass model has a third resonance and a second anti-resonance indicated as f_3 and f_B in Fig. 4b. In

addition f_1 has been moved to a slightly lower frequency, and f_2 may be moved either upward (for $f_b < f_p$) or downward (for $f_b > f_p$), depending upon the resonance frequencies f_p and f_b of the top and back alone (Christensen, 1982). In most guitars, $f_b > f_p$, so both f_1 and f_2 are shifted downward by interaction with the flexible back (Meyer, 1974).

Dickens (1981) has proposed a four-mass model that includes the mass of the ribs. The equivalent circuit now increases in complexity. By means of a computer, he has obtained solutions for 9 different cases. His model predicts another anti-resonance below f_1 , however, which is normally not observed.

Determining the response functions

In most of the experiments described in this paper, the guitar was driven at some selected point P (usually at or near the bridge) with a Bruel and Kjaer (B & K) 4810 vibration exciter used in conjunction with an 8001 impedance head, which has an effective mass load of 2.1 grams. The output from the force transducer is fed to a GenRad 1569 automatic level regulator and an audio amplifier to provide a constant driving force. The accelerometer output is amplified and integrated by a B & K 2651 charge amplifier. This velocity signal was fed through a tracking filter /amplifier (GenRad 1901) to a chart recorder (GenRad 1521) in order to obtain a graph of driving point mobility (v/F at point P) vs frequency.

The transfer mobility (v/F when $Q \neq P$) was obtained by affixing a BBN 501 accelerometer ($m \approx 2$ g) at Q and driving the guitar at constant force, as described above. The sound pressure levels were determined with a GenRad 1933 sound level meter. A B & K 2971 phase meter was used to determine the phases of the velocity and sound pressure with respect to the driving force.

In order to excite internal air vibrations or standing waves within the guitar, we used a driver consisting of a loudspeaker enclosed in a

box with a small rubber hose to transmit pressure variations to any desired point within the guitar. A small microphone was moved around within the guitar (with the help of a wire extending to the outside through the sound hole) in order to locate pressure nodes and antinodes.

Great care must be exercised in the selection of appropriate constraints or boundary conditions in order to observe the behavior of the component parts as well as the entire guitar. Seven different arrangements are illustrated in Fig. 5:

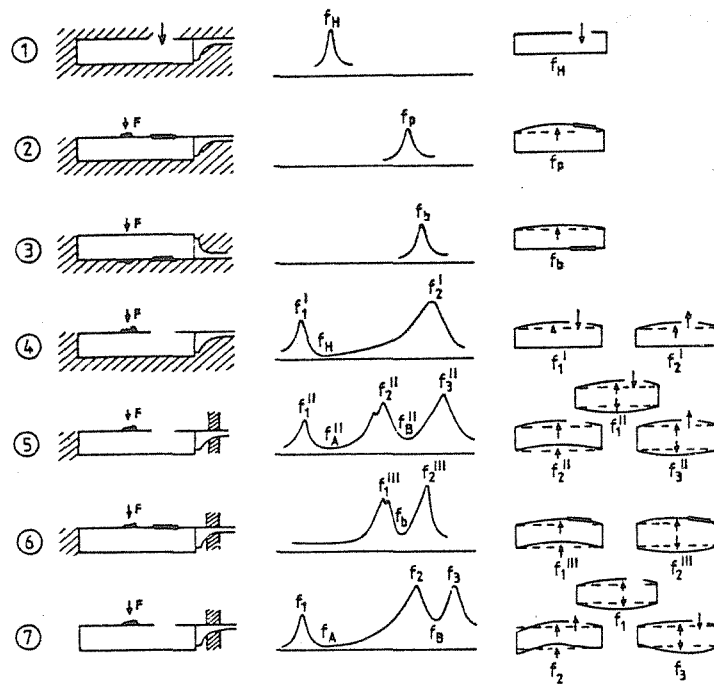


Fig. 5. Seven different boundary conditions used for measuring the vibrational behavior of a guitar and its component parts. In the first four arrangements, the guitar is placed in a sand box; in the latter three, the neck is clamped and the ribs are left free or immobilized with sand bags.

1. The entire guitar body is immobilized in a box of sand, so that only the enclosed air vibrates. This arrangement is used to determine the Helmholtz resonance frequency f_H , as well as those of the other modes of the air cavity which we designate as f_{A2} , f_{A3} , f_{A4} , etc.

2. The back and ribs are immobilized, and the sound hole is closed. As the top plate vibrates, the air pressure inside the guitar changes. The first mobility maximum occurs at the lowest top plate resonance frequency f_p , and successive maxima occur for other top plate modes (these are not the same as the free plate modes).
3. The top plate and ribs are immobilized in sand. The lowest back plate resonance frequency f_b and successive resonances of the back are determined.
4. The back and ribs are immobilized, as in (2), but the sound hole is open. The first top plate mode couples to the lowest air (Helmholtz) mode to produce resonances at f'_1 and f'_2 . An anti-resonance occurs at f_H . From the model shown in Figs. 2a and 3a, it can be shown that $f'^2_1 + f'^2_2 = f^2_H + f^2_p$.
5. The ribs are fixed, but the top and back plates are free to move, and the sound hole is open. The first top plate mode, the first back plate mode, and the lowest air mode couple to produce three resonances, designated as f''_1 , f''_2 , and f''_3 , plus two anti-resonances f''_A and f''_B . From the model in Figs. 2b and 3b, it can be shown that $f''^2_1 + f''^2_2 = f''^2_A + f''^2_B$.
6. The ribs are fixed, as in (5), but the sound hole is closed. There are now two resonances at f'''_1 and f'''_2 with an anti-resonance at the frequency of the first back plate mode f_b . It can be shown that $f'''^2_1 + f'''^2_2 = f^2_p + f^2_b$.
7. Finally, the neck of the guitar is fixed, but the entire body is allowed to vibrate freely. The three lowest resonances occur at f_1 , f_2 , and f_3 , and anti-resonances occur at f_A and f_B .

Along with these various conditions of constraint in Fig. 5 we show

the vibration configurations at the lowest resonances and typical driving-point mobility curves. Note that we are dealing only with the resonances that result from coupling between the lowest modes of the top plate, back plate, and the enclosed air. Similar coupling occurs between the higher modes of these vibrating components, but this coupling is less well understood.

Coupling at low frequency

The two-mass and three-mass models, discussed in the previous section, predict several interesting relationships between the various measured frequencies of vibration. These can be checked with the measured frequencies. The two-mass model, for example, predicts that $f_1'^2 + f_2'^2 = f_p^2 + f_H^2$. Given below are experimental values for these frequencies in several guitars f_1' .

	f_p	f_H	f_1'	f_2'	$\frac{f_1'^2 + f_2'^2}{f_p^2 + f_H^2}$
Martin D-28	163	121	105	180 Hz	1.05
Martin D-35	131	125	92	159	1.03
Guild	190	123	106	200	0.96
Kohno 30	183	122	104	211	0.99
Conrad	188	127	101	205	0.98

The first three guitars are steel-string folk guitars, and the last two are classical guitars. In all five instruments, the ratio is within 5% of unity, which supports the validity of the two-mass model.

In a previous study, guitar resonances were measured in a helium atmosphere (Ross and Rossing, 1979). Although the experimental conditions were slightly different, these data are also in reasonably good

agreement with the relationship predicted by the two-mass model.

	f_p'	f_H'	f_1'	f_2'	$\frac{f_1'^2 + f_2'^2}{f_p'^2 + f_H'^2}$
Conrad	195	205	148	255 Hz	0.91
Epiphone	193	198	150	245	1.08
Guild	198	180	142	220	0.96
Lyle	214	160	150	228	1.04

The three-mass model predicts that $f_A''^2 + f_B''^2 = f_H''^2 + f_b''^2$. This can be checked with data from two steel-string folk guitars and one classical guitar. Again the agreement is good.

	f_A''	f_B''	f_H''	f_b''	$\frac{f_A''^2 + f_B''^2}{f_H''^2 + f_b''^2}$
Martin D-38	110	180	121	165 Hz	1.06
Martin D-35	109	176	118	159	1.07
Kohno 30	118	209	119	204	1.03

Finally, the resonances f_1''' and f_2''' measured in arrangement 6 should follow the relationship $f_1'''^2 + f_2'''^2 = f_p''^2 + f_b''^2$. We have data on two steel-string guitars to check this.

	f_1'''	f_2'''	f_p''	f_b''	$\frac{f_1'''^2 + f_2'''^2}{f_p''^2 + f_b''^2}$
Martin D-28	157	178	163	165 Hz	1.05
Martin D-35	118	174	131	159	1.04

Thus the two-mass and three-mass models are seen to apply to the

vibrational behavior of the guitars under different conditions of constraint. It is essential, however, to use the parameters appropriate to each particular boundary condition.

Modes of vibration of component parts

Thus far we have discussed only the resonances that result from the interaction of the lowest vibrational modes of the top plate, the back plate, and the enclosed air. Each of these major components has many other modes of vibration, and combinations of these lead to abundant resonances throughout the audible range of frequency.

Several investigators have made hologram interferograms of a guitar top plate vibrating in its various modes under different conditions of constraint (Firth, 1977; Jansson, 1981; Richardson, 1982; Jovičić and Jovičić, 1977). Thus their modal frequencies are somewhat different, although the modal shapes are in rather good agreement. Richardson (1982) also shows hologram interferograms of several modes of vibration of the back plate of a classical guitar.

We have studied the vibrational modes of the top plates and back plates of several guitars with the ribs and other members immobilized in sand (arrangements 2 and 3, previously described). The plate was driven by a B & K vibrator, and the motion of the plate was determined by moving a small accelerometer ($m = 2$ g) across the surface of the plate. (While the mass of the accelerometer causes a small shift in the modal frequencies, it has negligible effect on the modal shapes. The modal frequencies were determined without the accelerometer attached).

The modal frequencies and configurations of the top and back plates of a Martin D28 guitar are shown in Fig. 6. The modal designations at the top give the numbers of nodes in the horizontal and vertical directions, respectively. The lowest frequencies for the top and back plates correspond to f_p and f_b , as discussed earlier. All modal frequencies are given for a closed sound hole (arrangement 2). With the sound hole open,

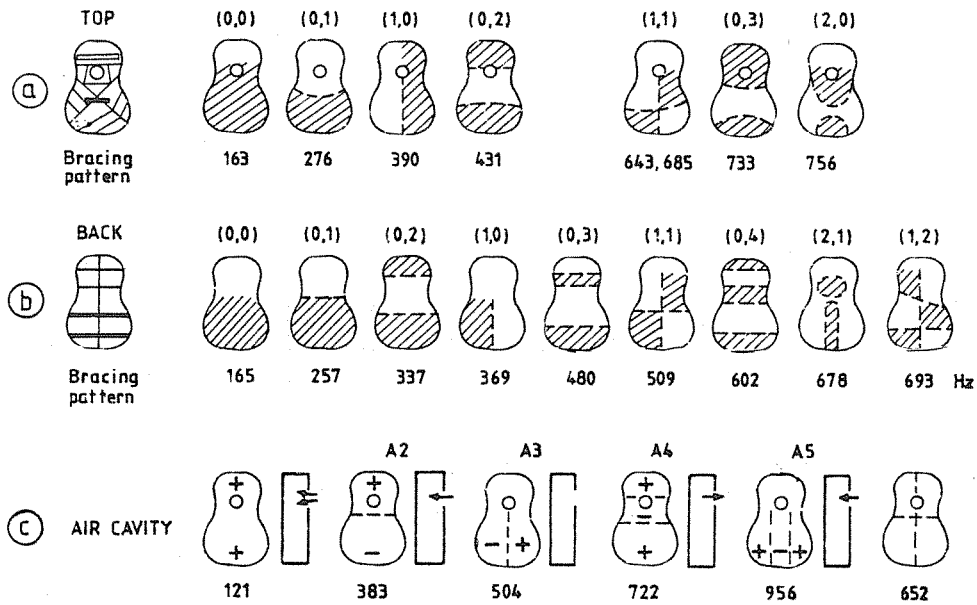


Fig. 6. (a) Modes of a folk guitar top (Martin D-28) with the back and ribs in sand; (b) Modes of the back with the top and ribs in sand; (c) Modes of the air cavity with the guitar body in sand. Modal designations are given above the figures and modal frequencies below.

the lowest top plate mode is replaced by resonances at 110 and 185 Hz (f'_1 and f'_2).

Also shown in Fig. 6 are the modes of vibration of the air inside the guitar body. The lowest air mode is the Helmholtz resonance of the cavity; air moves in and out of the sound hole as the pressure inside the cavity changes. The mode designated A2 resembles the first resonance of a pipe closed at both ends; air "sloshes" back and forth, creating a pressure node at the center and pressure maxima at the ends. The A4 mode resembles the second mode of this same pipe oriented vertically, while A3 and A5 resemble the first two resonances of a horizontal pipe having a length equal to the width of the guitar.

Several modes of the top and back plates and air cavity of a Kohno 30

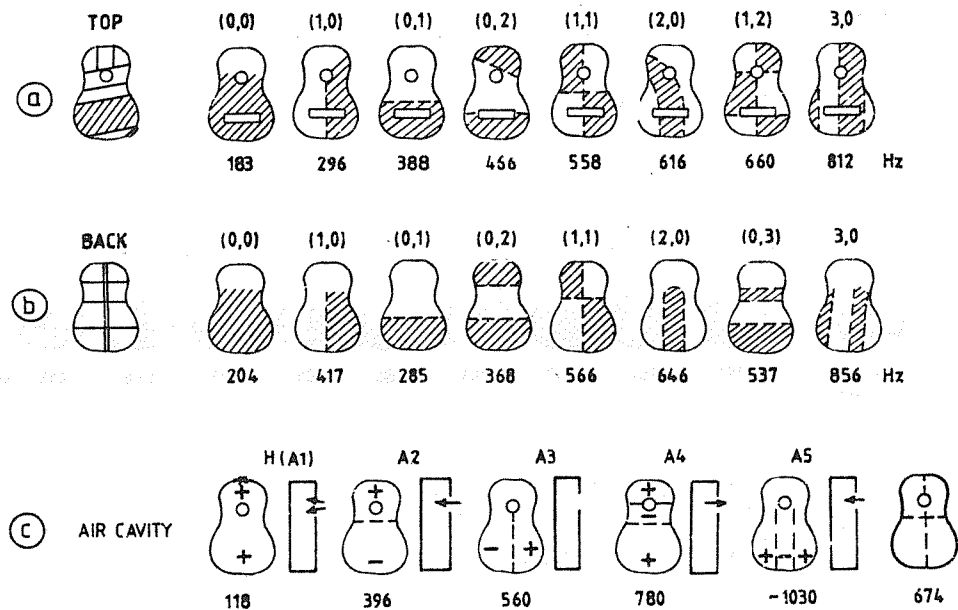


Fig. 7. (a) Modes of a classical guitar top (Kohno 30) with the back and ribs in sand, (b) Modes of the back with the top and ribs in sand; (c) Modes of the air cavity with the guitar body in sand. Modal designations are given above the figures and modal frequencies below.

(Professional model) guitar are shown in Fig. 7. Note that the (0,1) mode is higher in frequency than the (1,0) mode due to the fan bracing. Modes in the back plate nearly always occur at higher frequencies than the corresponding modes in the folk guitar of Fig. 6; this is partly due to the smaller size of the lower bout, partly due to the greater stiffness. The modes of the top and back are not as closely matched in frequency as in the folk guitar.

Table I compares the modal frequencies in four different guitars, two classical and two folk. Many interesting observations can be made. In the Martin D-28, for example, the fundamental modes of the top and back plate are tuned to almost the same frequency; in the other three guitars the back is tuned considerably higher (by two to six semitones on the musical scale). In the fan-braced top plates of the classical guitars the (0,1) mode occurs at a higher frequency than the (1,0) mode, in the cross-braced top plates and in all the back plates the reverse is true.

Table 1. Frequencies of the principal modes of the top plate, back plate, and air cavity in four guitars

<u>Top plate</u>								
	(0,0)	(0,1)	(1,0)	(0,2)	(1,1)	(0,3)	(2,0)	(1,2)
folk:								
Martin D28	163	276	390	431	643	733	756	
Martin D35	135	219	313	397	576	626	648	777
classical:								
Kohno 30	183	388	296	466	558		616	660
Conrad	163	261	228	382	474		497	
<u>Back plate</u>								
	(0,0)	(0,1)	(0,2)	(1,0)	(0,3)	(1,1)	(2,0)	(1,2)
folk:								
MartinD28	165	257	337	369	480	509	678	693
Martin D35	160	231	306	354	467	501	677	
classical:								
Kohno 30	204	285	368	417	537	566	646	856
Conrad	229	277	344	495	481	573	830	611
<u>Air cavity</u>								
	H (A1) (Helmholtz)	A2 (0,1)	A3 (1,0)	(1,1)	A4 (0,2)	A5 (2,0)		
folk:								
Martin D28	121	383	504	652	722	956		
Martin D35	118	392	512	666	730	975		
classical:								
Kohno 30	118	396	560	674	780			
Conrad	127	391	558	711	772	1033		

Guitar resonances

The main vibrational patterns of a Martin D-28 guitar with a fixed neck and free body are shown in Fig. 8. The first three resonances at 102, 193, and 201 Hz result from coupling between the lowest modes of the top plate, the back plate, and the air cavity; these occur at f_1 , f_2 , and f_3 , as previously discussed. Sound is radiated strongly from the sound hole at 102 Hz and 201 Hz, somewhat less strongly (about 20 dB less) at 193 Hz. The coupling at 102 Hz is mostly through the motion of the

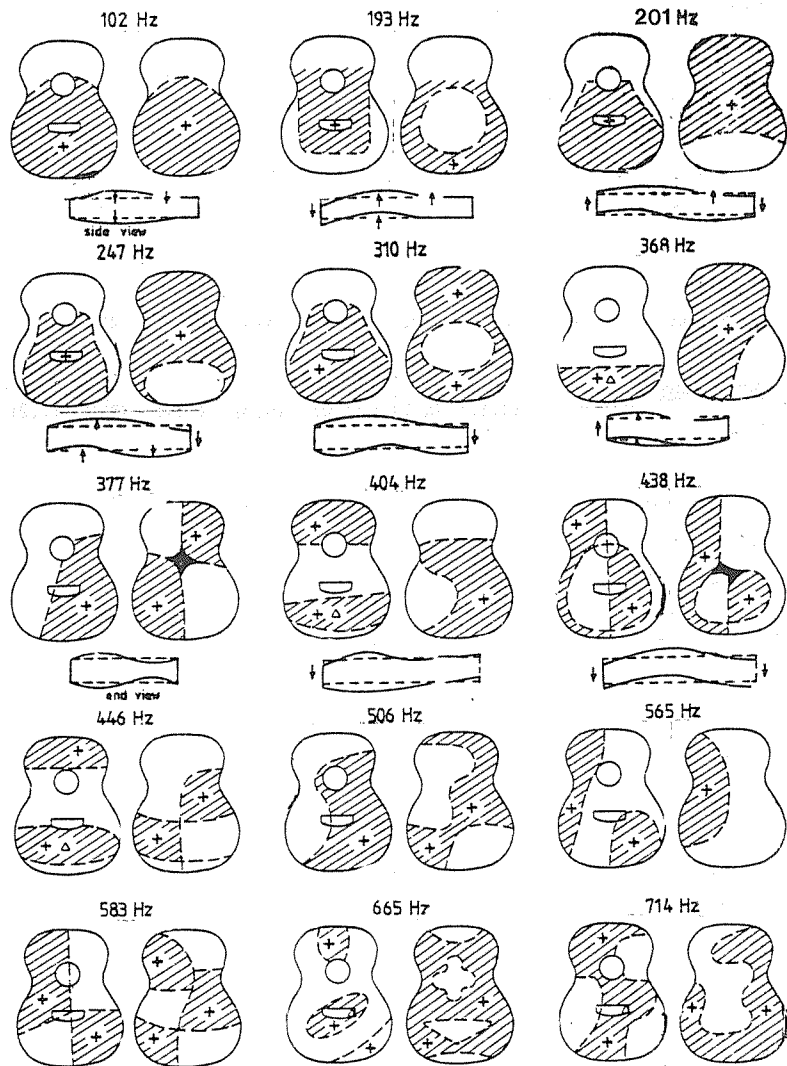


Fig. 8. Vibrational patterns of a Martin D28 guitar at some of the more important resonances below 800 Hz (neck fixed, body free).

enclosed air, at 193 Hz it is mostly through rib motion, and at 201 Hz there is an appreciable amount of both.

The next three resonances at 247, 310, and 368 Hz appear to result from a coupling between the (0,1) modes in the top plate and back plate

plus a weak coupling to the A2 air mode, which has the same modal shape. The radiation from the sound hole is considerably less (about 20 dB less at 247 Hz and 368 Hz, and about 30 dB less at 310 Hz) compared to the resonances at $f_1 = 102$ Hz and $f_3 = 201$ Hz, but nevertheless the sound hole radiation appears to make a notable contribution to the total sound output in this frequency range. The coupling scheme we have described is illustrated in Fig. 9.

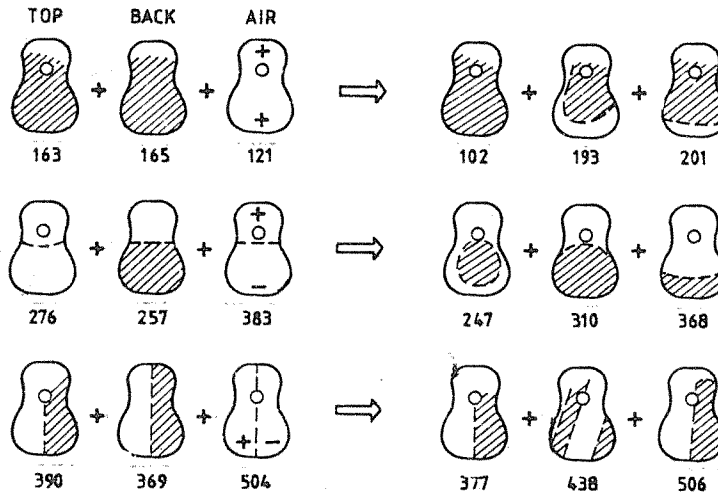


Fig. 9. Low-frequency coupling in a Martin D-28 folk guitar. In each case a top plate mode, a back plate mode, and a mode of the enclosed air couple together to produce one of the resonances shown in Fig. 8.

The (1,0) modes in the top and back plates appear to couple together and also to interact with the A3 air mode to produce resonances at 377, 438, and 506 Hz. Radiation from the sound hole is quite weak at these frequencies, because the sound hole lies on the line of symmetry of the plate motion. This coupling is also illustrated in Fig. 9.

Coupling between top and back plates in the Kohno 30 classical guitar, illustrated in Fig. 10, is quite different from that described in the

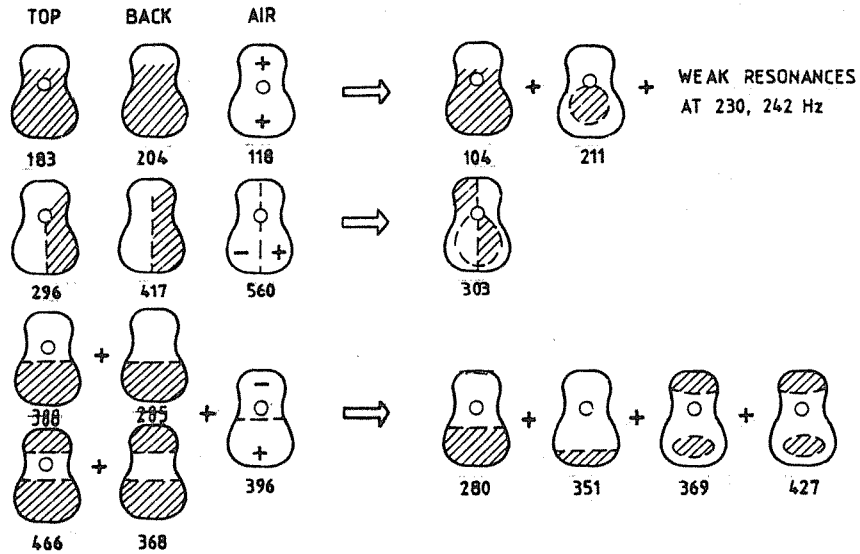


Fig. 10. Low-frequency coupling in a Kohno 30 classical guitar (neck fixed, body free). The coupling between top and back plates and the enclosed air modes is considerably more complicated than in the folk guitar shown in Fig. 9.

Martin D-28, because the relative frequencies of the same modes in the top and back are substantially different. The lowest modes of the top and back plates couple together to give strong resonances at 104 Hz and 211 Hz; weak resonances at 230 Hz and 242 Hz also appear to originate from this interaction.

Because there is much less transverse bracing, the (1,0) mode occurs at a much lower frequency in the top plate of a classical guitar than in a cross-braced folk guitar. Thus it couples only weakly to the (1,0) mode in the back plate and to the A3 air resonance, and the resonance at 303 Hz is mainly a mode of the top plate.

The (0,1) and (0,2) modes in the top and back plates plus the A2 air mode appear to couple together in a complicated way to produce at least four resonances, as shown in Fig. 10. The resonance at 280 Hz is mainly due to the (0,1) mode in the back plate. The sound hole radiates strongly at the upper two resonances, which are near the A2 air mode in fre-

quency; the sound level at the sound hole is only 8 to 10 dB below that observed at the lowest resonances, where the top and back plates move in their main (0,0) mode. Strong radiation around the frequency of the A2

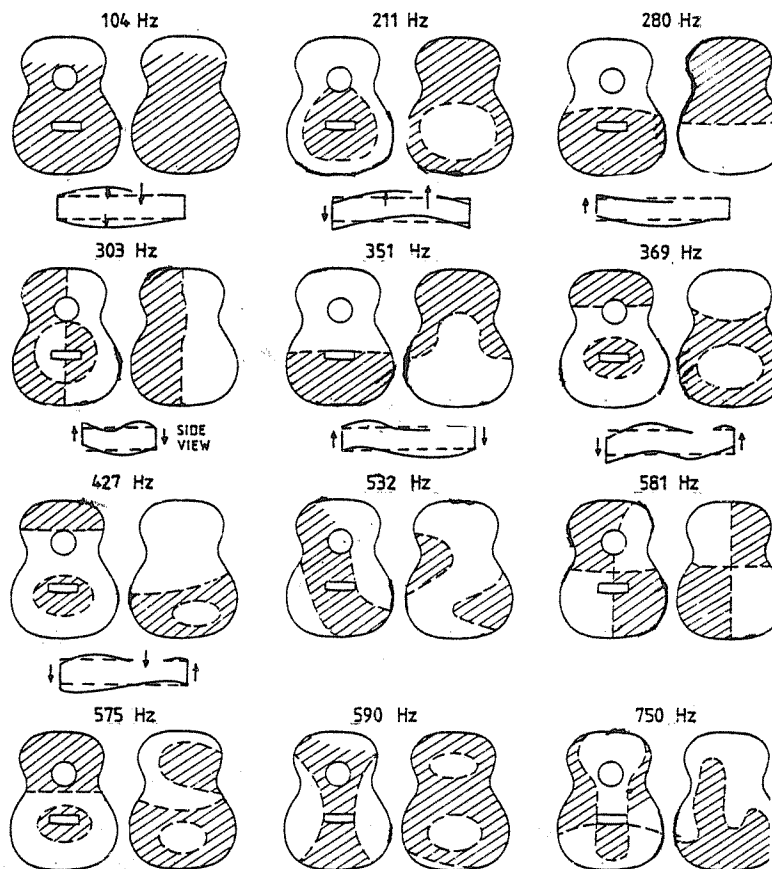


Fig. 11. Vibrational patterns of a Kohno 30 (Professional model) classical guitar at the most prominent resonances below 800 Hz.

air mode (about 400 Hz) is typical of good classical guitars. Meyer (1983) found that the acoustical response of classical guitars around 400 Hz show a particularly high correlation to quality.

Resonances of the Kohno 30 classical guitar are shown in Fig. 11.

They are quite different from the resonances of the Martin D-28 folk guitar in Fig. 8. In the Kohno classical guitar, only two prominent resonances are associated with the coupling of the fundamental (0,0) modes, whereas in the Martin folk guitar, each interaction leads to three fairly prominent resonances. This is due mainly to the larger differences between the modal frequencies in the top and back plates in the Kohno guitar.

In folk guitars the resonances based on the (1,0) modes generally lie at higher frequencies than in classical guitars because of greater cross-grain stiffness in the X-braced top plate.

The (1,0) top plate mode in the Kohno guitar appears to couple to the (0,2) mode as well as the (0,1) mode in the back plate, thus leading to a more complicated family of resonances than are observed in the Martin D-28.

Conclusion

The acoustical response of both classical and folk guitars is dominated by a series of resonances which are tracable to interactions between the vibrational modes of the various parts. These interactions at low frequency can be described fairly well by rather simple two-mass and three-mass models. Attempts are being made to similarly model the (1,0) and (0,1) mode interactions in order to understand the guitar as a system of coupled oscillators.

In order to successfully describe the acoustical response of the guitar, it is important that the boundary conditions be carefully selected and described when response measurements are made.

Acknowledgments

We wish to thank George Dauphinais, Larry Henrikson, and Richard Ross for the loan of guitars used in this study. Robert Witte assisted in

some of the response measurements. Conversations with Richard Ross were particularly enlightening.

References

Arnold, E.B. and Weinreich, G. (1982): "Acoustical spectroscopy of violins", *J.Acoust.Soc.Am.* 72, 1739.

Beranek, L.L. (1954): Acoustics, Section 3.4, McGraw-Hill, New York.

Boullosa, R.B. (1981): "The use of transient excitation for guitar frequency response testing", *Catgut Acoust.Soc. Newsletter* No. 36, 17.

Caldersmith, G. (1978): "Guitar as a reflex enclosure", *J.Acoust.Soc.Am.* 63, 1566.

Caldersmith, G. (1981): "Plate fundamental coupling and its musical importance", *Catgut Acoust.Soc. Newsletter* No. 36, 21.

Christensen, O. and Vistisen, B.B. (1980): "Simple model for low-frequency guitar function", *J.Acoust.Soc.Am.* 68, 758.

Cox, S. (1980): "An equivalent-circuit approach to the coupling between the Helmholtz and top-plate modes in a stringed instrument", *Catgut Acoust.Soc. Newsletter* No. 33, 30.

Dickens, F.T. (1981): "Analysis of the first and second vibration modes in a guitar using an equivalent electrical circuit", *Catgut Acoust.Soc. Newsletter* No. 35, 18.

Firth, I.M. (1977): "Physics of the guitar at the Helmholtz and the first top-plate resonances", *J.Acoust.Soc.Am.* 61, 588.

Jansson, E.V. (1981): "A study of acoustical and hologram interferometric measurements of the top plate vibrations of a guitar", *Acustica* 35, 95.

Jovičić, O. and Jovičić, J. (1977): "Le role des barres de raidissement sur la table de resonance de la guitare", *Acustica* 38, 175 and 180.

Meyer, J. (1974): "Die Abstimmung der Grundresonanzen von Gitarren", *Das Musikinstrument* 23, 179; English translation in *J. Guitar Acoustics* No. 5, 19 (1982).

Meyer, J. (1983): "Quality aspects of the guitar tone", in (E.Jansson ed.) Function, Construction and Quality of the Guitar, Publ. No. 38, Royal Swedish Academy of Music.

Morse, P.M. and Ingard, K.U. (1968): Theoretical Acoustics, McGraw-Hill, New York.

Richardson, B.E. (1982): "A physical investigation into some factors affecting the musical performance of the guitar", unpublished PhD. thesis, University College, Cardiff.

Ross, R.E. and Rossing, T.D. (1979): "Plate vibrations and resonances of classical and folk guitars", J.Acoust.Soc.Am. 65, 72; also R.E. Ross (1979): "The acoustics of the guitar: an analysis of the effect of bracing stiffness on resonance placement", unpublished M.S. Thesis, Northern Illinois University.

Rossing, T.D. (1981): "Physics of guitars: an introduction", J.Guitar Acoustics No. 4, 45.

Stetson, K.A. (1981): "On modal coupling in string instrument bodies", J.Guitar Acoustics No. 3, 23.

Strong, W.Y., Beyer, T.B., Bowen, D.J., Williams, E.G., and Maynard, J.D. (1982): "Studying a guitar's radiation properties with nearfield holography", J. Guitar Acoustics No. 6, 50.

To be added after the third piece in the section "Guitar resonances":

Although fixing the neck approximates the condition under which the guitar is played, suspending the guitar on rubber bands so that it is totally free to vibrate appears to give results that may be easier to interpret. In the free condition, the Martin D-28 has only two strong resonances (104 and 201 Hz) due to the interaction in the first row of Fig. 9.

TONAL QUALITIES OF THE INDIAN TANPURA
Ranjan Sengupta, B.M. Banerjee, Sumita Sengupta, Dipali Nag
Sangeet Research Academy, Calcutta, India

Abstract

Vocalists of North Indian Classical Music use the four-stringed "Tanpura" to get the drones with which to synchronize the notes they must produce accurately in their song. When the strings are struck by fingers in succession, the shell of its resonance chamber "Tumba" emits a characteristic melodious sound that creates the atmosphere of classical music. Though the four strings are tuned to three frequencies, the musicians can get the cue of all the notes from the harmonics, that are produced strongly and abundantly. The Tanpura drone, tuned and fingered by trained musicians, has been analyzed with a Kay Sonagraph. The sonagrams revealed spectra that extend over the full audio range. The sound persists with good amplitude and little decay over the first half of a period of 3 to 5 seconds. It starts to decay in the later half, when high frequency clusters are rapidly eliminated. There are vibratos, of a period of 0.1 second or greater, which may vary from cluster to cluster. This must be due to characteristic shell vibrations, which is complex for the Tumba has a complex shape. The Tanpura spectrum contains quite a number of unharmonic frequencies, that cannot be ascribed even to harmonics of strings other than that struck.

Introduction

Vocalists of North Indian classical music use the Tanpura (Tambura) as an indispensable accompanying instrument providing the drones, with which to synchronize the notes they must produce in their song, accurate in pitch. The Tanpura is a four-stringed instrument, the resounding twangs of which create the atmosphere of Indian classical music. Its sound is considered very sweet and melodious, and it stimulates both the musician and the audience.

Description

The Tanpura is a big four-stringed instrument (Fig. 1). Its first string - a steel wire - is tuned to the middle note of the lower octave. The second and third string - also of steel - are both tuned to the first note of the middle octave. The fourth string - a thick brass wire - is tuned to the first note of the lower octave. The strings go side by side over the bridge, and then along the neck almost to the top of the Tanpura, finally over the edge of "Ati" or "Atak", which is an ivory strip positioned securely in a slot cut into the convex surface of the neck, and then through the holes of "Targahan", yet another strip of ivory or



Fig. 1. Photo of Ladies and Gents Tanpura. The strings in Ladies Tanpura are tuned to nominal frequencies of 180, 240, 240 and 120 Hz; those of the Gents Tanpura are tuned to 120, 160, 160 and 80 Hz.

bone, to the four pegs on which they are twisted and tied. The pegs are held tightly in holes of the neck, by friction. By twisting the knobs on the pegs (Khutia), tension of individual strings can be adjusted separately. Fine adjustment of tension is obtained by positioning the "Mankas", through which the strings go, to be held securely in the wooden block of a triangular cross section, called Keel, Mongra or Longot, which is glued to the bottom of "Tumba", the resonance box. The Tumba is formed out of a dried shell of class of Indian gourd. This must have the shape of a flattened sphere, of nearly 50 cm in diameter, which is slightly re-entrant at the base, but elongated to a cone at the top, where it is attached to the hollow wooden, nearly semi-cylindrical neck (Dand) of about a metre in length.

About one-fourth of one side of the gourd is cut off to be covered by the slightly convex wooden surface called the "Tabli". The bridge - a rectangular strip of deer horn - rests elevated on the wooden blocks, which are glued to the middle of Tabli. The resonating shells of Tumba and Tabli are glued securely to the neck through decorative leaves of thin wood called "Pattia". The vibrations of the shells of Tabli and Tumba, and to a lesser extent that of the neck, contribute in major way to the volume, character and melody of the sound emitted. Periodic excitation by the strings vibrating at stable and controlled frequencies bestow the emitted sound, its musical character. This was well known to the ancient musicians who invented and developed this instrument. The Tanpura is perhaps the only instrument which places a knot of cotton thread between the string and the bridge, which, when placed correctly, dramatically improves the volume and quality of the sound bestowing it the Tanpura character. This is known as the adjustment of "jwari", which means strengthening.

Operation

Although the four strings are tuned to only three frequencies viz., the first note of the lower octave, the middle note of the lower octave and the first note of the middle octave, the musicians get the cue of all

the seven notes. This is because they are trained to hear the harmonics, and to match with the harmonics of their own sung tones. (Perhaps they also recall these tones from their memory to help in this matching.) This becomes easy due to the abundance and strength of harmonics in the Tanpura tones, which exceed the fundamental up to at least 1000-1500 Hz. In this frequency range, the sung tones also have similarly strong harmonics, particularly when the performer sings /^ud/, /^uæ/ and /^uε/ and in a slightly modified way /i/. For it is well known that harmonics are very strong in the first two formants, and extend to 2000 Hz with large amplitudes.

The eight notes of Hindusthani octave have the following nominal frequencies.

(Do)	(Re)	(Mi)	(Fa)	(Sol)	(La)	(Ti)	.
ॐ	ॐ	ॐ	ॐ	ॐ	ॐ	ॐ	ॐ
240	270	301	320	360	405	452	480

When the first wire is tuned to Sol = 180 Hz, it gives the cue

to ॐ ॐ ॐ as
La Ti Re

- 1) 180 Hz - Pancham - Middle tone of lower octave ॐ
- 2) 180 x 2 - 360 Hz - Middle tone of middle octave ॐ
- 3) 180 x 3 - 540 Hz - (270 x 2) - Re of upper octave ॐ
- 4) 180 x 4 - 720 Hz - Middle tone of upper octave (360 x 2) ॐ
- 5) 180 x 5 - 900 Hz - (450 x 2) Ti of upper octave ॐ
- 6) 180 x 6 - 1080 Hz - Re of fourth octave; 4th harmonic of Re (270 x 4) ॐ
- 7) 180 x 7 - 1260 Hz - Fa of fourth octave; (320 x 4) = 1280 Hz ॐ
- 8) 180 x 8 - 1440 Hz - Middle tone of 4th octave; 360 x 4 = 1440 Hz
- 9) 180 x 9 - 1620 Hz - La of 4th octave; 405 x 4 = 1620 Hz ॐ

The thick wire is tuned to 120 Hz, so it gives the cue to

ॐ ॐ ॐ
Do, Mi Sol (Middle note) and Fa

- 1) 120 Hz - First note of the lower octave ॐ
- 2) 120 x 2 - 240 Hz First note of Middle octave ॐ
- 3) 120 x 3 - 360 Hz Middle note of Middle octave ॐ
- 4) 120 x 4 - 480 " First note of upper octave; 2nd harmonic ॐ
- 5) 120 x 5 - 600 " Mi of upper octave; (301 x 2) ॐ
- 6) 120 x 6 - 720 " Middle note of upper octave; (360 x 2) ॐ
- 7) 120 x 7 - 860 " Very soft Ti of upper octave; (452 x 2)
- 8) 120 x 8 - 960 " 3rd harmonic of Fa; (320 x 3) ॐ
- 9) 120 x 9 - 1080 " 4th harmonic of Re; (270 x 4) ॐ

Experiments

The Tanpura drone, tuned and fingered by trained musicians, with and without jwari, was directly recorded into the memory, and then analysed by a Kay Sonagraph, model 7800. The experiments were conducted in a noise proof studio of the dimensions 18'x16'x12' with a reverberation time around 0.1 second. The sonagrams revealed spectra that extend over the full audio range (Figs. 2a and 2b; also Fig. 4a). The sound persists with good amplitude and insensible decay over the first half of a period of 3 to 10 seconds (Figs. 3a and 3b). It starts to decay in the later half, when high frequency clusters are rapidly eliminated (Figs. 3a and 3b). Notice that in the "3D spectra" recorded with a high frequency lift of 6 dB/octave (Fig. 3a), the maximum occurs at high frequencies - at about 5 kHz. This frequency of maximum response initially decreases with time - almost exponentially (Fig. 3a). Vibratos of different character and timing are visible in Fig. 2a, particularly in Figs. 3a and 4a, and are seen to be present in the different clusters. These must be due to the characteristic shell vibrations of the Tabli, Tumba and the neck. These must still be identified. The amplitude decay curve contains fluctuations at the fundamental frequency (Fig. 4a). These also come into the "3D spectra" as beautiful woven patterns. The spectra without jwari are shown in Figs. 6a and 6b. The frequency range is smaller, and there is a more rapid decay in amplitude which contains a smaller number of vibratos. Unharmonic frequencies reported in the abstract were not found in these direct recordings. The spectra of a Harmonium - an additional accompanying instrument sometimes used by musicians of classical music - do not extend beyond 6 kHz (Fig. 5). The Tanpura emits a characteristic twang $U-\alpha-\omega$. This is well explained by its formant structure - which contains formants similar to the vowel /æ/ in the first half. In the later half, high frequency clusters get dissipated, and the sound approaches that of the vowel /ω/. The Tanpura sound is valued, not only because of its melody and sweetness, but also because it contains strong harmonics and formants, extending over almost the full audio range. A musician can "hear" all the notes of the "song" he is going to sing in the twangs of the Tanpura. The performing artist adjusts the strings to his own octaves accurately. He perhaps recalls from his brain the notes of his octaves, and this he also hears in the Tanpura twangs. This stimulates him so that he gets set to produce the required pitches accurately, easily and naturally. This also stimulates the audience, who are,

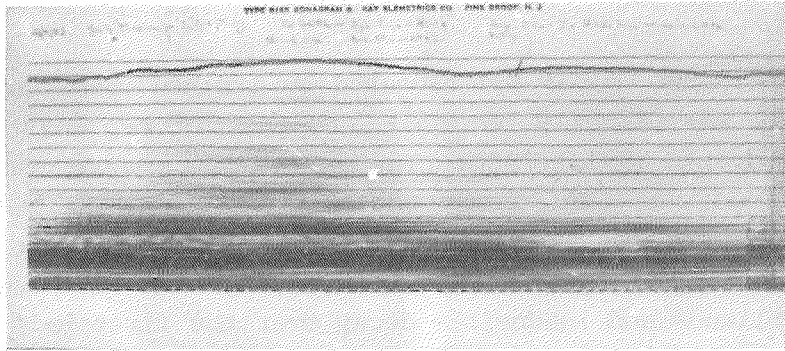


Fig. 2a. "3D Spectra" sonagram of middle string of Gents Tanpura; 16 kHz range (horizontal lines mark 1, 2...15, 16 kHz); Notice the vibratos in the formants within 1 kHz; that between 2 to 3 kHz; 4 to 5 kHz. Notice also the response between 6 to 7 kHz; 8 to 9 kHz; 9 to 10 kHz; 11 to 12 kHz; 13 to 14 kHz. The time span is 1.28 sec.

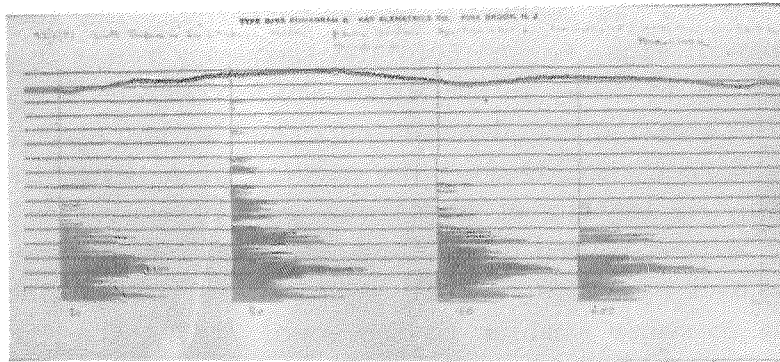


Fig. 2b. "Power Spectrum" of the same. Notice how the spectra extends clearly into 13 to 14 kHz marker lines; also how the upper frequency enhances at first and then dissipates with time; also that maximum amplitudes are obtained above 2 kHz. "Normal shape" spectra with no high frequency preemphasis.

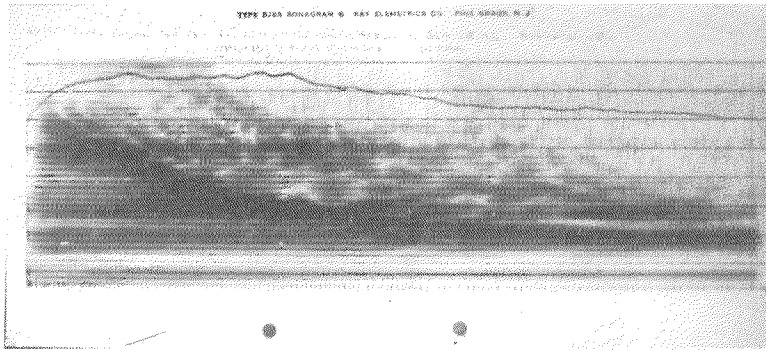


Fig. 3a. "3D Spectra" of the middle string of Ladies Tanpure recorded with 6 dB lift per octave (horizontal lines mark 1, 2...7, 8 kHz). Notice that the maximum amplitude, in this case, occurs above 5 kHz, at start. This frequency of maximum amplitude diminishes with time - almost exponentially. After about one second it rests at 3 kHz. Notice also the positions of maxima in the vibrato's on different harmonics. Time span = 2.56 sec.

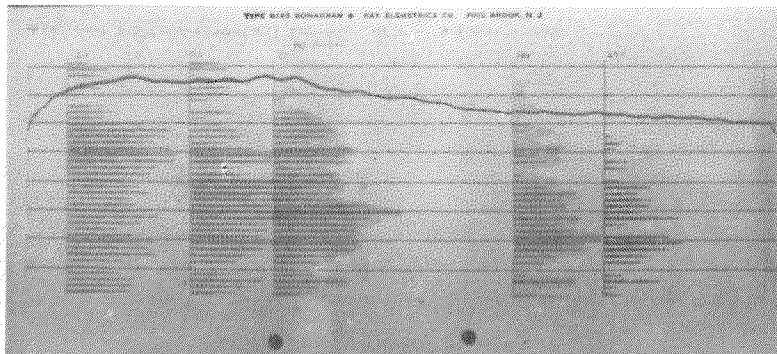


Fig. 3b. "Power Spectrum". Notice how the high frequency harmonics get dissipated with time.

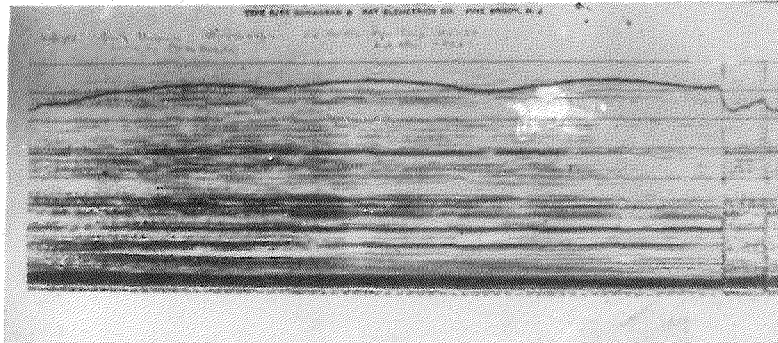


Fig. 4. "3D Spectra" of the lower Sa - thick string - of Gents Tanpura. Notice the rapid amplitude fluctuation that causes the "woven" patterns, also the vibrato's that are different in different clusters; compare the vibrato's with the amplitude fluctuation shown in the "amplitude display" curve. (8 kHz frequency span and 2.56 seconds time span.)

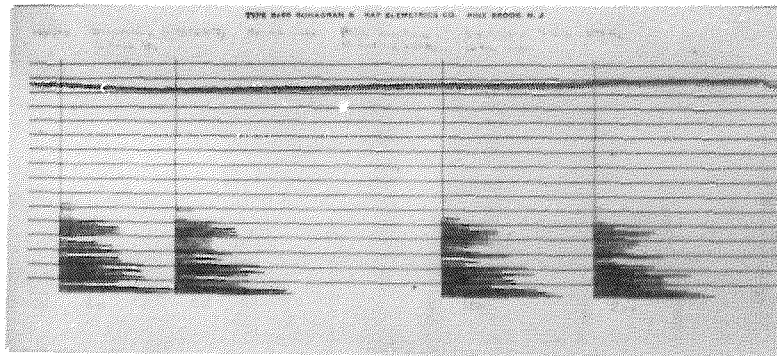


Fig. 5. "Power Spectrum" of a Harmonium. Notice that the frequency components do not extend beyond 6 kHz. (16 kHz frequency span and 1.28 seconds time span.)

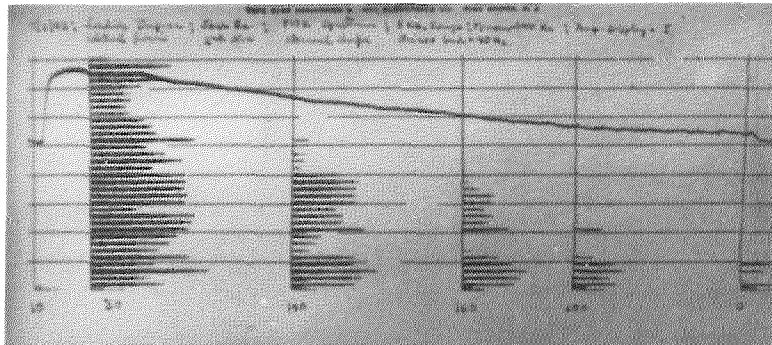
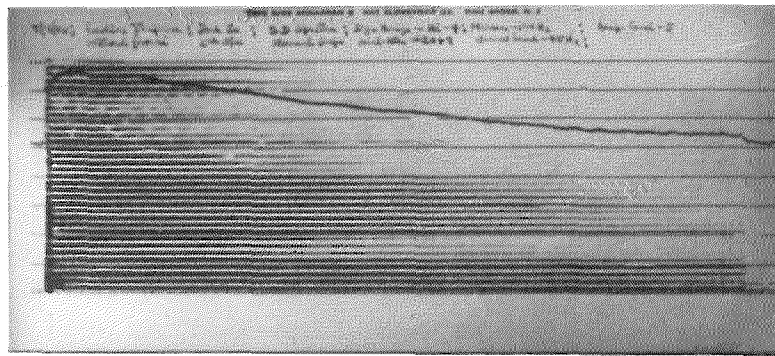


Fig. 6. 3D spectra and Power Spectrum of the middle string of a Tanpura without jwari. Notice how the amplitude decays rapidly, how the high frequency clusters get dissipated and how almost all frequencies above one kilohertz are eliminated after 2.5 seconds. (8 kHz frequency span and 2.56 seconds time span.)

mostly, musicians themselves and to them the Tanpura has a position of prize.

Conclusion

We report the beginning of a scientific research on the Tanpura. Only the characteristics of the Tanpura sound are presented here. Following investigations should concern the formant and antiformant positions that make the sound melodious. This may be done in two ways, viz., (a) by

applying statistical methods on the emissions of good Tanpuras; (b) by artificially positioning formants to create a sound which is considered sweet and melodious by expert musicians. However, the real Tanpura sound is even more complex, for it contains vibratos which are different in each respective formant. Our promised objective is to find out ways and means of fabricating Tanpuras of consistent good quality. So far, this has been done by families of experts with empirical knowledge about selection and processing of the gourd for the Tumba, the quality of wood and its shape for forming the Tabli and the Dand, as well as some crude methods of testing them. We shall have to find out scientific answers to their methods, and also, to devise apparatus and methods to support and supplement these tests.

